PhD thesis

Martin G. Klompmaker

Insights into carotenoid sequestration mechanisms in Tomato fruit (*Solanum lycopersicum*) and the effect of ectopic expression approaches on carotenoid biosynthesis

This thesis was submitted for the degree of Doctor of Philosophy at

Royal Holloway University of London, June 2017

Declaration of authorship

I hereby declare that the work presented in this thesis is the original work of the author unless otherwise stated. Original material used in the creation of this thesis has not been previously submitted either in part or whole for a degree of any description from any institution.

Martin G. Klompmaker

Abstract

Carotenoids are involved in a wide range of plant processes varying from development to defence, pollination and seed dispersal. The consumption benefits of carotenoids for human health and nutrition have led to development of an interest in the industrial application of carotenoids in food, feed and cosmetics. Tomato (*Solanum lycopersicum*) is the model plant for carotenoids related studies with its fruits which contain high levels of carotenoids.

Carotenoid sequestration is an important process linked to carotenoid biosynthesis which requires further elucidation. A selection of tomato lines perturbed in carotenoid biosynthesis was studied for their differences in sequestration mechanisms. Premature accumulation of carotenes in a tomato line constitutively expressing PSY1 led to the differentiation of chloroplasts to chromoplast in immature fruit to create a higher capacity for carotenoid accumulation. Tomato lines *rr*, og^{C} and *tan*, knock out lines for PSY1, LCY-B and CRT-ISO respectively, demonstrated different distributions between plastoglobules and crystalline membrane structures associated with *cis*-carotenes and *trans*-carotenes. The role of carotenoid accumulation and changes in carotenoid profiles suggests the plastid can adapt to changes in carotenoid content through plastid differentiation and preferential sequestration.

Ectopic expression of the MEP and bacterial carotenoid (*crtE*, *crtB*, *crtI*) pathway in the cytosol has hereby been attempted to enhance carotenoid content as an alternative to metabolic engineering of endogenous key enzymes. The isoprenoid biosynthesis clusters are spread over various cellular compartments in plants. A modular cloning system (GB Cloning) was used for the assembly of vectors with the genes of the MEP and bacterial carotenoid pathway in single or multi gene combinations. The ectopic expression of *crtB* led to the accumulation of phytoene (14-fold), phytofluene and lycopene, and increased levels of lutein and β-carotene. The impact of the enzyme on pathway intermediates beyond its function suggest a signalling cascade based on cytosolic apocarotenoids derived from the CRTB activity.

Acknowledgements

After finishing my master's degree in the Netherlands I was looking for a PhD project within the field of Plant Biotechnology focussing on metabolic engineering. I am very happy with the opportunity provided by Professor Paul Fraser to pursue a PhD-project in his laboratory at the Royal Holloway University and the support of the EU consortia DISCO and MultiBioPro.

A PhD-project is a personal achievement, but I would have never managed without help throughout the years I have worked on my project. I thank Professor Paul Fraser and Professor Peter Bramley, my supervisor and advisor respectively, for their support and questions to keep me focussed during the course of my PhD. Furthermore I would like to thank Dr Genny Enfissi and Dr Marilise Nogueira for the helpful discussions during our project meetings for the EU DISCO project and their help in the laboratory. Also Chris Gerrish for his very helpful technical support and my project student Veronica Czernik for her work on the cloning of carotenoid biosynthesis vectors. I am grateful for the fantastic group of colleagues who have all contributed to my project and in general to three pleasant years within this team.

I thank my family and friends, who have been supportive, helped me stay optimistic and have been great company to calm down after stressful moments.

Doing a PhD is a big challenge, but I am sure I can implement all the valuable lessons in my future carrier and life.

Thank you!

Martin Klompmaker

Table of Contents

List of Figures

List of tables

List of abbreviations

ACCD	Acetyl-CoA carboxylase D
ACT	Acetyl-CoA acetyltransferase
CAD	Coronary Artery Disease
CaMV35S	Cauliflower Mosaic Virus 35S
CDP-ME	4-diphosphocytidyl-methylerythritol
CDP-MEP	4-diphosphocytidyl-methylerythritol 2-phosphate
CMK	4-diphosphocytidyl-methylerythritol Kinase
CRISPR	Clustered Regularly Interspaced Short Palindromic Repeats
CRTB	Bacterial Phytoene Synthase
CRTE	Bacterial Geranylgeranyl Diphosphate
CRTI	Bacterial Phytoene Desaturase
CRT-ISO	Bacterial Carotenoid Isomerase
CRTW	Bacterial Carotenoid Ketolase
CRTZ	Bacterial Carotenoid Hydroxylase
DGDG	Digalactosyldiacylglycerol
DMAPP	Dimethylallyldiphosphate
DNA	DeoxyriboNucleic acid
DXP	Deoxyxylose 5-phosphate
DXR	Deoxyxylose 5-phosphate reductase
DXS	Deoxyxylose 5-phosphate synthase
FPP	Farnesyl Diphosphate
FPPS	Farnesyl Diphosphate Synthase
GB	Golden Braid
GC-MS	Gas Chromatography – Mass Spectrometry
GGPP	Geranylgeranyl Diphosphate
GGPPS	Geranylgeranyl Diphosphate Synthase
GMO	Genetically Modified Organism
GPP	Geranyl Diphosphate
GPPS	Geranyl Diphosphate Synthase

HDR	Hydroxymethylbutenyl Diphosphate Reductase
HDS	Hydroxymethylbutenyl Diphosphate Synthase
HMBPP	Hydroxymethylbutenyl Diphosphate
HMG	Hydroxymethylglutaryl-CoA
HMGR	3-hydroxy-3-methylglutaryl CoA Reductase
HMGS	3-hydroxy-3-methylglutaryl CoA Synthase
HPLC	High Performance Liquid Chromatography
IDI	Isopentenyl Diphosphate Delta Isomerase
IPP	Isopentenyl Diphosphate
LCY-B	Lycopene Cyclase β
LCY-E	Lycopene Cyclase ε
MCT	4-diphosphocytidyl-methylerythritol Synthase
MDS	Methylerythritol 2,4-cyclodiphosphate Synthase
MEcPP	Methylerythritol 2,4-cyclodiphosphate
MEP	Methylerythritol phosphate
MGDG	Monogalactodiacylglycerol
MK	Mevalonate kinase
MVA	Mevalonate pathway
og^c	*old gold crimson* (*LCY-B*) mutant
Or	"Orange" plastid associated gene with DnaJ Cys-domain
PCR	Polymerase Chain Reaction
PDS	Phytoene Desaturase
PIF	Phytochrome-interacting Factor
PMD	Pyrophosphomevalonate Decarboxylase
PMK	Phosphomevalonate Kinase
PSY	Phytoene Synthase
RNA	RiboNucleic Acid
rr	*psy1* mutant
RT	Retention Time
RT-PCR	Reverse Transcription-Polymerase Chain Reaction
TALEN	Transcription Activator-Like Effectors Nucleases

tan	*tangerine* (*crt-iso*) mutant
Thsp	*Arabidopsis thaliana* Heat Shock Protein Terminator
Tnos	*Agrobacterium tumefaciens* Nopaline Synthase terminator
TP	Transit Peptide
TU	Transcriptional Unit
UPLC	Ultra Performance Liquid Chromatography
UTR	Untranslated Region
VDE	Violaxanthin De-Epoxidase
ZDS	ζ-carotene desaturase
ZEP	Zeaxanthin epoxidase
Z-ISO	ζ-carotene isomerase

1. Introduction

1.1. The Isoprenoid network

1.1.1. Isoprenoids in nature

The cluster of metabolites which is called isoprenoids (or terpenoids) consists of over 55,000 compounds found (Mannen et al., 2014). A large part of these compounds can be found in plants (Rohmer et al., 1996; Zhou et al., 2012). Within this biochemical family a range of structural and functional variation is found which is unmatched by any other class of plant natural products. Classified based on the number of C_5-building blocks linked, this family is divided into hemiterpenes (C_5), monoterpenes (C_{10}), sesquiterpenes (C_{15}), diterpenes (C_{20}), triterpenes (C_{30}), tetraterpenes (C_{40}) and polyterpenes (>C_{40}). The starting point of the isoprenoid network is an isomeric duo of the aforementioned C_5-isoprene precursors: isopentenyl diphosphate (IPP) and dimethylallyl diphosphate (DMAPP), which an isopentenyl diphosphate delta isomerase (IDI) enzyme can change reversibly (Zhou et al., 2013). These two compounds can be synthesised via two distinctly different pathways: the mevalonate (MVA) pathway and the methylerythritol phosphate (MEP) pathway (Figure 1-1). The MVA-pathway is localised in the cytosol in animals, plants and fungi, whilst the MEP-pathway is found in bacteria, green algae and plastids of higher plants (Enfissi et al., 2005; Paetzold et al., 2010; Zhou et al., 2013). Besides the specificity in location and presence in organisms, the two precursor pathways interact distinctly with specific downstream isoprenoid branches. The MVA-pathway provides the precursors for e.g. sesquiterpenes and sterols. The MEP-pathway creates a flux of IPP/DMAPP utilised by plastidial isoprenoid branches like carotenoids, tocopherols and chlorophylls in plants (Chappell, 2002; Enfissi et al., 2005; Hsieh and Goodman, 2005; Kumar et al., 2012).

1.1.2. Isoprenoid precursors and prenyl extensions

While the two isoprenoid precursor pathways operate individually in different compartments, crosstalk is observed between them (Bick and Lange, 2003). The pathways are not demonstrating complete redundancy but are compatible. The linkage between the two pathways becomes clear in the interactive fluxes of IPP and DMAPP, despite being localised in

different compartments (Lange et al., 2015). A study executed by S. Kumar and others demonstrated the functionality of the MVA pathway when transferred to the plastids; When using fosmidomycin to inhibit the MEP-pathway, the transferred MVA-pathway took over IPP production and allowed regular growth (Kumar et al., 2012). An undefined level of redundancy is found between the pathways, as the pool of IPP/DMAPP can be used between the compartments if either pathway is inhibited. The rate of exchange between these pools is not defined [reviewed by Vranova et al.] (Enfissi et al., 2005; Vranova et al., 2013). A study on terpenoid volatiles synthesized in snapdragon flowers demonstrated the contribution of the MEP pathway to the volatiles produced in the cytosol; whereby the diurnal fluctuations of volatile synthesis seems to match with the circadian rhythm (Dudareva et al., 2005).

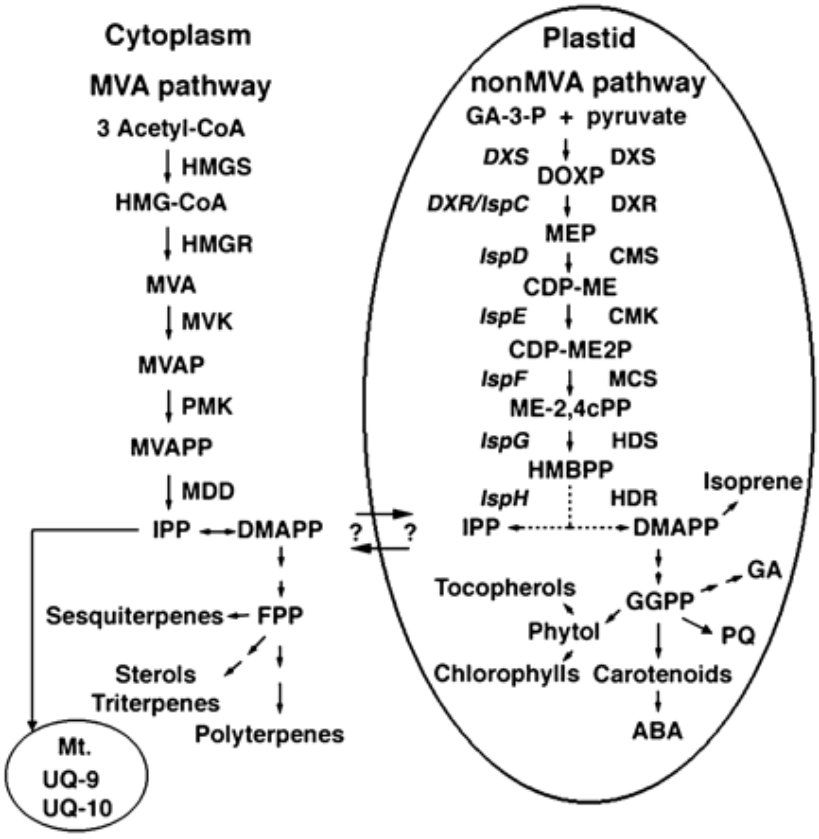

Figure 1-1. The plant isoprenoid network.
Schematic overview of the isoprenoid pathway cluster displaying the two isoprenoid precursor pathways (MVA & MEP) and the compartmentalised branches of isoprenoid compounds. linking the enzymatic steps involved in both pathways to a range of compounds specifically derived from either pathway (Hsieh and Goodman, 2005). Abbreviations of MVA and MEP pathway enzymes and intermediates are clarified in tables and text. Other abbreviations: GA = gibberellin, PQ = plastoquinones, ABA = abscisic acid, Mt. = mitochondrion, UQ =ubiquitin.

IPP and DMAPP are the C_5-precursor molecules of all isoprenoids, and by linking the IPP and DMAPP molecules in different combinations of size and ratio, the large variety in isoprenoids is generated. The balance of IPP and DMAPP is relevant for the synthesis of the various compounds, as the linkage of either solely IPP or DMAPP, or a combination of the two can lead to distinctly different compounds. E.g. geranyl diphosphate is a mixture of IPP and DMAPP and rubber consist mainly of IPP (Zhou et al., 2013). Some isoprenoids are synthesised from one C_5-molecule, e.g. isoprene from DMAPP, whilst the linkage of IPP/DMAPP molecules leads to the assembly of geranyl diphosphate (GPP), farnesyl diphosphate (FPP) and geranylgeranyl diphosphate (GGPP) (Zhou et al., 2013). GPP (C_{10}) is the precursor for e.g. monoterpenes, FPP (C_{15}) the precursor for sesquiterpenes. GGPP (C_{20}) is a precursor for e.g. diterpenes, which are found primarily in the plastids (Bick and Lange, 2003). Extended isoprenoid backbones, tri-, tetra-, and poly-terpenoids are constructed out of these three compounds, as reviewed by Fraser and Bramley (Fraser and Bramley, 2004; Kim et al., 2010).

1.1.3. MEP pathway

The non-mevalonate pathway or MEP-pathway was discovered via radiolabelled precursors for the pathway. Radiolabelled pyruvate and glyceraldehyde 3-phosphate proved to be integrated into the isoprenyl units produced in an *E. coli* strain fed with these compounds (Rohmer et al., 1996). Glyceraldehyde 3-phosphate and pyruvate are joined in a head-tail connection by deoxy-xylulose 5-phosphate (DXP) synthase (DXS) to form DXP at the start of the MEP pathway (Figure 1-2). DXP can be used as a substrate for DXP reductase (DXR) to produce methylerythritol 4-phosphate (MEP). DXR, not DXS, is the first committed step of the MEP-pathway as DXP can be used as a substrate for thiamine pyridoxal (Carretero-Paulet et al., 2006; Enfissi et al., 2010). MEP undergoes two enzymatic reactions to arrive to 4-diphosphocytidyl-methylerythritol 2-phosphate (CDP-MEP), via CDP-ME synthase (MCT) and CDP-ME kinase (CMK) which reattaches a phosphate to 4-diphosphocytidyl-methylerythritol (CDP-ME). The next step is the synthesis of methylerythritol 2,4-cyclodiphosphate (MEcPP); this reaction is catalysed by a MEcPP-synthase

(MDS). Hydroxymethylbutenyl diphosphate (HMBPP) is generated via HMBPP-synthase (HDS) and a HMBPP-reductase (HDR) carries out the final step of the pathway towards IPP and DMAPP (Carretero-Paulet et al., 2006; Li and Sharkey, 2013). An overview of the MEP pathway genes is provided in Table 1-1.

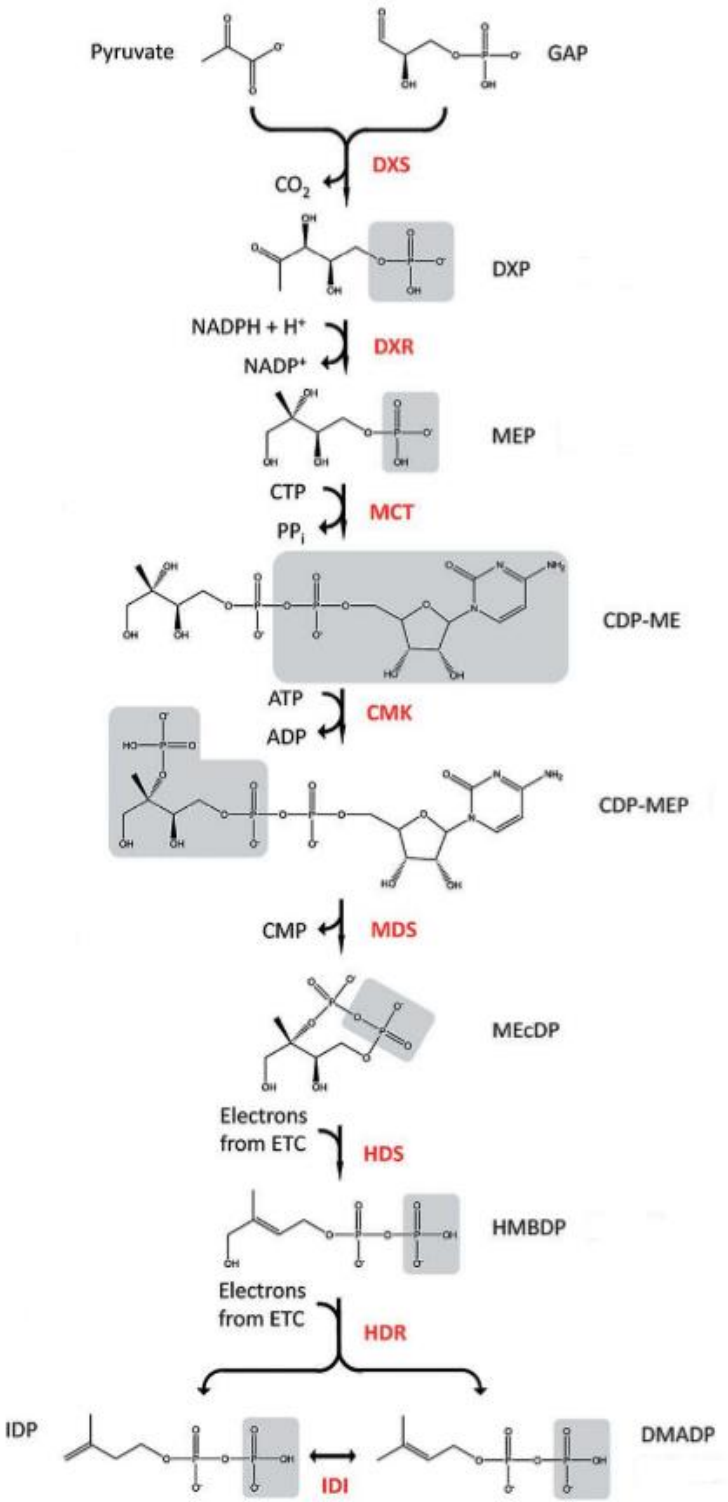

(figure on the previous page)

Figure 1-2. MEP-pathway.

DXS is the first step of the MEP-pathway; it synthesises deoxy-xylulose phosphate from pyruvate and glyceraldehyde-3-phosphate. The two products of the pathway are IPP and DMAPP, which are synthesised through six further enzymatic steps. DXR is the first committed step of the pathway producing MEP. MCT and CMK add phosphates in a linkage process with diphosphocytidyl. MDS, HDS and HDR modify the molecule to the final IPP or DMAPP molecules depending on the position of the double bond. Figure adapted from (Li and Sharkey, 2013).

Table 1-1 Overview of the genes of the MEP pathway.

Names of the genes for the enzymes of the MEP pathway. Abbreviations used in this thesis are place in the second column (Li and Sharkey, 2013). Enzyme number as depicted in the KEGG pathway platform are provided in the last column.

MEP pathway gene names	Abbreviations	Enzyme number (KEGG)
deoxyxylose 5-phosphate synthase	DXS	2.2.1.7
deoxyxylose 5-phosphate reductase	DXR	1.1.1.267
4-diphosphocytidyl-methylerythritol synthase	MCT	2.7.7.60
4-diphosphocytidyl-methylerythritol kinase	CMK	2.7.1.148
methylerythritol 2,4-cyclodiphosphate synthase	MDS	4.6.1.12
Hydroxymethylbutenyl diphosphate synthase	HDS	1.17.7.1
Hydroxymethylbutenyl diphosphate reductase	HDR	1.17.1.2

1.1.4. MVA pathway

The MVA pathway (Figure 1-3) - the other upstream pathway - is present in the cytosol. For this 3-hydroxy-3-methylglutaryl CoA reductase (HMGR) is the key enzyme of the pathway (Enfissi et al., 2005). The MVA pathway consists of six enzymatic steps starting with an Acetyl-CoA acetyltransferase (ACT) linking two acetyl-CoA molecules into acetoacetyl-CoA. This step is followed by the synthesis of hydroxymethylglutaryl-CoA (HMG) by HMG-synthase (HMGS). HMGR then catalyses the synthesis of mevalonate, the intermediate the pathway is named after. Two phosphates are added to create mevalonate 5-phosphate and mevalonate 5-pyrophosphate, these phosphates are attached via mevalonate kinase (MK) and phosphomevalonate kinase (PMK) respectively. The final step of the pathway is the synthesis of IPP via pyrophosphomevalonate decarboxylase (PMD). As PMD only generates IPP, not DMAPP, an IDI enzyme is required to generate DMAPP molecules (Gupta and Phulara, 2015; Lange et al., 2000).

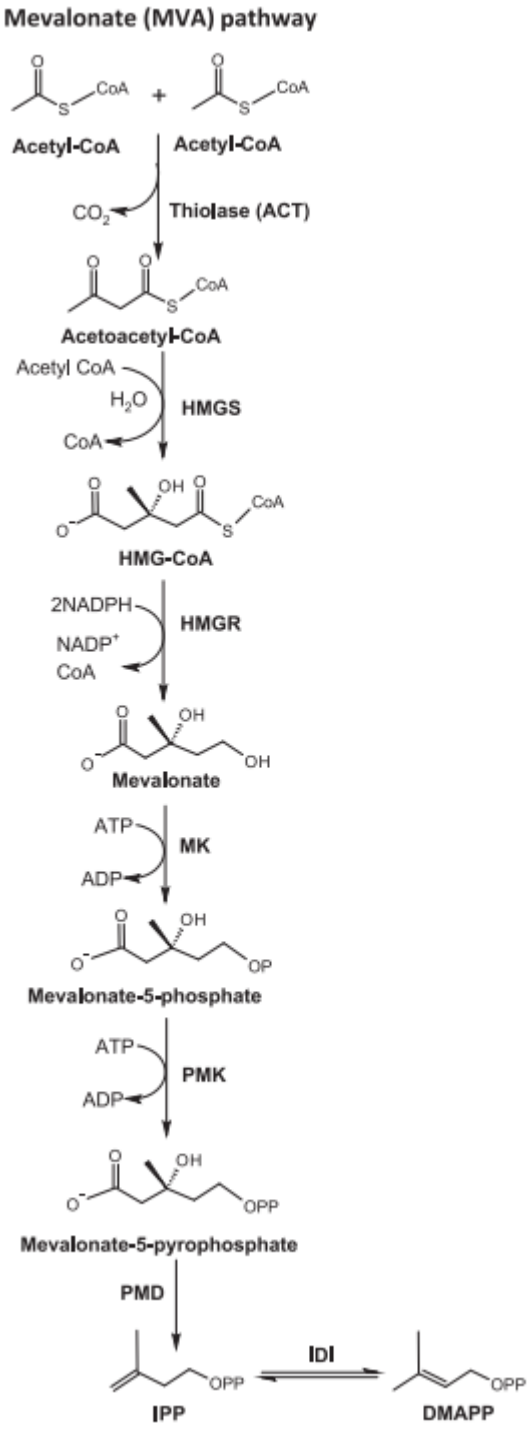

Figure 1-3. MVA pathway

Six enzymatic steps (ACT, HMGS, HMGR, MK, PMK, PMD) which synthesise IPP out of two acetyl-CoA molecules. HMGR is the key enzyme which synthesises mevalonate during the third step of the pathway. IDI is required for the isomerisation of IPP in the DMAPP in the cytosol. Figure adapted from (Gupta and Phulara, 2015).

1.1.5. Isoprenoid accumulation

1.1.5.1. Isoprenoid storage structures

The production of metabolites in plants is suggested to occur both continuously and on demand, as biochemical pathways are active over an extended period for developmental purposes or due to external triggers i.e. stresses (Hahlbrock et al., 2003; Morandini, 2013). For most primary metabolites a direct function can be found, or these compounds can be used directly in the maintenance or development of tissues. In the case of e.g. sugars, directly derived from photosynthesis, starch granules will be formed to store the sugars for later usage [reviewed by (Egea et al., 2010)]. Secondary metabolites, in their role towards plant protection, are often disruptive or toxic in high concentrations (Niinemets et al., 2013; Van Cutsem et al., 2011). Plants have developed inventive organelles and structures during evolution to allow accumulation of secondary metabolites without harming their own tissues. E.g. terpenoids involved in plant defences can be secreted into trichomes; trichomes are storage structures on the plant surface, in most cases the location where these compounds are required in the case of biotic stress (Xie et al., 2008). Similarly sterols, involved in plant microbe interactions, can be esterified with fatty acids (Halling and Slotte, 2004). Carotenoids on the other hand are required in the photosynthesis process, but their anti-oxidant function can disturb cellular processes by excessive scavenging of ROS. Therefore in plant plastids sequestration of carotenoids occurs in various types of storage sinks (Maass et al., 2009).

1.1.5.2. Plastid types

As the plastid contains a significant segment of the isoprenoid biosynthesis cluster, an insight of the plastid and how it adapts to the accumulation of isoprenoids in specific profiles is relevant. Plastids are former cyanobacteria which have been absorbed by plant cells and adapted into organelles [reviewed by (Gould et al., 2008)]. Therefore plastids still maintain their own genomic DNA, a significantly downgraded version of their former genome, from which proteins are derived. The plastid genome is commonly circularly mapped, but has been characterised as both circular and branched linear structures with many inverted repeats (Oldenburg and Bendich,

2004). Plastids are a common appearance in plant cells and tissues, and through differentiation can modify to specific roles required per tissue. An overview of plastid differentiation, with special attention for chloroplasts and chromoplast, is provided below. All plastid types known have their source as undifferentiated totipotent proplastids, which can differentiate into tissue specific plastids with distinct roles, and dedifferentiate in to the proplastid state (Allorent et al., 2013; Barsan et al., 2012). All plastid types maintain the same basic structure with two organelle membranes, stromules on the surface and their ancestral genomic DNA. Stromules are external plastid structures which are attached to the double membrane structure and can create tubular connections between plastid (Natesan et al., 2005). The major separation between plastid types found in "green" and "non-green" plastid types is strongly linked to the compounds and structures accumulated in the organelle (Figure 1-4). Green plastids can be either chloroplasts or chromoplasts which are respectively accumulating photosynthetic pigments (chlorophylls or carotenoids) in large quantities, whilst non-green plastids like amyloplasts or elaioplasts contain either high levels of starch or of sterols (Botté and Maréchal, 2013; Egea et al., 2010). These non-green plastids are grouped as leucoplasts, which allow for high levels of non-photosynthetic compounds or specific biosynthetic processes e.g. fatty acids (Natesan et al., 2005). Proplastids are considered non-green plastids as no photosynthetic compounds are present in these organelles. Etioplasts, the intermediates between proplastids and chloroplasts during the dark growth of seedlings, count as non-green plastids as well. The roles of each type of plastid described above are linked to specific tissues (Botté and Maréchal, 2013). Green vegetative tissues primarily contain chloroplasts with a high chlorophyll content captured in tightly stacked thylakoid membranes, which provide an efficient photosynthesis process. Chromoplasts, mainly functioning as carotenoids sequestration sites, generate coloured tissues e.g. flower petals, fruits and roots (Barsan et al., 2012). Other plastid types like amyloplasts contain large starch granules which are often found in storage organs like roots and tubers. Plastids are adaptable

to changes in the environment and can dedifferentiate if so required to differentiate into another plastid type [reviewed by (Gould et al., 2008)].

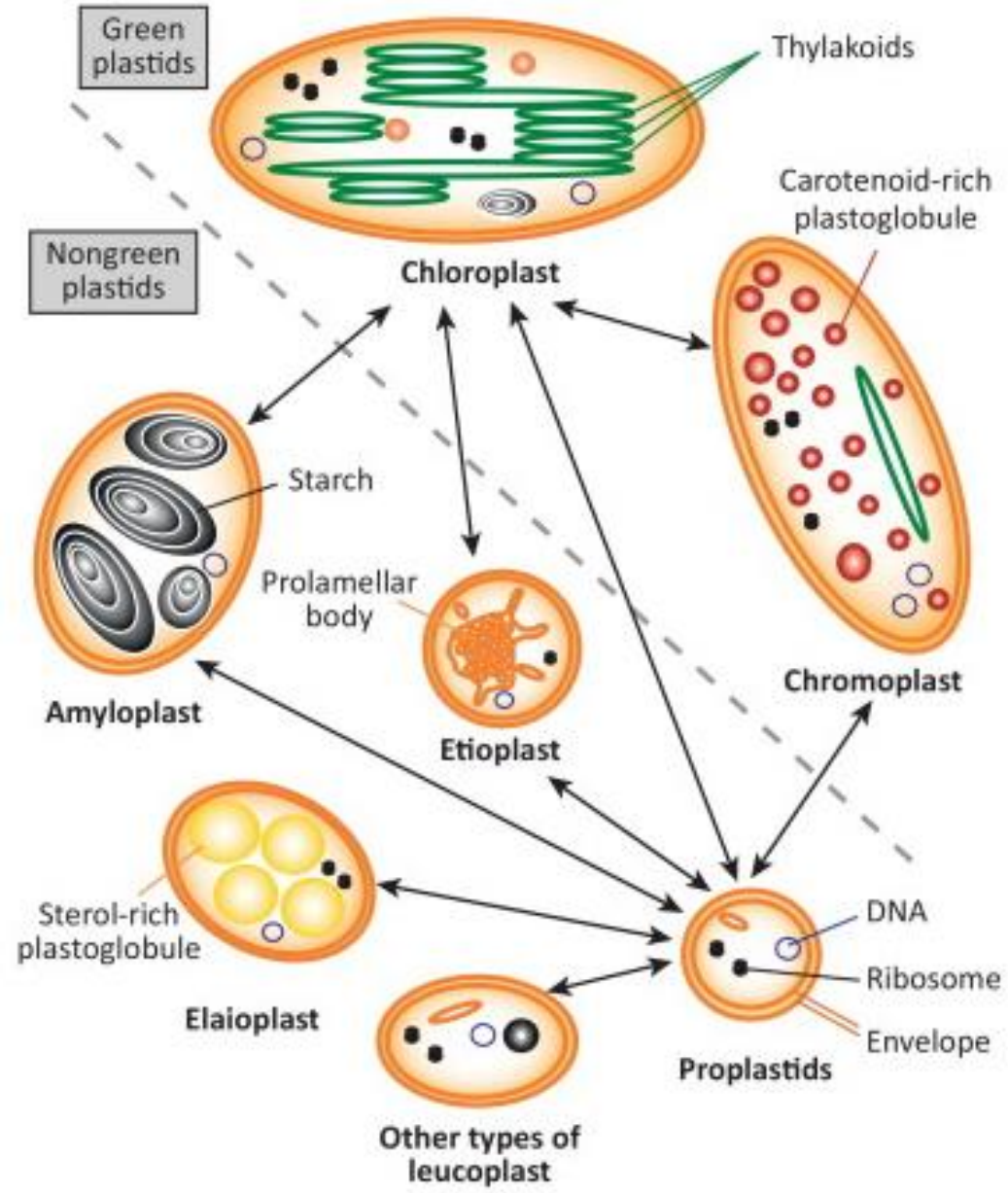

Figure 1-4. Plastid differentiation
An overview of the basic plastid and its various differentiated types. Plastid types are segregated between green and non-green tissues, arrows indicate differentiation potential. Proplastids are undifferentiated plastids which can differentiate into any type of plastid. Chloroplasts and chromoplasts are so-called green plastids and are common in vegetative tissues and fruits and flowers. Non-green plastids are leucoplasts like amyloplasts, elaioplasts or Etioplasts, which are commonly found in roots and tubers. Figure adapted from (Botté and Maréchal, 2013).

1.2. Carotenoids: biosynthesis and sequestration

1.2.1. Carotenoids

Carotenoids are C_{40}-compounds, generated from C_{20} geranylgeranyl pyrophosphate (GGPP) via phytoene synthase (PSY) - the first committed step of the carotenoid pathway in plants (Giuliano et al., 1993). Three enzymes, phytoene desaturase (PDS), *zeta*-carotene isomerase (Z-ISO) and *zeta*-carotene desaturase (ZDS), are responsible for the *cis*-configurations synthesising poly-*cis*-lycopene from phytoene via four intermediates, although the role of Z-ISO can be induced through light (Farré et al., 2011). All-*trans* lycopene is produced by carotene isomerase (CRT-ISO) from poly-*cis*-lycopene. Lycopene is a highly produced compound in carotenoid biosynthesis in tomato, and the molecule before branching of the pathway into a α-carotene branch leading to lutein and a β-carotene branch for xanthophylls (Fraser et al., 2009). Two enzymes are involved in the branching downstream of all-*trans* lycopene, lycopene cyclase-β (LCY-B) and lycopene cyclase-ε (LCY-E), reviewed by P.M.Bramley (Bramley, 2002; Fraser et al., 2009). These enzymes are proposed to act in complexes, bound to the membranes, in the plastids (Nogueira et al., 2013). Carotenoids are natural pigments, ranging from yellow to dark red, although intermediates phytoene and phytofluene are colourless carotenoids (Farré et al., 2011; von Oppen-Bezalel et al., 2015). An overview of the carotenoid biosynthesis pathway in plants, including associated pigment colours is provided in Figure 1-5.

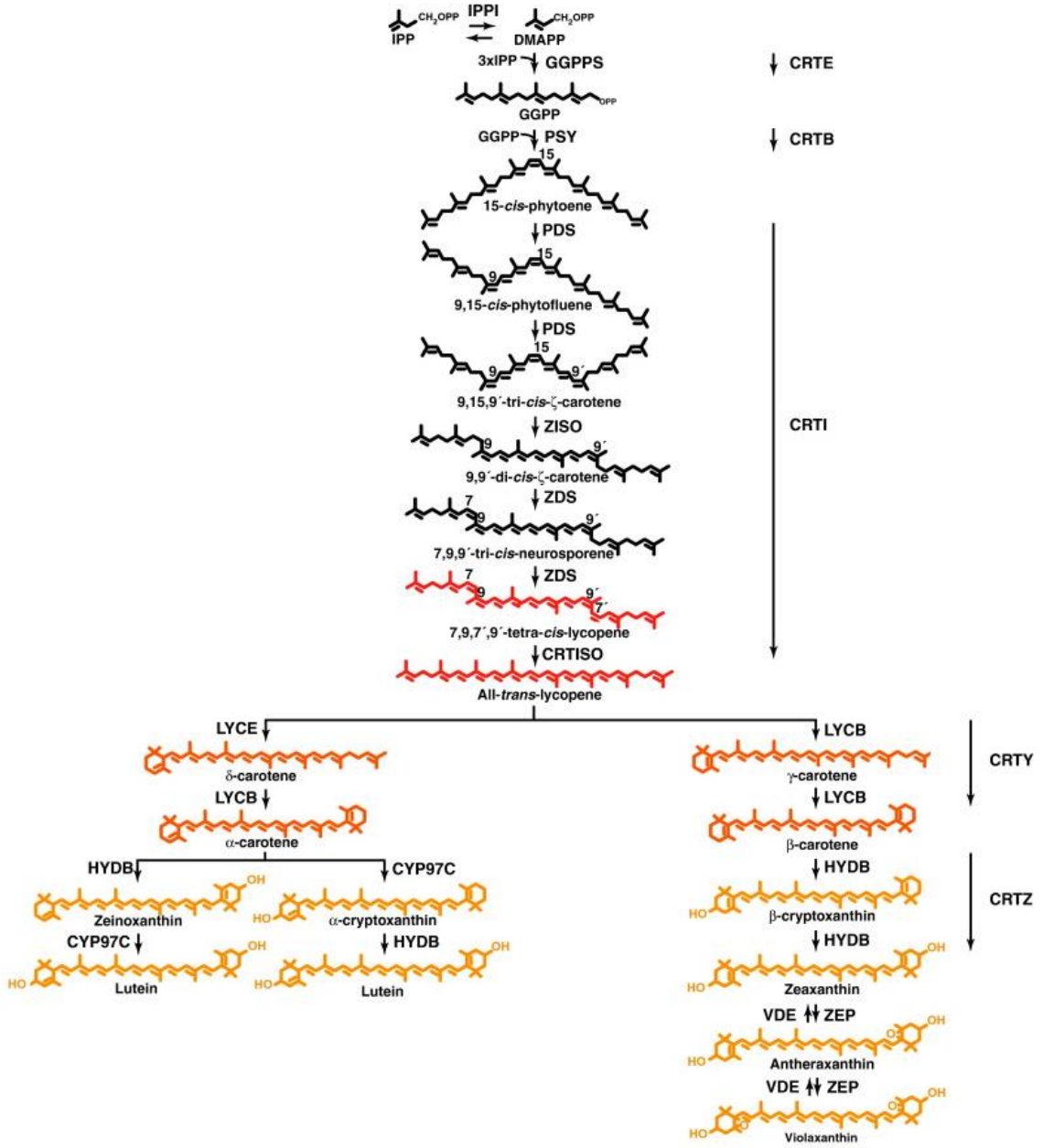

Figure 1-5. Carotenoid biosynthesis in higher plants.
Display of common plant carotenoids with their respective enzymes. Bacterial carotenoid enzymes with overlapping reaction roles are depicted on the right side. The carotenoid pathway starts with synthesis of phytoene out of two GGPP molecules, which through various steps of desaturation and isomerisation is adapted to all-*trans*-lycopene. Lycopene can undergo two different paths of cyclisation which in turn are adapted to xanthophylls such as lutein and violaxanthin. Colours of the carotenoid pigments are indicated in the structures. Figure adapted from (Farré et al., 2011)

1.2.2. Xanthophylls

Xanthophylls zeaxanthin, antheraxanthin, violaxanthin and neoxanthin are derived from β-carotene through a partly reversible enzymatic process in the xanthophyll cycle (Figure 1-6). The xanthophyll cycle is an important aspect of photo-protection through quenching of overexcited chlorophyll singlets and oxygen singlets (Bouvier et al., 2000; Jahns and Holzwarth, 2012). Under low light levels xanthophylls aid the efficient use of light energy, whilst in the situation of excess light xanthophylls dissipate the energy (Demmig-Adams and Adams, 1996b). The first enzyme β-carotene hydroxylase (HYBD) is responsible for the synthesis of β-cryptoxanthin and zeaxanthin. Zeaxanthin in turn is modified into violaxanthin via a zeaxanthin epoxidase (ZEP), a process that can be reversed by violaxanthin de-epoxidase (VDE) (Niyogi et al., 1998). From violaxanthin, neoxanthin can be generated through the neoxanthin synthase enzyme (Bouvier et al., 2000; Farré et al., 2011).

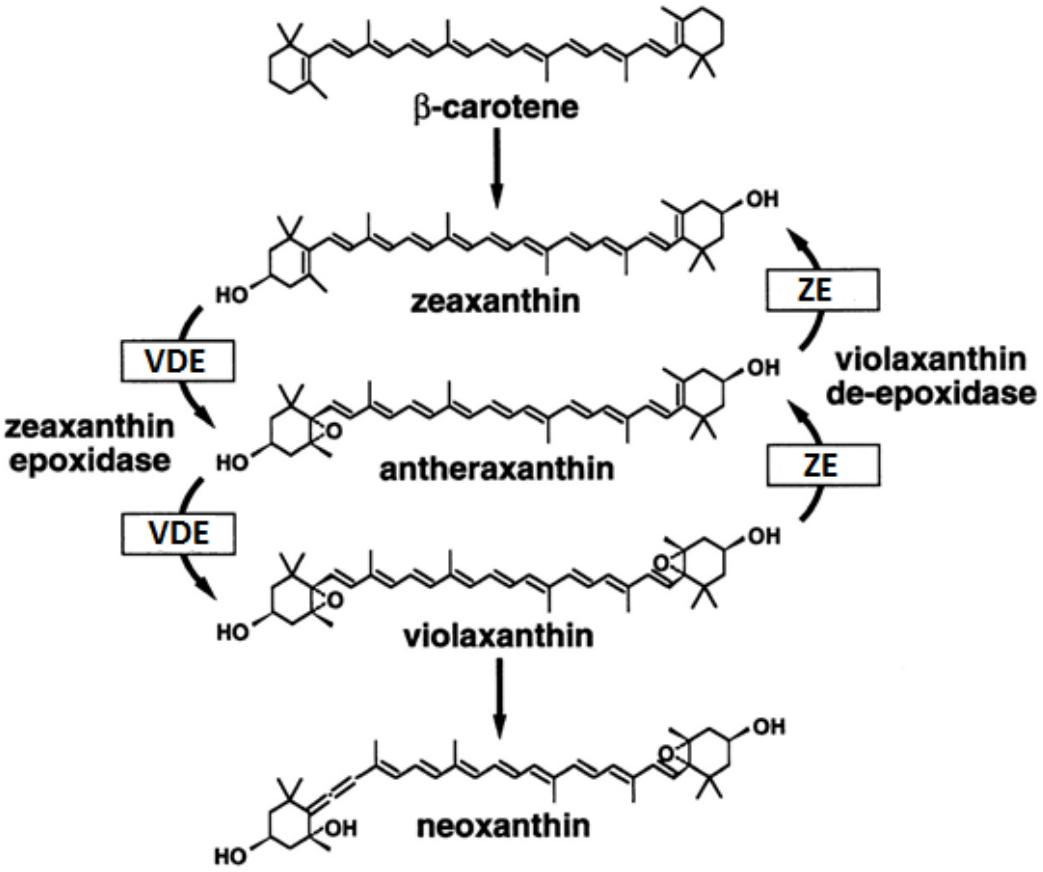

Figure 1-6. The xanthophyll cycle.
Violaxanthin de-epoxidase (VDE) and zeaxanthin epoxide (ZE) are the enzymes involved in the xanthophyll cycle, occurring in the membranes of the lumen. Zeaxanthin, antheraxanthin and violaxanthin are involved in the xanthophyll cycle whilst neoxanthin is the end-point of the xanthophyll pathway. Figure adapted from (Niyogi et al., 1998).

The enzyme HYBD is simultaneously involved in the α-carotene branch towards xanthophyll biosynthesis, more specifically lutein. In a two-step system complemented by a carotene e-ring hydroxylase (Farré et al., 2011). Lutein is another important photo protector in the light harvesting complexes through quenching of chlorophyll triplets, complementing the quenching of chlorophyll and oxygen singlets as regulated through the xanthophyll cycle (Dall'Osto et al., 2006; Jahns and Holzwarth, 2012).

1.2.3. Ketocarotenoids in bacteria

Carotenoid biosynthesis occurs in a wide range of organisms, and bacteria and fungi have a different setup for the pathway compared to plants and algae, reviewed by Fraser and Bramley (Fraser and Bramley, 2004; Nogueira et al., 2013). The biosynthesis of (keto)carotenoids in bacteria functions in a simplified manner, only seven enzymes are required for the biosynthesis from GGPP to the ketocarotenoid astaxanthin (Misawa and Shimada, 1998). Bacterial carotenoid genes can convert GGPP into all-*trans* lycopene via only two steps, a phytoene synthase (CRT-B) and a phytoene desaturase (CRT-I), a shorter track compared to the pathway present in plants (Ravanello et al., 2003). CRTY then functions as a lycopene cyclase towards β-carotene. The enzymes with compatible roles to the enzymes in the plant pathway are depicted in Figure 1-5. CRTZ (carotenoid hydroxylase) and CRTW (carotenoid ketolase) can perform an interactive set of modifications deriving astaxanthin from β-carotene via numerous intermediates (Misawa and Shimada, 1998). Especially the enzymatic activity of the ketolase, which add the keto-groups to the carotenoid molecules, adds a wide variety to the otherwise limited range of carotenoids as known in plants. The high value of ketocarotenoids in industry has led to a range of studies to integrate ketocarotenoid enzymes in plants. The transplastomic CRTZW in lettuce and transgenic CRTZW in potato are examples of the successful accumulation of ketocarotenoids, especially astaxanthin, in crop plants (Campbell et al., 2015; Harada et al., 2014). An overview of the reaction induced by CRTZ and CRTW is provided in Figure 1-7.

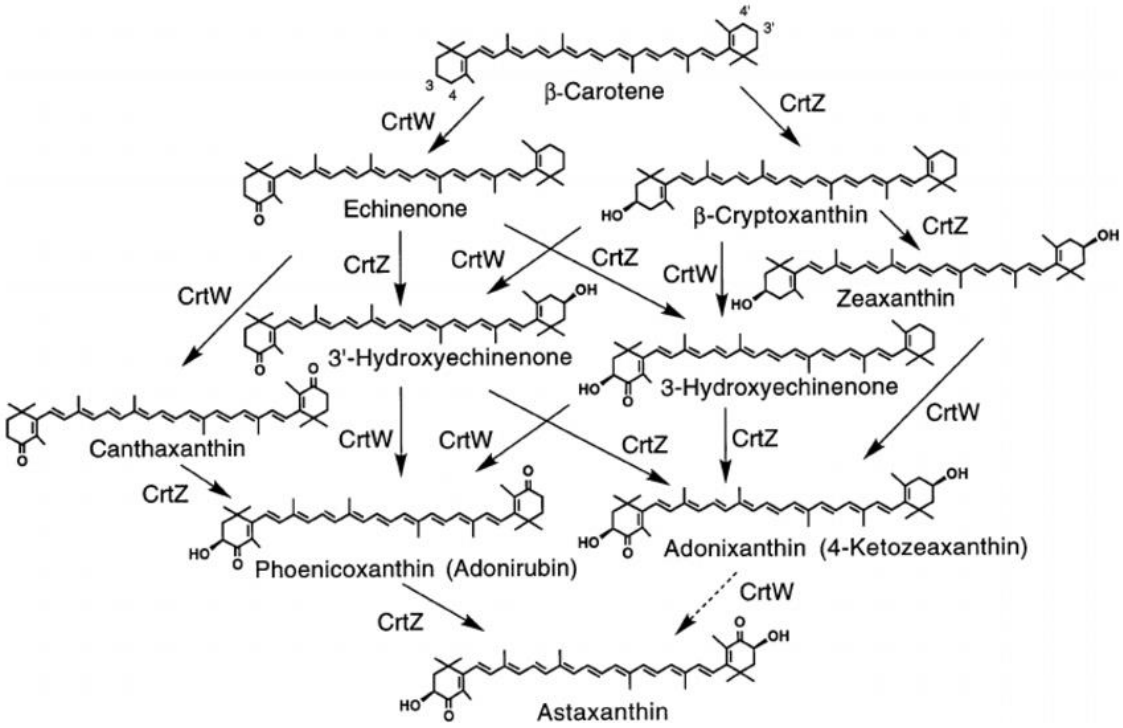

Figure 1-7. Ketocarotenoid biosynthesis.
Enzymatic steps performed by CRTZ (hydroxylase) and CRTW (ketolase) with β-carotene or derived products as substrates. Final compound of this interactive pathway is astaxanthin. Figure derived from (Misawa and Shimada, 1998).

1.2.4. Carotenoid sequestration

The localisation of carotenoids and their biosynthetic enzymes in the plastid has helped in the understanding of compartmentalisation of isoprenoids (Lichtenthaler et al., 1997; Rodríguez-Concepción and Boronat, 2002), which in turn has helped in the understanding of sequestration mechanisms for carotenoids in the plastid (Nogueira et al., 2013). The family tree of the tomato clade demonstrates a link between the sequestration of carotenoids and the increased production of coloured carotenoids, suggesting that green-fruited varieties of the *Solanum* clade lack a storage sink for carotenoids due to the absence of chromoplasts in the green fruit tissue. This theory provided the required evidence for the necessity of sequestration (Kilambi et al., 2014). The capacity of plastid membranes to stabilise and store carotenoids is linked to the regulation of carotenoid biosynthesis. A study by Nogueira et al. associates shifts in carotenoid patterns, obtained via mutant lines in the carotenoid pathway, with different models of sequestration in the plastid. (Nogueira et al., 2013). Various sequestration structures for carotenoids are described in literature which are not generally integrated in every carotenoid

accumulating species. The main sequestration structures are membrane crystalloids, crystals, plastoglobules, and fibrils. Chromoplasts in tomato mainly contain plastoglobules and membrane crystalloids (Harris and Spurr, 1969), whilst peppers (*Capsicum*) contain more fibrils (Deruère et al., 1994). Other plant species accumulating carotenoids, like carrot (*Daucus carota*), contain more free carotenoid crystals (Maass et al., 2009).

1.2.5. Plastid differentiation

1.2.5.1. Chloroplast

Plants rely on photosynthesis to sustain their energy supply, which takes place in the chloroplasts [reviewed by (Egea et al., 2010)]. Photosynthesis occurs in the chloroplasts where two photosystems process carbon dioxide and water into oxygen and sugars. In the thylakoid membranes, present in the chloroplasts, the photosynthetic activity takes place. A double layered membrane system with an outer and inner envelope membrane creates a large membrane surface on which photosynthetic activity occurs [reviewed by (López-Juez, 2007)]. In these membranes the chlorophylls and xanthophylls are involved in a complex energy balance with many redox-factors involved (Dall'Osto et al., 2006). Carotenoids can function as scavengers of ROS and photo-protectors, whereby carotenes function as anti-oxidants against ROS and xanthophylls can non-photochemical quench excited chlorophyll and oxygen singlets and chlorophyll triplets and are therefore very important in the protection of photosynthetic processes (Jahns and Holzwarth, 2012; Pogson et al., 1998). Chloroplasts consist primarily of the aforementioned thylakoids, although many other structures are present in the organelle (Figure 1-8). The sugar produced is stored as starch molecules in grain-like structures, and small plastoglobules are attached to the thylakoid membranes [reviewed by (Egea et al., 2010)].

1.2.5.2. Chromoplast

None of the plastid types can accumulate carotenoids at a level comparable to the chromoplast. As shown in Figure 1-4 chromoplasts can be generated from proplastids and chloroplasts, and therefore can occur in any tissue when a high carotenoid content is observed on site. Obvious examples for the range of tissues are tomato fruits, carrots (roots), and daffodil flower petals

(Beyer et al., 1989; Fraser et al., 2007; Rodriguez-Concepcion and Stange, 2013). The common example of chromoplast development is the differentiation from chloroplasts. Carrot root tissue does not develop chloroplasts underground, which shows the flexibility of the organelle in its (de-)differentiation process (Botté and Maréchal, 2013). Chromoplasts can contain a range of storage structures for carotenoids: plastoglobules, crystals, and membrane structures; the balance of these structures varies per tissue and species (Maass et al., 2009).

1.2.5.3. Chloroplast to chromoplast differentiation

Recent studies confirmed the development of chromoplasts from chloroplasts; proteomics and confocal microscopy studies demonstrated the differentiation process (Barsan et al., 2012; Kilambi et al., 2013). During this differentiation all photosynthetic structures, i.e. thylakoids and chlorophylls, are disintegrated and novel structures for the sequestration of carotenoids are assembled (Vishnevetsky et al., 1999). Accumulation of carotenoids in plastids occurs in various sequestration structures which are often species specific. Sequestration in tomato fruit commonly takes place in membrane integrated crystalloids (Harris and Spurr, 1969). Other structures normally sequestrating carotenoids are crystals, globules and fibrils. Found originally in cauliflower the Or-protein has been primary study case for its role in chromoplast development and the linked generation of a carotenoid deposition sink (Li et al., 2001). The OR gene does not have an effect on carotenoid biosynthesis and It is therefore assumed that OR is an important regulator of carotenoid sequestration through plastid differentiation (Zhou et al., 2015).

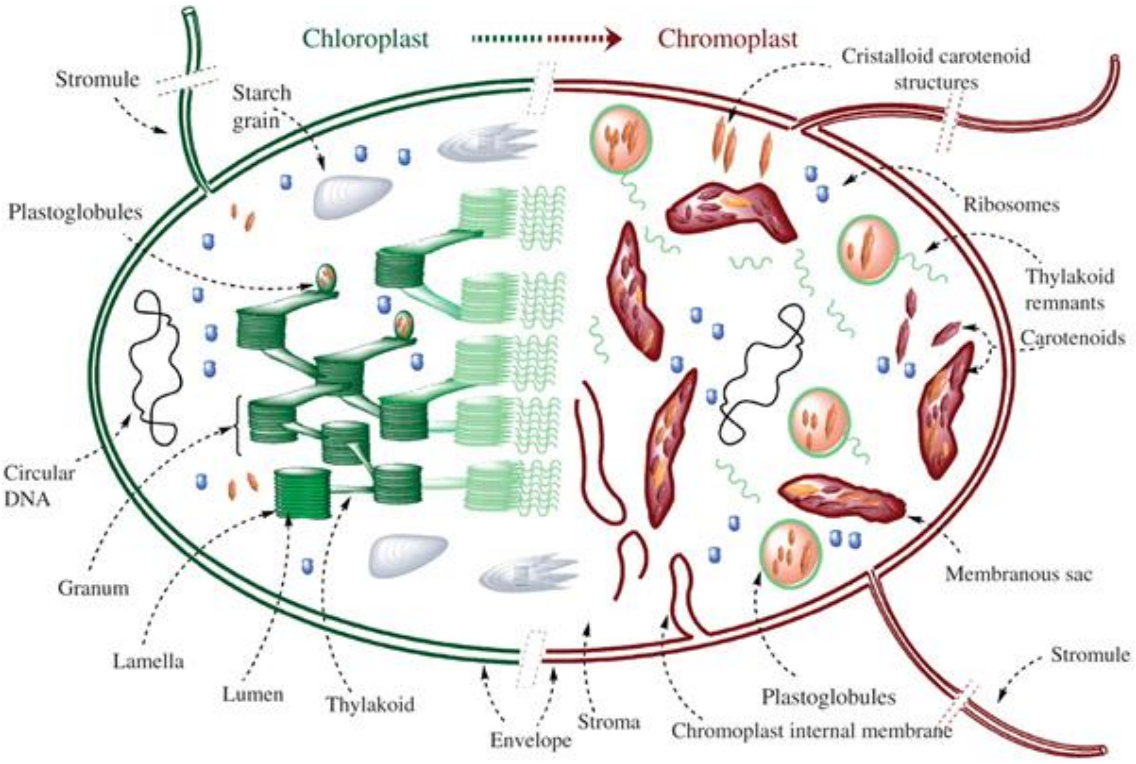

Figure 1-8. Chloroplast to chromoplast differentiation in tomato.
Main changes occurring during differentiation are the degradation of the thylakoid structures and starch, and the accumulation of sequestration structures like carotenoid crystals and crystalloid membranes. Plastoglobules are increasing in size during the differentiation, and are no longer attached to thylakoid structures. Figure adapted from (Egea et al., 2010).

1.3. Isoprenoid regulation and carotenoid functions in plants

1.3.1. Isoprenoid regulation in plants

In plants isoprenoids play a role in several developmental processes and other essential mechanisms. Carotenoids and tocopherols are scavengers of reactive oxygen species (ROS), which is a useful trait against UV-stress (Carretero-Paulet et al., 2006; Enfissi et al., 2005). Plant hormones like gibberellins and abscisic acid are involved in the growth of plants and their adaptation to stresses (Enfissi et al., 2005; Hsieh and Goodman, 2005). The activity of genes is determined *in vivo* by transcription factors, which themselves are activated through signals in the cells, tissues or the organism. Therefore, when looking at transcriptional regulation of isoprenoids and carotenoids in particular, looking beyond the transcription factor and investigating the signals is of interest. Stress-factors can be a trigger for modifications in transcription levels. Stress related hormones are involved in the upregulation of carotenoids, the same way some hormones can influence activity in the regulation of the MEP-pathway (Cordoba et al., 2009). Compounds of these pathways can have an effect on regulation as well. A study in tomato demonstrates that phytoene synthase and β-carotene hydroxylase activity at the breaker stage are associated with a strong increase in lycopene during ripening. Linking transcriptional regulation of these genes to metabolic levels clearly demonstrates the effect of regulation for these genes on carotenoid biosynthesis (Smita et al., 2013). With both the genes of the MEP pathway and the carotenoid pathway present in the plastids, linkage for these pathways has been proven. The many studies in which overexpression of MEP-pathway genes were linked to increased carotenoid content provided perhaps the best evidence. E.g. it has been shown that *hdr* expression levels rise during tomato fruit ripening and seedling de-etiolation in Arabidopsis (Botella-Pavía et al., 2004). A direct correlation between expression levels of *dxs* and *psy1* was found during fruit ripening in tomato, which suggests a coordinated impact in carotenoid regulation (Lois et al., 2000).

1.3.1.1. Regulation of the MEP pathway

A range of studies have been performed on the first two steps of the pathway DXS and DXR, both considered key regulatory steps of the pathway (Carretero-Paulet et al., 2006; Paetzold et al., 2010). The main aim of these studies has been to discover homologs of these enzymes in different plants. Next to sequence comparisons and expression levels, another focus was to reveal the system of regulation for these enzymes through feedback loops. For example: the functional analysis of DXS and DXR in *Amomum villosum Lour, w*hich suggested a more specific role in isoprenoid biosynthesis for DXR (Yang et al., 2012). Expression profiling of *dxr* in *Campotheca acuminate* demonstrated an elicitor-based expression system induced by the plant hormone jasmonate (Yao et al., 2008). Where these enzymes are considered the rate limiting factors among the enzymes within the pathway, the abundance and activity of these enzymes can be modified by various factors. Abscisic acid (ABA) is a cleavage product of the carotenoid pathway primarily derived from the xanthophyll zeaxanthin [reviewed by (Nambara and Marion-Poll, 2005)]. ABA induces up regulation of five MEP-genes (*dxr, mct, cmk, hds, hdr*) in hairy roots of *Rauvolfia verticillata* (Chang et al., 2014). PIF5, a phytochrome-interaction factor (PIF), can be linked to the positive regulation of the MEP-pathway. When tested in cell suspensions the increased activity of the PIF5 enzyme induced enhanced levels of chlorophylls and carotenoids, the effector of this increase is suggested to be enhanced IPP/DMAPP biosynthesis (Mannen et al., 2014). The regulation through PIFs is light induced as demonstrated in both Arabidopsis and Tomato fruit; PIFs modulate the photoreception of tissues via regulation of the light absorption, this has been directly linked to the regulation of carotenoid biosynthesis (Leivar et al., 2008; Llorente et al., 2016; Toledo-Ortiz et al., 2014). The example of the ABA feedback response described above is a trigger for enhanced gene expression. Once a gene has been transcribed, a few steps still separate it from being a functional or active protein. Several regulatory factors can play a role post-transcriptionally. In the MEP-pathway for example, DXS is regulated via feedback inhibition through IPP and DMAPP. Both IPP and DMAPP are able to bind to the enzyme in a similar manner as thiamine phosphate. Thiamine phosphate is a cofactor involved in the

catalysis of this enzyme's reaction (Banerjee et al., 2013). For both the MEP and carotenoid pathway post-transcriptional regulators are reported, suggesting that there is further regulation of the flux of precursors of the MEP pathway towards the carotenoid pathway.

1.3.1.2. Regulation of the carotenoid pathway

OR proteins found in higher plants are major post-transcriptional regulators of PSY in carotenoid biosynthesis through adaption of the carotenoid sequestration sinks; OR proteins regulate the differentiation of chromoplast development, the plastid type for optimised carotenoid storage (Li et al., 2001; Zhou et al., 2015). A strong correlation between OR-protein levels and PSY-protein levels is found in Arabidopsis, interaction of the OR protein with the PSY enzymes causes a higher percentage of active enzymes which directly affect the rate of carotenoid biosynthesis (Zhou et al., 2015). A similar correlation is found for ZDS, an enzyme involved in carotenoid biosynthesis, a knockout of ZDS showed reduced carotenoid content. The reduction in carotenoid content was linked to downregulation of various genes, which suggests carotenoids might be involved in retrograde signalling (Haili et al., 2007). Retrograde signalling is conceptualised as signals from sub-cellular organelles, plastids or mitochondria, to the nucleus were nuclear gene expression is modulated (Leister, 2012). Storage of carotenoids in membrane structures (sequestration) can enhance production by avoiding signals to the regulatory mechanisms. ZDS-mutants are supposed to have an effect on leaf development, which, similarly to the hypothesis of Haili et al., could suggest that carotenoids have regulatory functions (Avendaño-Vázquez et al., 2014). This correlation is present at the metabolite level as well as at the protein level, as demonstrated by a higher carotenoid content when PSY-levels are higher under the influence of OR (Zhou et al., 2015). An important element in feedback regulation is the availability of the compound that can trigger these processes. Sequestration of carotenoids can impact the regulation of carotenoid biosynthesis; therefore storage or sequestration of carotenoid needs to be studied simultaneously with regulation of biosynthesis. The capacity of plastid membranes to stabilise and store carotenoids is linked to the regulation of carotenoid

biosynthesis, especially in the chromoplasts, plastids with a large storage capacity for carotenoids [reviewed by (Egea et al., 2010)]. A study by Nogueira et al. 2013 associates shifts in carotenoid patterns, obtained via mutant lines in the carotenoid pathway, with different models of sequestration in the plastid. The models suggested increased sequestration capacity for the carotenoids accumulated at higher levels (Nogueira et al., 2013). In the complex system of isoprenoid regulation another relevant factor is the segregation between green and non-green tissues. In tomato, homologous genes exist for the tissue specific regulation of isoprenoids like carotenoids, as demonstrated by the genes for phytoene synthase 1 and 2 (*psy1* & *psy2*) among others. It is reported that *psy1* is active in the flowers and fruits and not in the leaves and stems of tomato plants, and *psy1* knock-out mutants cannot be compensated by *psy2* (Fray and Grierson, 1993). Similar outcomes have been observed for paralogous precursor genes *dxs*, *idi*, and *ggpps*, for which different expression patterns were found between tissue types in *Z. mays* (Vallabhaneni and Wurtzel, 2009).

1.3.1.3. Isoprenoid related stress regulation

Stress responses are strongly linked to the accumulation and release of secondary metabolites. Abiotic stress such as photobleaching, heat and cold stress, require metabolites to overcome these external impacts (Mahajan and Tuteja, 2005). Salt tolerant tomato varieties maintain a higher steady state jasmonate content, compared to salt sensitive varieties (Pedranzani et al., 2003). Hot climates often cause reduction of process efficiency in plants, which can cause a drop in secondary metabolites like carotenoids and anthocyanins (Chan et al., 2010b; Morison and Lawlor, 1999). Light intensity can trigger the activity of secondary metabolites production as compounds like xanthophylls can aid in photoquenching (Bino et al., 2005; Demmig-Adams and Adams, 1996a). Proline levels increase up to 10-fold in salt tolerant *Medicago sativa* (Petrusa and Winicov, 1997). Increased anthocyanin content can be observed in various species under the influence of various abiotic stresses, including salt, drought, cold, and metal stress (Chalker-Scott, 1999; Chan et al., 2010b; Christie et al., 1994). Other compounds which are increased by

cold stress are sugars, sugar alcohols, flavonoids, phenolics and jasmonates (Janská et al., 2010; Pedranzani et al., 2007). Biotic stresses like pathogens or herbivores can be fought off through toxic compounds or bad tasting aromas. Indirect defence mechanisms can be induced through attraction of e.g. predators in the case of herbivores, often terpenoids volatiles (Takabayashi et al., 1994). Terpenoid indole alkaloids are triggered in biotic stress responses through the ERF-transcription factor, which is involved in most stress related signalling cascades (Singh et al., 2002). An expression study in Arabidopsis demonstrated the increased gene expression of various genes of the p450 cytochrome superfamily during biotic stresses like fungal infections and mechanical wounding, suggesting the effect of terpenoids in plant defence (Narusaka et al., 2004). Processes in the plastids are tightly regulated by the nucleus. A suggestion for this level of control is the communication between the plastids and the nucleus, a process known as retrograde signalling (Chan et al., 2010a). The synthesis of carotenoids and the activity of the MEP-pathway is suggested to be linked to this process. A retrograde model for the MEP-intermediate MEcPP has recently been proposed, modifying epigenetic structures in the nucleus (Xiao et al., 2012). The fifth intermediate of the MEP-pathway, methylerythritol cyclodiphosphate (MEcPP), functions as a trigger for retrograde signalling for the expression of selected stress-responsive nuclear-encoded plastidial proteins, which is suggested to work as an epigenetic system. MEcPP itself or another factor induced via a signalling cascade could induce the switch from heterochromatin to euchromatin allowing for transcription in the opened chromatin structure. While there is no proof the compound actually moves to the nucleus when it is highly accumulated, correlation between increased synthesis of MEcPP and gene-expression of these stress-responsive genes is found (Xiao et al., 2012). Other reports mention alternative systems having an impact on protein folding in the endoplasmic reticulum or activation of a stress response transcription factor called CAMTA3 (Benn et al., 2016; Walley et al., 2015). Responses as described above can be linked to the triggers caused by ZDS inhibition, proposed as a carotenoid retrograde signal (Haili et al., 2007).

1.3.2. Role of carotenoids in plant

Over 600 carotenoids are found in nature, reviewed by Fraser and Bramley, Approximately 60 of those carotenoids are found in higher plants; other sources of carotenoids like various marine bacteria, *Erwinia* species, and fungi provide the extended range (Fraser and Bramley, 2004; Visser et al., 2003). Keto-carotenoids are a class of carotenoids not commonly present in higher plants, although the accumulation of astaxanthin has been observed in flowers of *Adonis genus* (Cunningham and Gantt, 2011). Carotenoids, carotenes and xanthophylls, can function as ROS scavengers, aid in photo-reception and photo-protection, and function as membrane-stabilisers. As carotenoid can be sequestered in various structures including the membrane structures, it can affect the membrane characteristics (McNulty et al., 2007),[reviewed by (Ruiz-Sola and Rodríguez-Concepción, 2012)].

1.3.2.1. Photo protection and ROS scavenging in the photosystem complex

Plants use carotenoids in various processes, of which most are present in the plastid. Carotenoid-derived compounds or signals can be found in other regions of the cell. In the plastid the carotenoids are involved in photosynthesis in two different ways. Carotenoids cover the area of the light spectrum which is not efficiently absorbed by chlorophyll, improving the efficiency of the photosynthetic systems in the plastid (Park et al., 2002). While involved in the improvement of photosynthesis carotenoids function as photo protectors against light as well. Carotenoids can protect plant tissues as antioxidants against reactive oxygen species or by maintaining the electron balance during the various processes ongoing in the cell. Therefore carotenoids are important in the balance of light absorbance, as light is required for the plants maintenance and development but excess light causes damage (Horton and Ruban, 2005; Müller et al., 2001). Next to light, other environmental stresses causing ROS molecules can be counteracted (Demmig-Adams and Adams, 2002). Xanthophylls are the main carotenoids involved in the photosystems; two independent xanthophyll branches aid the systems with photo protection. Both the α-carotene- and β-carotene-derived xanthophylls, lutein and violaxanthin, respectively function in a xanthophyll cycle to quench chlorophyll triplets and

chlorophyll and oxygen singlets (Dall'Osto et al., 2006; Jahns and Holzwarth, 2012; Niyogi et al., 1998).

1.3.2.2. Attraction of pollinators and seed dispersers

In their role as pigments, carotenoids are responsible for the yellow to red colour spectrum in plants, which is used for the attraction of pollinators to flowers or for the dispersers of seeds for seeds and fruits (Park et al., 2002). Furthermore, carotenoids, when cleaved into apo-carotenoids, are involved in the production of growth regulators like abscisic acid and strigolactones [reviewed by Nambara and Marion-Poll] (Nambara and Marion-Poll, 2005; Rodríguez-Villalón et al., 2009; Van Norman and Sieburth, 2007). Fragrant volatiles and bright colours can attract various types of animal that utilise plant material - predominantly flowers and fruits - and therefore indirectly generate pollination activity or seed dispersal. Flower volatiles in the wild tobacco species *N.attenuata* demonstrated a clear effect of pollinator visits and length of nectaring (Kessler and Baldwin, 2007). Several hypotheses exist for the accumulation of secondary metabolites like carotenoids in fleshy fruit tissues related to attraction and seed dispersal, including i.e. inhibition of germination during the digestion process (M.L.Cipollini and D.J.Levey, 1997). Carotenoids, as e.g. in tomato fruit, are responsible for both colour and scent for the attraction of pollinators and seed dispersers (Howitt and Pogson, 2006).

1.4. Applications of carotenoids in health and industry

1.4.1. Carotenoids in health

1.4.1.1. Health promoting compounds in Tomato

The interest towards isoprenoids goes beyond the scientific studies focussed on plant processes, many applications in nutrients, pharmaceuticals or colourants, are based on or derived from isoprenoid sources. Carotenoids are known to have an alleviating effect on age-related diseases like cancer and macular degeneration, reviewed by Fraser and Bramley (Enfissi et al., 2005; Fraser and Bramley, 2004). Phytosterols can reduce cholesterol levels (Halling and Slotte, 2004). The impact of anthocyanins on health through their role as antioxidant and other roles such as inhibiting high glucose levels can prevent symptoms of diabetes or reduction of lipid biosynthesis in the liver during the onset of obesity (Tsuda, 2012). Accumulation of anthocyanins in tomatoes is not commonly as high as in berry varieties such as blackcurrants and blueberries, but various reports demonstrate enrichment of tomato varieties with anthocyanins through expression of anthocyanin specific transcription factors (Bovy et al., 2002; Butelli et al., 2008; Gonzali et al., 2009). Vitamin C (ascorbic acid) and E (tocopherols) are present in tomato in sufficient amounts to have a beneficial impact on health, mainly achieved through their antioxidant functions (Frusciante et al., 2007; George et al., 2004).

1.4.1.2. Preventive health benefits of carotenoids

A variety of carotenoids function as antioxidants. Since oxidation of various structures in the human body - lipids, nucleotides and proteins - can lead to chronic diseases like cardiovascular diseases, cancer, or age-related degeneration, these compounds working against oxidation are valuable heath benefactors [reviewed by (Mayne, 2003)]. Lycopene has been correlated with a reduced risk of prostate cancer (Giovannucci et al., 2002). Both β-carotene and α-carotene have been proven to have an inverse association with coronary artery disease (CAD) and the development of opacities in lenses in the eye (Osganian et al., 2003; Taylor et al., 2002). Not all carotenoids have a significant effect against those diseases; lutein and zeaxanthin do not help against CAD (Osganian et al., 2003). Besides β-carotene and α-carotene only total carotenoid

intake helps against opacities (Taylor et al., 2002). A range of carotenoids, including zeaxanthin, β-carotene, astaxanthin and lycopene, have a suppressing effect on antigen induced mast cell degranulation. Mast cell degranulation is linked with inflammations occurring during allergic responses, carotenoids can inhibit the degranulation and therefore reduce allergic responses (Manabe et al., 2014). Lipid peroxidation of membranes can be affected by the integration of carotenoids. Apolar carotenoids like lycopene and β-carotene proved to have a pro-oxidant effect, while for example astaxanthin has an anti-oxidant effect as well as preserving membrane structures. The way these compounds affect the membranes can explain the beneficial effect on health they might generate (McNulty et al., 2007).

1.4.1.3. Nutritional value of carotenoids

The nutritional value of carotenoids for human health has been extensively studied. The best known example is the pro-vitamin A activity of β-carotene. The structure of β-carotene represents two retinol compounds, which when absorbed in the body can be cleaved into two retinol compounds via an oxygenase step [review by (Fraser and Bramley, 2004)]. Since vitamin A deficiency is a problem in third-world areas, induction of pro-vitamin A production in rice has been studied (Beyer et al., 2002). Although studies have not been conclusive on the full range of effects of β-carotene, both positive and negative, the advised daily intake is currently set to 4.8mg (Engel and Wyss, 2010). 4.8mg daily would relate to the relative intake of ~800µg of vitamin A, this advice is especially useful for countries where vitamin A deficiencies are common (Engel and Wyss, 2010). A break-through in carotenoid enhanced products is the development of Golden Rice to combat the vitamin A deficiency in third world countries. The positive influence of poly-unsaturated fatty acids from marine fishes and seafood has been known to man for a long time. The combination of carotenoids like astaxanthin and Omega-3 fatty acids proved to be viable for the sustainability of cognitive capacities and can inhibit processes related to neuro-degeneration (Barros et al., 2014).

1.4.2. Carotenoids in industry

1.4.2.1. Carotenoids in food

Humans have been using a large range of natural products to sustain themselves through history, most of these products are directly or indirectly plant derived. Whether flowers have been used for their aroma or colour, or herbs for their medicinal properties, humanity has utilised the wide variety of metabolic compounds to improve their health and enhance their ways of life. The use of carotenoids and anthocyanins as vitamins (pro-vitamin A) and antioxidants, is advised to be integrated in diets world-wide. To improve vitamin intake in countries with insufficient carotenoids in their diets, Golden rice was developed; β-carotene levels have been enhanced in rice via transgenic systems to reduce vitamin A deficiency in third-world countries. A successful insertion of carotenoid biosynthesis genes has been accomplished, and orange endosperm, due to β-carotene, has been achieved (Beyer et al., 2002; Tsuda, 2012). The initial development of Golden rice was a proof of concept with total carotenoid accumulation of ~1.6µg/g, optimised rice mutant lines (Golden Rice 2.0) demonstrate higher levels of total carotenoid at ~37µg/g (Beyer et al., 2002; Paine et al., 2005; Ye et al., 2000). Therefore 100g of Golden Rice 2.0 would approximately fulfil the recommended daily intake of β-carotene. Carotenoids, derived from flowers or fruits, are used for their colour in food, feed and dyes [reviewed by Fraser and Bramley] (Fraser and Bramley, 2004; Noviendri et al., 2011).

1.4.2.2. Carotenoids in feed

The colourful range displayed during carotenoid biosynthesis allows for the use of these compounds as food pigments. This purpose is perhaps best described by the ketocarotenoid astaxanthin, which is used to add colour to the flesh of e.g. salmon and trout, when integrated into fish feed (Kumar et al., 2012). Ketocarotenoids, for example used in the production of fish feed, can be chemically synthesised. Genetic engineering of various crops demonstrates the possibility of utilising plant sources for the production of keto-carotenoids (Campbell et al., 2015; Huang et al., 2013). A recent study in trout demonstrates the use of powdered tomato fruit from GMO lines producing keto-carotenoids (3mg/g DW), mixing this powder with fish feed

resulted in fish fillets enriched with keto-carotenoids at ~40µg/g DW (Nogueira et al., 2017). Dietary supplementation of poultry with carotenoids enhances pigment levels in egg yolk. Studies have been successfully performed with different carotenoids e.g. lutein, lycopene, β-carotene and zeaxanthin, which increased carotenoid content in sampled egg yolks (Handelman et al., 1999; Karadas et al., 2006).

1.4.2.3. Cosmetics

The developments in industrial chemistry have led to a large set of compounds that can be chemically synthesised, although these processes are expensive. Current developments are returning to the original plant sources and aim to enhance or transfer biochemical pathway to high biomass sources and model crops. Colourless carotenoids for example, extracted from a tomato variety high in phytoene and phytofluene, demonstrate a positive effect on skin health under exposure to sunlight (von Oppen-Bezalel et al., 2015). Other sources of carotenoids are being used in the cosmetic industry. Algae are presented as a novel source of carotenoids to be used as vitamin supplements for health and cosmetic purposes (Del Campo et al., 2007).

1.4.2.4. Industrial production of carotenoids

Feed supplements astaxanthin and canthaxanthin are estimated to represent approximately 20% of total aquaculture costs for salmon, trout and shrimp industry (Lorenz and Cysewski, 2000). A wide range of algae produce ketocarotenoids, but not many have been targeted for industrial processing. Algae species *Haematococcus pluvialis* is used commercially for the production of astaxanthin (1.5-3% of DW), but its slow growth with its need for high intensity sunlight make it costly to produce these compound (Yuan and Chen, 2000). The yeast *Xanthophyllomyces dendrorhous* is an alternative source of astaxanthin, but the synthesis is occurring at lower rates than in *Haematococcus pluvialis* at only 0.4% of its DW (Christiansen et al., 1995). Natural sources alone are not sufficient to cover the demand of astaxanthin for e.g. the aquaculture industry. To meet the demand for ketocarotenoids i.e. astaxanthin, industrial production uses total chemical synthesis of compounds such as astaxanthin (Jackson et al.,

2008). Starting materials are often petroleum or petrochemical based substrates. The products of the two industrial producers of synthetic astaxanthin, BASF and DSM, are marketed as Carophyll® Pink and Lucantin® Pink respectively. The chemical synthesis of carotenoids leads to a mixture of the compounds of interest and by-products of the process, and furthermore, the produced carotenoids are mixtures of racemic isomers. This method of manufacturing is still covering 95% of the total astaxanthin on the market, due to the significant difference in production cost between chemically synthesised ($2000/kg) and natural synthesised ($7000/kg) (LE Frucht and S Kanon, 2005). Novel natural sources of ketocarotenoids have been developed in recent years; Higher plant species, tomato and mais, have been genetically modified to produced ketocarotenoids in fruit (3mg/g DW) and kernels (~10µg/g) for integration in feed (Moreno et al., 2016; Nogueira et al., 2017). Colourless carotenes, important compounds in cosmetic products to protect skin damage, are in high demand in the cosmetic industry due to their application in diverse formulations (von Oppen-Bezalel, 2007). Sources of colourless carotenes, such as phytoene and phytofluene, are not common in nature, therefore the current source for these compounds is chemically treated algal cultures (von Oppen-Bezalel et al., 2006). Given the difficult growing conditions for algal systems and the isomeric issues of chemical synthesis, attempts towards renewable sources are being investigated. For these attempts to be successful, the application of genetic modifications is required in most cases (Mann et al., 2000), [reviewed by (Schmidt et al., 2011)].

1.5. Genetic engineering and model plants

1.5.1. Genetic engineering of isoprenoids

1.5.1.1. Overexpression of MEP pathway genes

A recent study in Arabidopsis compared the impact of all individual genes of both the MVA and MEP pathway on isoprenoid biosynthesis. Overexpression of these genes and linked gene-to-metabolism integration led to the conclusion that only HMGR for the MVA-pathway and DXR and MDS for the MEP-pathway are to be considered key regulators (Lange et al., 2015). DXS was not found to be a key regulator of the MEP pathway. Although the characterisation and overexpression of a range of *dxs* genes makes the role of DXS on isoprenoid regulation difficult to exclude (Battilana et al., 2011; Enfissi et al., 2005; Kudoh et al., 2014; Yang et al., 2012). Various attempts towards enhancements of the isoprenoid precursor flux or specific isoprenoids have been performed, during these attempts key regulatory steps have been found and utilised. The overexpression of *dxs* and *hmgr* in tomato led to enhanced levels of carotenoid and sterol content respectively (Enfissi et al., 2005). Whilst overexpression of *hmgs* resulted in an increase of downstream isoprenoid products, this was matched with an increased expression level of *hmgr* (Wang et al., 2012). Overexpression of *dxr* in *Camptotheca acuminata* showed similar effects on carotenoids and chlorophylls compared to *dxs*, combined with negative effects on the plants chloroplast development when *dxr* was down-regulated (Avendaño-Vázquez et al., 2014; Yao et al., 2008). Different from the *hmgs* overexpression construct, *dxr* did not result in increased expression levels of *dxs*, excluding the option of compensational regulation (Carretero-Paulet et al., 2006). The elucidation of key steps in the MEP pathway can be extended and linked to the regulation of downstream pathway elements such as the carotenoid pathway. Interaction between DXS and PSY1, first committed steps of the MEP and the carotenoid pathway respectively, demonstrates that the presence of PSY1 enzymes can only be fully utilised when DXS aids the synthesis of sufficient precursors for GGPP as the building block for carotenoids (Lois et al., 2000).

1.5.1.2. Overexpression of key genes in the carotenoid pathway

The effects of gene expression and metabolic engineering have been studied in carotenoid biosynthesis. For example, downregulation of phytoene synthase in tomato results in a yellow phenotype in fruits due to a lack of carotenoid biosynthesis (Kang et al., 2014). The aforementioned result is similar to the results described for the *psy1* knock-out in tomato (Fray and Grierson, 1993). Later studies demonstrated the positive impact of constitutive expression of *psy1* on carotenoid content (Fraser et al., 2007). An interesting experiment conducted was the construction of a homologous carotenoid pathway in rice endosperm for the accumulation of β-carotene, in which three vectors containing transcriptional units (TUs) for *psy1*, *crtI* and *lcy-b* were successfully transformed, a novelty result since rice endosperm is normally carotenoid free (Ye et al., 2000). Other studies utilising bacterial carotenoid genes such as *crtB* and *crtI* had similar successes. Seed specific expression of *crtB* from *Erwinia uredovora* in *Brassica napus* led to a 50-fold increase of carotenoids in the seeds (Shewmaker et al., 1999). Extended upon this research, seed specific expression of *crtB* was studied in combination with seed specific expression of *crtE* and *crtI*, which lead to further increased carotenoid levels. The triple construct led to a significant change in the profile with a ratio increase for β-carotene (Ravanello et al., 2003). In tomato fruit specifically expressed *crtE* and *crtB* and constitutively expressed *crtI* were crossed and screened for interesting phenotypes, focussing on carotenoid content. Significant increases in carotenoid content were found for CRTI, independently or crossed with CRTE or CRTB, as well as interesting changes in carotenoid sequestration (Nogueira et al., 2013).

1.5.1.3. Synthetic and Systems Biology

In recent years, the progress in synthetic biology and its methodologies has been significant. The development of systems utilising type IIs restriction enzymes to allow for the construction of large multi-gene constructs has proven helpful. The idea to design and use genetic elements as parts that can be assembled as one would build a machine required standardisation of common elements utilised in molecular biology. In micro-organisms the BioBrick system was the first application of a standardised system for synthetic biology (Knight, 2003). Current methods for

the modular assembly of DNA fragments are the Golden Gate and MoClo methods, which are overlapping in design and compatibility (Engler et al., 2008; Weber et al., 2011). Where the Golden Gate cloning method's prime quality is its flexibility, Gibson Cloning is designed for more complex single reaction assemblies (Engler et al., 2008; Gibson et al., 2009). The Golden Gate method after an update allows for easy shuffling of modular parts within a single reaction (Engler et al., 2009). Both Golden Gate and Gibson cloning were initially designed for microbial and biomedical studies in fungi, rat embryonic cells, and yeast, and were adapted to plant systems later (Gibson et al., 2008; Terfrüchte et al., 2014; Tong et al., 2012). A synthetic biology technique for plant biotechnology was developed using the same concept as the Golden Gate methods; the Golden Braid (GB) method uses a scar-benign method consisting of four vectors, allowing for endless linkage of parts until the size of the vector interferes with the effectivity (Sarrion-Perdigones et al., 2011). GB cloning has gone through various updates and extensions, as the addition of an entry vector (GB2.0), utilising the method for CRISPR/cas9, and a generic update to GB3.0 (Sarrion-Perdigones et al., 2013; Vazquez-Vilar et al., 2016).

1.5.2. Model plants for metabolic engineering

1.5.2.1. Tomato (Solanum lycopersicum)

Tomato is considered to be the most important fruit worldwide. Since its domestication in South America it has been bred to optimise quality traits like growth, productivity, fruit quality and disease resistance. Tomato has become a model plant for plant biotechnology because of its interesting features (Canene-Adams et al., 2005) e.g. fleshy fruit, sympodial shoots and compound leaves. Research performed in tomato can be extrapolated to other species within the *Solanaceae* family, for example potato, pepper and tobacco (Kimura and Sinha, 2008). With the sequence of the tomato genome available, its position as major model plant is becoming stronger (The Tomato Genome Consortium, 2012). Over the duration of the tomato genome sequencing project it has been predicted that tomato can become a model for plant pathogen interaction, one of the key aspects that affect tomato crop efficiency (Arie et al., 2007). Ailsa Craig, together with the miniature variety MicroTom, is considered one of the staple crop of

plant molecular biology especially on the aspect of fruit biology (Giovannoni, 2007). Tomato is ideally suited for fruit biology studies as the broad variety of wild species can be used to elucidate quality locus traits for fruit quality (Schauer et al., 2006). MicroTom has become a strong model for tomato genetics, as with its compact size and fast growth it can be used in high throughput systems for e.g. mutagenesis-based genetic studies (Meissner et al., 1997).

1.5.2.2. Nicotiana benthamiana

Tobacco varieties, e.g. *Nicotiana Tabaccum* and *Nicotiana benthamiana*, are a common model plant cluster within the field of plant biology. *N.benthamiana* is widely used as an experimental host for plant virology as it can be infected by a high number of viruses (Goodin et al., 2008). A draft genome sequence has been published, which can be utilised to broaden the scope of research performed with *N.benthamiana* (Bombarely et al., 2012). An effective transient transformation system is available for *N. benthamiana* (Wydro et al., 2006). Stable genetic transformations followed by regeneration can be executed at good efficiency, which makes *N. benthamiana* a popular species for studies on protein localisation, interaction, expression and purification (Goodin et al., 2008). With the CRISPR-cas9 system becoming available for plant biotechnology it has since been implemented in experiments with *N. benthamiana*. It has been used in for example genome editing through CRISPR mutagenesis or multiplex and homologous recombination (Li et al., 2013; Nekrasov et al., 2013). Virus Induced Gene silencing is a system that also works in *N. benthamiana* (Liu et al., 2004).

1.6. Aims and objectives

In this PhD project the aim is to (i) elucidate and characterise carotenoid sequestration mechanisms in plants and (ii) to implement ectopic engineering approaches to enhance carotenoid content *in planta*.

Objective 1: To elucidate the effect of carotenoid contents and profiles from different tomato lines perturbed in carotenoid biosynthesis on carotenoid sequestration mechanisms in *Tomato*. Sub-plastid analysis of tomato fruit from PSY1, *rr*, og^c, *tan* and *tan-crtI* lines (Ailsa Craig background) was used to characterise differences in carotenoid sequestration mechanisms (chapter 3). Plastid differentiation triggers and preferential carotenoid deposition within the plastid were the focus of this study.

Objective 2: To develop a Synthetic Biology platform for ectopic engineering of the MEP and carotenoid pathway in plants. Golden Braid cloning, a plant modular cloning system, was used for the assembly of a vector library for ectopic engineering of the MEP and carotenoid pathway (chapter 4). Transcriptional units for the entire MEP pathway (*C. annuum*, *E. coli*) and three carotenoid genes (*P. ananatis*) were constructed, targeted to the cytosol. A set of modular transcriptional units targeted to the plastid were created for the MEP pathway as an endogenous reference.

Objective 3: To evaluate the impact of ectopic engineering approaches for the MEP and carotenoid pathway on carotenoid content in *Nicotiana benthamiana*. Vectors with single or multiple transcriptional units for both the MEP and carotenoid pathway were tested via transient transformation in *Nicotiana benthamiana* (chapter 5). Profiling of carotenoid content was performed using liquid chromatography techniques and the outcomes suggest potential advantages of ectopic engineering approaches.

1.7. Scientific and economic rationale

1.7.1. Carotenoid sequestration mechanisms

As described earlier in this chapter, carotenoids can be stored in plastids within cells in various structures. Whereas chromoplasts in tomato fruit predominantly accumulate their carotenoids in plastoglobules and membrane crystalloids, an interest has been developed in the way carotenoids integrate within those structures and whether specific carotenoids are sequestered in specific structures. As shown in recent work, the sequestration of e.g. phytoene and β-carotene can be traced to the plastoglobules and membrane crystalloids (Nogueira et al., 2013). The presumption is made that carotenoids due to their unique characteristics can function as modulators of membrane structures, a hypothesis that has been tested in model bilayers of lipid, mixed with various carotenoids in vitro. The length of the C_{40}-molecules gives the opportunity for integration between the fatty acid tails of lipids. The way different carotenoids behave within the membrane depends on the *trans*-/*cis* configuration, as shown in Figure 1-9.

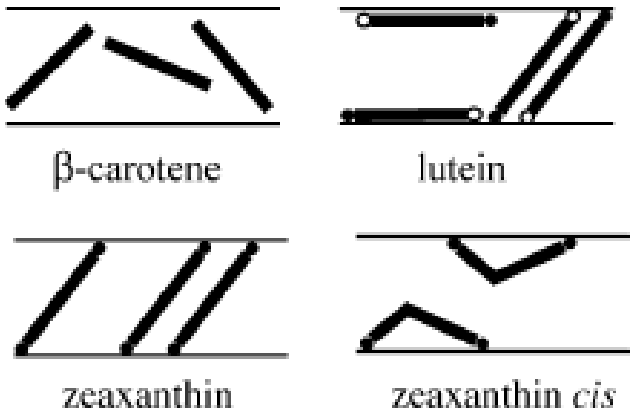

Figure 1-9. Proposed carotenoid-lipid interactions.
Hypothetical interaction of various carotenoids within lipid bilayers in the membrane. It is proposed that the difference in *cis*-/*trans*-composition of the carotenoids leads to alternative ways of integration within the membrane. Figure derived from (Widomska et al., 2009).

Next to the *trans*-/*cis*-configuration, the polar heads of carotenoids can anchor themselves in the opposite polar sections of lipid bilayers. Such anchors will lead to a more stable membrane structure inhibiting oxidative degradation. All-*trans*-lycopene, the main carotenoid accumulated in ripe tomato fruits, affects the stability of membranes severely (McNulty et al., 2007). This

effect is found as well for all-*trans*-zeaxanthin, while *cis*-zeaxanthin has a stabilising effect (Gruszecki and Strzałka, 2005; Widomska et al., 2009). This could suggest that the ratio of carotenoids with different effects on membrane stability generate an adapted sequestration preference, and therefore change the ratio of carotenoid sequestration between the structure types.

1.7.2. Modular cloning systems

The development of the Golden Braid system is focussed on plant biotechnology and synthetic biology approaches for plant systems (Sarrion-Perdigones et al., 2011; Sarrion-Perdigones et al., 2013). Since the development of the first GB-system, two updated versions have been presented - GB2.0 and GB3.0. The main advantage of GB over other modular cloning systems is the double loop topology, which allows for continuous combining of TUs as long as biological factors, i.e. maximum functional vector size, allow for it (Figure 1-10). The vectors on both sides of the loop, the Ω and α vectors, have reversed cloning sites containing the recognition sites for two type II enzymes which allow for the unlimited assembling of multi-gene vectors (Sarrion-Perdigones et al., 2011).

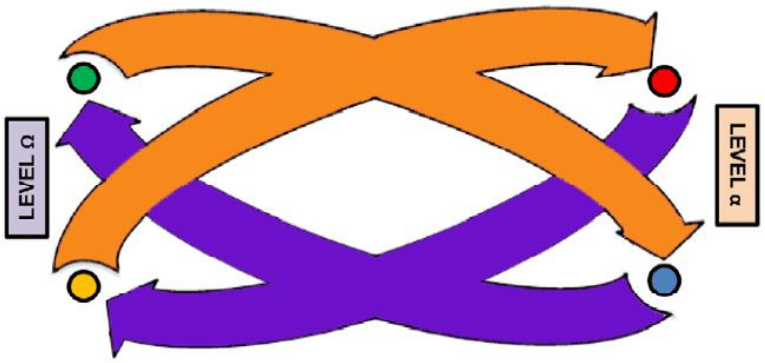

Figure 1-10. Double loop design of the GB-system.
The loop has two sides, which can be used for linking TUs. E.g. TUs can be cut out of individual Ω-vectors and be united and transferred to an α-vector to create a multi-gene vector. Figure derived from (Sarrion-Perdigones et al., 2011).

GB version 1.0 allowed for parts to be prepared by PCR and directly be cloned into α or Ω binary vectors. GB2.0 has as main advantage compared to the earlier version, that parts (promoters, terminators, coding sequences) can be built in an entry vector, and a library of parts can be

created rapidly in these entry vectors (Sarrion-Perdigones et al., 2013). This novel cloning method is presented as the new standard for Synthetic Biology within the field of Plant Biotechnology (Patron et al., 2015). Therefore, the technique will be utilised for objective two, to construct a vector library for ectopic expression of isoprenoid genes. One successful report has been published recently on the use of GB in a broad study on phytosterols in *Solanaceae* species. A part of this study involved the construction of a phytosterol pathway, using nine phytosterol genes assembled in a single vector (Sonawane et al., 2016).

1.7.3. Ectopic expression of isoprenoid pathways

As described earlier in this chapter, the regulation of pathways in their endogenous sites of activity is strictly controlled through various mechanisms which include feedback loops. In an attempt to circumvent the regulatory mechanisms present on the endogenous sites of activity, ectopic expression in another cellular compartment could be an option. The suggestion has been tested previously for the MVA pathway, targeting to the plastid, and enhanced both carotenoid and phytosterol levels. The impact therefore could be traced back to both the compartment in which the pathway is ectopically expressed and the endogenous compartment (Kumar et al., 2012). Undirected transport of isoprenoid intermediates between intercellular compartments has been suggested for e.g. the cytosol and the plastid (Bick and Lange, 2003). With the substrates for the selected enzymes of the MEP and carotenoid pathways present in the cytosol, the ectopic expression approach should generate enhanced levels of isoprenoids such as carotenoids and chlorophylls.

1.7.4. Economic importance of carotenoids and tomatoes

Tomato (*Solanum lycopersicum*) is one of the main cultivated crops worldwide, being cultivated with the 7th highest yield in amount per hectare and the 12th highest production capacity at ~45-50 tons/ha and 170 million tonnes respectively in 2014 (FAOSTAT2014; Kimura and Sinha, 2008). Originally from the Andes region in South America, tomatoes are currently a widespread crop around the world (Vincent et al., 2013). As a crop plant tomato produces fruits with a large range

of nutritional compounds such as carotenoids, flavonoids, vitamins and various phenolic compounds [reviewed by Gerszberg et al.] (Gerszberg et al., 2015; Raiola et al., 2014). A study on the consumption of tomato products states that tomato, the 4th most consumed fruit in the USA, is of undeniable importance to the American diet (Canene-Adams et al., 2005). The impact of these statistics has led to a range of studies to improve the health promoting traits of tomato through enhancing the levels of e.g. carotenoids (Raiola et al., 2014). Carotenoids are considered high value compounds for industry and in foodstuffs. The global carotenoid market is expected to grow to a value of $1.95 billion by 2025, based on a compound annual growth rate of 5.1%. This is based on a range of valuable compounds such as astaxanthin, canthaxanthin, capsanthin, lycopene, zeaxanthin, lutein, β-carotene and other (Accuray Research LLP, 2017). The industrial value of carotenoids is high; therefore it is of interest to focus on approaches to enhance carotenoid content in natural sources such as plant, algae, bacteria and fungi. Biological sources of carotenoids could compete with the chemical synthesis currently used for .e.g. astaxanthin. A recent study attempted to integrate maize-derived keto-carotenoids in fish feed to compete with feed with chemically synthesised keto-carotenoids; it was a successful experiment in which comparable results were obtained between biological and chemically derived keto-carotenoid uptake (Breitenbach et al., 2016). Studies on sequestration mechanisms could aid further applications by determining how better targeted sequestration can be arranged. Metabolic engineering of the isoprenoid pathway, focussed on carotenoids, can boost concentrations, which in turn can improve the chances to compete with chemical synthesis.

2. Materials and Methods

2.1. Starting materials and sampling

2.1.1. Starting materials

Tomato (*Solanum lycopersicum*) variety Ailsa Craig, control line, and lines perturbed in carotenoid biosynthesis, were grown under greenhouse conditions in a 16h light and 8h darkness regime, at approximate temperatures of 25°C and 20°C respectively. Genetic material for the designed GB-parts was obtained from several sources. DNA for coding sequences of the MEP genes was obtained from *Escherichia coli* DH5α genomic DNA and *Capsicum annuum* (sweet pepper) leaf RNA samples. An optimised vector used for the overexpression of bacterial carotenoid genes *crtZ* and *crtW* was used as the source for the promoter and terminator parts of the created constructs (Misawa and Shimada, 1998). *N.benthamiana* plants were grown under greenhouse conditions, in a 16h light and 8h darkness regime, at approximate temperatures of 25°C and 20°C respectively, for the agro-infiltration experiments. Competent cells, *E. coli* DH5α and *Agrobacterium tumefaciens* GV3101, for the GB cloning and plant transformations were made on site. Lubia-Bertani (LB) broth (1lt: 5g yeast extract (Oxoid Ltd.), 5g tryptone (Oxoid Ltd.), 10g NaCl, pH5.7 + 15g agar for plating) and antibiotic stocks used were prepared on site, and sterilised by autoclaving and filter sterilisation respectively. Chemicals, unless mentioned otherwise, were bought from Sigma-Aldrich.

2.1.2. Methods for sampling and stocks

Samples of plant material were quenched in liquid nitrogen seconds after harvesting and stored at -80°C until further processing. Samples used for metabolite analysis were freeze-dried and ground using a tissue lyser (Tissue lyser II, Qiagen). For RNA extractions plant material was ground to powder using a mortar and pestle cooled with liquid nitrogen, to be stored at -80°C until further use. Bacterial strains were maintained in glycerol stocks at -80°. For the preparation of glycerol stocks 700µl of culture was mixed with 300µl of glycerol (100%) and flash frozen in liquid nitrogen and stored at -80°C. For experiments such as sub-plastid fractionations and inhibitor studies that require fresh material, samples were prepared according to these specific

protocols e.g. kept cool (4°C) or at room temperature (~23°C). Tomato seeds were collected during fruit harvesting, fruit jelly with seeds was resuspended in an HCl solution (~16%) and left for 2-3h before washing and collecting in a sieve. Seeds were dried on filter paper (Whatmann) before storage. Tobacco seeds were collected from dried seed pods on the plants, seeds were separated from the pods and stored. Seeds were stored at ambient temperatures in the dark.

2.2. General molecular biology techniques

2.2.1. Bacterial chromosomal DNA extraction

A 5ml LB-broth culture of *E. coli* DH5α was grown overnight, and 1ml of the cell suspension was used for genomic DNA extraction [protocol derived from (Cheng and Jiang, 2006)]. The cell suspension was spun down in a centrifuge at 8000g for 2 min, and supernatant was removed. Thereafter the pellet was washed twice with 400µl STE-buffer (100mM NaCl, 10mM Tris-HCl, 1mM EDTA, pH8.0) and centrifuged again at 8000g for 2 min. Then the pellet was resuspended in 200µl TE-buffer (10mM Tris-HCl, 1mM EDTA, pH8.0) before 100µl Tris-saturated phenol (pH8.0) was added, followed by vortexing the mixture for 60s. A 5 min centrifuge step at 13000g at 4°C is performed next to separate the aqueous and organic phases in the mixture. 160µl of the aqueous phase was transferred to a new tube, after which 40µl of TE-buffer was added before 100µl of chloroform (HPLC-grade, Fischer scientific) was mixed in. The mixture was centrifuged again for 5 min at 13000g and at 4°C. The aforementioned step was repeated until an initially occurring white interface had disappeared, repetitions varied between two and three times. Again 160µl of the aqueous phase was transferred to a new tube and 40µl of TE-buffer and 5µl RNAse (10mg/ml, Qiagen) were added. The mixture containing RNAse incubated at 37°C for 10min, followed by a final chloroform extraction. 150µl of the aqueous phase was transferred to a new tube and screened for its DNA concentration. The purified DNA was then stored at -20°C, or used for subsequent experiments.

2.2.2. Extraction of RNA from leaf material

Leaf material was collected and flash frozen in liquid nitrogen. Samples were ground to a fine powder with a mortar and pestle, continuously adding liquid nitrogen to keep the sample cool. Approximately 80mg of ground material was used for a RNA extraction, the extraction was performed with an RNeasy Plant Mini kit (Qiagen). No modifications to the extraction protocol provided with the kit were made. The obtained RNA sample was tested for its quantity and purity via A_{230}/A_{260} ratio measurements and via gel electrophoresis. Samples were stored at -80°C and further processed to cDNA for isolation of the required coding sequence via PCR.

2.2.3. Plasmid extraction

Cultures (5ml LB-broth, plus required antibiotics) of *E. coli* or *A. tumefaciens* grown for the purpose of plastid extraction were centrifuged at 9391*g* for 3 min. Normally 4ml of culture was spun down, twice 2ml in an Eppendorf, before the first solution of the miniprep kit was added. The kit and its protocol as provided (Wizard plus SV minipreps DNA purification, Promega) were used for the extraction of vector DNA from bacteria. The only modification was the amount of nuclease free water, 50µl instead of 100µl, used for the elution of the DNA from the column. Eluted samples were quantified and checked for their purity by analysing the A_{260}/A_{280} ratio, and could be stored at -20°C or used for further applications.

2.2.4. Gel electrophoresis

Size based separation of DNA/RNA samples was performed via gel electrophoresis. A solution of TBE-buffer (Tris-borate-EDTA) and 1-2% agarose (Bioline) was heated by microwaving to boiling point or until all agarose dissolved. Before pouring the liquid agarose gel in a mold, GelRed-solution (10.000x, Biotium) was added at 1µl/10ml. Samples, mixed with 6xloading dye (Promega), were loaded in the wells. Ladders (100bp & 1Kb, Promega) were loaded next to the samples. After the gels had been run in the electrophoresis device, gels were placed under a UV-camera for visualisation and analysis of bands. When bands needed to be cut out of gels for further processing, gels would be placed on a UV-lamp (U:Genius3, Syngene) and bands would be cut out with a laboratory scalpel.

2.2.5. Gel purification and DNA extraction

Cut out gel bands, or PCR reactions containing DNA fragments of interest, would be processed using a Wizard SV Gel and PCR Clean-up System (Promega). The approximate weight in mg of the cut-out DNA fragment would be matched with the resuspension buffer of the kit (1µl/1mg) and the agarose would be dissolved at 65°C. PCR fragments were mixed with an equal volume of resuspension buffer. The standard extraction provided with the kit instructions were followed, and again the elution volume was reduced by half. The samples would be checked for their purity and quantity as mentioned before.

2.2.6. DNA sequencing

Sequencing services for the confirmation of sequences and their accuracy were provided by MWG Eurofins (Wolverhampton, UK). An Eppendorf tube contain either 5ng/µl for PCR products or 10ng/µl for vector DNA was supplemented with 2µl of sequencing primers (10µM) and sent off for sequencing.

2.2.7. Restriction digests

Standard digestions performed for the confirmation of cloning steps were performed using a selection of restriction enzymes (New England Biolabs). Type I restriction enzymes, HindIII and EcoRI, were used for the confirmation based on digestion patterns. Whilst the GB designated type II enzymes BsaI and BsmBI were used for the isolation and size quantification of GB parts and GB TUs. The reaction protocols were enzyme specific, temperatures varied between 37°C and 55°C and incubation time varied between 5-60 min depending on enzymes having high fidelity traits. The ratios of the reaction mixtures were kept as described by the producer, but total reaction was reduced by half (0.5µl restriction enzyme, 2.5µl Buffer, 0.5µg template DNA, total reaction volume 25µl). The reaction was stopped by adding 6x gel loading dye (5µl per reaction), which was provided by New England Biolabs.

2.2.8. cDNA synthesis

Synthesis of cDNA was performed with the Quantitect Reverse Transcription Kit (QiaGen), via the standard protocol as provided with the kit. 1µg RNA was used for reverse transcription and

any traces of RNA were removed with the optional RNAse treatment. cDNA samples were purified using the Wizard SV Gel and PCR Clean-up System (Promega) and cDNA concentration was measured using a nanodrop spectrophotometer. cDNA was used directly or stored -20°C.

2.2.9. RT-PCR

Qualitative confirmation for expression of coding sequences was performed through PCR using illustra PuReTaq Ready-to-go PCR beads (GE healthcare). 25ng cDNA and 1µl primer solution (10µM) per primer were added to the pre-mix bead and total volume was made up to 25µl. Gene specific primers were added per reaction based on samples screened, and reference genes were included in analysis. PCR runs were performed for 25 cycles (30"95°C, 30"60°C*, 30"72°C *=primer specific) to avoid depletion of reagents and untargeted DNA multiplication. PCR reactions were run on agarose gels to confirm fragment appearance and size. An overview of all primers used for RT-PCR analysis is provided in Table A-3.

2.3. Competent cells and transformations of bacteria

2.3.1. Chemically competent cells (*E. coli*) for heat shock transformation

Transformation of vectors into *E. coli* DH5α was done performing a heat shock to chemically competent cells. Competent cells were prepared as follows. Untransformed *E. coli* DH5α was cultured in 50ml LB-broth, shaking (180rpm) at 37°C. This culture would be started in the morning from a 5ml overnight culture, adding a 1:100 inoculum. When the culture reached OD_{600}=0.6-0.8, the cultures were pelleted in a centrifuge (2465*g*, 10 min, 4°C). The cells were resuspended in a 10ml solution (10% glycerol, 0.1M $CaCl_2$) and incubated on ice for 15 min. After a second centrifugation step (2465*g*, 10 min, 4°C), cells were resuspended in 1ml of the Glycerol/$CaCl_2$-solution and split into 25µl aliquots. After flash freezing the aliquots in liquid nitrogen, the competent cells were stored at -80°C.

2.3.2. Heat shock transformation of *E. coli*

To perform the heat shock transformation, an aliquot per transformation would be thawed on ice, before 1-3µl of DNA-solution would be added. After the DNA and the cells have been gently

mixed, the suspension was left incubating on ice for approximately 30 min. Thereafter the heat shock was performed: tubes are placed in a water bath (45°C) for 45 seconds, and put back on ice for 2 minutes after that. 250µl of LB-broth was added to the cell suspension and this culture was left shaking at 37°C for 1h. The transformation mixes were plated on plates with LB-agar and the required antibiotics in two volumes (50µl and 225µl) and incubated at 37°C.

2.3.3. Electro-competent cells (*A. tumefaciens*)

For plant transformations *A. tumefaciens* is a commonly used carrier of vector DNA. Electroporation of *A. tumefaciens* is a regularly used method to insert vector into the bacterium. In order to prepare *A. tumefaciens* cells for electroporation, these cells need to be electro competent. For this procedure a 5ml culture of *A. tumefaciens* in LB with tetracycline (2.5µg/ml) was incubated overnight shaking (180rpm) at 28°C. Followed by the preparation of a second overnight culture (200ml LB + 5µg/ml tetracycline), 1ml of the initial overnight culture was added as an inoculum. The culture was left shaking until the culture reached OD_{600}=0.5-0.7, then the culture was split into two centrifuge bottles and left on ice for 30 min. The culture was then spun down at 4°C (2465*g*, 15 min), the cells were resuspended in 50ml 10% glycerol (4°C). The cells were centrifuged again and washed a second time with 50ml of 10% glycerol. After the second washing 200µl of 10% glycerol was added, and 50µl aliquots were prepared. After being flash frozen in liquid nitrogen the electro competent cells were ready for use or could be stored at -80°C.

2.3.4. Electroporation of *Agrobacterium tumefaciens*

For the electroporation of *A.tumefaciens* an aliquot per vector sample was thawed on ice, before 1µl of DNA solution was added. The gently mixed DNA/cell suspension was transferred to an electroporation cuvette (1mm gene pulser cuvette, Bio-Rad), and the cuvette was tapped on a flat surface to remove any air bubbles. It is important to keep the sample-filled cuvettes on ice during the preparation phase. The cuvette was then placed in the pre-cooled cuvette holder of the electroporation device (Multiporator® Electroporator 2510, Eppendorf UK), and given a

pulse to perform the electroporation (1440v, 5ms). To allow for a quick recovery of the cells, 250µl of LB-broth was added to the cuvette and the content of the cuvette was transferred to a falcon tube (15ml) to incubate the cells at 28°C, shaking (180rpm), 1h. After the incubation the culture was plated in two volumes (50 and 250 µl) on LB-agar with the required antibiotics. The plates were incubated for 36-48h, or until colonies were spotted.

2.4. Golden Braid Cloning

The GB-cloning system has established three software tools for the main steps of the cloning strategy. All three tools are to be found on the GB-cloning website (https://gbcloning.upv.es/, currently providing version GB3.0), and will be discussed further on in order of application. TUs design and created for this chapter all have been "basic" constructs (promoter, coding sequence, and terminator), therefore the descriptions following will be for the preparation of such constructs.

2.4.1. GB domestication design

The sequences for the various GB-parts that were created were entered in the domestication tool, to receive GB-specific primer sets for the addition of type II enzyme recognition sites on the ends of the sequence and the removal of any internal binding sites for those enzymes. Primers, custom oligos, were ordered from Eurofins MWG. The outcome of sourcing the domestication tool is a short description of the primers required for the domestication (patches), including a short protocol for the part assembly in a one-pot restriction/ligation reaction.

2.4.2. GB domestication PCR

Required fragments (primers provided in the appendix), were synthesised using either the KOD-PCR kit (Merck-Millipore) or illustra PuReTaq Ready-to-go PCR beads (GE healthcare), standard reactions set-up was followed. Due to the normally extended length of the primers (>35bp), the T_m was most often above 72°C [primer list: Table A-1**Error! Reference source not found.**, Appendix]. To create a feasible programme for the cycler, all were run on an annealing

temperature of 65°C as standard. The outcome of the PCR-reaction was checked on gel. PCR fragments were purified with the gel extraction and PCR clean-up kit (Promega) as described before. The fragments were either cleaned up straight from the PCR mix or after being isolated from agarose gels, depending on the outcome of the PCR (single or multiple bands).

2.4.3. GB domestication assembly

Confirmed bands were mixed into a reaction assembly to build the GB-part. 40ng patch DNA, 75ng vector DNA (pUPD), 1µl BsmBI (New England Biolabs), 1µl T4-ligase (Promega), 1µl 10xligase buffer, reaction volume was made up to 10µl with molecular biology grade water (VWR). The reaction tube was placed in a thermo-cycler and a 25-cycle programme was run (25x 2'37°C, 5'16°C). After the cycler finished the ligation mix was ready for heat shock transformation to *E. coli* DH5α. 1µl of the ligation-mix was added to an aliquot of *E. coli* competent cells and the heat shock protocol was performed as described before. Cells were plated on LB-agar with 100µg/ml ampicillin and 20µg/ml X-gal and 16µg/ml IPTG (X-gal/IPTG-solution, Melfords). After overnight incubation the plates were checked for white colonies, four colonies were striped on a fresh LB-plate and made into cultures for a plastid extraction (miniprep kit, Promega) to be used in the next step of the GB-cloning system.

2.4.4. TU assembly

The assembly of a TU were prepared *in silico* with the second tool on the GB-website. Parts that make a basic TU were inserted in the tool and the required binary vector (α1, α2, Ω1, Ω2) was be selected. A similar ligation mix was prepared, with BsaI and BsmBI/BgtZI (New England Biolabs) for α-vectors and Ω-vectors respectively. 75ng of each part (pUPD-vector) and 75ng of the binary vector (pDGB1) was added to the enzyme mixture, and the same thermo-cycler programme as described for the domestication procedure used. Heat shock transformation was performed with the assembly mix, as the efficiency of the Ω-vectors is lower 3µl was added to the competent cells instead of 1µl. The transformed *E. coli* cells were plated on LB-agar with X-gal/IPTG solution and the vector specific antibiotics (50ug/ml kanamycin for α-vectors and

50ug/ml spectinomycin for Ω-vectors). Colonies were picked after overnight incubation and cultures were prepared for plastid extraction.

2.4.5. Binary assembly

The third software tool on the GB-website provided for the *in silico* preparation of multi-gene constructs is the binary assembly. Units on either the α- or Ω-side of the double loop system can be cut out, linked and placed in either vector 1 or 2 on the other side. E.g. TUs from pDGB1α1 and pDGB1α2 can be linked in series and placed into pDGB1Ω1 or pDGB1Ω2. The simplicity of the GB-cloning method reveals itself, as for the binary assembly the same thermocycler programme as described before was used again, and furthermore the same restriction/ligation mix is prepared. For the binary assembly again 75ng of each vector was required and either BsmBI (for α to Ω) or BsaI (for Ω to α) is added. Chemically competent *E. coli* cells were transformed as described before and transformed cells were plated on LB-agar containing X-gal/IPTG and the required antibiotics. White colonies were selected for miniprep cultures and the obtained vector DNA was checked for its properties and used for further cloning steps or transformation into *A. tumefaciens*.

2.5. Subplastid fractionation

Experiments were performed as reported in a bio-protocol article by (Nogueira et al., 2016). Tomato fruit was harvested from the glasshouse and washed and deseeded in the laboratory, the remaining pericarp tissue was cut into small cubes (+/- 1cm^2). Approximately 50 grams of pericarp tissue per gradient tube was stored overnight at 4°C to allow for starch degradation (Nogueira et al., 2016). Samples were kept on ice or in a 4°C room during the remaining part of the procedure. After the overnight incubation the pericarp was mixed with extraction buffer (0.4M sucrose, 50mM Tris, 1mM DTT, 1mM EDTA, pH: 7.8) in a blender (21/8010ES, Waring Products UK). The pericarp-buffer suspension was homogenised for twice 3 seconds (1 second at speed I, 2 seconds at speed II) until a rough mixture was obtained suitable for plastid isolation.

The suspension was put onto four layers of muslin and the obtained slurry was divided over centrifuge bottles (500ml) and centrifuged for 10 min at 5000*g*. Supernatant was discarded, a small fraction of the supernatant was used to resuspend the pellet in. The plastid suspension was transferred to a smaller tube (50ml) and tubes were topped up with extraction buffer. Samples were centrifuged at 9000*g* for 10 min, all supernatant was discarded afterwards. The plastid pellets were disrupted by resuspending the pellets in 45% sucrose buffer (3ml), sucrose buffer consisted of: 45% sucrose (or lower, see below), 50mM tricine, 2mM EDTA, 2mM DTT, 5mM sodium bisulfite, pH:7.9, and the same fruit samples were pooled in a hand-held potter homogenizer. Plastid samples were homogenised by repeating the motion disruption at least ten times. The samples were collected in a 50ml falcon tube and topped up with sucrose buffer (45%) up to 16ml. The homogenised plastid material was divided over two ultra-centrifuge tubes (8ml each). A stepwise sucrose gradient was created by adding 38% sucrose buffer (6ml) followed by 20% (6ml), 15% (4ml) and 5% (8ml). Gradient tubes were balanced and placed in an ultra-centrifuge to be spun at 100000*g* for ~18h. After the gradient has been build up during the ultra-centrifugation, the gradients were fractionated into 1ml fractions using a Minipuls®3 peristaltic pump and FC203B fraction collector (Gilson, UK). Fractions can be used directly or stored at -20°C.

2.6. Transient transformation in *N.benthamiana*

2.6.1. *A. tumefaciens* culture preparations

For the transient expression of the GB-vectors, those vectors were transformed to *A. tumefaciens* using an electroporator as described before. *A. tumefaciens* strains containing the GB-vectors were grown in a 5ml overnight culture (LB-broth, 50µg/ml rifampicllin, 50µg/ml gentamycin, 50µg/ml kanamycin or 100µg/ml spectinomycin), simultaneously *A.tumefaciens* CV58 (vector p19) was grown in LB-broth (50µg/ml rifampicllin, 36µg/ml chloramphenicol, 50µg/ml kanamycin), and all strains were incubated shaking at 28°C. The P19 vector reduced gene silencing effects which could occur during overexpression experiments (Voinnet et al.,

2003). Next, a 50ml culture was prepared for each strain and grown in 250ml flasks, containing induction medium (yeast extract 1g/L, beef extract 5g/L (Oxoid Ltd), peptone 5g/L (Merck KGaA), sucrose 5g/L, 2mM $MgSo_4$, 20µM acetosyringone, 10mM MES, pH5.6) under the same conditions overnight. These cultures were centrifuged for 10 min at 3000*g* and washed in 5ml infiltration medium (10mM MES, 10mM $MgCl_2$, 100µM acetosyringone). The cells were centrifuged again (10 min, 3000*g*) and brought into suspension by carefully rolling them for 2h. The OD_{600} was measured and samples were diluted till the OD_{600} was 0.5, before preparing the final culture mixtures for infiltration. Depending on the amount of co-infiltrated vectors, the ratios of the GB-vectors were mixed in equal volumes with the p19 vector (1:1 for 1 GB-vector, 1:1:1 when 2 GB-vectors are used, etc.).

2.6.2. Agro-infiltration of *N.benthamiana* leaves

N.benthamiana plants were grown from seeds under greenhouse conditions, for approximately 5-7 weeks until the plants had developed about 6-8 fully developed leaves (10-12 leaves in total). On the infiltration day plants were not watered and were provided with extra light (white fluorescent light, for 1h) to aid the infiltration efficiency. The four middle leaves of each plant were marked and infiltrated with the selected cell suspension using a 10ml syringe without a needle to prevent piercing. Three plants were infiltrated per construct to allow for enough viable leaf material per construct. The infiltrated plants were left for 7 days, before the leaves were harvested. Whole leaves were quickly placed into falcon tubes and flash frozen in liquid nitrogen, to be stored in -80°C. Method adapted from (Sparkes et al., 2006).

2.7. Metabolite extractions

2.7.1. Metabolite extraction

For analysis of carotenoid, chlorophyll and tocopherol content in the leaf material, those compounds were extracted from the material using a chloroform/methanol extraction. 10mg of freeze-dried material was weighed in an Eppendorf tube and 250µl of methanol (HPLC-grade, Fischer Scientific) was added to be vortexed intensively. 500µl chloroform was added, the

mixture was vortexed and placed on ice for 20 min. 250µl of 100mM Tris-HCl (pH7.5) was added and the content of the tube was mixed again by vortexing. The sample was centrifuged at minimum 20238*g* for 5 min, and the separated chloroform phase was transferred to a new tube. Another 500µl of chloroform was added, the tube again vortexed and centrifuged. The second chloroform phase was added to the first chloroform phase in the second tube and the tube was placed in vacuum evaporator to evaporate all the chloroform in the sample. Dried samples were stored at -20°C or used for chromatography analysis directly.

2.7.2. Carotenoid extraction from fractions

Fractions were extracted into three phases (carotenoids (non-polar), proteins and a polar phase). Methanol (250µl) was added and the sample vortexed, next chloroform (750µl) was added and the sample was vortexed again before being placed on ice for 20 min. Samples were spun down at minimum 20238*g* in a table top centrifuge for 5 min and the bottom chloroform phase was transferred to a new Eppendorf tube. A second volume of chloroform (750µl) was added to the sample, the sample was then vortexed and spun down again. The second chloroform phase was pooled with the first phase and the total volume was dried down in a vacuum evaporator (Genevac). The sample was topped up with methanol (750µl), mixed and spun down at max speed. The methanol phase was transferred to a new Eppendorf tube. All three phases, the non-polar, polar, and proteins, were stored at -20°C or used for further analysis.

2.7.3. Phytosterol extractions

For sterol extractions 20mg was weighed out per sample and placed in a 2ml Eppendorf tube. Samples were saponified using 6% KOH in Tris-HCl pH: 7.5 (600µl) at 65°C for 60 minutes. Following the incubation, 400µl MeOH and 1ml $CHCl_3$ were added and the samples were vortexed and placed on ice for 20 minutes. After incubation, samples were centrifuged at 20238*g* for 5 minutes and the $CHCl_3$ phase was collected in a 2ml glass vial, re-extraction with $CHCl_3$ was performed and both $CHCl_3$ phases were merged. Myristic acide-D27 (50 µg) was added

to the $CHCl_3$ phase before drying the sample in a vacuum evaporator (Genevac). Samples are ready for derivatisation at this stage or can be stored at -20°C. Derivatisation was performed in two steps, firstly methoxyvamine-HCl (30µl at 20mg/ml pyridine) was added and the mixture was incubated at 40°C for 60 minutes. Secondly, methyltrimethylsilyltrifluoroacetaminde (70µl) was added followed by another incubation at 40°C for 60 minutes. Samples were ready to be used for Gas Chromatography – Mass Spectrometry (GC-MS) analysis immediately.

2.8. Chromatography techniques

2.8.1. UPLC analysis

Samples to be run with Ultra Performance Liquid Chromatography (UPLC) were resuspended in 50µl ethyl acetate (HPLC-grade, Fischer Scientific). Any debris was pelleted by centrifuging the samples for 5 min at 20238*g*, 20µl of the sample was transferred to a glass vial (2ml) containing an insert. Vials were placed in the cooled auto sampler of the UPLC, to keep sample degradation to a minimum.

2.8.1.1. Carotenoids and chlorophylls

For the analysis of carotenoids, chlorophyll and tocopherols an Acquity Ultra Performance Liquid Chromatography (UPLC) system was used with photo diode array (PDA-detector). The system was set up with an Ethylene Bridged Hybrid column (BEH C18, reverse phase (RP)) (2.13100mm, 1.7mm with BEH C18 VanGuard precolumns (2.1350mm, 1.7mm) attached. In the mobile phase a binary solvent gradient was used: solvent A, methanol/water (50/50) and solvent B, acetonitrile/ethyl acetate (75/25). The gradient started at A/B (30/70%) for 0.5 min, to be stepped up to A/B (0.1/99.9%) for 5.5 min and back to A/B (30/70%) for 2 min. The column temperature was set to 30°C, meanwhile the samples were maintain at 8°C in the auto sampler. A volume of 3µl was loaded on the column per sample.

2.8.1.2. Keto-carotenoids

Keto-carotenoids were detected and quantified on the previously mentioned Acquity UPLC system, using the BEH C18 column and the same solvents for the binary gradient. A different

gradient was set up for the detection of keto-carotenoids. The gradient ran as follows: A(50%)/B(50%) for 0.5 min, followed by a stepwise gradient of 4.5 min to reach A(30%)/B(70%), 2 min at A(0%)/B(100%) before going to a(30%)/B(70%) for 1 min and finishing with A(50%)/B(50%) for 2 min.

2.8.2. HPLC analysis

For samples with minor abundances of certain compounds analysis was performed using High Performance Liquid Chromatography (HPLC) with integrated PDA, an Agilent HPLC system. The method for the analysis of plant isoprenoids has been described in the literature (Fraser et al., 2000). The system was set up with a C30 reverse phase (RP) 5 µm column (150 x 4.6 mm) coupled to a C30 guard column (50 x 4.6mm, 5 µm) (YMC Inc., USA). A triple solvent gradient consisted of mobile phases A, methanol; B water/methanol (20/80 by volume), containing 0.2% ammonium acetate, and C, tert-methyl butyl ether. The gradient started with A (95%)/B(5%) for twelve minutes, stepped to A(80%)/B(5%)/C(15%) at twelve minutes. This was followed by a linear gradient to A (30%)/B(5%)/C(65%) from minute twelve to thirty. From minute thirty to sixty a conditioning phase was used to return to the starting point of the gradient at A (95%)/B(5%). The column was kept at 25°C, autosampler temperature was set on 12°C.

2.8.3. GC-MS analysis of phytosterols

Detection of phytosterols was performed with GC-MS as described previously (Enfissi et al., 2010). Samples were injected on a gas chromatograph, Agilent HP6890 (UK), with attached 5973 Mass Spectrometer (MS). Injections were performed with 1µl per sample at 290°C. For the GC a temperature gradient was used, starting at 70°C for 4 minutes, followed by a 5°C/min increase up to 310°C. Final temperature was kept for 10 minutes. The MS interface was set at 290°C at full scan mode scanning at 10-800D using 70eV EI.

2.9. Data analysis and statistics

2.9.1. Molecular biology software

In silico work performed for the design of primers, parts and vector was done through the freely accessible online molecular biology suite Benchling (www.benchling.com, San Francisco, USA). Design of primers for cloning purposes, sequencing and RT-PCR was performed through Primer3, integrated in the molecular biology suite. Fasta files of the sequences of genes of interest, vectors and other parts were added to a personal section on the suite and applications of the suite used for in silico cloning steps, PCR reactions and digests and ligations. Sequencing data was analysed through the DNAStar molecular biology software package (Lasergene12, core suite, Wisconsin, USA). Software application SeqMan was used for the screening of sequencing files and alignment with control sequences of genes and vector elements and backbones.

2.9.2. Chromatography software

UPLC and HPLC chromatography traces were analysed using Empower chromatography data software (Waters US, Milford, USA). Peak area was determined for compounds of interest based on their spectra and retention times. Spectra detection settings were set to specific compound clusters to obtain accurate peak areas per compound screened (see appendix Table A-4). Standard curves as available were used to determine absolute quantities per compound (see appendix Table A-4). Data analysis of sterols and phytosterols from traces obtained from the GC-MS device was performed through AMDIS32 (NIST, USA) in combination with a NIST-library (National Institute of Standards and Technology, Gaithersburg, USA). NIST08 MS library was constructed based on in-house standards for a wide range of compounds. Samples were aligned via retention time calibration and MS identification. Relative quantification was analysed through comparison to the internal standard.

2.9.3. Processing and statistics

Following the data mining in the respective software packages of specific chromatography devices further processing was performed using EXCEL2013 (Microsoft Office software).

Processing of data, construction and formatting of graphs as well as statistical formatting and analysis was performed within the EXCEL suite. Via advanced statistical analysis, e.g. Dunnett's test, comparisons between all samples and the control were performed using the statistical software package SPSS (IBM SPSS-21, New York, USA).

3. Analysis of plastidial carotenoid sequestration in mutants and transgenic varieties with different carotenoid contents.

3.1. Introduction

In plants carotenoids are synthesised and accumulated in the plastids within their cells [reviewed by (Neuhaus and Emes, 2000)]. Besides their involvement in various plant development processes carotenoids are sequestered in plastid lipid structures to accumulate colour [reviewed (DellaPenna and Pogson, 2006; Li et al., 2009; López-Juez, 2007)]. Chloroplasts can be differentiated into chromoplasts to allow for more carotenoid accumulation by modifying the plastid structures to generate an enhanced sequestration of carotenoids [reviewed by (Cazzonelli and Pogson, 2010)]. Differentiation of chloroplasts to chromoplasts happens in tomato fruit during ripening when ripening related carotenoids start accumulating. Carotenes like phytoene, phytofluene and lycopene do not accumulate in photosynthetic tissues, as they are not involved with the photosynthetic complexes, this role is mainly conducted by xanthophylls (Pogson et al., 1998).

The *PSY*sense overexpression line demonstrates an interesting phenotype in which "ripening" related carotenes accumulate at the onset of fruit development, resulting in a pink to orange background colour of the mature green fruit (Fraser et al., 2007). Previous studies showed chromoplast-like structures in the mature green tissues. In this chapter an insight is provided of the interaction between plastid differentiation and carotenoid accumulation, and which of these two processes pushes chloroplast to chromoplast differentiation. The hypothesis for this chapter is that chloroplast to chromoplast differentiation can be accelerated by a premature increase in carotene content in plastids.

In a similar study a range of tomato mutant lines perturbed in carotenoid biosynthesis are screened for changes in sub-organelle carotenoid storage location. Via sub-chromoplast fractionations the objective is to explain how accumulation of specific carotenoids or changes in the carotenoid profile can lead to changes in preferential sequestration sites. A potentially important modifier of sequestration preference can lie in the difference between "*cis*" and

"*trans*" geometric chemical structures for the different carotenoids (Widomska et al., 2009). These structural changes could modify the integration within the membrane and globule membrane structures in a specific manner (Gruszecki and Strzałka, 2005). The hypothesis for this chapter is that *cis*- and *trans*-carotenoids have different preferred sites of sequestration within chromoplasts.

3.2. Resources: tomato mutant lines perturbed in carotenoid biosynthesis

For this chapter a selection of tomato lines perturbed in carotenoid biosynthesis was utilised. The selected lines were lines with overexpression or knock-out mutants of key genes of the carotenoid pathway, including *psy1*, *crt-iso*, *LCY-b* and *crtI.* A detailed description of the different lines and their background is presented below.

- **Ailsa Craig**

Ailsa Craig is a common tomato variety (*Solanum lycopersicum)* cherished for its flavoursome fruit, medium sized round shape and early ripening, commonly grown by home growers and commercial growers in the UK. Furthermore, it is a standardised variety for plant molecular biology. Besides, this line is the isogenic background for all tomato lines used in this study.

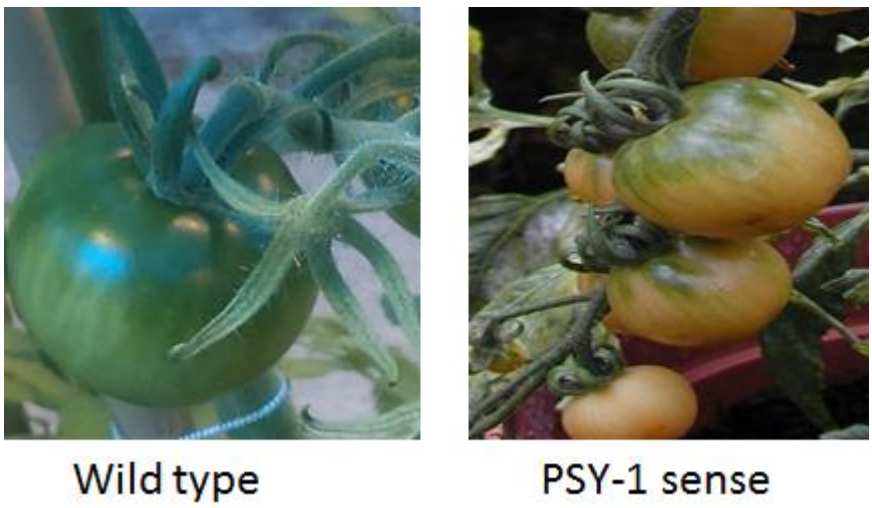

Figure 3-1. Phenotype of PSY1sense during fruit development.

The early activation of the PSY1 enzyme causes the accumulation of carotenoids and differentiation of chloroplasts to chromoplasts in immature fruit. Immature fruit will still possess the green crown, as common in Ailsa Craig, but the otherwise pale green tissues have coloured pink to orange.

- **PSY1sense**

The PSY1sense overexpression line, constitutively expressing *psy1,* was used to study the effects of constant activity for the PSY1 enzyme, which is normally expressed during fruit development in wild type lines (Fraser et al., 2007). The PSY1sense line shows a carotenoid enriched phenotype from the onset of fruit development (Figure 3-1), a trait that can be linked to the enhanced PSY1 enzyme activity and "ripening" related carotenoid accumulation. The early accumulation of these carotenoid is linked to the appearance of chromoplasts in unripe fruit, where normally primarily chloroplasts are found.

- ***rr*-mutant**

The *rr*-mutant is a naturally occurring knock-out of the PSY1 enzyme, and has historically been called a "yellow" flesh variety. Studies with overexpression lines for PSY1 have confirmed the lack of function of the *rr*-mutant (Fray and Grierson, 1993). The *psy2* gene which is active in the photosynthetic tissues of the plant cannot compensate for this loss of function of *psy1* (Fray and Grierson, 1993). The fruit contains a dramatically reduced level of carotenoids, which results in a pale yellow fruit colour (Figure 3-2). Therefore during the studies performed for this chapter it is considered a null-mutant for carotenoid biosynthesis in tomato fruit.

- ***Tangerine* mutant**

The tangerine t^{3183} mutant (*tan,* accession LA3183*)* is a knock-out mutant for *crt-iso* gene, for which the transcription of this gene is impaired, a second allele of this gene $tangerine^{mic}$ is confirmed as a deletion mutant (not used in this study). The relevance of CRT-ISO is primarily found in non-photosynthetic tissues, as light can induce the reaction catalysed by the enzyme (Isaacson et al., 2002). The enzyme's absence inhibits the isomerisation of poly-*cis*-lycopene to

all-trans-lycopene, this results in the accumulation of neurosporene and poly-*cis*-lycopene (Isaacson et al., 2002). The reduction in lycopene accumulation in the ripe tomato fruit results in an orange colour phenotype (Figure 3-2).

Figure 3-2. Phenotypes of the tan and yellow flesh (*rr*) mutant lines.
The knock-out mutants of CRT-ISO and PSY1 results in an orange and yellow colour respectively in the fruit, a significant difference compared to the wild type fruit. Photo modified from (Kachanovsky et al., 2012).

- ***tan*-CRTI mutant**

As described in the introduction, the bacterial CRTI enzyme (phytoene desaturase) can perform a range of desaturation and isomerisation steps, from phytoene up to lycopene, of the carotenoid pathway (Misawa and Shimada, 1998; Ravanello et al., 2003). A cross of the *tan* and CRTI mutant lines resulted in a phenotype where CRT-ISO is still inhibited but the CRTI enzyme can partially overcome the blocked synthesis of lycopene (Enfissi et al., 2017).

- ***og^c*-mutant**

The *old-gold-crimson* (*og^c, accession LA3179*) is a recessive allelic mutation found in tomato (Ronen et al., 2000), and is linked to the gene responsible for the cyclase activity that synthesises β-carotene from lycopene. The mutant phenotype therefore is a reduced content of β-carotene favouring lycopene accumulation, demonstrated by the darker red fruit colour when ripe. The visual phenotype presents itself most clearly in the pericarp and seed jelly where the intensity of the deep red colour is intensified compared to the wild type (Figure 3-3).

Figure 3-3. The og^c phenotype.
For the og^C mutant line a higher lycopene and lower β-carotene content, can be observed well in the fruit pericarp. The pericarp, and the seed jelly as well, demonstrate a darker red colouration (arrows). Photo adapted from (TGRC, 2004).

3.3. Subplastid fractionation: description of expected outcomes

To make the analyses presented further on in this chapter more accessible, a brief description of expected outcomes of the procedure will be provided below. In this description, a summary of the protocol is included, a full version of the protocol is available in chapter 2 (materials and methods).

At the start of the procedure, tomato fruit is harvested and the pericarp is collected and diced into small cubes. These pericarp cubes are disrupted in a plastid specific osmotic buffer and plastids are isolated and purified in a quick washing process. Plastid isolates are disrupted further to allow sub-organelle separation during the formation of a stepwise sucrose gradient, which is formed during a prolonged ultra-centrifugation step. Established gradients are split into 1ml fractions, which are analysed for their carotenoid and chlorophyll content using UPLC techniques.

A standard gradient for ripe tomato fruit material should contain two distinct layers (Figure 3-4). The top layer consists of primarily plastoglobules, the second layer is the membrane phase and contains various membrane structures and can contain carotenoid crystals. Any particles that do not fit the density range of the sucrose gradient will cluster in a pellet at the bottom of the

tube. The described layers are based on previous experiments with this technique, in which the sub-plastid structures were observed in samples of distinct layers through microscopy techniques (Nogueira et al., 2013).

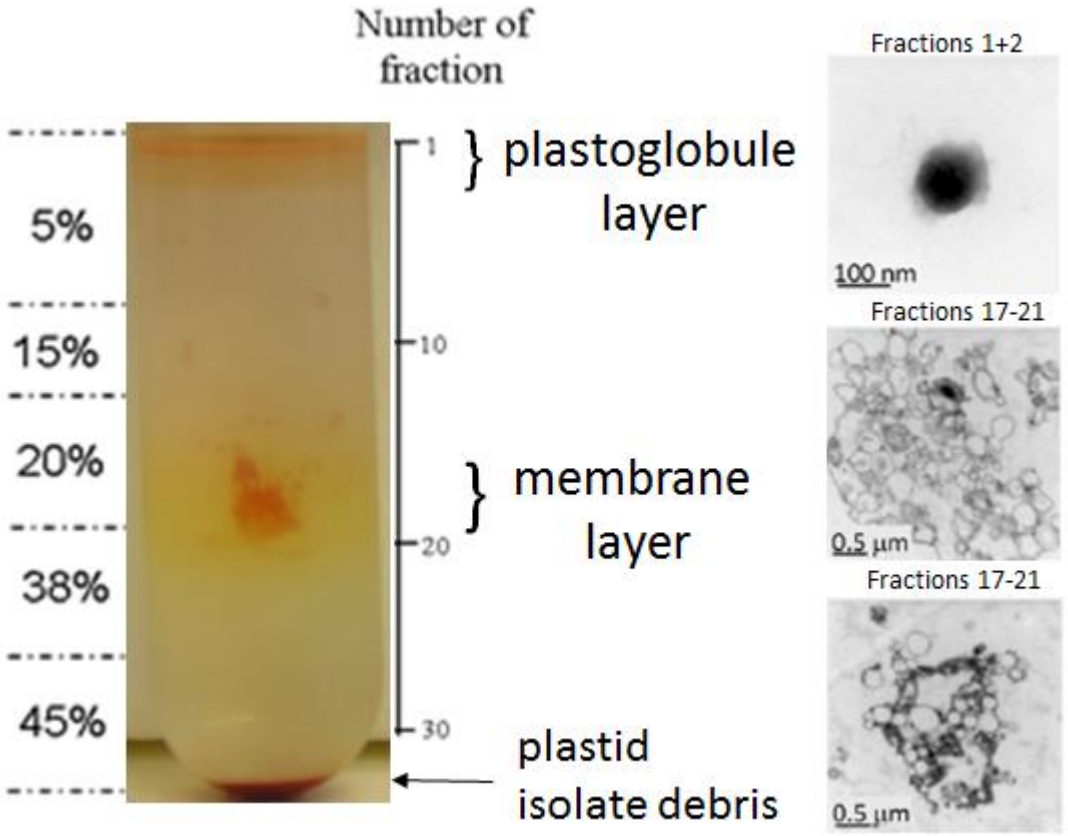

Figure 3-4. Visualisation of a standard sucrose gradient for subplastid fractionations.
The step-wise built sucrose gradients consist of five different concentrations of sucrose buffer (5, 15, 20, 38 and 45%). Three distinct layers can be found in a subchromoplast sucrose gradient for ripe fruit material. The top layer is a deposition of primarily plastoglobules, which has been confirmed by electron microscopy as visualised in the top right photo (Fractions 1+). The second layer, at the 20% segment, contains mainly membrane structures and carotenoid crystals. Membranoid crystals were observed, again via electron microscopy, in this phase as shown in the bottom right photos (Fractions 17-21). At the bottom of the tube any debris and impurities of the plastid isolation and preparation are pelleted. Microscopy photos were derived from earlier work with the fractionation technique as published by (Nogueira et al., 2013).

3.4. Results

3.4.1. Accelerated chloroplast to chromoplast differentiation related to early accumulation of "ripe" carotenoids

To determine whether altered carotenoid accumulation effects plastid differentiation, a sub-plastid study was performed with a PSY1 overexpression line (PSY1sense) and an Ailsa Craig control line in tomato. Three different subplastid fractionations were performed at different ripening stages - mature green, breaker stage, and ripe fruit. A fourth subplastid fractionation was performed with only Ailsa Craig tomato fruit, comparing ripe and mature green samples to a mix of both. This experiment was included based on the results of the PSY1sense and Ailsa Craig three-stage fractionation as a control of differentiating chloroplasts and chromoplasts. In this section the key in comparing the results is the absolute difference of accumulation between the overexpression line and the control, therefore the graphic display in the different figures will be depicted in µg/fraction.

3.4.1.1. Analysis of PSY1sense and Ailsa Craig at mature green stage

For the first subplastid study ~150grams of mature green pericarp was collected for both the PSY1 sense line and the Ailsa Craig control line. The subplastid fractionations were performed as described in Materials and Methods, and per gradient ~32 fractions were collected. Two sets of gradients were analysed per experiment for comparative accuracy. Figure 3-5 provides an overview of one of the gradients analysed, similar results were obtained for the second analysed gradient set (Figure 3-6). Fractions were extracted and analysed using UPLC techniques; chromatograms of AC (ripe and mature green) can be found in the appendix (Figure A-2, Figure A-3).

In insert A of Figure 3-5 the two gradients representing the Ailsa Craig and PSY1sense lines are compared. Clear differences can be detected in various areas of the gradients (Figure 3-5 (A), red squares), for example at the top of the gradient where a plastoglobule phase has appeared for the PSY1sense line. Secondly, above the green segment of the gradient of PSY1sense a

colourful area is present at fractions 18-20. Furthermore, local differences in the intensity of the green segments of both lines can be observed. The collected fractions were screened for their carotenoid and chlorophyll content using UPLC techniques, and a general increase of carotenoids was detected for the PSY1sense line compared to the control. The chlorophyll profile was generated based on the sum of all fractions (Figure 3-5, B). A 2-fold increase in total carotenoid content was observed for the PSY1sense line compared to the control. The increase can be explained by the appearance of phytoene (6.4µg), phytofluene (4.3µg), ζ-carotene (4.7µg) and lycopene (2.0µg), and increases in lutein (1.5-fold), β-carotene (2-fold) and xanthophylls (1.5-fold). Simultaneously chlorophyll content increased by 36% and 23% respectively for chlorophyll B and chlorophyll A. Depicted in Figure 3-5 (C) are the individual abundances of a selection of measured compounds from the gradients, quantities in µg were plotted per fraction. A separation can be made between gradient distributions of carotenoids like phytoene and lycopene and other carotenoid like β-carotene and lutein or xanthophylls and chlorophylls for the PSY1sense line. Phytoene and lycopene primarily accumulate in fractions 18-20 and the plastoglobules, whilst the other afore mentioned compounds demonstrate a three peak distribution.

A

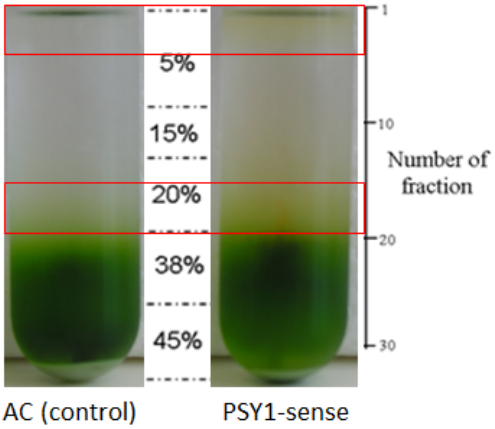

B

	phytoene	phyto-fluene	ζ-carotene	lycopene	lutein	β-Carotene	neo-xanthin	viola-xanthin	total carotenoid	α-toco-pherol	chloro-phyll B	chloro-phyll A
AC (control)	0.1	n.d.	n.d.	0.5	27.1	18	24.6	5.1	75.3	33.7	141.5	598.9
PSY1-sense	6.4	4.3	4.7	2	45.6	36.7	36.9	8	144.5	50.6	192.4	736.8

C

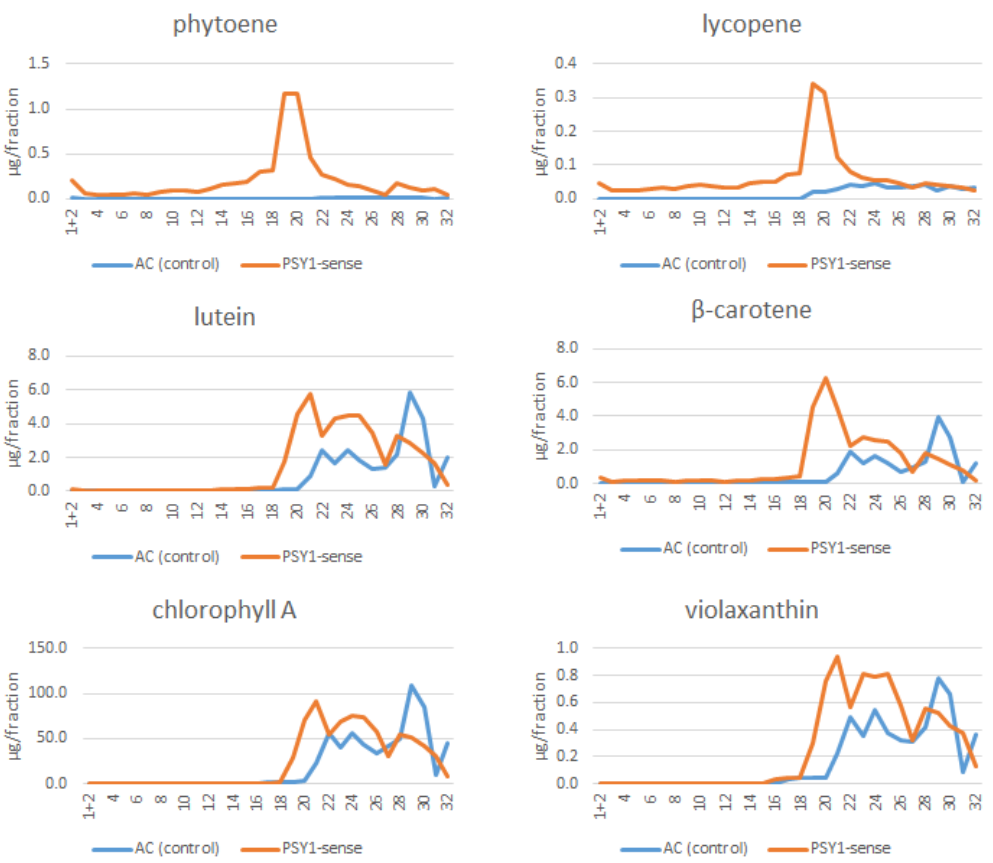

Figure 3-5: Subchromoplast fractionation of Ailsa Craig and PSY1sense at the mature green stage.

(A) Visualisation of sucrose gradients; demonstrating the effects of the overexpressed PSY1 enzyme. Appearance of a plastoglobule phase and a "ripe" carotenoid specific membrane phase at fraction 18-20. (B) Table overview of overall carotenoid and chlorophyll content in the individual gradients, units in µg. (n.d. = not detected) (c) Compounds specific abundances through the sucrose gradients based on UPLC analysis. The abundances correlate with intensely coloured phases in the gradients. Graphs for other compounds presented in table (B) can be found in the appendix (Figure A-11).

A

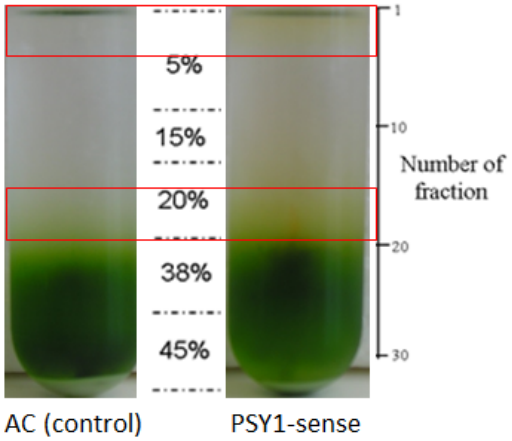

B

	phytoene	phyto-fluene	ζ-carotene	lycopene	β-carotene	lutein	viola-xanthin	neo-xanthin	total carotenoids	chloro-phyll B	chloro-phyll A	α-toco-pherol
AC	0.1	n.d.	n.d.	0.0	12.2	29.8	8.5	18.0	68.6	189.7	596.3	25.6
PSY-1 sense	5.7	3.5	4.3	0.6	21.2	38.7	10.1	18.9	103.0	191.9	594.3	38.4

C

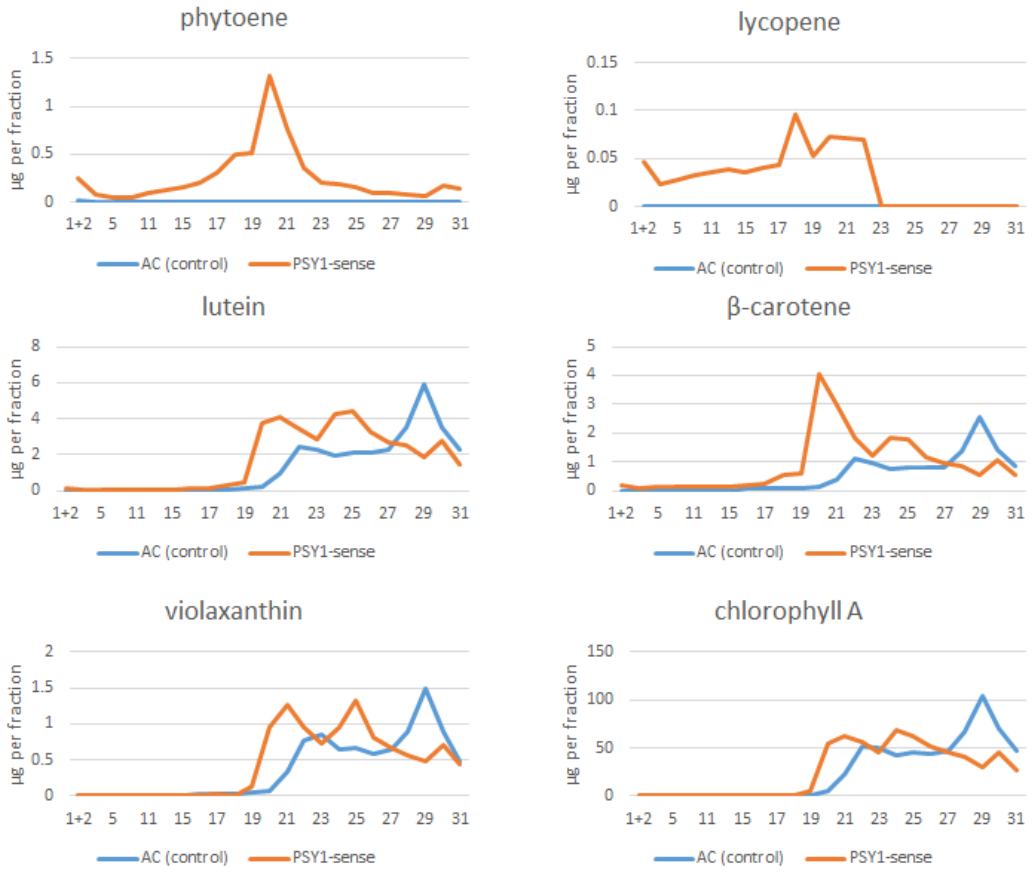

Figure 3-6. Second gradient set of PSY1sense and AC at mature green stage.
The trends for the different carotenoids and chlorophylls are overlapping with data in Figure 3-5. Three different membrane phases can be observed for the PSY1sense line, whilst the AC-line has only two membrane phases. A: sub-chloroplast gradients with outline of sucrose layers and collected fractions. B: table with summed quantities of carotenoids and chlorophylls in the gradients (units in µg, n.d. = not detected). C: compounds specific distribution per fraction of the gradient.

An important observation is the change that can be seen between the two analysed lines. The three peaks for PSY1sense are positioned at fractions 18-20, 23-25 and 28-30, the two peaks for the control line are positioned at fractions 22-24, and 28-30. β-carotene shows a change in ratio between the three peaks compared to lutein, violaxanthin and chlorophyll in the PSY1sense line. Where the other compounds have a roughly equal distribution over the three peaks, β-carotene is mainly accumulated in the peak that matches the single peaks for phytoene and lycopene, linking these three compounds based on their accumulation in ripe fruit. The control line demonstrates the opposite distribution, i.e. the highest peak for lutein, β-carotene, violaxanthin and chlorophyll A is the peak at fractions 28-30. Given the chromoplast phenotype of the PSY1sense mutant during early fruit development as described in section 3.2, the areas at fractions 18-20 and 23-25 can be linked to chromoplasts and differentiating chloroplasts respectively.

The duplicate gradient displays similar outcomes with a main peak at fractions 18-21 for the carotenes, whilst xanthophylls and chlorophylls are distributed over two and three membrane phases for the AC and PSY1sense lines respectively (Figure 3-6).

3.4.1.2. Analysis of PSY1sense and Ailsa Craig at breaker stage

Following the subplastid analysis of the mature green tissue the same approach was performed with material of the PSY1sense and Ailsa Craig lines at the breaker stage. For this study ~130 gram of pericarp material was used. The plastid isolation samples were placed in fractionation gradients for separation of the different structures. Gradients of both lines were analysed using UPLC techniques and the results are presented in Figure 3-7 and Figure 3-8. The gradients displayed in Figure 3-7 are used as the representative results for the description below, both sets of gradients depict similar trends and patterns.

As can be observed in Figure 3-7 (A), differences between the mutant and the control line have changed in contrast compared to the results with the mature green material. Both lines show a similar pattern through the gradient; the gradients both have a visible plastoglobule phase

(fractions 1 and 2) and contain two membrane phases at fractions 20-22 and 23-25. The PSY1sense line contains more carotenoids (Figure 3-7, B), the total carotenoid content in the PSY1sense gradient is approximately 50% higher than the control. Photosynthesis involved xanthophylls and chlorophylls are at approximately the same levels in both lines, as well as lutein. PSY1sense accumulated phytoene (7.5-fold), phytofluene (4-fold), lycopene (3.5-fold) and β-carotene (1.8-fold) at a higher level (Figure 3-7, B), which correlates with the stronger orange to red coloured areas in the gradients (fractions 1-2, 14-17: Figure 3-7, A). Looking in more details at the alignment of peaks in the membrane phase, it can be observed that in contrast to the mature green experiment the peaks are aligned at breaker stage. When comparing the distribution of the compounds between the two lines the ratio is different (Figure 3-7, C). Where for PSY1sense phytoene and lycopene show an equal division of abundance between the two peaks, and the plastoglobule phase for phytoene represents ~25% of the membrane peak's abundance, the peak height at fractions 20-22 for the control line is roughly 2-fold higher than the other peak at fractions 23-25. The other compounds displayed show a 2-fold higher peak at fractions 20-22 for PSY1sense, whilst for the control line the area at fractions 23-25 displays a plateau rather than a peak increasing the fold change between the two membrane phases to 2.5 fold.

A

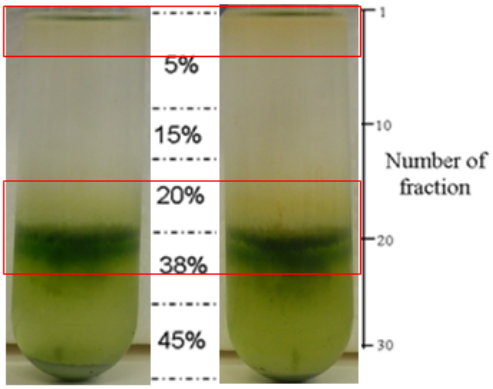

B

	phytoene	phyto-fluene	ζ-carotene	lycopene	lutein	β-carotene	viola-xanthin	neo-xanthin	total carotenoid	chloro-phyll B	chloro-phyll A	α-toco-pherol
AC (control)	0.6	0.6	0.0	2.6	28.6	29.1	18.9	3.7	84.0	79.0	393.1	49.3
PSY1sense	4.3	2.4	3.6	9.3	31.7	51.5	19.2	4.6	126.7	81.5	425.7	54.8

C

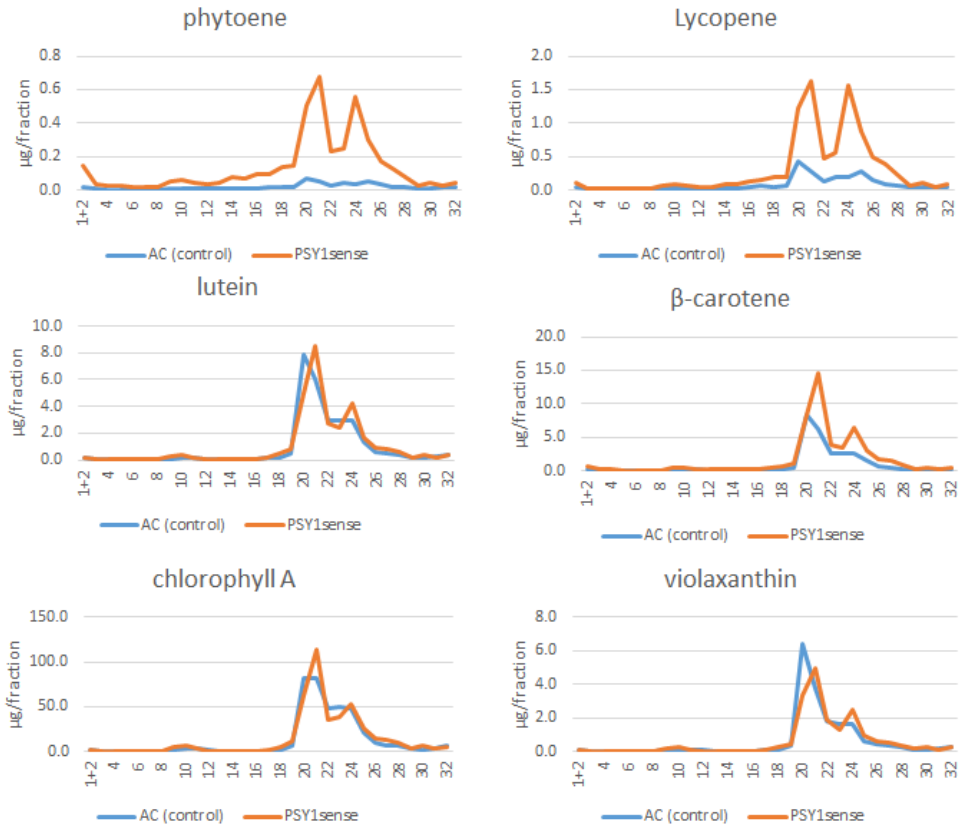

Figure 3-7. Subchromoplast fractionation of Ailsa Craig and PSY1sense at the breaker stage. (A) Visualisation of sucrose gradients; demonstrating the effects of the overexpressed PSY1 enzyme. Higher colour intensity of carotenoid enriched phases in the plastoglobule phase and a "ripe" carotenoid specific membrane phases at fraction 19-22 and 22-25. (B) Table overview of overall carotenoid and chlorophyll content in the individual gradients, units in µg. (n.d. = not detected) (c) Compounds specific abundances through the sucrose gradients based on UPLC analysis. The abundances correlate with intensely coloured phases in the gradients. Graphs for other compounds presented in table (B) can be found in the appendix (Figure A-12).

A

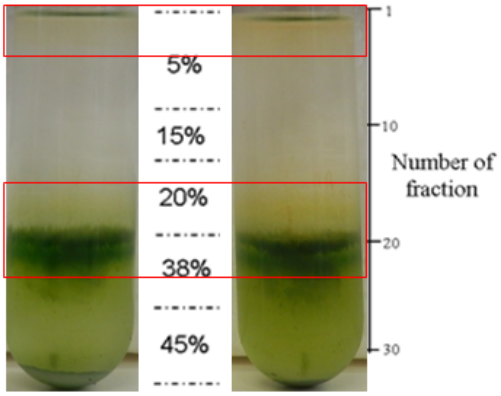

B

	phytoene	phyto-fluene	ζ-carotene	lycopene	β-carotene	lutein	viola-xanthin	neo-xanthin	total carotenoids	chloro-phyll B	chloro-phyll A	α-toco-pherol
AC	0.5	0.5	0.0	1.4	25.1	30.9	13.1	9.3	80.9	101.3	394.3	51.3
PSY-1 sense	4.8	2.8	4.3	6.7	51.3	39.1	14.8	12.4	136.1	115.0	476.3	61.7

C

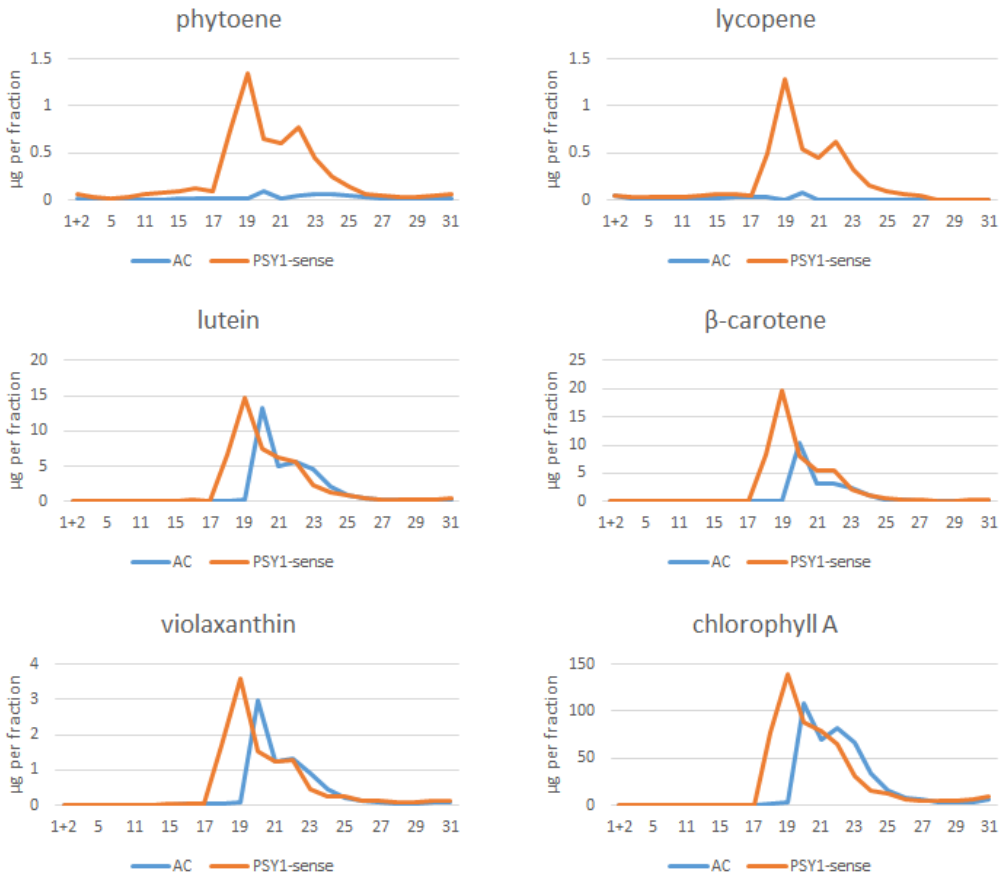

Figure 3-8. Second set of gradients for sub-plastid fractionation of PSY1sense and AC at breaker stage.

The two peak membrane phase pattern is found as well for these gradients. A shift in the distribution can be found for PSY1sense (C), this artefact is an effect of the method for fractionation. A: depiction of gradients and outline of stepwise sucrose gradient and fractions collected. B: table with abundances of carotenoids and chlorophylls, for sum of all fractions, units in µg. C: distribution of individual compounds per fraction.

Despite the shift in the outcome of the gradient for PSY1sense in the duplicate gradient (Figure 3-8, C), the two gradient sets can be considered equal. The visualisation of the gradients (Figure 3-8, A) displays no such shift, which suggests an artefact during the fraction collection.

In the sub-plastid experiments with the PSY1sense line, a relatively lower starch content could be observed in the gradient pellets compared to the control at the mature green and breaker stage (Figure 3-1, Figure 3-5 (A), Figure 3-7 (A)). This suggest a higher rate of starch degradation in the premature fruit where *psy1* is overexpressed.

3.4.1.3. Analysis of PSY1sense and Ailsa Craig at the ripe stage

Once the PSY1sense reaches the ripe stage the early carotenoid accumulation phenomenon is lost, and the fruit is not distinguishable anymore compared to the control except for an increase in carotenoid content (Figure 3-9, A-B). For this fractionation study ~100grams of ripened pericarp tissue per line was used to produce fractionation gradients from which 32 (1ml) fractions each were collected. Results described below are directly linked to the gradients displayed in Figure 3-9. Similar trends in carotenoid sequestration deposition were found in both gradient sets.

Similar to the results at the breaker stage, there is no difference in distribution over the gradients, both lines show the standard outcome for ripe tomato fruit with a plastoglobule layer and a single membrane layer. The effect of the overexpressed PSY1 enzyme is demonstrated by the 2-fold increase in both lycopene and β-carotene (Figure 3-9: B). No differences in carotenoid distribution can be observed between the two gradients when looking at the individual compounds presented in Figure 3-9 (C), but for lycopene with an increased sequestration in the plastoglobule phase. Any desynchronised effects on plastid development have been overcome by all chloroplasts being differentiated to chromoplast during the process of ripening.

Figure 3-10 displays the second set of gradients, which was analysed separately as a replicate of the first set. As the visualisations of the gradients of both sets demonstrate, outcomes were equal. The performed analyses suggest a similar trend between the two sets.

A

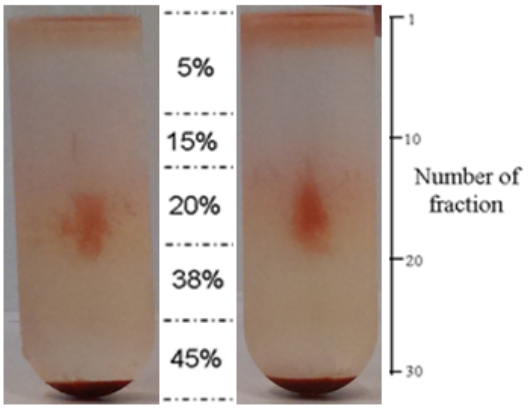

B

	AC (control)		PSY1-sense				
	phytoene	phytofluene	ζ-carotene	lycopene	β-carotene	lutein	total carotenoid	α-tocopherol
AC (control)	4.8	4.5	1.7	27.8	4.4	2.5	45.7	7.3
PSY1-sense	4.5	4.4	1.7	60.1	9.5	3.1	83.2	10.4

C

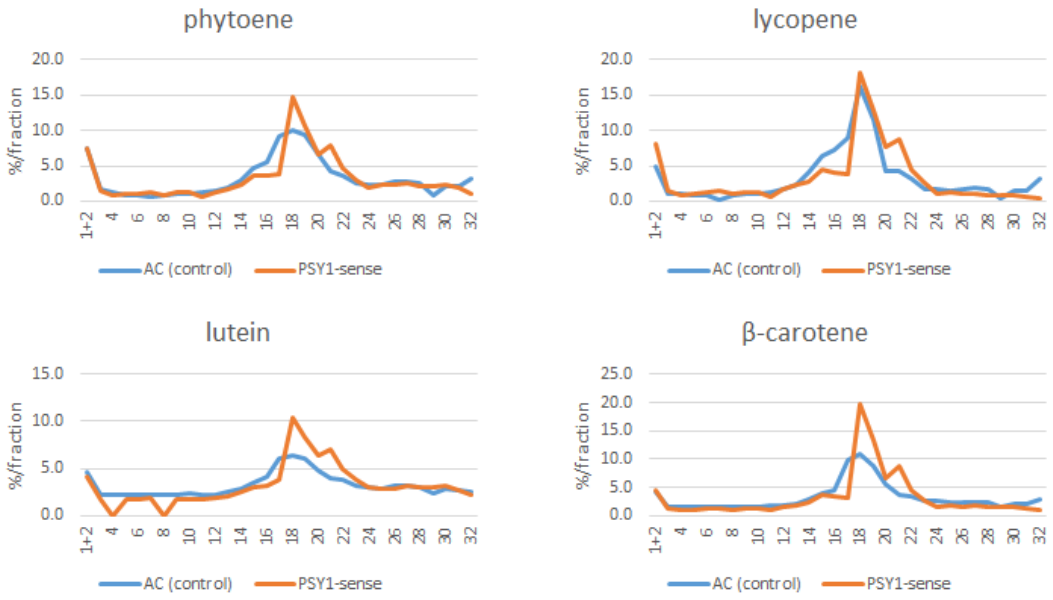

Figure 3-9. Subchromoplast fraction of PSY1sense and AC (control).

(A) Sucrose gradients of both lines with a coloured plastoglobule layer and a single membrane phase at fractions17-19. (B) Table presents carotenoid quantities (µg), sum of all fractions. (C) Overview of distribution of phytoene, lycopene, lutein and β-carotene abundances over the gradients, based on percentage ratios. Graphs for other compounds presented in table (B) can be found in the appendix (Figure A-13).

A

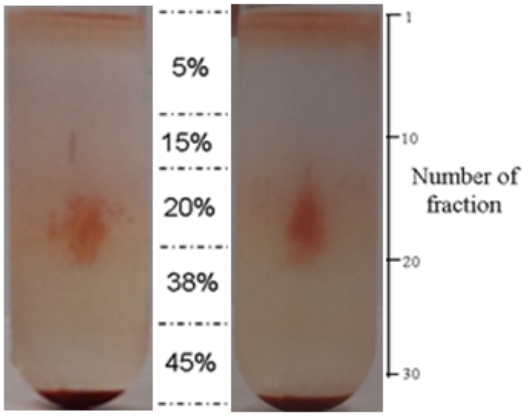

B

	phytoene	phyto-fluene	ζ-carotene	lycopene	β-carotene	lutein	total carotenoids	α-toco-pherol
AC	4.2	3.9	1.4	25.2	3.8	2.0	40.5	6.4
PSY1-sense	3.9	3.8	1.3	55.3	8.4	2.6	75.5	9.1

C

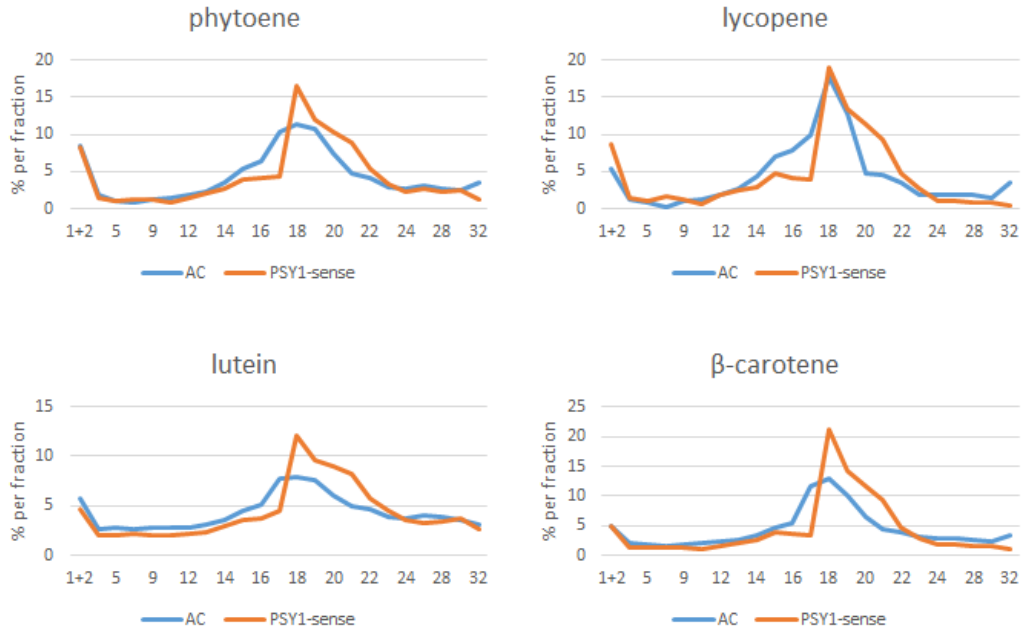

Figure 3-10. Gradient set two for the PSY1sense and AC line at the ripe stage.
This replicate displays a similar trend as observed for the first set presented in Figure 3-9. A: overview of gradients as observed after the establishment of the sucrose gradient. B: table presenting the quantities detected per compound as sum of the fractions (units in µg). C: relative distribution of individual compounds between the fractions.

3.4.1.4. Comparison of mature green and ripe Ailsa Craig fruit

In order to compare results from the PSY1sense mutant with an independent control a chloroplast/chromoplast mixture was created by making up a gradient with a chloroplast isolate and chromoplast isolate from mature green and ripe fruit respectively. This mixture can potentially clarify the appearance of additional membrane layers and shifts of those phases through the gradient. Therefore ~130 gram of pericarp material for both ripening stages was used for the plastid isolation after which one fourth of each isolate was added to a sucrose gradient tube. Six tubes were prepared in total, of which two contained one fourth of each isolate, creating a mix of both chloroplasts and chromoplasts. Two sets of gradients, consisting of ripe, mature green and mixed plastid isolates, were analysed. The outcomes are presented in Figure 3-11 and Figure 3-12; the two sets can be considered equal. Therefore the results as displayed in Figure 3-11 are described as a representation of both sets.

The sucrose gradients of the ripe and mature green samples turned out to be as expected, with a plastoglobule layer and membrane layer (fractions 18-21) for the ripe Ailsa Craig, and a membrane layer (fractions 23-29) but no plastoglobule layer for the mature green samples (Figure 3-11, A,C). When comparing the mixed sucrose gradients to the ripe and mature green gradients various visual differences can be detected. The stronger colour intensity of the “ripe” membrane and plastoglobule layers in the mixed samples on the one hand, and the absence of the “mature green” membrane layer at fractions 23-29 are distinctively different from the unmixed samples. When comparing the quantitative data for the individual compounds analysed, more specific differences can be found between the unmixed samples and the mixed sample. Compared to the sum of both unmixed samples, the mixed sample contains double the amount of lycopene, 20 and 40% less phytoene and β-carotene respectively, and a 90% loss of

A

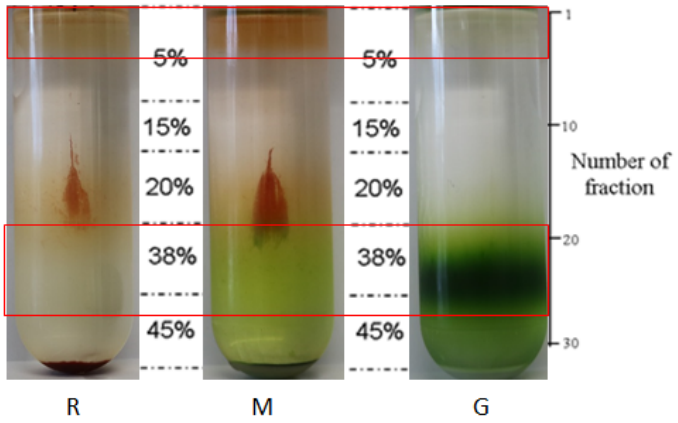

B

	phytoene	phyto-fluene	ζ-carotene	lycopene	β-carotene	lutein	neo-xanthin	viola-xanthin	total caro-tenoids	chloro-phyll B	chloro-phyll A	α-toco-pherol
ripe	6.25	4.11	2.06	29.42	4.53	2.73	n.d.	n.d.	49.10	n.d.	n.d.	1.46
mixed	4.88	4.81	2.09	60.02	7.97	5.06	0.88	0.47	86.18	11.31	45.57	2.38
mature green	0.13	n.d.	n.d.	0.14	9.57	23.61	9.60	4.23	47.28	139.60	451.14	3.09

C

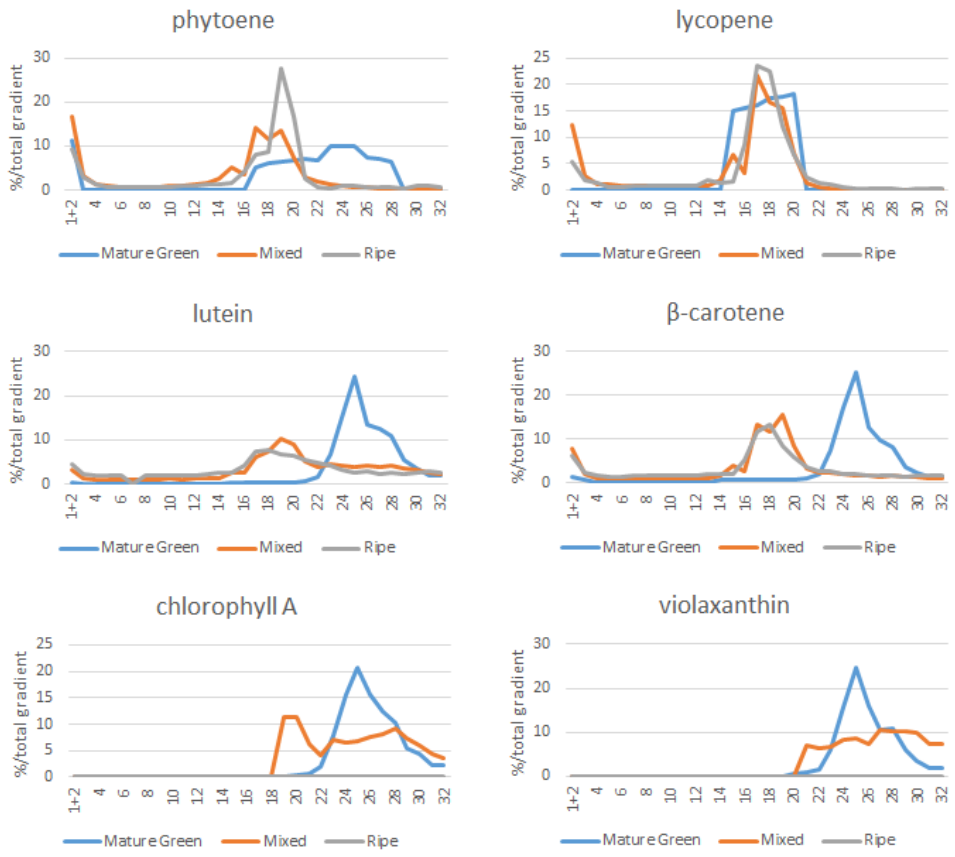

Figure 3-11. Comparing mature green and ripe fruit, material from the Ailsa Craig control line. (A) Gradient overview for ripe (R), mixed (M) and mature green (G). Key areas are marked in red: plastoglobule area and chloroplast membrane phase. (B) Table overview of detected carotenoids and the quantities for the sum of the gradients. Units in µg. (n.d. = not detected) (C) Gradient distributions per detected compound, data is presented as a percentage of the total amount per gradient. Key carotenoid representatives and a xanthophyll and chlorophyll representative are presented. Graphs for other compounds presented in table (B) can be found in the appendix (Figure A-14).

A

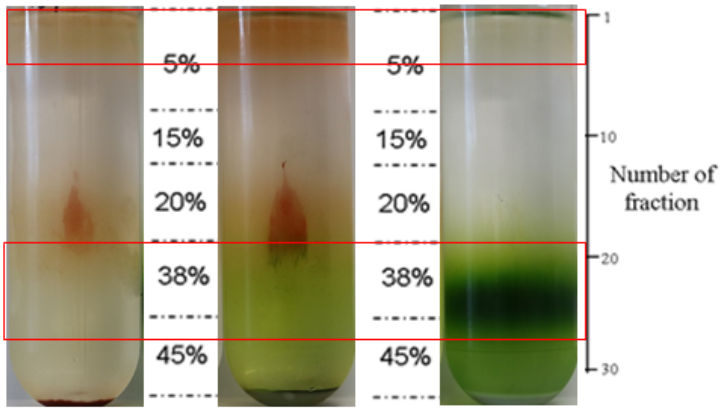

B

	Phyto-phytoene	Phyto-fluene	ζ-carotene	lycopene	β-carotene	lutein	Viola-xanthin	Neo-xanthin	total carotenoids	Chloro-phyll B	Chloro-phyll A	α-toco-pherol
ripe	3.5	3.4	1.5	26.9	4.6	3	n.d.	n.d.	42.9	n.d.	n.d.	1
mixed	5.5	5.5	1.8	65.3	10.5	4.7	0.6	1	94.9	9	43.6	2.7
mature green	0.1	n.d.	n.d.	0.3	21.1	28.6	7	13.1	70.2	142.9	522.3	4.3

C

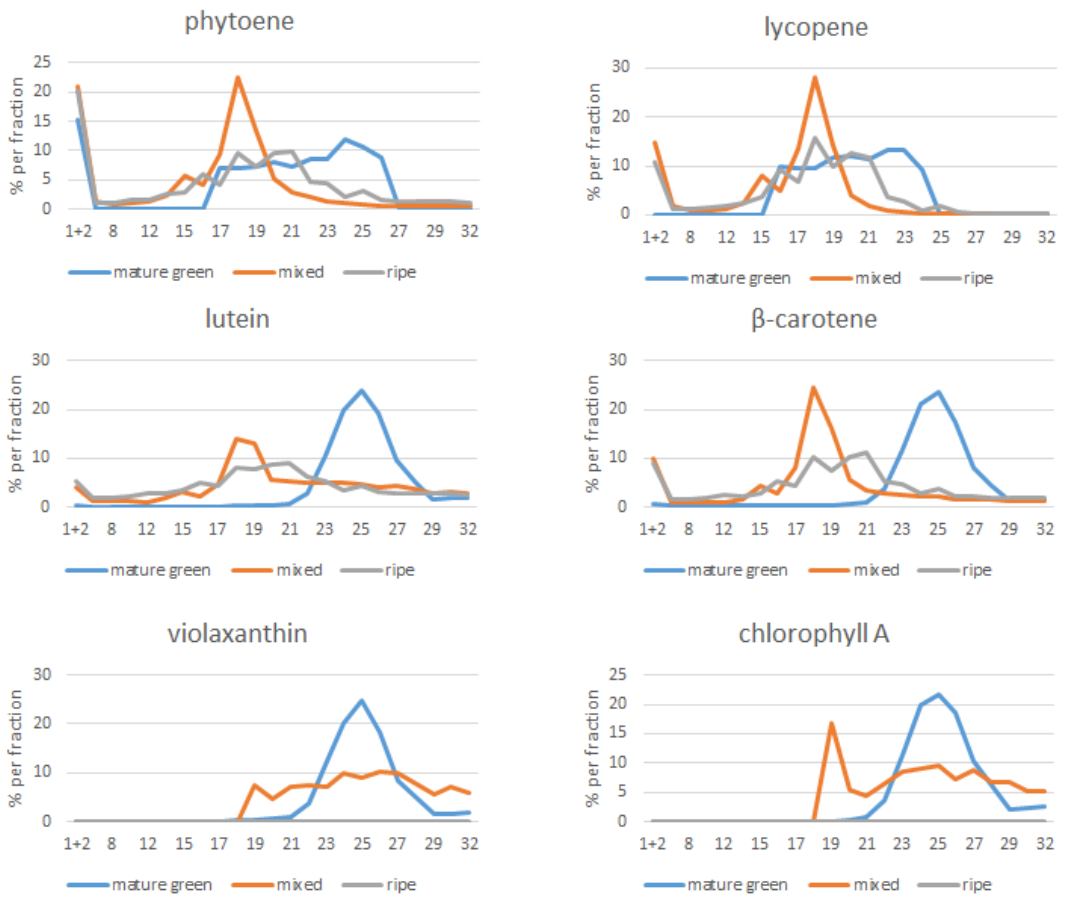

Figure 3-12. Second set of sub-plastid fractionation for ripe, mature green and mixed plastid isolates.

A similar trend can be observed comparing the outcomes presented in Figure 3-11. A: visualisation of sucrose gradients. B: table with carotenoid and chlorophyll content as sum of the gradients (units in µg, n.d. = not detected). C: graphical overview of distribution through the gradient for a selected cluster of compounds analysed.

xanthophylls and chlorophylls was observed (Figure 3-11, B). Interestingly no loss in carotenoid content was found for the mixed sample, which might be caused by differences in plastid isolate loaded. If the disintegration of the chloroplast structures occurred during the initial mixing of the isolates, these substrates and precursors could be released and utilised by enzymes present in the mixture. Such an event could explain the difference in carotene content between the individual gradients and the mixed gradients.

The abundances shown in Table 3-1, from the pellets of the gradients, display differences in carotenoid content between samples. The absence of the dark green membrane layer and the loss of 90% of xanthophylls and chlorophylls can be explained by investigating the debris-pellet in the tube. The pellet of the mixed sample gradients contained a thick green layer, which was missing in the unmixed mature green gradients. Analysis of carotenoid and chlorophyll content in the pellets shows a clear increase in xanthophyll and chlorophyll increase in the mixed pellets (Table 3-1).

Table 3-1. Carotenoid and chlorophyll abundances of sucrose gradients.
Analysis was performed to clarify the observations on the distribution pattern in the gradients of mixed plastid isolates (3.4.1.4). Outcomes for both gradients are displayed. Pellets of ripe, mature green and mixed sampled gradients were screened. Units in µg/pellet, 3 replicates per gradient screened. Underlined values indicate loss of compound from the gradient.

	gradient set I			**gradient set II**		
	ripe	**mixed**	**mature green**	**ripe**	**mixed**	**mature green**
phytoene	24 ±0.4	28 ±0.3	0.1 ±0	29 ±0.4	23 ±0.2	0.1 ±0.0
phytofluene	22 ±0.7	27 ±1.0	n.d.	26 ±0.3	22 ±0.2	n.d.
ζ-carotene	6 ±0.2	10 ±2	n.d.	7 ±0.0	6 ±1	n.d.
lycopene	101 ±2	119 ±2	n.d.	94 ±9	121 ±5	n.d.
β-carotene	72 ±2	118 ±4	8 ±0.5	84 ±0.6	104 ±1	8 ±1.0
lutein	13 ±0.3	63 ±2	13 ±0.8	15 ±0.1	53 ±1.2	14 ±1
violaxanthin	n.d.	24 ±2	8 ±0.2	n.d.	22 ±1	8 ±0.8
neoxanthin	n.d.	8 ±2	3 ±0.1	n.d.	6 ±0.6	3 ±0.3
chlorophyll B	n.d.	239 ±2	78 ±3	n.d.	200 ±2	82 ±4
chlorophyll A	n.d.	739 ±12	266 ±10	n.d.	654 ±3	261 ±15
α-tocopherol	68 ±2	98 ±2	18 ±2	75 ±1	83 ±2	18 ±2

This could explain the absence of any dark green layer in the gradient itself, as by an unknown reason the membrane structures of that specific layer might have been disrupted which could cause the deposition of these membrane structures in the pellet. At the base of the red “ripe” membrane layer a small layer of green membrane structures can be found. The localisation of the different membrane structures can be linked to the distribution of the individual compounds quantified using UPLC techniques. The distribution data of the mixed samples shows a peak between fractions 16 and 22, with e.g. phytoene at the top side of the segment and chlorophyll A on the bottom side of the segment (Figure 3-11, C). At a much lower intensity, the mixed sample also shows a “green” membrane layer at the same segment of the gradient as the unmixed mature green samples, primarily found for the xanthophylls and chlorophylls. All compounds presented in Figure 3-11 (C) are solely or simultaneously accumulated at fractions 16-22, showing that compounds like β-carotene and lutein have been sequestered in those membrane structures. Although mixing the samples of the unripe and ripe fruit, development stages showed some distinctly different outcomes compared to the unmixed samples, as the two individual peaks of the unmixed samples were not disturbed. No third peak that could be linked to differentiating chloroplasts could be detected during the analysis.

3.4.2. Adaptations in chromoplast sequestration stimulated by changes in carotenoid profiles.

Within the range of selected mutant lines, a variety of carotenoid profiles is available. These profiles occur due to overactivity or inactivity of key steps in the carotenoid pathway. The different carotenoid types and their respective ratios can alter sequestration pattern within the plastid sub-structures. A comparison between *cis*-carotenoid enriched and high *trans*-lycopene lines was performed and their sequestration pattern has been studied. Changes in deposition in different storage parts can be observed between *cis*- and *trans*-carotenoids, furthermore xanthophylls play a role. While in section 3.4.1.The comparison of the carotenoid content was based on absolute levels per fraction, a different approach is required for this section. As the aim is to determine ratio changes in accumulation between plastid sub-structures a relative

comparison is performed whereby the relative amount per carotenoid is determined through calculation of the percentage of the fraction content compared to the sum of each carotenoid indicated as %/fraction.

3.4.2.1. The influence of all-trans lycopene and β-carotene on carotenoid sequestration.

A subplastid study was performed on ripe fruit material of Ailsa Craig, *rr*-mutant and *og^c*, to obtain insights in any alteration of carotenoid sequestration within chromoplasts with a high lycopene/ low β-carotene profile (*og^c*). Furthermore, the *rr*-mutant, functioning as a null-mutant, can dilucidate how chromoplasts sequester carotenoids at low quantities. For this study ~150 grams of pericarp tissue was used per line and the obtained plastid isolate per sample was assembled into sucrose gradients to separate the different plastid structures. Collected fractions were subjected to a chloroform/methanol extraction before analysis using UPLC techniques took place. Figure 3-13 provides an overview of the achieved outcomes, displaying one of the two gradients per tube as a representative for the experiment. Chromatograms of the *rr*-mutant, the null-mutant, can be found in the appendix (Figure A-4).

When comparing the Ailsa Craig to the pale yellow *rr*-mutant the main observations are the difference in colour intensity and the similar distribution within their gradients. The plastids in the *rr*-mutant isolate can be considered chromoplast with the distinct plastoglobule layer at the top of the gradient (Figure 3-13, A). The range of carotenoids present in the *rr*-mutant fruit is reduced to lutein and β-carotene, and a trace of lycopene. Besides those carotenoids α-tocopherol has been detected, as the knock-out mutation generating the phenotype is targeting the carotenoid biosynthesis specifically. The amounts of lutein and β-carotene were reduced 2-fold and 8-fold respectively. Lycopene content diminished to ~0.3% of the content in the control

A

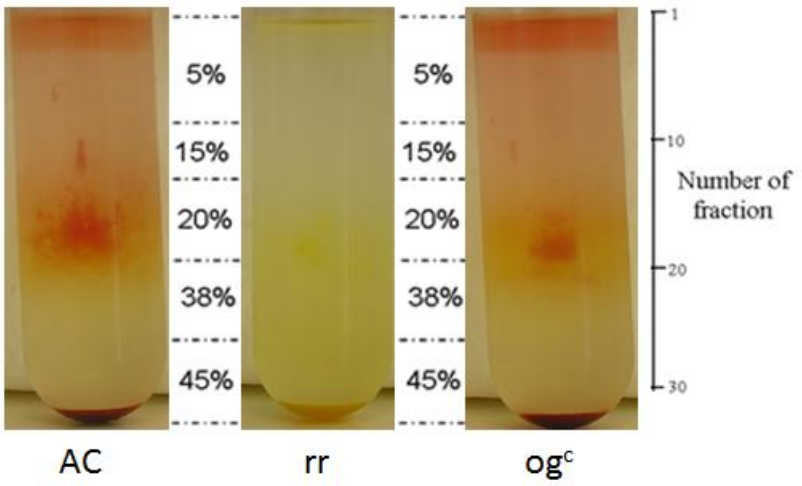

B

	phytoene	phyto-fluene	ζ-carotene	lycopene	β-carotene	lutein	total carotenoid content	α-tocopherol
AC (control)	11.5	10.6	3.2	104.5	17.4	4.6	151.8	19.3
ogᶜ (mutant)	11.5	10.0	4.8	100.9	6.0	6.7	139.8	16.0
rr (mutant)	0.0	0.0	0.0	0.3	2.2	2.1	4.6	13.3

C

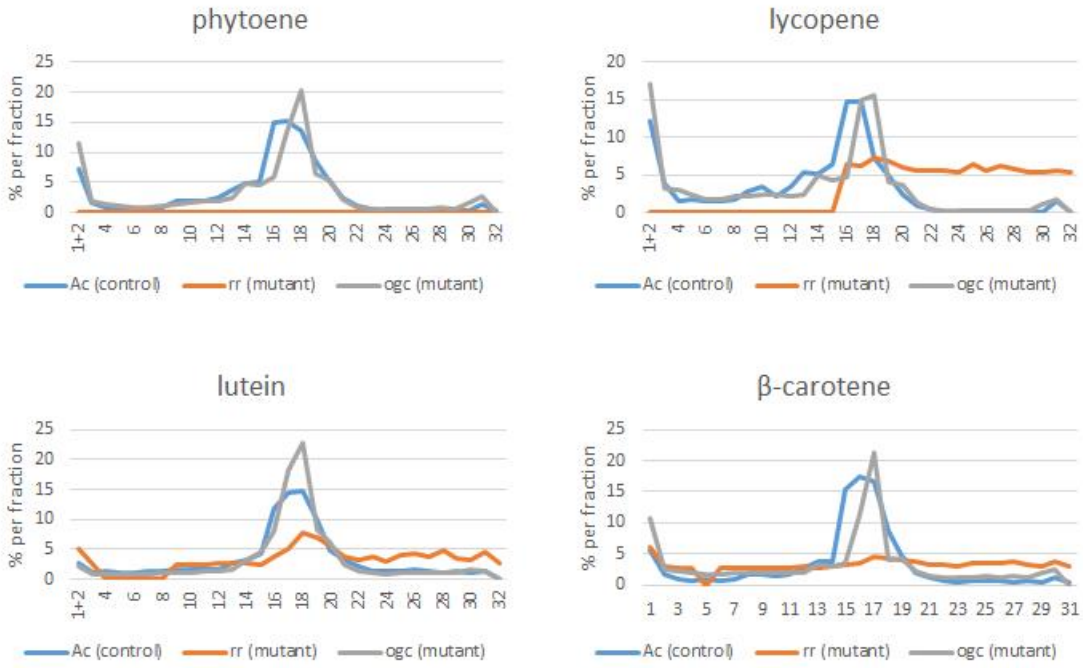

Figure 3-13. Overview of subchromoplast fractionation for Ailsa Craig, rr-mutant and ogᶜ.
All three samples show the expected distribution with a plastoglobule and membrane phase (A), although the intensity of the phases differs between them. (B) Table depicts the abundances measured for the different compounds units in µg per full gradient. (C) Graphical visualisation of distribution through the gradient for phytoene, lycopene, lutein and β-carotene, matching the visual appearance of the gradients as shown in section A. Graphs for other compounds presented in table (B) can be found in the appendix (Figure A-15).

A

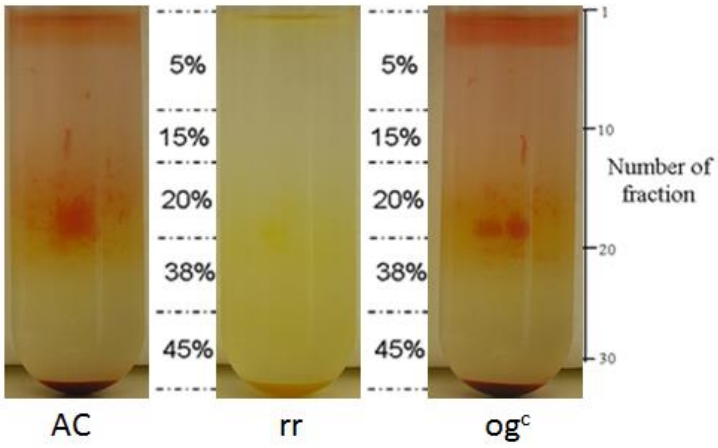

B

	phytoene	phyto-fluene	ζ-carotene	lycopene	β-carotene	lutein	total carotenoids	α-toco pherol
AC	10.3	9.3	2.8	91.6	15.5	4.4	133.9	18.1
rr-mutant	0.0	0.0	0.0	0.0	1.4	1.8	3.2	10.5
ogC	11.0	8.6	3.1	38.5	3.2	5.9	70.3	13.1

C

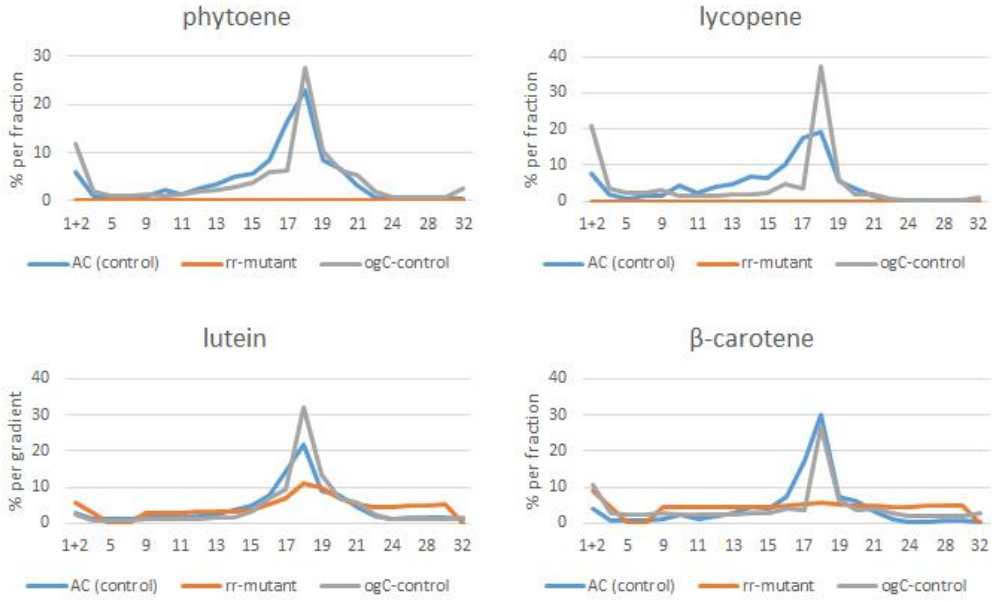

Figure 3-14. Duplicate gradients for the AC, rr and ogᶜ lines.
Outcomes between the two sets of gradients depict the same trends on deposition of carotenoids (set 1 displayed in Figure 3-13). A: Display of gradients, outlined with fractions and sucrose percentage indicators. B: abundances of carotenoids detected, summed amounts for each gradient. C: visual outline for selected carotenoids, distribution per fraction for each compound.

line, which sums up the total carotenoid content to be reduced by 97%. From the three carotenoids identified, lycopene was only found from the 16th fractions down. The two carotenoids, lutein and β-carotene, display a regular pattern with minor peaks at the plastoglobule and membranes phases. The *og^c* mutant and the Ailsa Craig control display the same phases at roughly the same positions in the gradients. Both samples have the same shades of colour going through the gradient, from the top down pink, orange and pale yellow respectively. The *og^c* plastoglobule phase is visually more intense than the Ailsa Craig phase, however the membrane phase of the Ailsa Craig line is more dense and seems to contain more crystals than for the *og^c* line (Figure 3-13,A). Investigating the carotenoid content in more depth, the general content within the gradients is approximately the same at ~150 and 140µg per gradient for Ailsa Craig and *og^c* respectively. Screening the individual carotenoids shows equal amounts of phytoene, phytofluene, and increases for ζ-carotene and lutein. A 3-fold decrease in β-carotene content is most noticeable. Since the lycopene β-cyclase is inhibited, the drop in β-carotene levels is a logical consequence. The absolute differences in lycopene levels seem contrasting with the expected higher accumulation in the *og^c* line, however, comparing the relative abundances in both lines the lycopene content is ~5% higher in the *og^c* line. The visual differences between the *og^c* line and the control in both the plastoglobule and membrane phase are depicted in more detail in Figure 3-13 (C). The fractional distribution of the different compounds measured confirms the stronger colouration of the plastoglobule phase for the *og^c* line. As laid out in Figure 3-13 (C), the sequestration of phytoene, lycopene and β-carotene in the plastoglobules of the *og^c* line is approximately 5% higher for all three carotenoids. Lutein on the other hand does not show the same trend, as its sequestration in the plastoglobule phase is equal to the control.

Figure 3-14 displays the second set of gradients with sub-plastid samples for the AC, *rr* and *og^c* lines. A similar trend in accumulation of carotenoids in the plastoglobules can be observed for the *og^c* line.

3.4.2.2. The role of cis-carotenoids in carotenoid deposition in chromoplasts

Both the *tan* and *tan*-CRTI lines are inhibited in the activity of the CRT-ISO enzymes which executes the biosynthetic step from poly-*cis*-lycopene to all-*trans*-lycopene. The *tan*-CRTI line contains an expression vector for the bacterial CRTI gene, its corresponding enzyme bypasses the endogenous biosynthesis to all-*trans*-lycopene. To study the effect of *cis*-carotenoids and specifically poly-*cis*-lycopene, a sub-plastid study was conducted on pericarp tissue from ripe fruit for the above mentioned lines. ~100 grams of pericarp tissue was collected per line for the plastid isolations. Like aforementioned sub-plastid experiments, plastid isolates were disrupted, separated on density in a sucrose gradient and fractions were analysed using UPLC techniques. Chromatograms and spectra of the increased *cis*-carotenoids, and other detected compounds, can be found in the appendix (Figure A-1, Figure A-5). Clusters of gradients were analysed and presented in Figure 3-15 and Figure 3-16, Figure 3-15 is referred to in the description below.

The gradients, depicted in Figure 3-15 (A), show a standard distribution profile with a plastoglobule phase and a membrane phase. The diminished levels of the red all-*trans*-lycopene is clearly noticeable in both the *tan* lines by the distinct yellow to orange colouration. Furthermore, the *tan-crtI* line shows a larger and lower membrane phase than the control and the *tan* line, covering fractions 18-24 of the gradient instead of 16-20. The plastoglobule phase of the *tan* is paler than the *tan*-CRTI phase, moreover in general the background seems more yellow for the *tan* than the *tan*-CRTI line. The inhibition of CRT-ISO in the *tan* line caused the accumulation of a range of *cis*-carotenoids, especially neurosporene and poly-*cis*-lycopene. The high *cis*-carotenoid content showed a phenotype in which carotenoids are accumulated in the plastoglobules to a lesser extent. Instead the sequestration in the membrane structures was relatively higher compared to the control line.

Despite the 50% higher carotenoid content the *tan* line does not look particularly more intense in colour than the *tan*-CRTI line, this can be explained by the carotenoid profile with 3- and 2-fold increase in colourless phytoene and phytofluene respectively (Figure 3-15, B). The block at

the CRT-ISO enzyme as it occurs in the *tan* line allows for the accumulation of the precursors of all-*trans*-lycopene; poly-*cis*-lycopene, neurosporene, ζ-carotene, phytofluene and phytoene. Poly-*cis*-lycopene and neurosporene are not accumulated in red ripe fruit, where the CRT-ISO enzyme is still functional, however phytofluene and ζ-carotene are normally found. A 4-, 2- and 9-fold increase in accumulation of phytoene, phytofluene and ζ-carotene was found respectively.

As the change in fruit colour suggests, orange instead of red, lycopene content in the *tan* sample is reduced by ~90% (Figure 3-15, B). Likewise, both β-carotene and lutein show a 50% decrease in abundance. In Figure 3-15 (C), the individual carotenoids are put out in graphs displaying the distribution per fraction. When comparing the *tan* line to the control, it demonstrates a reduction in carotenoid deposition in the plastoglobules for all carotenoids presented in Figure 3-15 (C), when detected in both lines. As well compared to the *tan*-CRTI line, a reduction for all presented carotenoids, except for all-*trans*-lycopene and poly-*cis*-lycopene is observed.

Activity of the CRTI enzyme in the *tan*-CRTI line modifies the carotenoid profile as observed in the *tan* line on several aspects. All-*trans*-lycopene content covers 58% of the total carotenoid content in the control line, in the *tan* line this is reduced to 4%, for the *tan*-CRTI line the all-*trans*-lycopene level is recovered to 13%. The ability of the CRTI enzyme to bypass the endogenous pathway and utilise the pool of phytoene, which accumulates in the *tan* line due to the CRT-ISO inhibition, diminishes the excess phytoene. Moreover, the phytoene that would otherwise be used as a precursor for the endogenous pathway, does not end up being utilised by the enzymes up-stream of CRT-ISO and therefore an increase in phytofluene and ζ-carotene is not found. The amount of poly-*cis*-lycopene present in the *tan*-CRTI line represents 37% of the total carotenoid content, which is higher than the 27% found in the *tan* line (Figure 3-15, B).

A

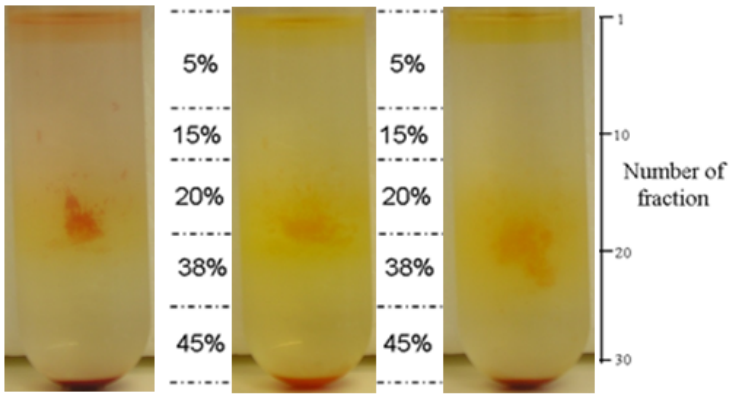

B

	phytoene	phyto-fluene	ζ-carotene	neuro-sporene	poly-cis-lycopene	all-trans-lycopene	β-carotene	lutein	total carotenoids	α-tocopherol
AC (control)	4.3	4.2	1.7	0.0	0.0	24.4	4.8	2.4	41.8	6.6
tangerine	15.8	9.9	14.7	6.8	21.1	2.7	4.5	1.4	77.0	7.3
tangerine/ crtI	3.5	4.8	3.2	5.3	18.6	6.6	5.8	2.5	50.2	17.4

C

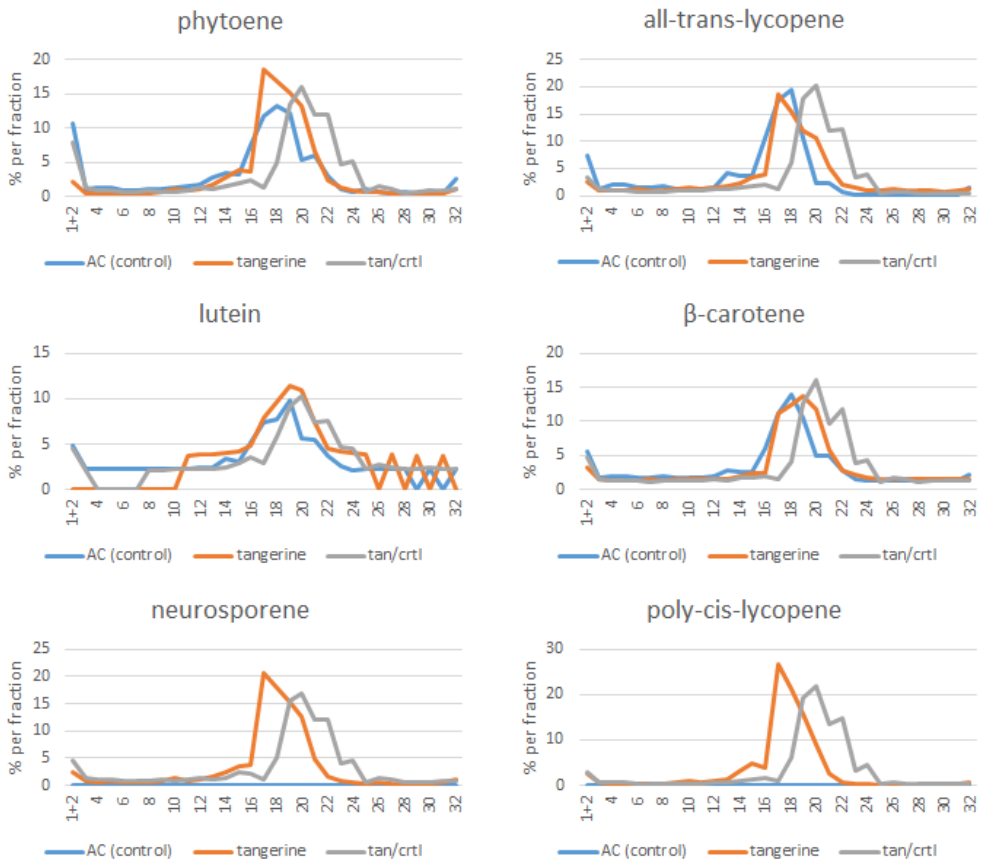

Figure 3-15. AC, tan and tan-CRTI subchromoplast fractionation.
(A) Sucrose gradients of the three plastid isolates, after plastid disruption. All three gradients show a visible plastoglobule phase and a distinct membrane phase. (B) Quantitative overview of carotenoid content in the gradients, sum of all fractions (µg). (C) Graphical display of individually analysed fractions per gradient. Visualising the pattern of colour deposition in the gradients. Graphs for other compounds presented in table (B) can be found in the appendix (Figure A-16).

A

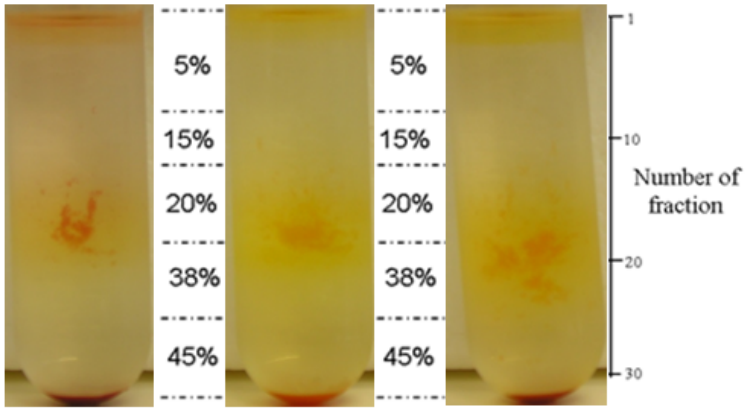

B

	phytoene	phyto-fluene	ζ-carotene	neuro-Sporene	poly-cis-lycopene	lycopene	β-carotene	lutein	total carotenoids	α-tocopherol
AC	4.0	3.8	1.5	0.0	0.0	22.4	4.2	2.1	37.9	6.4
tan	13.9	8.6	12.8	5.8	18.4	2.3	3.8	1.1	66.7	7.1
tan-crtl	3.5	4.0	4.4	3.8	5.7	2.1	5.2	2.4	31.1	19.0

C

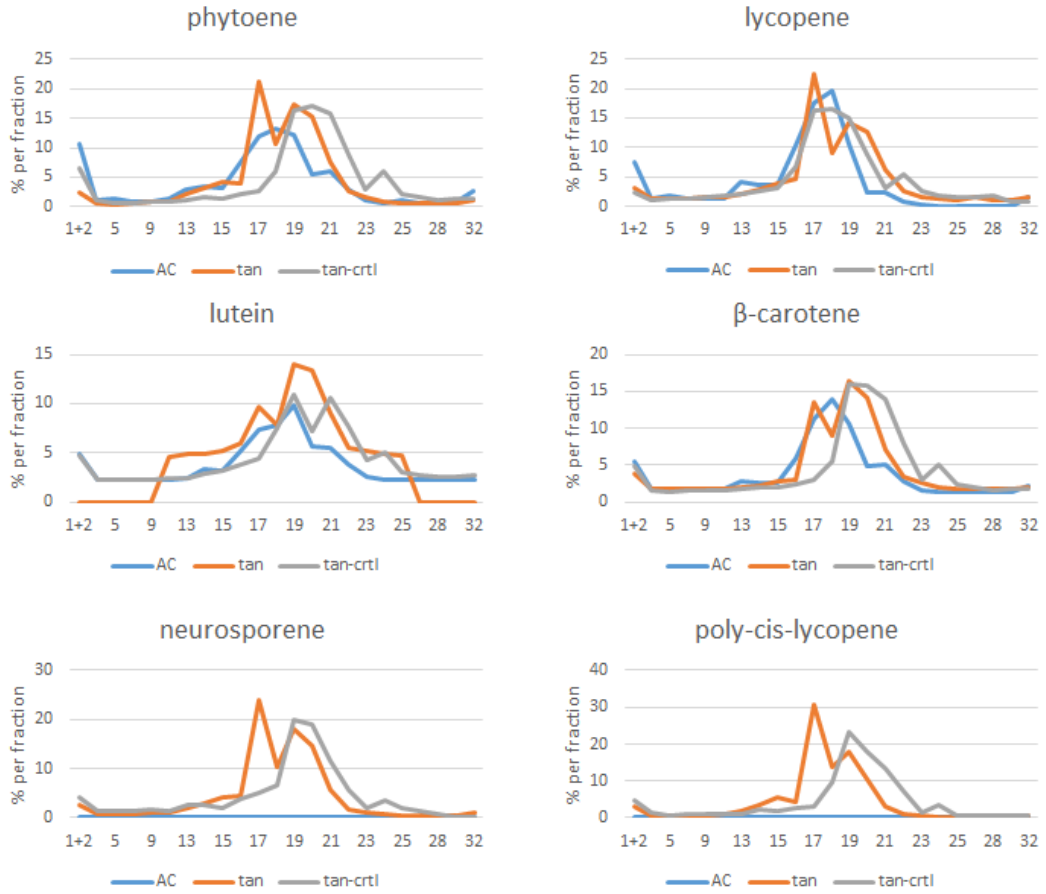

Figure 3-16. Duplicate gradients for AC, tan and tan-CRTI.
Gradient profiles display the same trends as seen for the gradients described in Figure 3-15. A: display of sucrose gradients and outline of sucrose abundances as stacked in gradient. B: abundances of compounds detected in the gradients. C: outline of relative distribution for selected compounds per fraction.

When looking at the distribution of the individual carotenoids through the gradient (Figure 3-15, C), the *tan*-CRTI resembles the control more than the *tan* line. For lutein, phytoene and β-carotene the pattern matches the control, for neurosporene and all-*trans*-lycopene the pattern is more similar to the *tan* line. Poly-*cis*-lycopene cannot be compared to the control line, as it is not accumulated in the wild type Ailsa Craig, however the ratio of accumulation in the plastoglobules is higher for the *tan*-CRTI line. As the control line shows a trend of higher carotenoid content in the plastoglobules, this trend can be linked to poly-*cis*-lycopene.

3.4.3. Preliminary screening of plastid and sequestration proteins

As described in the methods chapter (section 2.5) sub plastid fraction were processed into multiple extracts. The analysis for the studies on the various tomato mutant lines perturbed in carotenoid biosynthesis as displayed in section 3.4.1 and 3.4.2 was performed using the carotenoid extracts. To obtain more in depth information on the sequestration mechanisms and plastid adaptability towards altered carotenoid content fraction protein extracts can be used to determine the presence of relevant proteins in specific fractions as presented previously in literature (Nogueira et al., 2013). Targets for protein analysis are for example carotenoid biosynthesis enzymes (PSY1, LCY-B), Chloroplast membrane proteins (TIC, TOC), and sequestration enzyme (Plastoglobulin and fibrillin). Following the carotenoid analysis of the samples of the various fractionation samples preliminary screen were performed to calibrate protein levels for the protein gels and western blots. Protein levels in the performed studies were not sufficient for consistent analysis of the selected fractions. For further analysis of the sequestration mechanisms on the protein level higher amounts of starting material could be considered to obtain a higher yield of proteins.

3.5. Discussion

3.5.1. Carotenoids and chloroplasts to chromoplasts differentiation

Chromoplast differentiation in tomato fruit takes place at the onset of ripening. Various processes are involved in the differentiation process, of which starch degradation and induction by light play an important role (Llorente et al., 2016; Télef et al., 2006). As mentioned earlier in this thesis, PIFs are involved in the modulation of the responses to light signals and therefore regulate carotenoid biosynthesis on a transcriptional level (Leivar et al., 2008; Llorente et al., 2016; Toledo-Ortiz et al., 2014). PIFs control carotenoid biosynthesis by restricting carotenoid gene expression, based on the light intensity during shading effects; the impact of direct sunlight during the fruit ripening, abolishes the presence of these PIFs, which in turn elevates the regulation on the genes in the carotenoid pathway. The unhindered activity of the carotenoid pathway allows for the high carotenoid accumulation as observed in ripe tomato fruit (Llorente et al., 2016). In a way the overexpression of *psy1* in the PSY1sense line gives a similar response in immature fruit as during ripening, although the activity is still regulated to maintain the xanthophyll balance for photosynthetic activity. Different compared to the ripening stage were the β-carotene hydroxylase is inactive. The process of de-starching during fruit ripening is another influential factor that can regulate carotenoid accumulation. Experiments in which mature green pericarp discs were subjected to different sucrose levels demonstrate a delayed accumulation of lycopene; this delay is linked to the expression levels of *psy1*, which are promoted by lower sucrose levels in the fruit (Télef et al., 2006). The correlation between ripening and a declining starch content, which is reduced to soluble sugars, was found during a study on plastid starch synthesis and degradation. The balance between the synthesis and degradation of starch, as found in immature fruit, switches towards degradation at the mature stage of the fruit (Luengwilai and Beckles, 2009).Therefore both light and sugars can be considered triggers of carotenoid accumulation during ripening, although the direct effect of sugars on *psy1* expression would suggest a stronger influence.

The flux of the intermediate carotenoids in the respective pathway seems to be restricted at the β-carotene hydroxylase step, which is responsible for the biosynthesis of xanthophylls. As PIFs are tightly regulating the carotenoid content in chloroplasts the balance and abundance of xanthophylls is maintained and accumulation of “ripe fruit” related carotenes takes place. (Llorente et al., 2016). Carotenes are not normally involved in the photo protection of the photosystems present in chloroplasts, this suggests the need for of premature chromoplast differentiation (Figure 3-17). The significantly larger capacity of chromoplasts allows these plastid types to function as better storage sinks for carotenoids, compared to chloroplasts [reviewed by (Egea et al., 2010)].

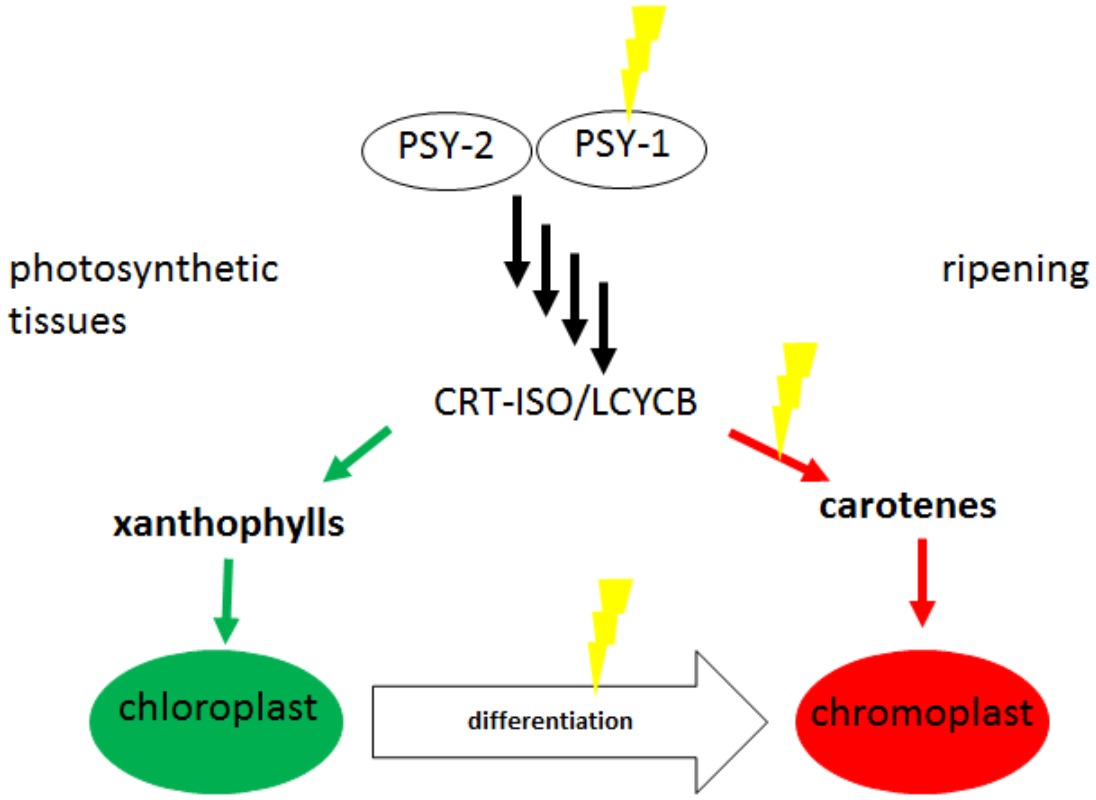

Figure 3-17. The effect of constitutive expression of *psy1* in tomato plants.
With a higher concentration of the PSY1 enzyme more carotenoid precursors are synthesised, the excess carotenes are accumulated and require a storage sink (indicated by lightning symbol). To provide a sequestration site, premature chromoplast biogenesis occurs to facilitate this.

-

Research on *psy* overexpression in Arabidopsis demonstrates similar effects on chromoplast differentiation in callus, roots, and seeds, where chromoplast structures, carotenoid crystals and/or increased carotenoid levels are observed (Maass et al., 2009; Shewmaker et al., 1999). It is important to mention that screened tissue types in which the chromoplast-like structures were found are not endogenous sites of chloroplast biogenesis. The PSY1sense mutant line displays an interesting phenotype, taking into account the aforementioned processes, where carotene accumulation takes place before ripening commences. The accumulation of carotenes besides xanthophylls in the developing tomato fruit is directly linked to the constitutive overexpression of the *psy1* gene. The presence of chlorophylls and xanthophylls is maintained since the fruit is still developing. For optimised photosynthesis activity a conserved profile of xanthophylls as dominant carotenoids is required [reviewed by (DellaPenna and Pogson, 2006)]. The increased carotenoid content, carotenes especially, occurs simultaneously with chloroplast to chromoplast differentiation; as chromoplast-like structures are found in the immature fruit of the PSY1sense line (Fraser et al., 2007). The sub organelle modifications found during the sub-plastid fractionations performed demonstrate the changes in plastid organisation. The presence of a carotene enriched phase in the sucrose gradients of mature green samples from PSY1sense material suggests the partial differentiation of chloroplasts to chromoplasts. Therefore it could be suggested that this additional phase in the gradients is indeed consisting of intermediate plastid structures. Proof for intermediate plastids between chloroplasts and chromoplasts has been found via confocal microscopy and transcriptomics (Egea et al., 2011; Kahlau and Bock, 2008); this “intermediate” phase could consist of differentiating membrane structures.

The breaker stage is a natural point for the wild-type fruit to start its chromoplast biogenesis, therefore most plastids have differentiated to chromoplasts or are in the differentiation process. The synthesised compounds are present earlier than normal chromoplast biogenesis occurs, and the high capacity sequestration sink is not fully available. Therefore it is likely that the excess of

carotenoids is stored in any plastid membrane structure, before chromoplast biogenesis has caught up. The degradation of the chloroplast derived structures as observed when mature green and ripe material are mixed for sub-plastid fractionation does not fit in with the assumption of adaptability as demonstrated in the single source samples of the AC and PSY-1 lines for sub-plastid analysis. This suggests that the interaction between chloroplast and chromoplast structures potentially disintegrates the chloroplasts structures e.g. thylakoid membranes, an effect that is prevented at the breaker stage due to the capacity of differentiating plastid structures to adopt the role of chloroplast structures.

3.5.2. The integration of *cis*- and *trans*-carotenoids into chromoplast specific lipid structures

From all plastid types, the chromoplast has the highest sequestration capacity for carotenoids. Out of the five types of chromoplast substructures, tomato chromoplasts consist of globules, membranes and crystals in an interactive manner i.e. crystalloids in membranous structures (Harris and Spurr, 1969). Plastoglobules are considered carotenoid storage sinks, which start to increase in numbers and size during chromoplast formation (Bian et al., 2011). It is proposed that phytoene is transported to the plastoglobules when the membranous structures of the chromoplasts are saturated; the accumulated carotenoids, which cause the saturation, in the membrane structures are often crystalline lycopene and β-carotene (Nogueira et al., 2013). Differences in distribution of carotenoids between the sub-chromoplast structures were detected during the analysis of sub-plastid fractionations of various mutant lines perturbed in carotenoid biosynthesis. A clear difference between the isomers of lycopene, specifically *cis*- and *trans*-lycopene configuration, was found when investigating the sequestration ratios between sub-chromoplast structures.

The inhibition of CRT-ISO in the *tan* line caused the accumulation of a range of *cis*-carotenoids, especially neurosporene and poly-*cis*-lycopene. The high *cis*-carotenoid content showed a phenotype in which carotenoids are accumulated in the plastoglobules to a lesser extent.

Instead the sequestration in the membrane structures was relatively higher compared to the control line. A hypothesised concept on the interaction between carotenoids and fatty acid chains in chromoplast lipids, studied in models consisting of mono-lipid bilayers and purified carotenoids, demonstrated the effect of *cis*-carotenoids on the structural interaction between fatty acid chains and carotenoids during sequestration (Widomska et al., 2009). The modelling on *cis*- and *trans*-carotenoids was executed on xanthophylls, which with their polar ends are predicted to anchor outside of the hydrophobic core of lipid bilayers. The accumulation of otherwise transient precursor carotenoids, can change the membrane structure of the lipid bilayer compared to the normally accumulated all-*trans*-lycopene. The structural alignment of hydrophobic carotenes within the hydrophobic environment could cause structural changes to the membranes allowing for more efficient sequestration. Moreover, the integration of single carotenoid molecules, compared to crystals, could be less disruptive for membrane activity and stability. Crystal formation would be the case for all-*trans*-lycopene and β-carotene, which is turn would saturate the membrane structures sooner.

Previous studies on sub-organelle sequestration of carotenoids demonstrated a matching effect for β-carotene, compared to the PSY1sense line, when two bacterial carotenoid genes (*crtB* and *crtI*) are expressed in plants and β-carotene levels are increased (Nogueira et al., 2013). In the case of the high β-carotene line the accumulation in the membrane phase is higher than in the control line, demonstrating the effect of this carotenoid on the plastoglobule to membrane sequestration ratio. The effect of xanthophylls on the membrane structural and dynamic properties could play a role in the sequestration potential of carotenoids in general (Gruszecki and Strzałka, 2005). In chromoplasts a higher all-*trans*-lycopene content, as found in the og^c and PSY1sense lines, caused a higher carotenoid deposition of lycopene in the plastoglobules. Increased carotenoid distribution towards the plastoglobules was not as widespread for the PSY1sense line as for the og^c line. For PSY1sense most carotenoids did not display any change in distribution, apart from all-*trans*-lycopene where a higher plastoglobule content was observed.

The occurrence of chloroplast structure degradation and the parallel sequestration of carotenoids in the chromoplast structures confirms this hypothesis; a relative increase in *trans*-lycopene content is shown and the ratio of accumulation preference is shifted to the plastoglobules.

4. Ectopic expression of isoprenoid pathways: the development of a synthetic biology vector library using the Golden Braid modular cloning system.

4.1. Introduction

The study of secondary metabolites has been focussed on increasing levels by overexpressing biosynthesis genes. While the positive outcomes of these attempt are numerous, the actual absolute increases are not as dramatic to warrant the cost of commercialising GMO products. In the example of carotenoids, isoprenoids synthesised in the plastid, overexpression of *psy1* or *dxs* (upstream pathway) in tomato led to a 1.5- and 1.6-fold increase respectively (Enfissi et al., 2005; Fraser et al., 2007). It is suggested that a reason for the restricted increases is due to the strict feedback regulation that is present at the endogenous sites of biosynthesis for these metabolites. Targeting a pathway segment or branch to another cellular compartment, where no such regulatory systems are in place, could therefore potentially allow for a stronger response to increased biosynthetic activity.

As shown in chapter 3, carotenoids can cause organelle structures and membranes to change depending on changes in carotenoid profiles and quantities. This leads to the hypothesis that carotenoids can accumulate in other cellular compartments, different than their endogenous sites of sequestration, when synthesised there. Given the presence of an upstream isoprenoid precursor pathway (MVA) in the cytosol, this cellular location was selected as a potential exogenous location. In a similar way, generating an enlarged pool of isoprenoid precursors by co-expressing the MEP pathway, endogenous to the plastid, in the cytosol could boost isoprenoid levels in a broader scheme. The objectives of this chapter are related to the assembly of a library of overexpression constructs using a novel plant cloning method: Golden Braid Cloning.

In order to meet the objective a synthetic biology approach was set up utilising the cloning method mentioned above. The Golden Braid method allows for scar-benign cloning and assembly of multi-gene constructs containing independent TUs per gene of interest (Sarrion-Perdigones et al., 2011). To achieve the biosynthesis of carotenoids in the cytosol, bacterial

(*P. ananatis*) carotenoid genes were used for overexpression constructs in an attempt to generate cytosolic carotenoid biosynthesis (Misawa and Shimada, 1998). For genes of the 2-C-methyl-D-erythritol 4-phosphate (MEP) pathway, genes of *C. annuum* were used when available, otherwise bacterial genes from *E. coli* were utilised. Design and assembly of GB patches, parts and constructs are described.

4.2. Golden Braid cloning

A general overview of modular cloning systems including Golden Braid Cloning is presented in chapter 1 (Synthetic and Systems Biology & Modular cloning systems). One of the developments described is the two updates of the GB-system, GB2.0 and GB3.0. Since at the start of this project GB2.0 was available, this version is utilised during the project and will therefore be the version to be described and discussed in more detail.

GB cloning is based on the utility of type IIs restriction enzymes, the GB2.0 version uses the enzymes *BsaI*, *BtgZI* and *BsmBI* for its cloning steps (Sarrion-Perdigones et al., 2013). The digestion overhang created by these enzymes is located near but not on the recognition site, which allows for elimination of the recognition site upon ligation with a DNA fragment containing a matching overhang. The GB-vectors are designed including a complicated system of these restriction sites in both orientations, to allow for targeted elimination and maintenance of the restriction sites depending on their requirements for future cloning steps (Sarrion-Perdigones et al., 2011).

The GB system consist of three different stages to assemble TUs: patches, parts and super parts. The super parts represent the three main elements of a TU: the promoter, terminator and coding sequence. The range of sub-elements, which are part of these super parts i.e. untranslated regions (UTRs), signalling peptides, un-transcribed regions, are divided over eleven parts that can be used in standardised combinations. A variety of constructs used in molecular biology have been included in the system; an overview can be found in Figure 4-1. GB cloning offers a

design website (https://gbcloning.upv.es/, GB3.0) for the design of any part or vector and contains a database with standardised vectors, a range of tutorials and assembly tools.

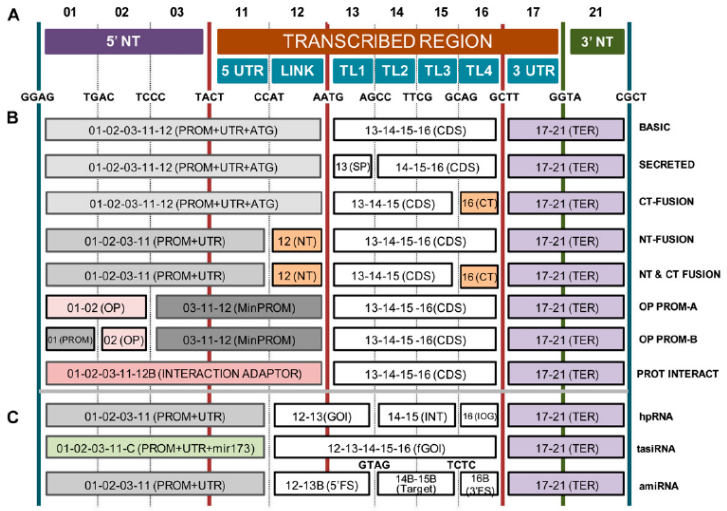

Figure 4-1. Display of standardised parts and super parts available in GB2.0.
The range varies from overexpression to silencing constructs to protein fusions. Eleven different parts are available split over three different super parts representing promoter, terminator and coding sequence segments. Parts as indicated in this overview have distinct sequences for linking parts in the TU-assembly phase. Figure adapted from (Sarrion-Perdigones et al., 2013).

The first step of the system is to select the DNA sequences to clone and use the GB-software to establish the protocols for domestication and assembly. Domestication is required to add the right extensions to the DNA fragment to enable a smooth assembly of the different parts. Furthermore, any restriction sites for the enzymes *BsaI*, *BtgZI* and *BsmBI* should be removed from the sequences to avoid any unspecific digestions during the process of cloning. For this purpose the GB system includes a procedure of single nucleotide mismatch incorporation via PCR (Sarrion-Perdigones et al., 2013). The PCR fragments generated during this process are called “patches” and will be linked into parts or super parts during assembly into the entry vector (pUPD) of the system. The entry vectors can be used to assemble TUs in the binary vectors when matched in the right combinations of parts.

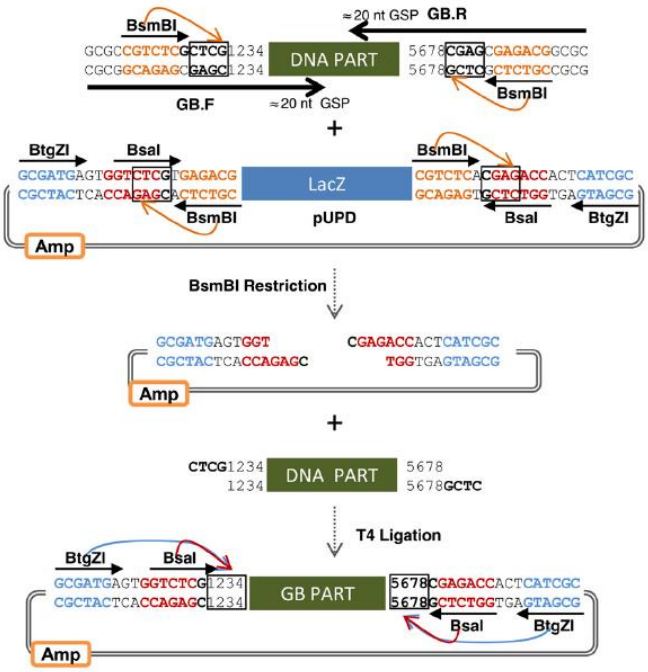

Figure 4-2. Overview of assembly of domesticated DNA parts in the entry vector (pUPD).
The setup of the entry vector includes all three restriction enzymes and allows for an easy assembly into the entry vector and further steps towards the binary vectors. Type IIs enzymes cut away from the restriction site and therefore allow for scar benign cloning of TU's and complex binary assemblies. Figure adapted from (Sarrion-Perdigones et al., 2013).

Assembly of TUs is a straightforward system with the use of type IIs restriction enzymes. The overhang sequences are designed in such a way that GB-parts are assembled in the order as designed and the repeated restriction and ligation steps allow for a very efficient cloning reaction. Screening of positive clones can be easily performed via blue/white screening since any unmodified vector (entry or binary) contains a *lacZ*-gene on the cloning site (Figure 4-2**Error! eference source not found.**). The binary vectors of the GB system are split into two branches, α and Ω vectors, and these branches require different enzymes for the construction of TUs in those vectors. In order to construct TUs in the α-vectors the *BsaI* enzyme is required, while a combination of *BsmBI*/*BtgZI* enzymes is required for the Ω-vectors.

Once TUs are assembled in the binary vectors, these cassettes can be linked via the "braiding" setup of the GB system. The borders of the cloning sites of the binary vectors contain the three restriction sites, in different orientations, that make up the GB-system and are therefore interchangeable between α- and Ω-vectors. An infinite loop exchange and addition of TUs

between α- and Ω-vectors can occur as long as vector size and stability do not interfere with the process (Sarrion-Perdigones et al., 2011). Every exchange merges two TUs into a multi-gene vector, or multi-gene vectors into a larger multi-gene vector. For example transcriptional unit A in vector α1 and transcriptional unit B in vector α2 can be jointed and transferred to vector Ω1 in a single restriction/ligation reaction. A simple schematic is depicted in Figure 4-3.

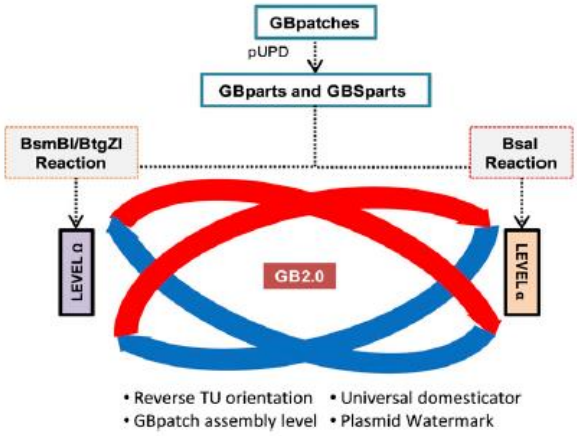

Figure 4-3. Generic overview of the GB process.
Patches are assembled into parts in the entry vector, after which TUs are generated in the binary vectors. Linking of TUs can take place between binary vectors via the "braiding" concept, where due to the scar-benign system no limitations to the number of linkages should exist. Figure adapted from (Sarrion-Perdigones et al., 2013).

4.3. Results: modular cloning library for isoprenoid biosynthesis

4.3.1. Selection of coding sequences and design of parts

The objective of this chapter was the ectopic expression approach to determine whether isoprenoids pathway genes can synthesise isoprenoids in cellular compartments where these enzymes are normally not present. Typically an isoprenoid pathway branch requires several gene products to utilise common precursors and generate a functional pathway. Therefore the GB-system, with its potential for multi-gene constructs, is a very appealing cloning system, as all required genes can be constructed into TUs and linked into a single vector. Two pathway segments of the plastidial isoprenoid pathway, the carotenoid pathway and the upstream MEP

pathway, were selected. Both pathways have been intensely studied in a range of organisms and their functions in the plastids or bacterial cells have been elucidated. In an attempt to avoid any regulatory mechanisms, the sequences for the genes of interest were selected from organisms other than *S. lycopersicum* and *N. benthamiana* to avoid any inhibitory effects in the model plants commonly utilised within the research group. Sources of the genes were *P. ananatis* for the bacterial carotenoid genes, and *C. annuum* and *E. coli* for the genes of the MEP-pathway. C. annuum was selected, despite its close relation to S. lycopersicum, for its high accumulation of carotenoids and the release of the genomic sequence (Guzman et al., 2010; Qin et al., 2014). The high accumulation of carotenoids is proposed to be the result of strong biochemical flux through the carotenoid pathway and the upstream MEP pathway (Hornero-Méndez et al., 2000). Parts were generated using the software available on the GB cloning website, which allows for the *in silico* design and assembly for all stages of the system (Vazquez-Vilar et al., 2015).

With the pepper (*Capsicum*) genome sequenced (Qin et al., 2014), and the matching intensity of carotenoid accumulation compared to tomato, using MEP pathway genes from pepper appeared a logical solution. Annotations of the MEP genes were limited and only the 1-deoxy-D-xylulose-5-phosphate synthase (DXS) was available. Therefore the other gene sequences of the pathway were taken from *E. coli*. The biosynthesis of carotenoids in micro-organisms differs from plants on the level of enzyme functionality; one of these enzymes is the CRTI enzyme which can perform all steps from phytoene to lycopene (Fraser et al., 1992). This is a simplified version of the process in plants where four enzymes (PDS, Z-ISO, ZDS, and CRT-ISO) are required. With only three enzymes required to produce lycopene from isoprenoid precursors, CRTE, CRTB and CRTI, choosing these enzymes reduces the required cloning steps. Moreover, stable overexpression lines of these genes in various combinations in tomato, have been studied targeting these heterologous gene products to the plastid (Nogueira et al., 2013). For the overexpression of these genes TUs were designed with a Cauliflower Mosaic virus 35s-promoter

(CaMV35S) with an optimised 5'UTR region and a double terminator, consisting of Thsp (terminator of the *Arabidopsis thaliana* heat shock protein 18.2 gene) and Tnos (terminator of nopaline synthase gene from *Agrobacterium tumefaciens*) terminators. The promoter and terminator parts are based on a successful construct which resulted in interesting outcomes on ketocarotenoid biosynthesis in tomato (Nogueira et al., 2017). The CaMV35S-promoter without a targeting peptide (tp) is expected to deliver the enzymes to the cytosol. A second promoter part was designed which, in addition to the actual promoter included a new transcription start site and a transcribed tp (transit peptide of the *Pisum sativum* L. RuBisCO small subunit) for the plastid, to be used as a comparison during the screening experiments. The sequences used for the generation of the GB parts can be found in the appendix (Fasta sequences for cloning), a summarised overview of the parts is presented in Table 4-1.

Table 4-1. Overview of generated parts for the GB system.
13 parts created via the domestication procedure. Two promoter part, one terminator part and 10 coding sequences. Removal of internal type IIs restriction sites was done by incorporation of single nucleotide mismatches by PCR, number of patches indicated the relevant restrictions sites in the sequences. Patches created by PCR were cloned into the entry vector.

DNA part	*Function*	*Size (bp)*	*Patches*
CaMV35S-5'UTR	Promoter	977	2
CaMV35S-5'UTR-TP	Promoter	1148	2
Thsp/Tnos	Terminator	539	2
DXS_{ca}	Coding sequence	2159	3
DXR_{ec}	Coding sequence	1197	3
MCT_{ec}	Coding sequence	711	1
CMK_{ec}	Coding sequence	852	2
MDS_{ec}	Coding sequence	480	2
HDS_{ec}	Coding sequence	1119	3
HDR_{ec}	Coding sequence	951	1

$CRTE_{pa}$	Coding sequence	909	2
$CRTB_{pa}$	Coding sequence	930	1
$CRTI_{pa}$	Coding sequence	1479	2

The first stage of the GB system is the domestication; this step was successfully performed for all parts presented in Table 4-1. The patches generated by PCR have the required extensions for the GB system and help to remove any internal type IIs restriction sites in the sequences. The expected patch size for the two promoter parts were 124bp and 918bp for the cytosolic CaMV35S promoter and 124bp and 1088bp for the plastid transient peptide and promoter combination part, the Thsp/Tnos terminator required two patches (370bp and 233bp). Confirmation of PCR fragments with the correct sizes is displayed in Figure 4-4. Primers for each patch designed per part are displayed in the appendix (Table A-1).

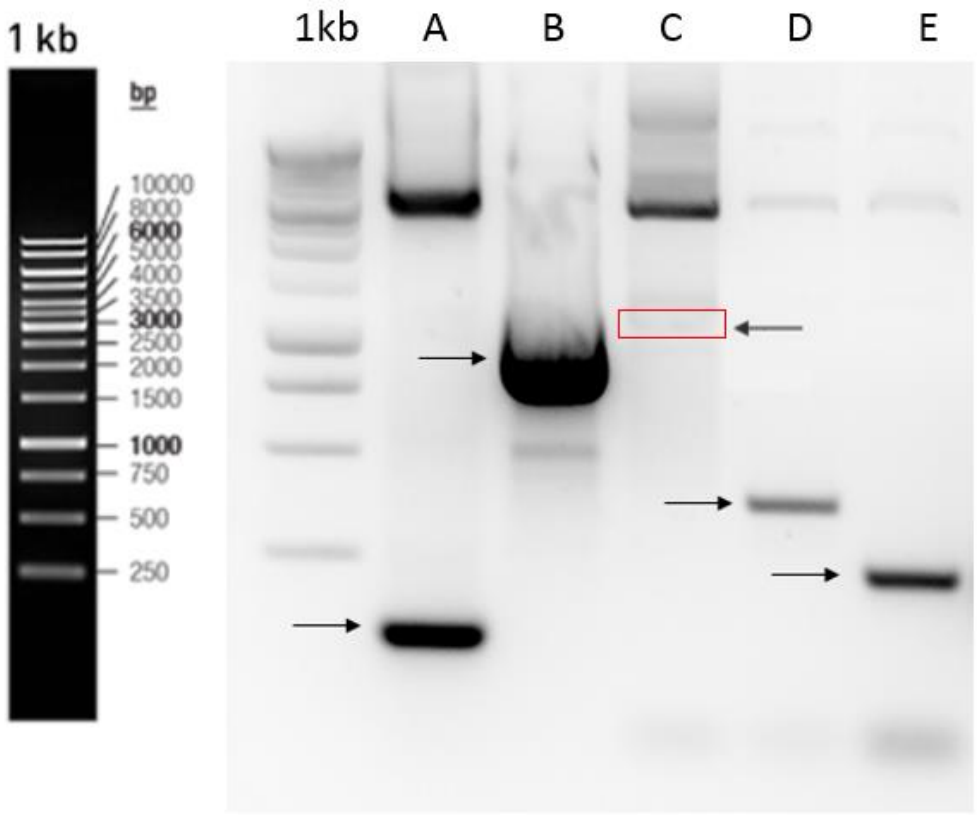

Figure 4-4. Display of gel electrophoresis for patches of the promoter and terminator parts. Domestication PCR fragments of Promoter and terminator parts for the GB-library. GB patches: (A) CaMV35S promoter patch I, (B) CaMV35S promoter patch II, (C) CaMV35S promoter +transit peptide patch II, weak band indicated by the red square, (D) Thsp/Tnos terminator patch I, (E) Thsp/Tnos terminator patch II. Index of the 1kb ladder on the left hand side.

The coding sequences for the MEP pathway were derived from RNA of *C. annuum* (bell pepper leaves) and genomic DNA from *E. coli* (strain: DH5α), RNA and genomic DNA were extracted as described in materials and methods. The GB parts for *dxs* and *dxr* were split into three patches each of 238bp, 1759bp, 176bp and 607bp, 410bp, 267bp respectively. The sequence for *hds* was split into three patches of 100bp, 759bp and 347bp, while *mct* and *hdr* did not possess any internal type IIs restriction sites and both were generated as one patch of 746bp and 986bp respectively. The parts for *cmk* and *mds* contained one internal type IIs restriction site each and their preparation required two patches each, sizes were 340bp, 573bp and 325bp and 216bp respectively. Confirmation of PCR generated patches via gel electrophoresis is displayed in Figure 4-5.

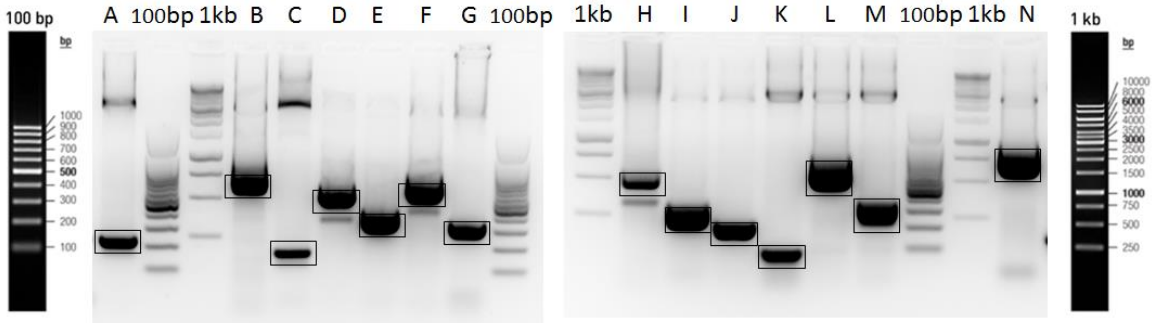

Figure 4-5. PCR fragments generated for the patches of MEP gene GB parts.
Domestication PCR products for GB-library. PCR products of interest are indicated with black squares. (A-C) patches DXS_{ca}, (D-E) patches DXR_{ec}, (F) patch MCT_{ec}, (G-H) patches CMK_{ec}, (I-J) patches MDS_{ec}, (K-M) patches HDS_{ec} and (N) patch HDR_{ec}. Index of 100bp and 1kb ladders on the left and right hand side

The bacterial carotenoid genes *crtE*, *crtB* and *crtI* were obtained from a bacterial vector containing all three gene sequences. Genetic material for this vector was obtained from *P. ananatis*. The sequence for the *crtB* part (965bp) required extensions to fit the GB system, a single nucleotide polymorphism was not necessary to eliminate restriction sites. *CrtE* and *crtI* were split into two patches each, the patches were 157bp, 813bp and 379bp, 1161bp respectively. Patches were generated using PCR and screening for their size using gel electrophoresis (Figure 4-6).

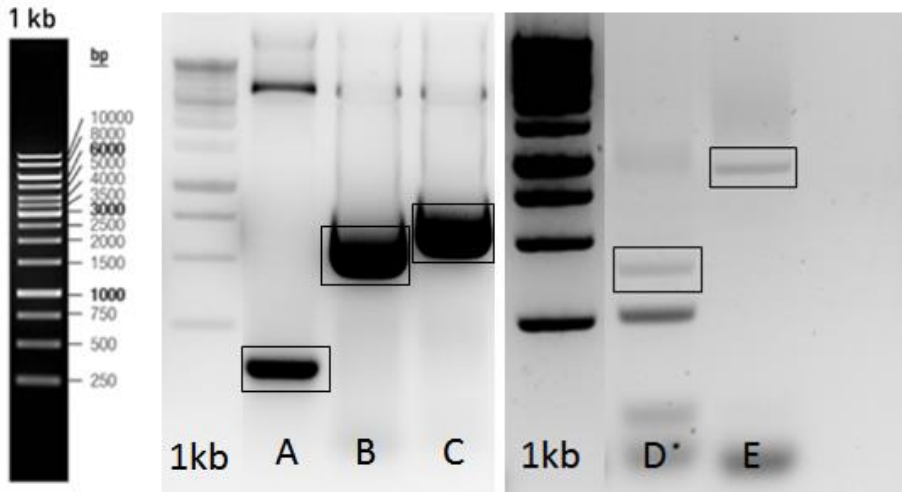

Figure 4-6. PCR fragments for patches of *crtE*, *crtB* and *crtI*.
Domestication PCR products of bacterial carotenoid pathway, parts for the GB-library. GB patches are indicated by the black squares. (A) Patch I CRTE, (B) patch II CRTE, (C) patch I CRTB, (D) patch I CRTI, and (E) patch II CRTI. Samples are aligned to 1kb ladder, index of the 1kb ladder is provided on the left hand side.

Once patches were assembled in the pUPD entry vector, the vectors were sent for sequencing to confirm the sequences of the parts generated. All parts were confirmed via sequencing; gene specific primers for sequencing are presented in the appendix (Table A-2). Assembly of sequences is presented for constructed TUs in “Assembly of transcriptional units”.

4.3.2. Assembly of transcriptional units

With the GB parts created, the following step is the assembly of TUs in binary vectors. The braiding loop of the GB system consists of four backbone vectors, α1, α2, Ω1 and Ω2, which allow for the construction of multi-gene constructs, as will be described further on in this chapter. In order to generate an efficient cloning setup, it is important to design a braiding schedule and place TUs in the vectors required for the schedule. Therefore the list of binary vectors containing the TUs created from the GB parts consists of various duplicates with different backbone vectors (Table 4-2). For all coding sequence parts created for the MEP and carotenoid pathway, binary vectors were assembled in combination with the CaMV35S promoter without targeting peptide. The MEP pathway genes were also combined with the CaMV35S promoter part containing the targeting peptide.

Table 4-2. Transcriptional units constructed in GB binary vectors.
TUs were constructed in different binary vectors of the GB system for braiding purposes. The TUs for the carotenoid pathway were constructed without a targeting peptide for the plastid. The MEP pathway genes were placed in TUs with and without the targeting peptide to the plastid. The "c" and "p" in front of the gene abbreviations represent targeting to the cytosol or plastid respectively.

backbone vector	expression cassette	backbone vector	expression cassette	backbone vector	expression cassette
pDGB1α1	cDXS	pDGB1α1	cCRTE	**pDGB1α1**	pDXS
pDGB1α2	cDXR	pDGB1α2	cCRTB	**pDGB1α2**	pDXR
pDGB1α1	cMCT	pDGB1α1	cCRTI	**pDGB1α1**	pMCT
pDGB1α2	cCMK			**pDGB1α2**	pCMK
pDGB1α1	cMDS			**pDGB1α1**	pMDS
pDGB1α2	cHDS			**pDGB1α2**	pHDS
pDGB1Ω1	cHDR			**pDGB1Ω1**	pHDR
pDGB1α2	cMDS			**pDGB1α2**	pMDS
pDGB1Ω1	cMDS			**pDGB1Ω1**	pMDS
pDGB1Ω2	cHDS			**pDGB1Ω2**	pHDS
pDGB1Ω2	pMCT			**pDGB1Ω2**	pMCT

The assembly into α-vectors requires a restriction reaction with *BsaI* to cut the GB parts out of the entry vectors. The Ω-vectors require a combination of *BtgZI* and *BsmBI* for the assembly of binary vectors, which is a more complicated reaction with reduced efficiency (Sarrion-Perdigones et al., 2013). This prevented the assembly of a TU for c*rtI* in pDGB1Ω2, which is

required for the assembly of a triple gene construct for the carotenoid pathway. The successful assemblies are displayed in Table 4-2, and were confirmed by digestions and sequencing. Digestions were performed with the HindIII enzyme, which provided distinct patterns based on the individual TUs. An overview of the TUs for the MEP genes is displayed in Figure 4-7.

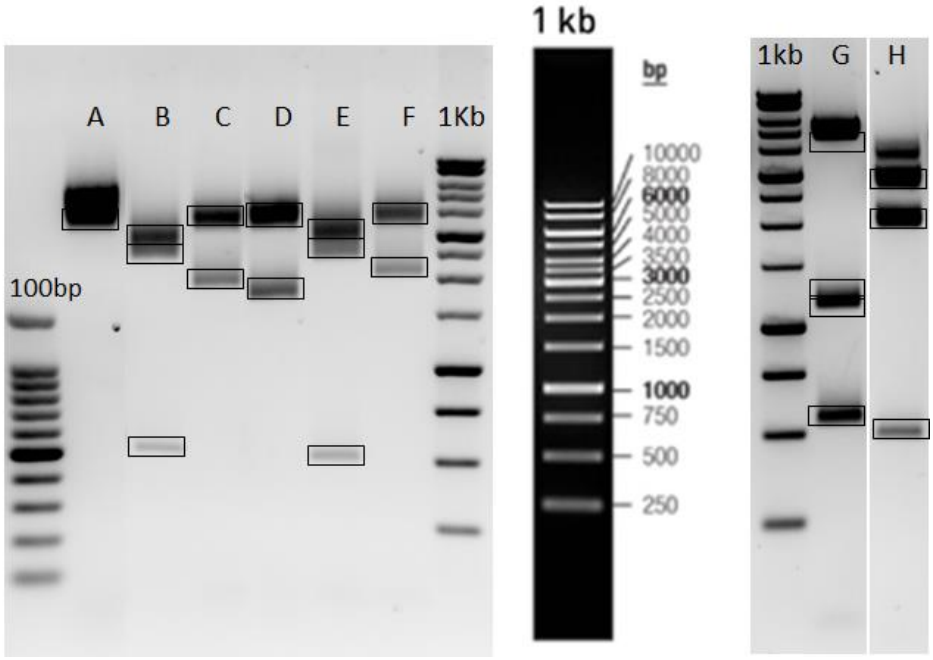

Figure 4-7. Digestion of GB-vectors with assembled TUs for the MEP genes.
Confirmation of successful assembly of TU's of the MEP pathway. 1 µg of plasmid DNA was digested with the HindIII restriction enzyme. Fragments are indicated by black squares (fragments under a 100bp were not detectable). A, pDGB1α1 (empty): 3194bp. B, pDGB1α2-DXR: 2.5kb, 2.4kb, 498bp, 21bp. C, pDGB1α1-MCT: 3.1kb, 1.9kb, 58bp. D, pDGB1α1-MDS: 3.1kb, 1.7kb. E, pDGB1α2-HDS: 2.6kb, 2.3kb, 498bp, 58bp, 21bp. F, pDGB1α1-HDR: 3.1kb, 2.1kb, 58bp. G, 3.5kb, 1.4kb, 1.3kb, 575bp, 58bp. H, 3.0kb, 2.0kb, 499bp, 58bp. 100bp ladder and 1kb ladder were used as a reference. Index of 1kb ladder is provided in the centre.

Completed TUs were sequenced with primers that target the borders between the three parts assembled. Using primers specific for the promoter and terminator parts allowed for the screening of successful assembly of the TUs. A sequence alignment display with sequence reads for the junctions of each of the TUs of the MEP pathway is provided below (Figure 4-8 - Figure 4-14). All sequence data was matched against the *in silico* sequences for the backbone vectors with the respective TUs and the individual elements of the TUs. Nucleotide comparisons between consensus sequences and outcomes of sequence analysis can be found in the appendix (Sequencing data).

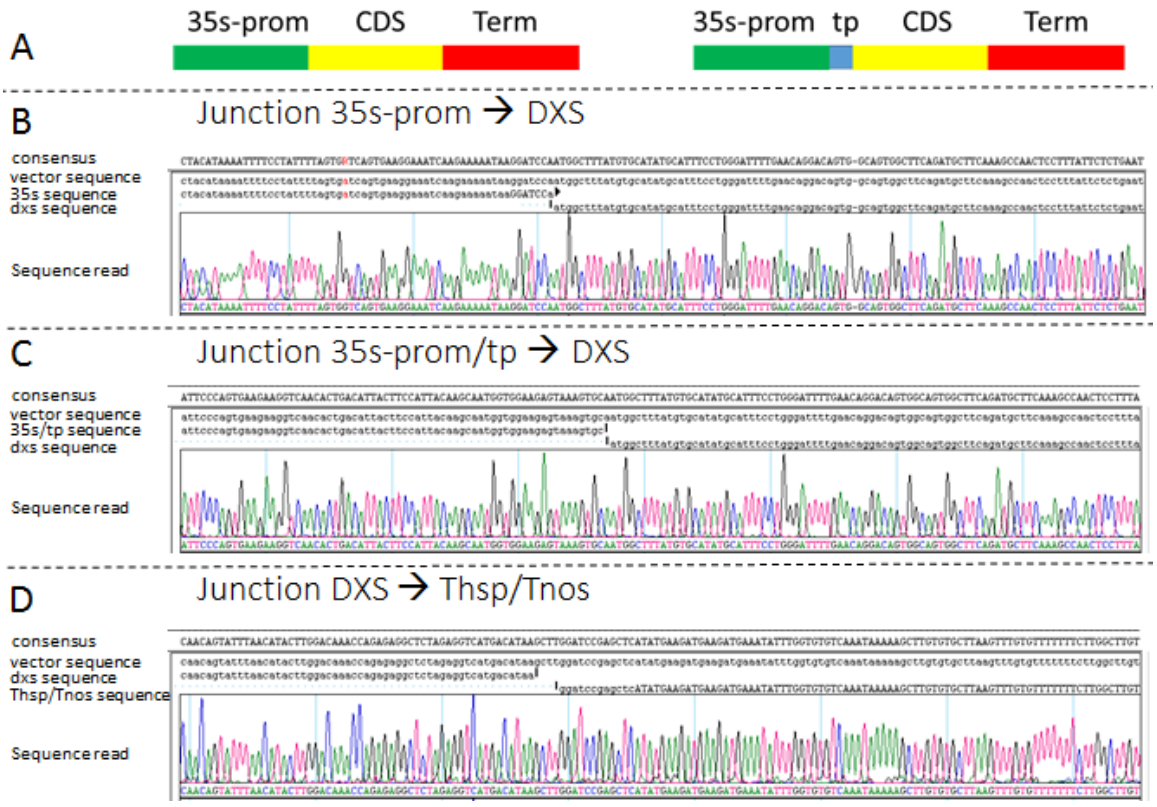

Figure 4-8. Assembly of TU for DXS_{ca} with CaMV35S promoter and Thsp/Tnos terminator.
Sequence reads (Sanger sequencing) of the assembly junctions of the *dxs*-expression cassettes compared to the *in silico* sequences of the vector and individual parts. (A) Expression cassette maps for the cytosolic and plastid targeted vectors. (B) Junction for the 35s promoter and *dxs* coding sequence. (C) Junction for the 35s promoter with targeting peptide with the *dxs* coding sequence (D) Junction for the *dxs* coding sequence with the Thsp/Tnos terminator.

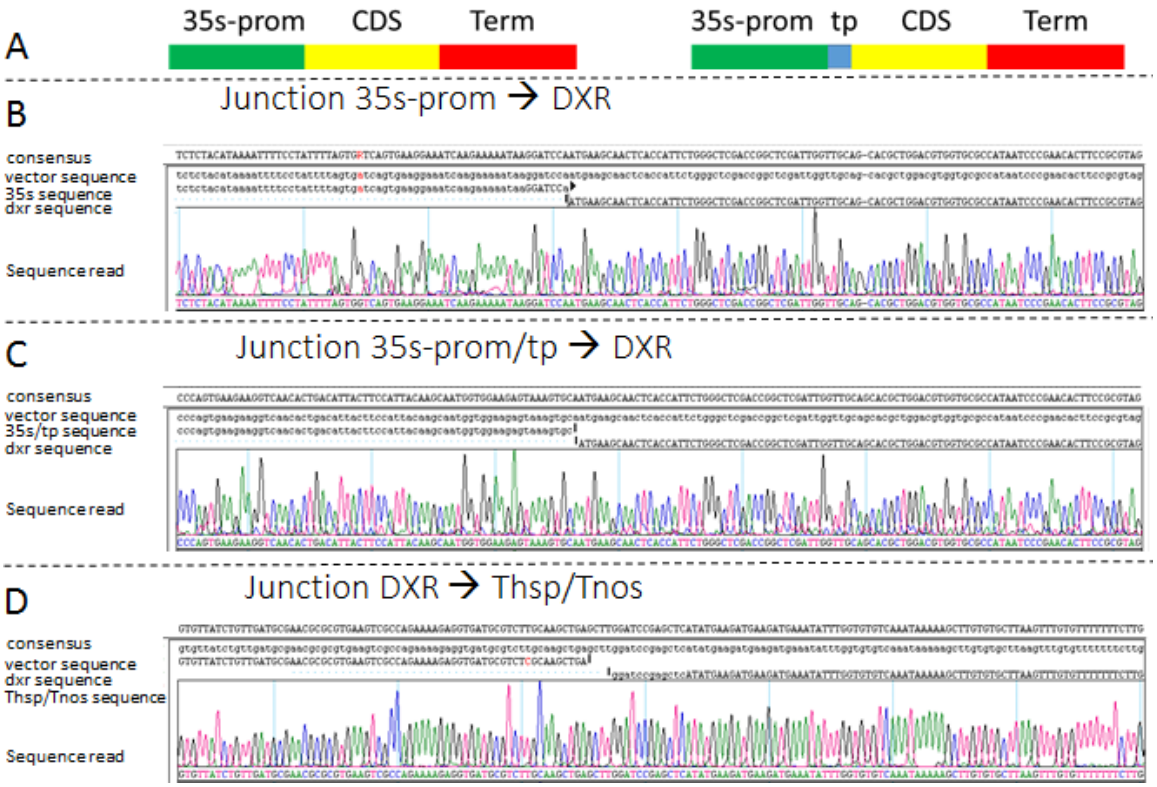

Figure 4-9. TU assembly of DXR_{ec} with CaMV35S promoter and Thsp/Tnos promoter.
Sequence reads (Sanger sequencing) of the assembly junctions of the *dxr*-expression cassettes compared to the *in silico* sequences of the vector and individual parts. (A) Expression cassette maps for the cytosolic and plastid targeted vectors. (B) Junction for the 35s promoter and *dxr* coding sequence. (C) Junction for the 35s promoter with targeting peptide with the *dxr* coding sequence (D) Junction for the *dxr* coding sequence with the Thsp/Tnos terminator.

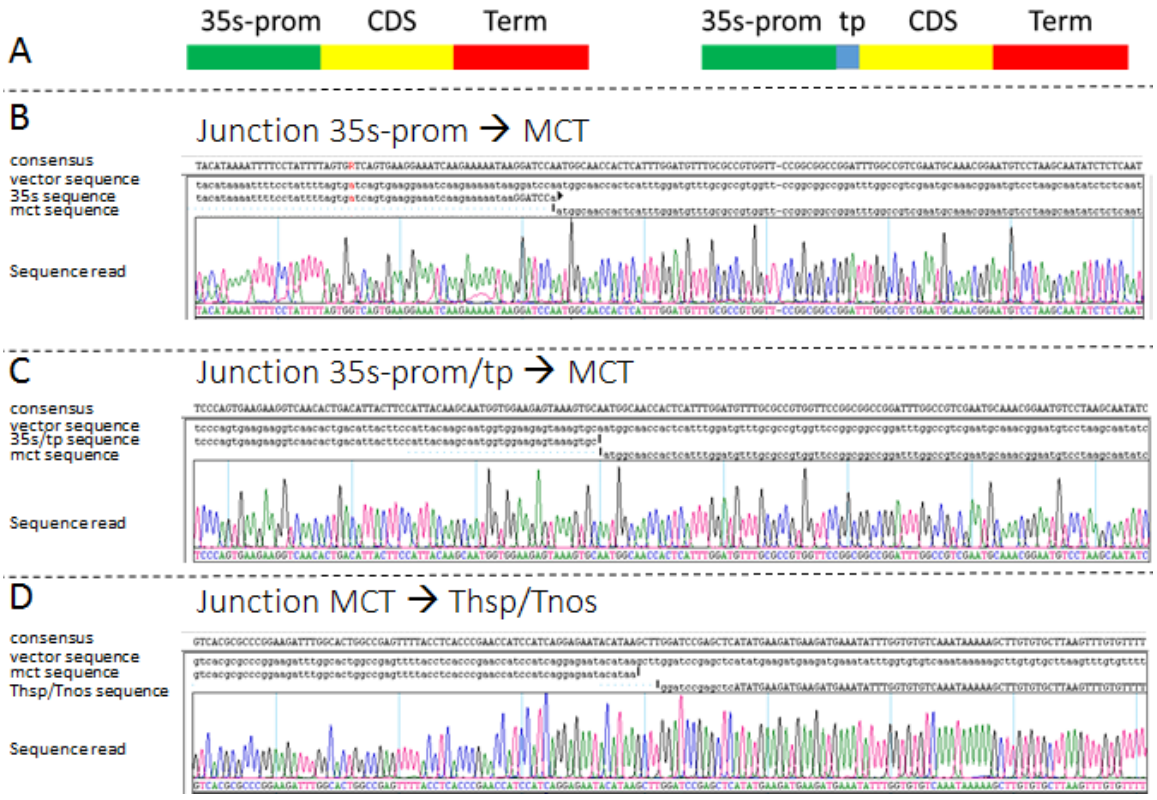

Figure 4-10. Generation of MCT$_{ec}$ TU.
Sequence reads (Sanger sequencing) of the assembly junctions of the *mct*-expression cassettes compared to the *in silico* sequences of the vector and individual parts. (A) Expression cassette maps for the cytosolic and plastid targeted vectors. (B) Junction for the 35s promoter and *mct* coding sequence. (C) Junction for the 35s promoter with targeting peptide with the *mct* coding sequence (D) Junction for the *mct* coding sequence with the Thsp/Tnos terminator.

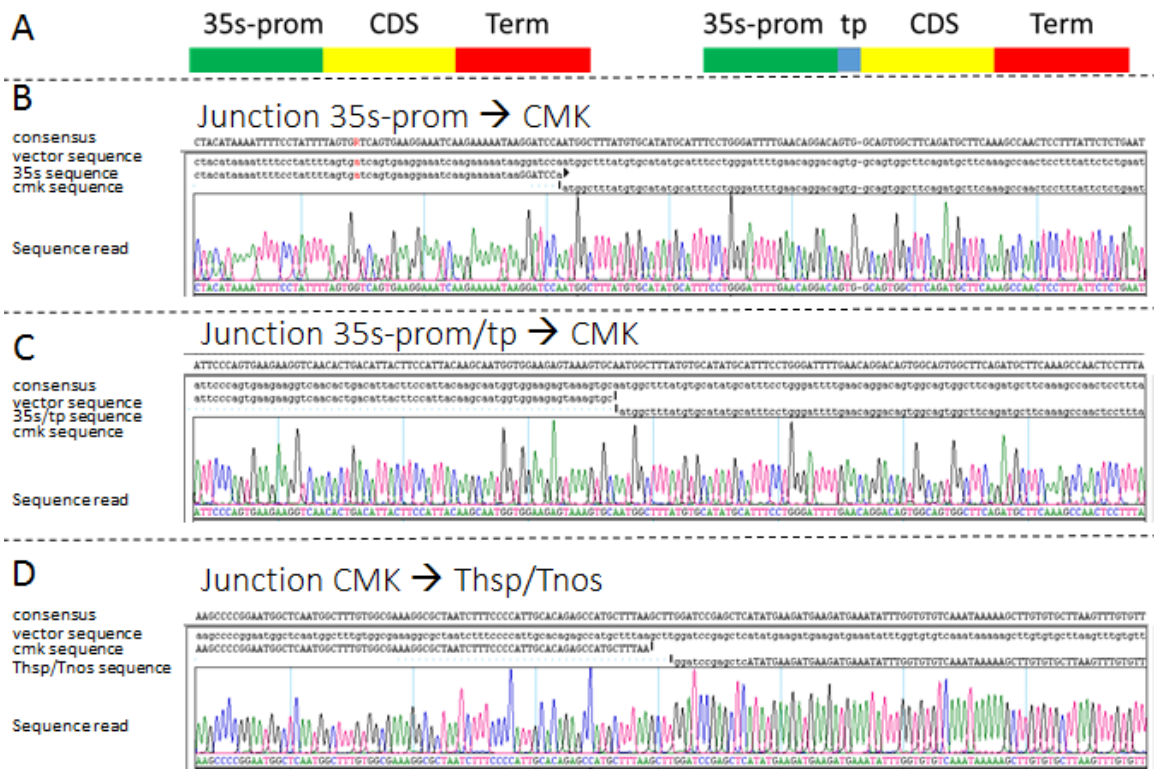

Figure 4-11. Assembly of CMK_{ec} TU with CaMV35S promoter and Thsp/Tnos terminator.
Sequence reads (Sanger sequencing) of the assembly junctions of the *cmk*-expression cassettes compared to the *in silico* sequences of the vector and individual parts. (A) Expression cassette maps for the cytosolic and plastid targeted vectors. (B) Junction for the 35s promoter and *cmk* coding sequence. (C) Junction for the 35s promoter with targeting peptide with the *cmk* coding sequence (D) Junction for the *cmk* coding sequence with the Thsp/Tnos terminator.

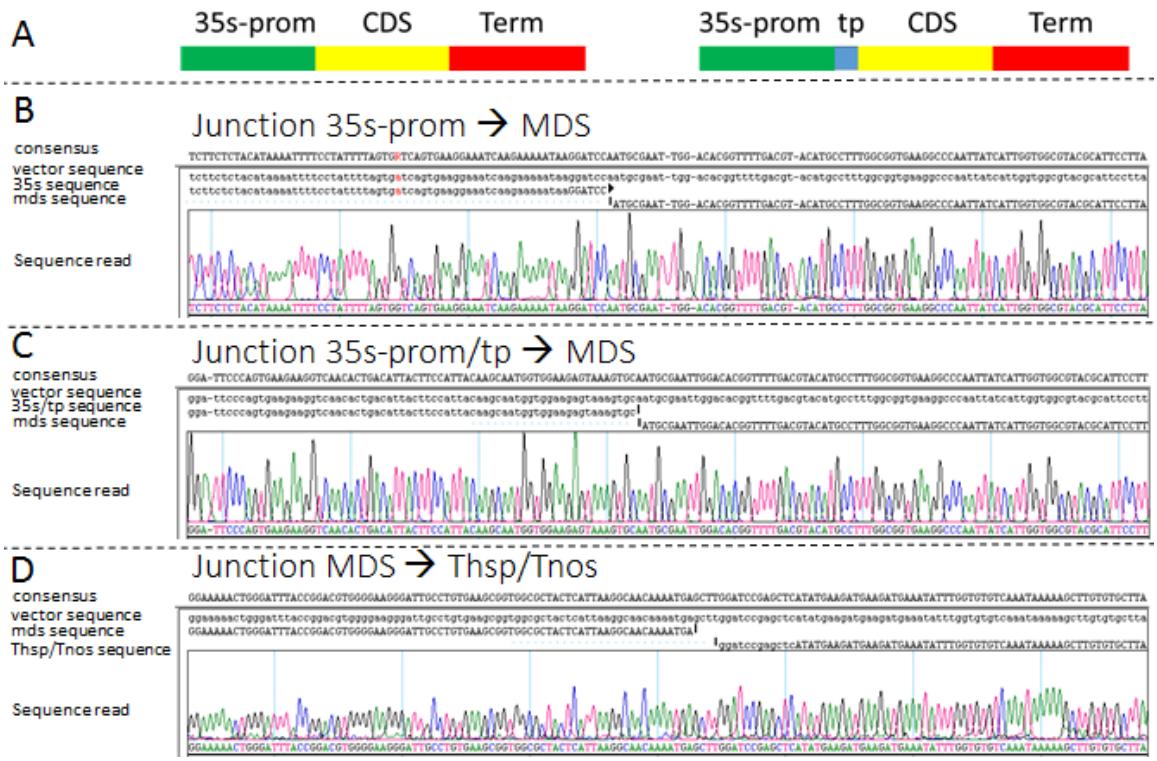

Figure 4-12. Sequencing of MDS_{ec} TU-assembly.
Sequence reads (Sanger sequencing) of the assembly junctions of the *mds*-expression cassettes compared to the *in silico* sequences of the vector and individual parts. (A) Expression cassette maps for the cytosolic and plastid targeted vectors. (B) Junction for the 35s promoter and *mds* coding sequence. (C) Junction for the 35s promoter with targeting peptide with the *mds* coding sequence (D) Junction for the *mds* coding sequence with the Thsp/Tnos terminator.

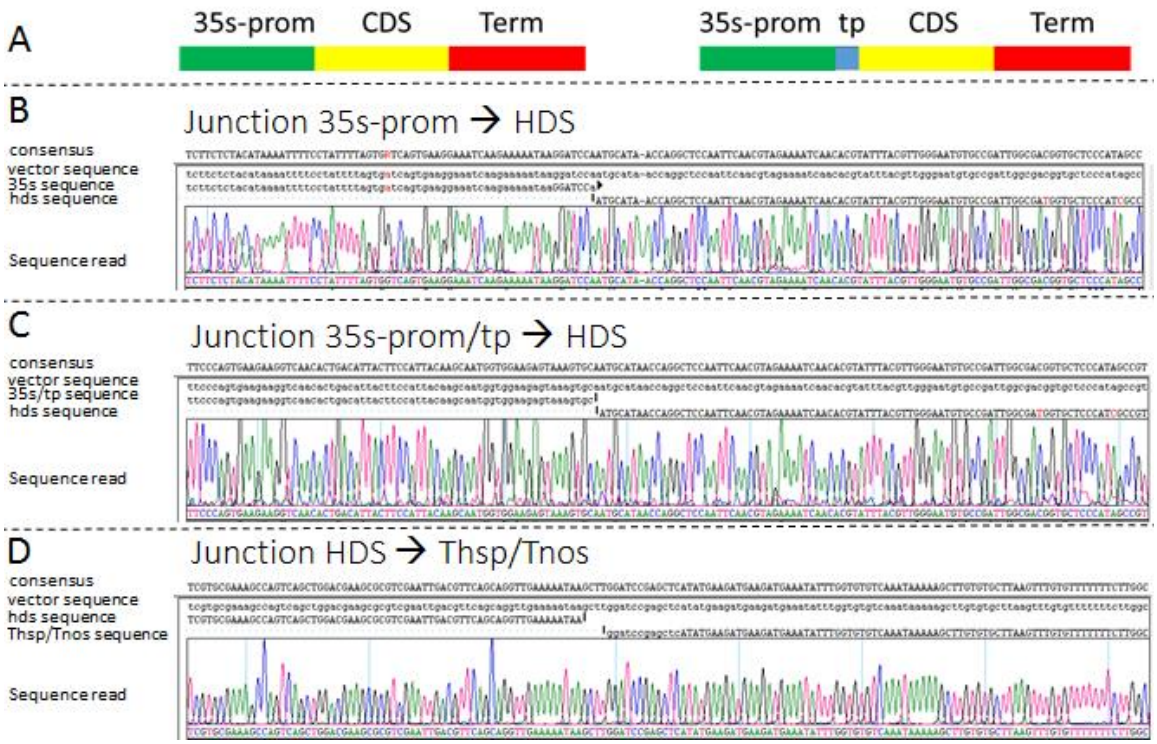

Figure 4-13. Sequence analysis of TU assembly for HDS_{ec}.
Sequence reads (Sanger sequencing) of the assembly junctions of the *hds*-expression cassettes compared to the *in silico* sequences of the vector and individual parts. (A) Expression cassette maps for the cytosolic and plastid targeted vectors. (B) Junction for the 35s promoter and *hds* coding sequence. (C) Junction for the 35s promoter with targeting peptide with the *hds* coding sequence (D) Junction for the *hds* coding sequence with the Thsp/Tnos terminator.

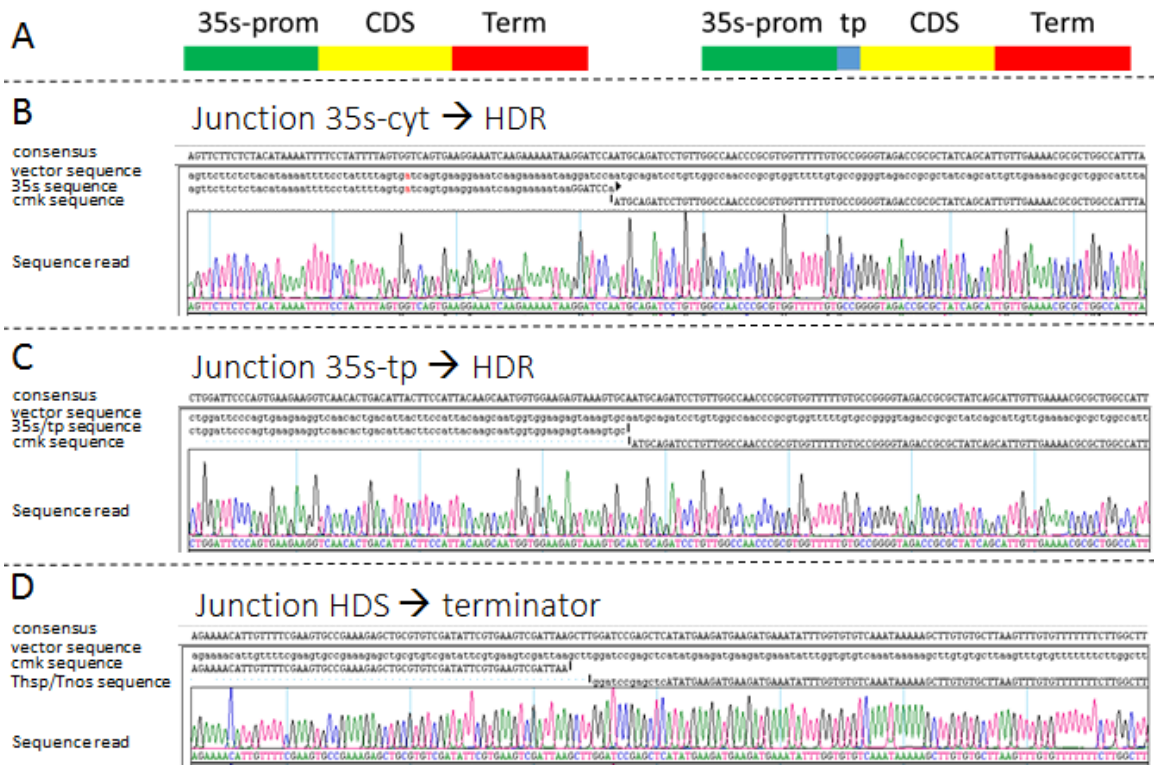

Figure 4-14. Sequence analysis of TU assembly for HDR_{ec}.
Sequence reads (Sanger sequencing) of the assembly junctions of the *hdr*-expression cassettes compared to the *in silico* sequences of the vector and individual parts. (A) Expression cassette maps for the cytosolic and plastid targeted vectors. (B) Junction for the 35s promoter and *hdr* coding sequence. (C) Junction for the 35s promoter with targeting peptide with the *hdr* coding sequence (D) Junction for the *hdr* coding sequence with the Thsp/Tnos terminator.

The TUs for the bacterial carotenoid genes *crtE*, *crtB* and *crtI* were planned to be assembled in pDGB1α1, pDGB1α2 and pDGB1Ω2 respectively, to facilitate the assembly of a multi-gene construct containing all three TUs. The assembly of crtI in a Ω-vector was not successful and therefore the *crtI* TU was planned to be assembled into pDGB1α2. As the outcome of the digest shows the TU for *crtI* was assembled in vector pDGB1α1, even though this was not followed up by the assembly of *crtE* and *crtB* in Ω-vectors. The confirmation of the positive clones for all three TUs via restriction digestions is displayed in Figure 4-15.

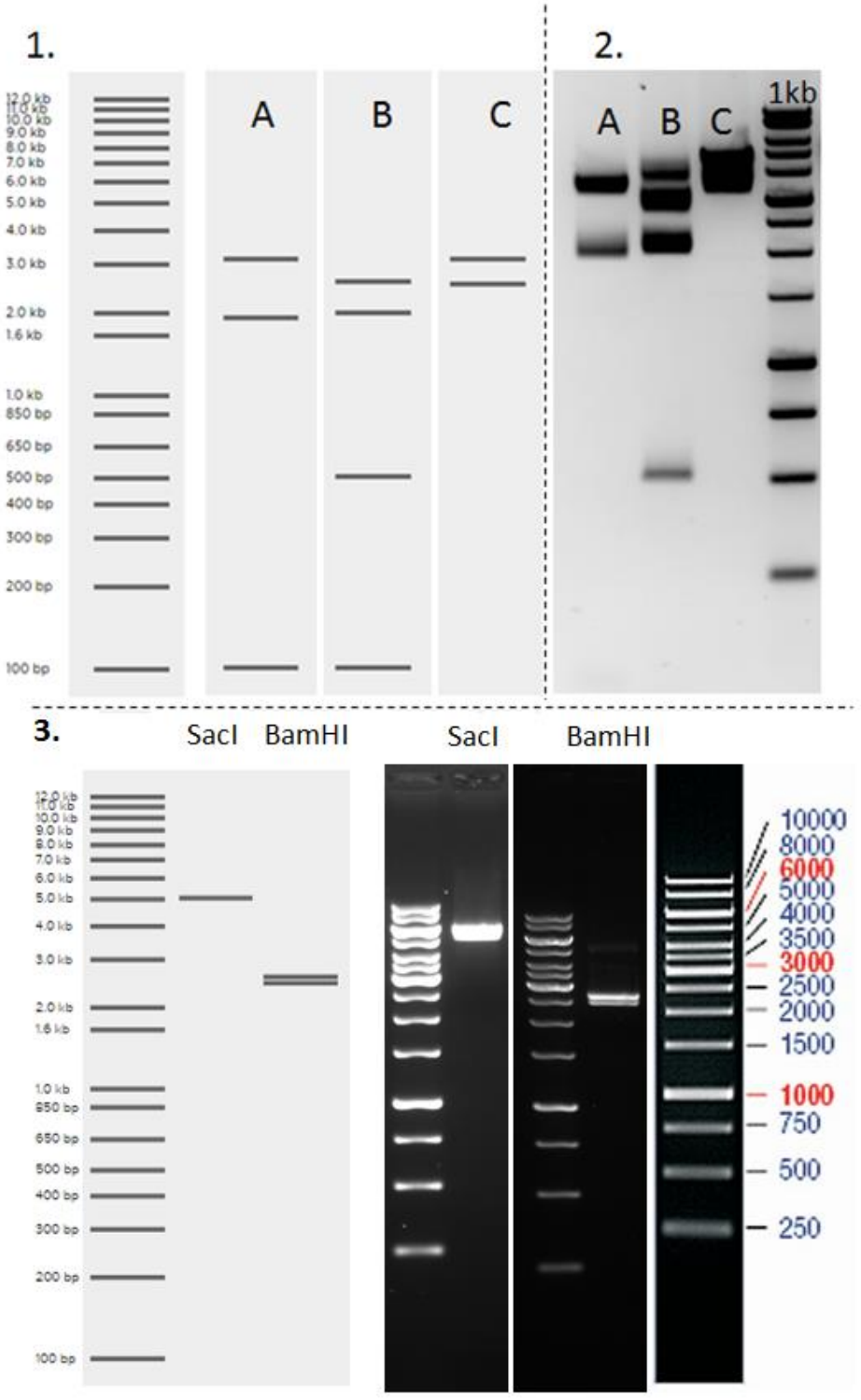

Figure 4-15. Assembly of CRTE, CRTB and CRTI TUs in α-vectors.
Confirmation of assembly of carotenoid gene TU's. (1) Predicted digestion patterns for pDGB1α1-CRTE (A), pDGB1α2-CRTB (B) and pDGB1α1-CRTI (C). (2) Digest of pDGB1α1-CRTE (A), pDGB1α2-CRTB (B) and pDGB1α1-CRTI (C) with the HindIII restriction enzyme. The fragments at 100bp were not detected for pDGB1α1-CRTE and pDGB1α2-CRTB, otherwise the patterns match the predictions. Digests were checked by the reference ladder (1kb). (3) Complementary digestions with SacI and BamHI for pDGB1α2-CRTB: left side displays the predictions and right side displays the digests. Reference ladder is the 1kb Gene plus ladder.

4.3.3. "Braiding" of multi-gene constructs

With the TUs assembled in the binary vectors, the assembly of multi-gene constructs was the next step. For the seven MEP genes a scheme was prepared to perform the braiding of the single-gene constructs. As displayed in Figure 4-16, the GB setup allows for rapid linkage of TUs into multi-gene constructs. It requires two cycles of restriction/ligation to create a multi-gene construct containing four TUs, derived from vectors with a single TU. With all single-gene vectors for the MEP pathway available, three rounds of braiding were required to construct a binary vector containing seven TUs. The braiding plan was executed for both the sets with targeting to the cytosol and the plastid, resulting in the assembly of pDGB1Ω1-MEP^{tp} and pDGB1Ω1-MEP^{cyt}. Furthermore, in a similar fashion, partial MEP pathway assemblies were generated covering one up to seven genes of the pathway (listed in Table 4-3).

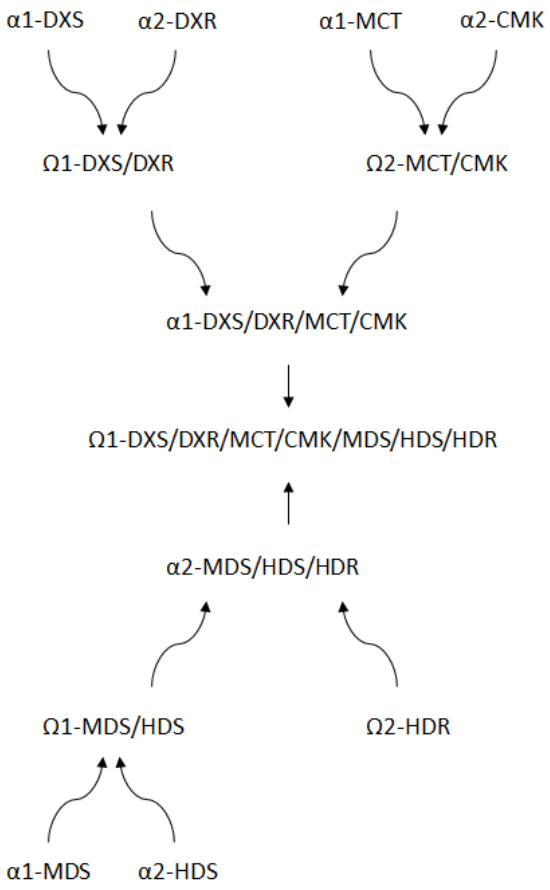

Figure 4-16. Schematic of braiding plan for the MEP pathway.
The unlimited loop between the α- and Ω-vectors allows for braiding of single gene vectors into multi-gene constructs. Assembly of a binary vector with seven TU's starts with the assembly of coupled TU vectors for the combination DXS-DXR, MCT-CMK, MDS-HDS in the Ω-backbone, given the odd number of TU's HDR is assembled directly into pDGB-1Ω2. A second binary assembly results in two multi-TU vectors of four and three TU's in the α-backbone vector respectively. These combinations, DXS-DXR-MCT-CMK and MDS-HDS-HDR respectively, can be united in a final assembly round for a vector with seven TU's in the Ω-backbone.

The assembly of the complete set of MEP genes was checked for accuracy via digestions and partial sequencing of the coding sequences. Digestions of the MEP^{tp} and MEP^{cyt} assemblies resulted with BsaI, BamHI and SacI are displayed in Figure 4-17 and Figure 4-19. As can be clearly observed from gel electrophoresis the presented digestion patterns do not match the prediction for either vector. The absence of expected bands and the appearance of unexpected bands makes it complicated to analyse the exact cause of the mismatch between the predicted and actual digests. A plausible reason for this issue is errors in the assembly of the vectors, possibly caused by the overlap in assembly sites between TUs. The similarity between the designs of the TUs could provide conflicts in the assembly of the multigene binary vectors.

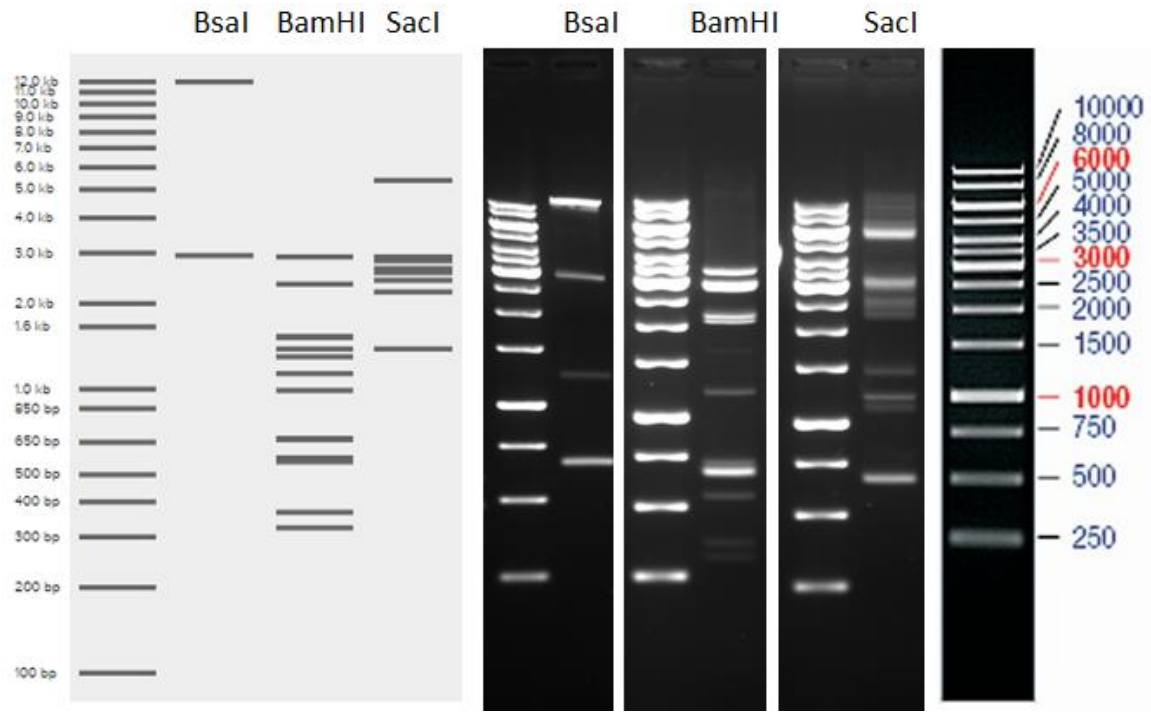

Figure 4-17. Restriction digestions of pDGB1Ω1-MEP^{tp} vector.
Screening of MEP Pathway multigene vector with plastid targeting. 0.5ug of vector DNA was digested with the BsaI, BamHI and SacI restriction enzymes respectively. Left panel: Predicted digests for the pDGB1Ω1-MEP^{tp} vector with each enzyme. Right panel: outcome of digests for pDGB1Ω1-MEP^{tp}. Digest are presented with their respective reference ladders (1kb); Nevertheless expected bands failed to appear and unexpected bands appear.

Screening for the presence of the coding sequence through PCR analysis led to the confirmation of the fragments of all MEP genes in the MEP^{tp} vector (Figure 4-18). Full length fragments, except for DXR for which only the 2nd and 3rd patch were amplified, were amplified via domestication primers as used for the formation of the GB-parts in the first phase of the cloning method. As can be observed in the figure fragments match the predicted sizes for each segment: dxs (2194bp), dxr (1001bp), mct (746bp), cmk (887bp), mds (515bp), hds (1154bp) and hdr (951bp). A comparison of the backbone vector, the vectors with the individual TUs for the MEP pathway, and the "full" MEP pathway was performed and for the MEP^{TP} vector all seven coding were confirmed.

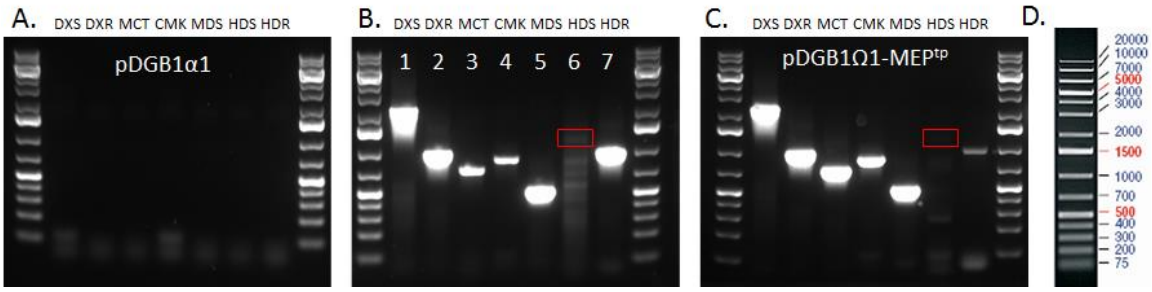

Figure 4-18 PCR confirmation coding sequences MEP^{tp} vector

PCR analysis of MEP pathway coding sequences in binary vectors. (A) pDGB1α1 negative control tested with primer sets for all seven genes. (B) Screening of the individual TUs in the binary vectors with their respective primer sets*. (C) Screening for presence of coding sequences in the MEP^{tp} multigene vector*. (D) Generuler 1kb Plus ladder. (* = correct fragment for HDS, had it appeared, is indicated with a red square)

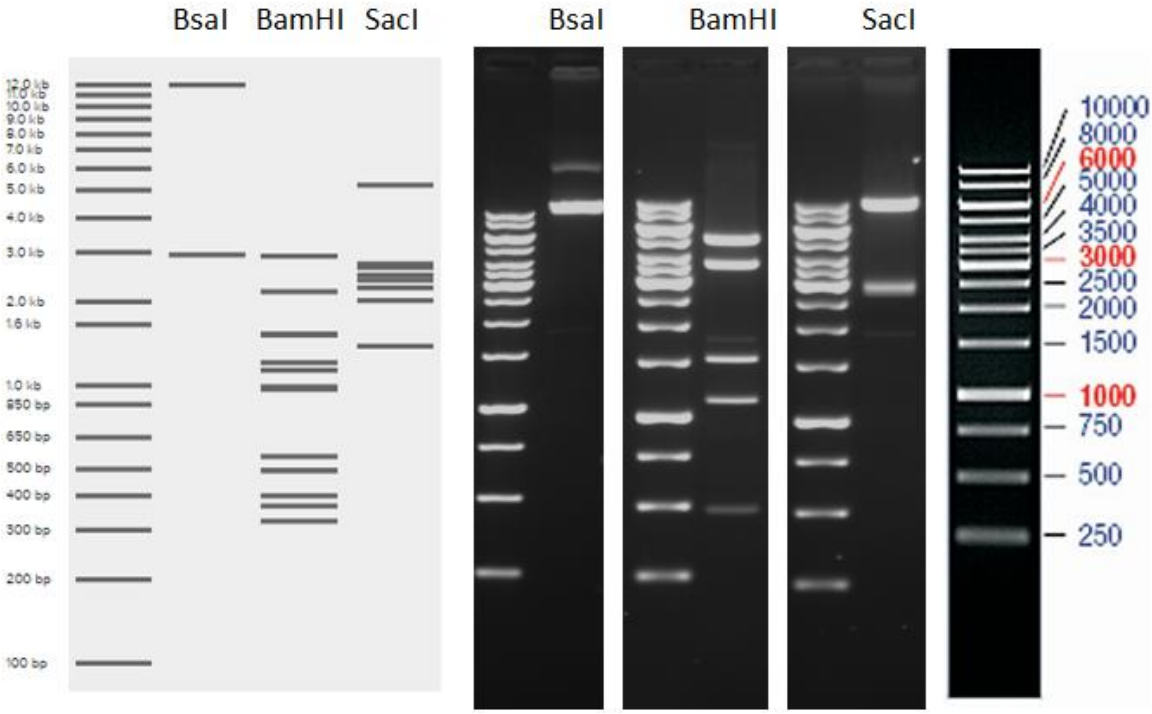

Figure 4-19. Restriction digestions of pDGB1Ω1-MEP^{cyt} vector.

Assembled multi-gene vectors for the MEP pathway with a targeting peptide for the plastid. 0.5ug of vector DNA was digested with the BsaI, BamHI and SacI restriction enzymes respectively. Left panel: Predicted digests for the pDGB1Ω1-MEP^{cyt} vector with each enzyme. Right panel: outcome of digests for pDGB1Ω1-MEP^{cyt}. Digest are presented with their respective reference ladders (1kb); Nevertheless expected bands failed to appear and unexpected bands appear. 100bp digestion fragments were not detected.

In a similar fashion the screening for the presence of MEP coding sequences was performed for the MEP^{cyt} multigene vector. As displayed in Figure 4-20 fragment for the six out of seven MEP genes were detected, the amplification of hdr was not successful. As can be observed in the figure fragments match the predicted sizes for each segment: dxs (2194bp), dxr (1001bp), mct

(746bp), cmk (887bp), mds (515bp), hds (1154bp) and hdr (951bp). The absence of a coding sequence, possibly the entire TU, in the multigene vector supports the issues with the assembly in the binary assembly as stated based on the restriction patterns displayed in Figure 4-17 and Figure 4-19.

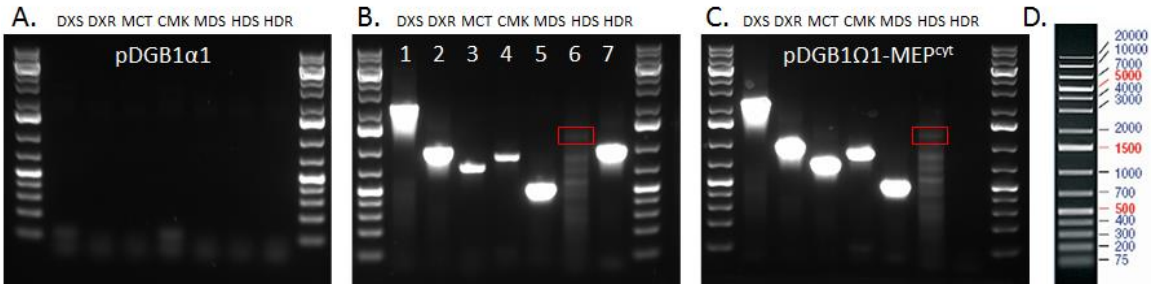

Figure 4-20 PCR confirmation coding sequences MEP^{cyt} vector
PCR analysis of MEP pathway coding sequences in binary vectors. (A) pDGB1α1 negative control tested with primer sets for all seven genes. (B) Screening of the individual TUs in the binary vectors with their respective primer sets*. (C) Screening for presence of coding sequences in the MEP^{cyt} multigene vector*. (D) Generuler 1kb Plus ladder. (* = correct fragment for HDS, had it appeared, is indicated with a red square)

For the constructed multi-gene vectors sequencing was performed to confirm the presence of TUs. Gene specific primers for *dxs*$_{ca}$, *mct*$_{ec}$ and *hds*$_{ec}$ were used to determine accuracy of the assembly in combination with the digestions performed earlier. A schematic overview of the sequence analysis aligned to the in silico sequences of the plasmid and the individual TUs is displayed in Figure 4-21. Given the mismatches found, through digestion analysis, in the assembly of the multigene vectors presence of the coding sequences sequenced can only provide confirmation of these sections in the vector independent of accurate assembly.

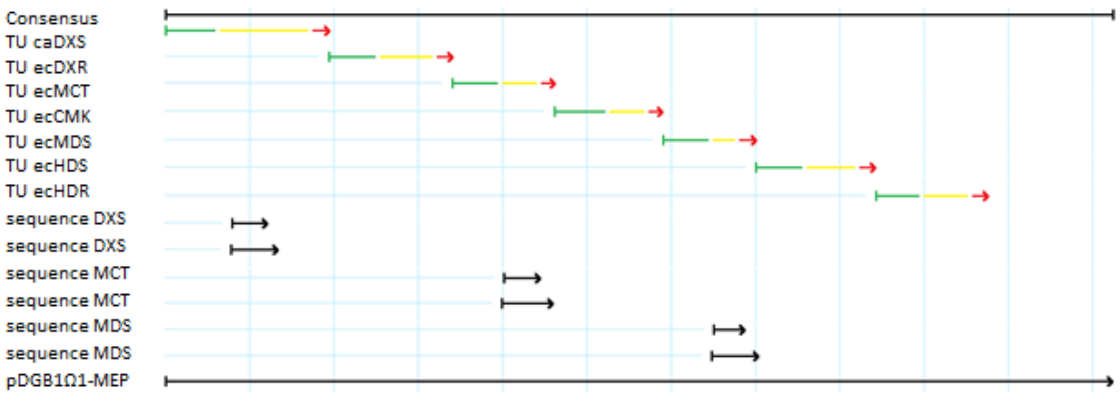

Figure 4-21. Sequencing schematic for the multi-gene vector of the MEP pathway.
An alignment of sequencing data of DXS_{ca}, MCT_{ec} and MDS_{ec} compared to in silico sequences of the MEP TUs and the full vector sequence. *In silico* TU's of MEP genes are indicated with colours per part (green = promoter, yellow = coding sequence, red = terminator). Full *in silico* sequence of assembled multi-gene vector is placed at the bottom of the figure.

Besides the two vectors that contain all the seven genes of the MEP pathway, the constructs with partial MEP pathway genes were assembled through the binary assembly method of the Golden Braid system. Digests with BsaI or BsmBI (depending on the vector background: α or Ω respectively), BamHI and SacI restriction enzymes demonstrated similar issues as observed for the "complete" MEP pathway vectors. Mismatches for the presented vectors compared to the predicted digestion pattern with all three enzymes (Displayed in Figure 4-22). Either the appearance of unexpected bands or the absence of expected can be observed for the presented vectors in the digests of one or more enzymes. The multigene vector for DXS^{tp}-DXR^{tp} is displays two correct patterns for BsaI and SacI respectively, although BamHI displays an entirely incorrect pattern. The level of deviation from the predicted patterns as observed between the DXS^{tp}-DXR^{tp} vector and the extended assemblies would suggest that repetitive use of the infinite loop generates a higher chance on assembly errors. The confirmation of the proper assembly of the pDGB1Ω1-crtEcrtB vector (Figure 4-23) enforces this suggestion.

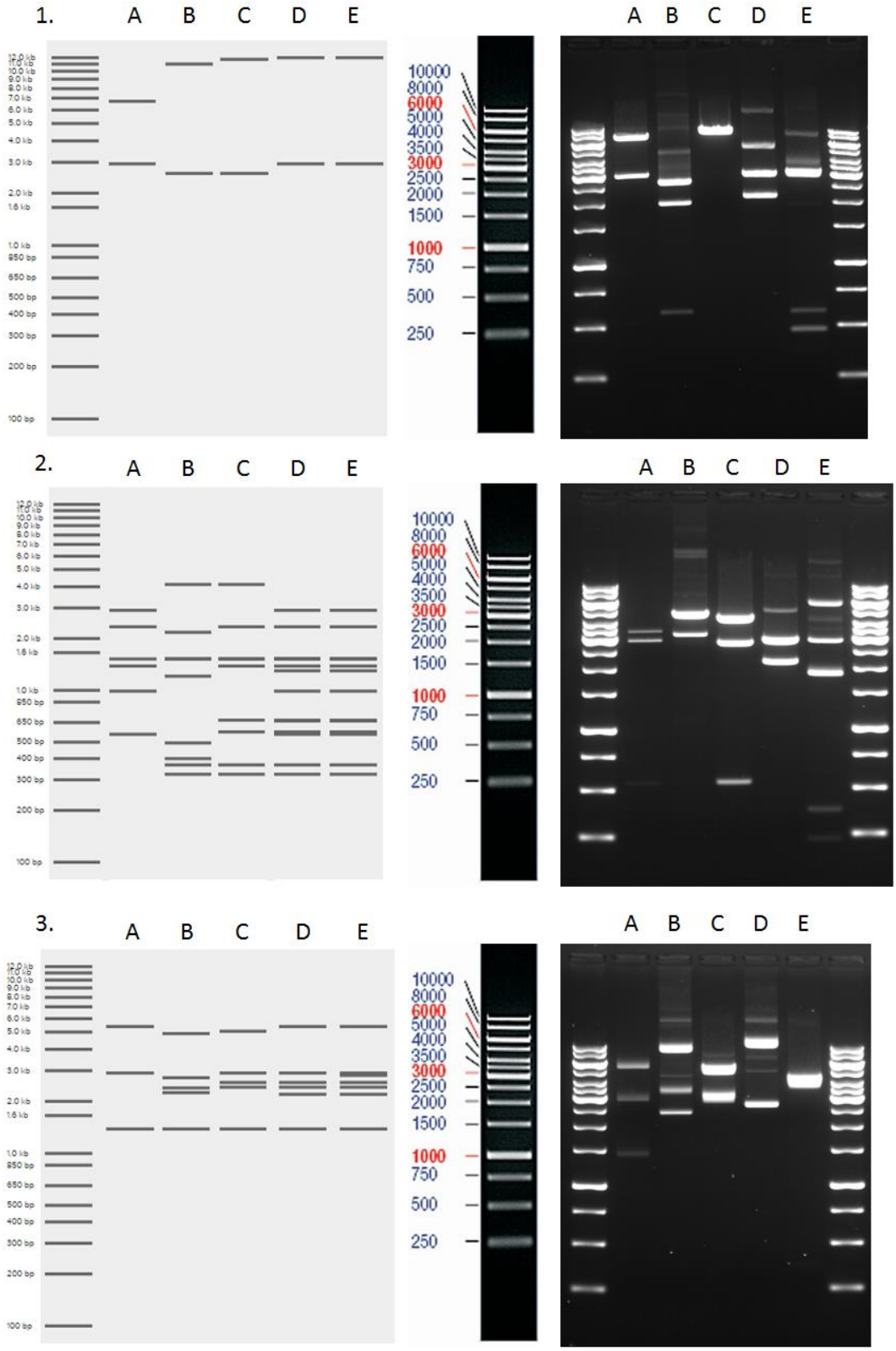

Figure 4-22. GB vectors of step-wise build-up of MEP multi-TU vectors.

Vectors presented: pDGB1Ω1_DXS-DXR (A), pDGB1α1_DXS-MCT (B), pDGB1α1_DXS-CMK (C), pDGB1Ω_DXS-MDS (D), pDGB1Ω_DXS-HDS (E). (1) Digestion with BsaI or BsmBI (respectively for α or Ω backbone) left panel predicted pattern, right panel: outcome of digestion. (2) Digestion with BamHI (respectively for α or Ω backbone) left panel predicted pattern, right panel: outcome of digestion. (3) Digestion with SacI (respectively for α or Ω backbone) left panel predicted pattern, right panel: outcome of digestion. Nevertheless expected bands failed to appear and unexpected bands appear 100bp fragments were not detected. 1kb ladder used as a reference.

All performed assemblies for multi-gene vectors using the GB cloning method are summarised in Table 4-3. For the MEP genes TUs for both plastid and cytosolic targeting were assembled into multi-gene vectors and were tested for functionality through expression analysis, despite concerns on assembly accuracy. The bacterial carotenoid genes were generated for cytosolic targeting only, and were integrated in screens with the single gene vectors for the carotenoid genes.

Table 4-3. Overview of multi-gene vectors generated via the GB braiding method.
Vectors with multiple TU's were assembled via the GB-system. For the MEP pathway combinations up to seven TU's were created (the complete MEP pathway), for both targeting to the plastid and cytosol. A double TU vector was created for *crtE* and *crtB*, *crtI* could not be included due to issues with the TU assembly.

MEP^{tp}	**MEP^{cyt}**	**CRT^{cyt}**
dxs+dxr	*dxs+dxr*	*crtE+crtE*
dxs-mct	*dxs-mct*	
dxs-cmk	*dxs-cmk*	
dxs-mds	*dxs-mds*	
dxs-hds	*dxs-hds*	
dxs-hdr	*dxs-hdr*	

With the unsuccessful attempt to assemble the TU for CRTI into the Ω2-vector, which was part of the design plan for the carotenoid pathway: α1-CRTE and α2-CRTB to Ω1-CRTE/CRTB, and link with Ω2-CRTI, only the CRTE/CRTB vector was constructed. The confirmation of this vector via restriction digestion, using the enzymes BamHI, BsaI and SacI, is displayed in Figure 4-23.

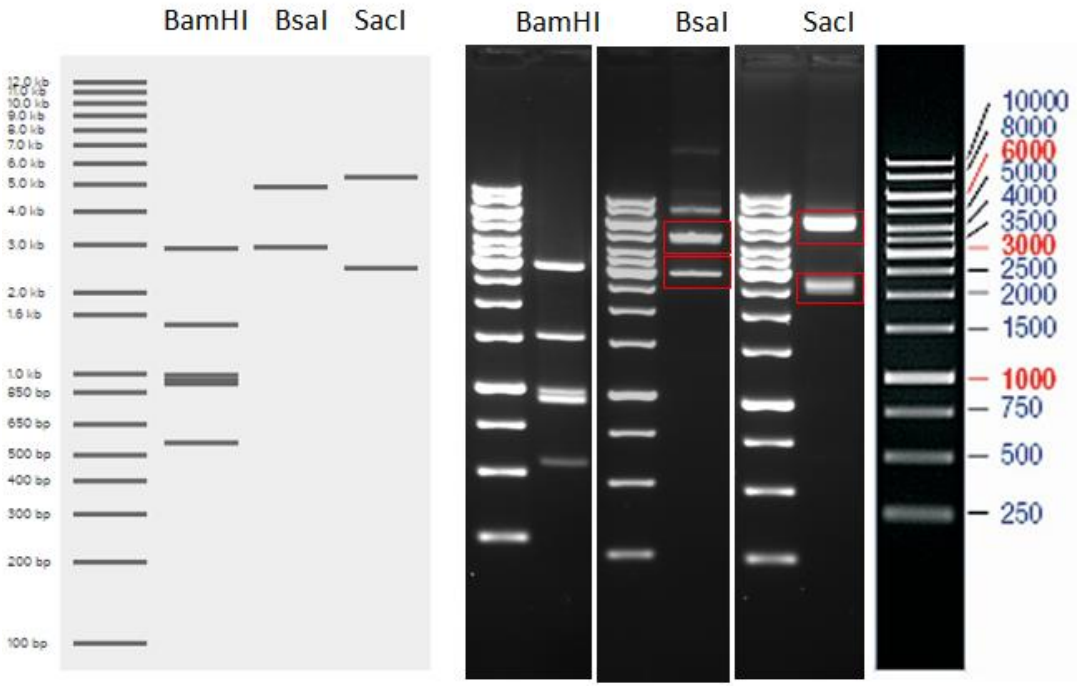

Figure 4-23. Confirmation of the multi-gene vector pDGB1Ω1-CRTE_CRTB.
Restriction digestion of multi-TU vector for *crtE* and *crtB*. Predicted pattern for the digests on the left. On the right the outcome of the digests including a display of their reference ladder. Matching patterns are found for all enzymes and marked by red squares for BsaI and SacI, as additional bands were detected due to partial digests.

To further determine the accuracy of the CRTE_CRTB multigene vector sequencing of assembly junctions was performed for the TUs of *crtE* and *crtB*. Sequence reads covering the junctions between the assembled parts, promoter to coding sequence and coding sequence to terminator, display accurate linking of these parts for both the CRTE and CRTB TUs (Figure 4-24 & Figure 4-26). Additional analysis of the connecting junction between the two TUs in the multigene vector shows the correct assembly of these two TUs with each other (Figure 4-25). This is in line with the match between the predicted restriction digestion patterns and the outcome of the digestions (Figure 4-23).

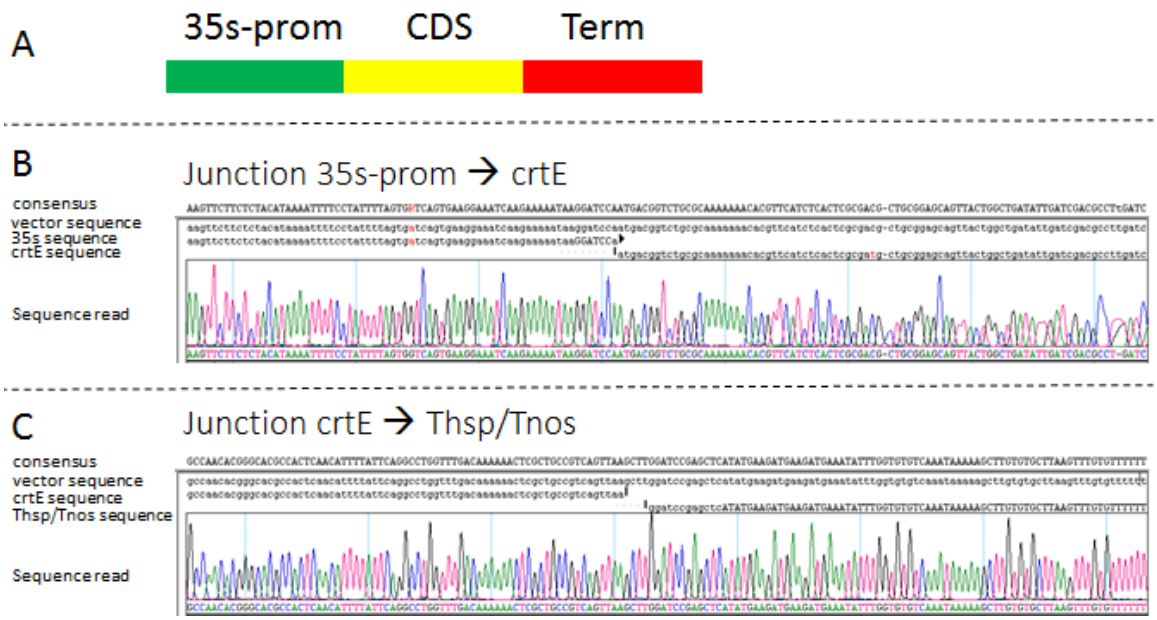

Figure 4-24 Sequence analysis of the junctions for crtE in the CRTE_CRTB binary vector.
Sequence analysis was performed with Sanger Sequencing techniques covering the junctions between the promoter and coding sequence and coding sequence and terminator. (A) Map of the transcriptional unit as designed. (B) Sequencing read of the junction between CMV-35s and *crtE*, compared *in silico* sequences. (C) Sequencing read of the junction between *crtE* and the Thsp/Tnos terminator, compared *in silico* sequences.

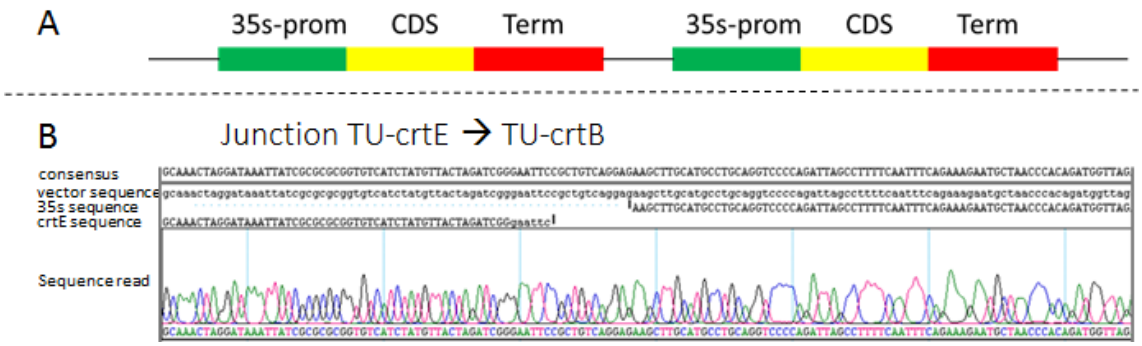

Figure 4-25. Sequence analysis of assembly junctions between expression cassettes

Sequence analysis of the junction between the TUs of crtE and crtB after binary assembly into multigene vector pDGB1Ω1-CRTE_CRTB. Sequence reads derived through Sanger sequencing. (A) Map of linked TUs as assembled in the multigene vector. (B)

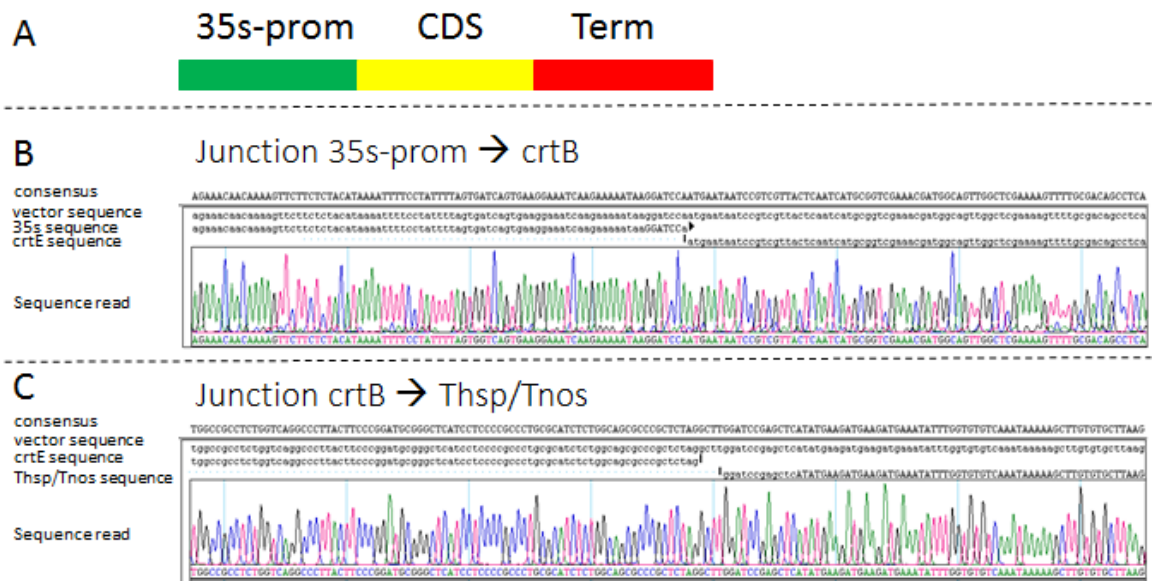

Figure 4-26. Sequence analysis of the junctions for crtB in the CRTE_CRTB binary vector. Sequence analysis was performed with Sanger Sequencing techniques covering the junctions between the promoter and coding sequence and coding sequence and terminator. (A) Map of the transcriptional unit as designed. (B) Sequencing read of the junction between CMV-35s and *crtE*, compared *in silico* sequences. (C) Sequencing read of the junction between *crtE* and the Thsp/Tnos terminator, compared *in silico* sequences.

4.3.4. Confirmation of functionality

A subset of the assembled single-gene and multi-gene constructs were screened via transient transformation in *N. benthamiana*. Leaf infiltrations were performed to determine functionality of the constructs for expression of the coding sequences and their potential impact on the isoprenoid pathway metabolism. The effect on the isoprenoid metabolism of the various constructs tested will be described in detail in chapter 5, while an overview of expression analysis is provided below. Based on confirmed stable internal reference genes from *N. tabacum* matching transcriptional sequences were selected and screened for in *N. benthamiana* (Schmidt and Delaney, 2010). *N. benthamiana* genes coding for Elongation factor 1α (EF1α), L23 ribosomal protein (L23) and Ubiquitin conjugating-enzyme (Ubi) were considered suitable and used as reference genes for the different RT-PCR analyses.

Expression analysis of RNA samples derived from leaf infiltrations with the MEP vectors demonstrated a partial successful outcome for the constructed multi-gene TUs. The RT-PCR outcomes are displayed in Figure 4-27. Outcome of the RT-PCR screening showed the expression of dxs_{ca}, mct_{ec}, mds_{ec} and hds_{ec} for the multi-gene vectors, the empty vector (EV) control (pDGB1α1) displayed no detectable expression for those genes. In the same infiltrations no expression was detected for the dxr_{ec}, cmk_{ec} and hdr_{ec} genes, similar to the findings for the EV-control. Visual differences can be observed for the dxs_{ca} gene in the single gene vector and the multi-gene vectors with targeting to the different cellular locations. Similarly mct_{ec} and hds_{ec} display a lower expression for the vector containing the six TUs from *dxr* to *hds*, compared to the vectors containing all seven genes of the MEP pathway. Transcription of mds_{ec} was detected in the MEP^{cyt} vector but not the MEP^{tp} vector.

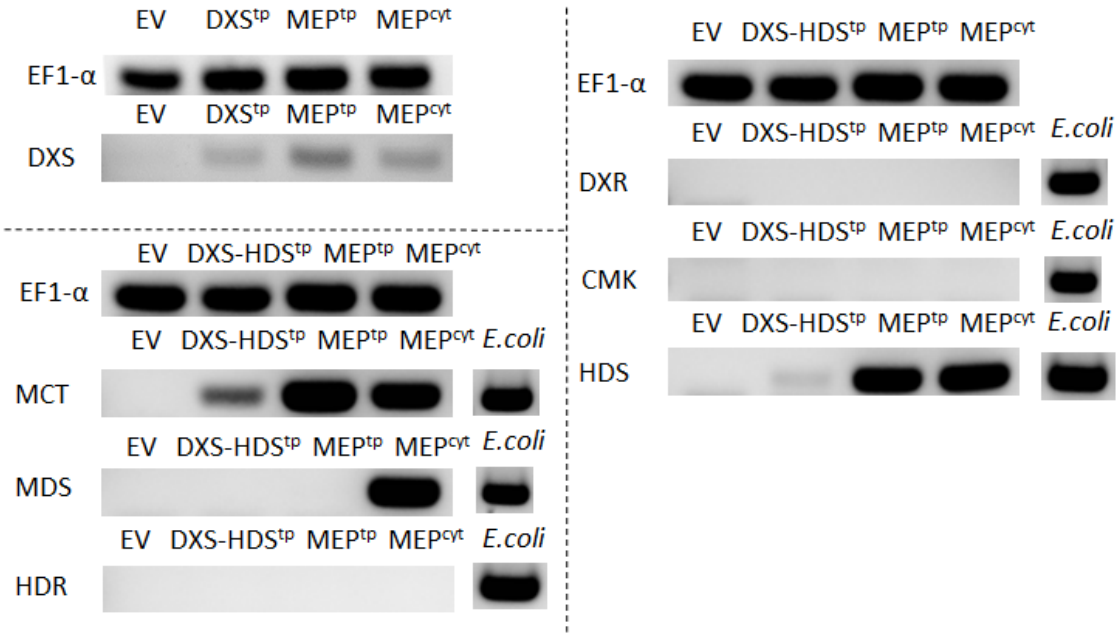

Figure 4-27. Expression analysis of MEP vectors.
RT-PCR analysis of the pDXS vector and the multi-gene constructs with six or seven out of seven genes assembled. Increase and appearance of expression was found for a sub-set of MEP genes: dxs_{ca}, mct_{ec}, mds_{ec} and hds_{ec}. Whilst for dxr_{ec}, cmk_{ec} and hdr_{ec} no expression in the multi-gene constructs was detected. EF1-α was used as a reference gene to confirm sample cDNA quality.

The transformation of the binary vector containing the *crtI* sequence was not successful. Therefore the single-gene constructs for *crtE* and *crtB* and their multi-gene assembly were tested and single-gene constructs were co-infiltrated as a comparison for the multi-gene construct. Leaf infiltrations were performed and leaf material was harvested. Samples were quenched and split into portions for RNA extractions and metabolite extractions. RNA was extracted and synthesised into cDNA for PCR confirmation of *crtE* and *crtB* expression. Samples were screened for the presence of *crtE* and *crtB* transcripts, EF1α was used as a reference gene. The outcomes presented in Figure 4-28 display the expression of *crtE* and *crtB* in the single-gene constructs. Both individually infiltrated samples as well as co-infiltrated single-gene constructs demonstrated expression of the transcripts, while the multi-gene construct did not show transcripts for either gene. The absence of transcripts in the multi-gene constructs suggests the vector to be dysfunctional.

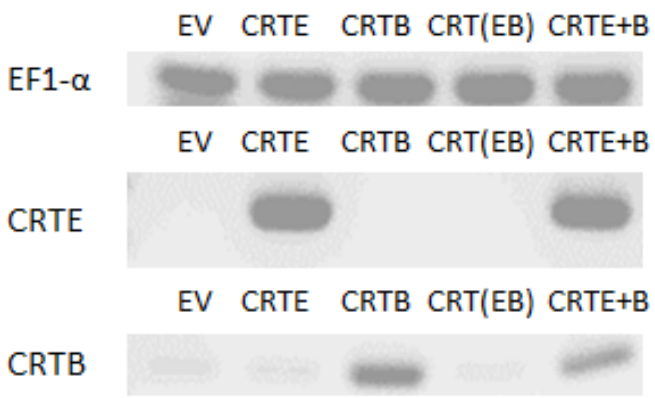

Figure 4-28. Expression analysis of CRTE and CRTB constructs.
RT-PCR of samples from infiltrated leaves of N.benthamiana. Expression of transcripts of the *crtE* and *crtB* genes with EF1-α as the reference gene. Samples of CRTE, CRTB and CRT(EB) compared the empty vector control (EV). Expression of *crtE* and *crtB* is confirmed in samples of single-gene constructs for both, for the individual infiltrations and the co-infiltrated samples (CRTE+B). The multi-gene construct "CRT(EB)" does not demonstrate expression of either *crtE* or *crtB*.

The analysis of the transiently transformed leaves of *N. benthamiana* was performed on both transcriptomics and metabolomics levels, i.e. gene expression levels and quantification of carotenoids and chlorophylls. Outcomes of these leaf infiltration experiments are discussed in chapter 5.

4.4. Discussion

4.4.1. Modular cloning system for synthetic biology

With the rise of systems and synthetic biology the need for modular cloning systems evolved. The idea to design and use genetic elements as parts, similar to parts for mechanical assembly, required standardisation of common elements utilised in molecular biology. I.e. like the universal parts to build a car, universal parts to build a vector could be generated according to this concept. In micro-organisms the BioBrick system was the first application of standardised system for synthetic biology (Knight, 2003). The development of such systems for plants started with the scar-benign cloning systems like Golden Gate cloning and Gibson cloning (Engler et al., 2008; Gibson et al., 2009). Although the systems are different in their technical execution, both systems allow for the assembly of large sets of DNA fragments. Gibson cloning makes use of DNA overhangs designed for the linking of DNA fragments. The system is scar-benign but designed assemblies do not provide flexibility (Gibson et al., 2009). Golden Gate cloning utilises standardised parts, based on type IIS restriction sites, which can be used in set combinations where similar parts are interchangeable for quick gene exchange and rapid assembly of transcriptional units (Engler et al., 2009). Both Golden Gate and Gibson cloning were designed for microbial and biomedical studies initially, in fungi, rat embryonic cells, and yeast respectively, and have been adapted to plant systems later (Gibson et al., 2008; Terfrüchte et al., 2014; Tong et al., 2012). GB-cloning offers similar flexibility as presented for the Golden Gate system and was directly designed for plant biotechnology experiments (Sarrion-Perdigones et al., 2011).

Golden Braid cloning, adapted from the Golden Gate method, was the first modular cloning method available for plant biotechnology (Sarrion-Perdigones et al., 2011). Implementation of this cloning technique for this thesis project demonstrated the advantages and disadvantages of the technique which are described below and summarised in Table 4-4. The first update, GB2.0, allowed for the assembly of GB-parts in entry vectors, which was found to be a useful

addition to the system both by the designers of the system and during the cloning procedures performed for this thesis (Sarrion-Perdigones et al., 2013). Once a library of parts is in place for cloning elements commonly used by a given molecular biologist, compatible parts can be assembled into TU's in a high throughput manner. This was demonstrated by the collection of TU's assembled during this PhD project. The difficulties with the assembly of TU's in the Ω backbone vectors is an issue, especially since the assembly of multi-gene vector will require at least one Ω-TU for any assembly with an odd number of TU's. Besides this concern, the flexibility of the system would require the assembly of a commonly used TU to be assembled in various backbone vectors to facilitate assembly of multi-gene vectors in different strategical setups. Furthermore, as the "binary" backbone vector does not possess a resistance marker gene for plant transformations, such elements need to be included in an assembly which automatically forces the user to assemble a multi-gene vector in case of a stable plant transformation strategy. While the assembly of multi-gene vectors can be performed rapidly, there are complications concerning the accuracy of the assembly and therefore the functionality of the created multi-gene vectors. Screen of the assembly process demonstrated both accurate and inaccurate assemblies, and only limited success for the expression of TU's. As demonstrated through the transient expression experiments the outcomes of transcription analysis were not consistent for these multi-gene vectors. A comparison of the presence of modular cloning systems in recently published studies shows the level of successful implementation of either Golden Braid Cloning or Golden Gate Cloning. Where the Golden Gate method has been successfully reported in various publications, showing the use of the method in genetic engineering of rat embryonic and human cell lines and genome editing in mono- and dicot plants, Golden Braid has been reported in only two publications other than the work presented by the designers (Ma et al., 2015; Sakuma et al., 2014; Sonawane et al., 2016; Tong et al., 2012). Especially the development of a generic CRISPR/cas9 system linked to the Golden Gate method has launched the application

of the technique for a range of organisms. In plants especially utilising the combined power of the techniques allows for efficient genomic editing (Lowder et al., 2015).

Table 4-4. Advantages and disadvantages of the Golden Braid Cloning System.
Overview of positive and negative aspects of the GB cloning system. Observations made in comparison with presented work of the designers and experiences obtained during the experiments performed for this thesis (Sarrion-Perdigones et al., 2013).

Positive aspects	Negative Aspects
1. The software available at the GB-website is helpful for rapid *in silico* design and preparation of any cloning strategies.	1."Binary" vectors of the GB-system do not possess a marker gene for plant transformation. Such marker element would have to be added as an independent TU to a multi-gene assembly.
2. Construction of GB-parts and TU's can be performed in a high throughput fashion.	2. The "Ω" backbone vectors demonstrate a very low efficiency for the assembly of TU's, a difficult issue concerning assembly strategies for multi-gene vectors.
3. Binary assembly can be performed in a similar fashion as for GB-parts and TUs. Although assembly accuracy requires improvement	3. The transcription of multi-gene expression vectors is not consistent, partial or no expression was observed in various cases. Issues with the binary assembly probably caused these issues in the vectors tested
4. The implementation of the system allows for the rapid generation of a library of GB-parts and vectors.	4. For an efficient use of the GB cloning system, TU's would need to be assembled in different versions of the backbone vectors to maintain the flexible and versatile nature of the system.
5. The cloning method allows for the quick assembly of vectors with different parts (promoter, terminator and/or CDS) to compare efficiency or determine the effect per CDS.	

4.4.2. Functionality of GB assembled TUs

For a set of ~30 different Golden Braid vectors assembly was attempted, with the aim for this vector library to function as a platform for the metabolic engineering of isoprenoids in plants, focussing on the overexpression of pathways and pathway segments. Both genes for the MEP

pathway, upstream of isoprenoid biosynthesis, and a segment of the microbial carotenoid pathway were selected for this platform in an attempt to increase the pool of isoprenoid precursors and more specifically enhance the biosynthesis of carotenoids in plants. In order to avoid strict regulatory regulation of biosynthesis for these compounds, cytosolic targeting was implemented to locate the synthetic pathways outside of their endogenous cellular location, as in plant cells the MEP and carotenoid pathways are normally active in the plastids. After assembly, the binary vectors were screened for functionality via leaf infiltrations in *N. benthamiana*. Analysis was performed for both transcription and metabolomics changes, of which the latter will be discussed in chapter 5.

Since the discovery of the MEP pathway as the second isoprenoid precursor pathway in bacteria and plastids (Lichtenthaler et al., 1997; Rodríguez-Concepción and Boronat, 2002), a wide range of studies have been performed. For most genes of the MEP pathway overexpression and knock-out mutants have been developed to study the impact of the individual enzymes on isoprenoid biosynthesis. Overexpression of *dxs*, *dxr* and *hdr*, in tomato, Arabidopsis and orchids respectively, have demonstrated those steps to be rate limiting for the flux of isoprenoid precursors, and are therefore considered important regulatory enzymes in the pathway (Carretero-Paulet et al., 2006; Enfissi et al., 2005; Huang et al., 2009). The knock-out mutant of HDS resulted in the accumulation of its substrate, which is linked to retro-grade signalling (Zhou et al., 2012). An advanced study on both the MEP and MVA pathways confirmed the effect of overexpressing individual MEP genes in Arabidopsis, suggesting a significant impact for the MDS enzyme (Lange et al., 2015). Alternatively various studies on feedback regulation link isoprenoid building blocks IPP and DMAPP to the expression of *dxs*, suggesting a negative feedback loop to control isoprenoid levels (Banerjee et al., 2013). To advance upon the elucidation of MEP pathway functionality a synthetic biology strategy was defined using the GB cloning method, with the aim to overexpress the MEP pathway in a modular vector containing all genes of the pathway as individual TUs. Partly focussed on increased isoprenoid levels, the TUs were

designed for targeting to the cytosol, to reduce the chances of any regulatory inhibition in the plastids as the endogenous site of activity. The reverse track has been performed with the MVA pathway, for which an operon with all six genes was targeted to the plastid demonstrating higher carotenoid and sterol levels (Kumar et al., 2012) .

The constructed vectors for the MEP pathway were found to be assembled inaccurately through screening via restriction digestions, although presence of coding sequences was detected. To determine the functionality of the vectors expression analysis was performed and the findings demonstrated a semi-positive outcome for the multi-gene vectors screened. The increase or appearance of transcripts for *dxs*, *mct*, and *hds* were found in multi-gene vector targeting both the cytosol and the plastid, whilst transcripts of the *E. coli mds* were only detected for the cytosolic targeted vector. Analysis of gene expression for the TUs containing the *crtE* and *crtB* genes displayed the expression of both genes in single-gene vectors, while the multi-gene vectors containing both genes failed to express either gene. The absence of expression is similar to the lack of expression of some of the MEP genes in their respective multi-gene constructs. Whilst the plasmids containing a single TU for either *crtE* or *crtB* demonstrate expression, the purpose of using the Golden Braid method is the assembly of multi-gene constructs to simplify overexpression experiments in plant transformations. The outcomes of the expression analysis suggest that the GB technique requires improvements to allow for successful application of the modular cloning system. A fully functional vector as a result of the assembly process is important to utilise the system to its full extent.

5. Ectopic expression of isoprenoid pathway genes: screening and validation of an isoprenoid Synthetic Biology vector library

5.1. Introduction

The discovery and functional elucidation of the isoprenoid genes and their products present in various organisms (Carretero-Paulet et al., 2006; Jinfen et al., 2012) has led to the production of a large number of overexpression lines and knockout mutants for key enzymes in the pathway (Enfissi et al., 2005; Fraser et al., 2007; Fray and Grierson, 1993). An important aspect of the biosynthesis of isoprenoid is its strict regulation at the transcriptional and post-transcriptional level. The results on sequestration mechanisms, described in chapter 3 of this thesis, could play a role in the regulatory processes involved in the MEP and carotenoid pathway. The accumulation of carotenoids in plastid membranes could prevent feedback regulation within the pathway. However, evidence has been found for feedback interaction between compounds of the carotenoid pathway and regulation of MEP pathway (Lois et al., 2000).

A strategy to circumvent the strict regulation of plastidial isoprenoid biosynthesis could be achieved by relocating the pathway to an exogenous compartment such as the cytosol. Such experiments have been performed for the cytosolic MVA pathway, for which attempts to overexpress these genes in plastids were made (Kumar et al., 2012). With no known regulatory mechanisms for the intermediates of the ectopic MVA pathway acquired in the plastid, regulation of the process is restricted and expression is not hindered. Furthermore, the plastid has the biosynthetic elements available to utilise the extra generated isoprene precursors synthesised via the MVA enzymes. In a similar fashion one could imagine a cytosolic overexpression of MEP and carotenoid genes will result in unregulated accumulation of more isoprenoid building blocks and carotenoids. Moreover, the suggested exchange of IPP and DMAPP between the cytosol and the plastid could lead to a higher general yield of isoprenoid, not only at the site of overexpression.

Chapter 4 described the design and assembly of a set of overexpression vectors for genes of the isoprenoid pathway: the carotenoid pathway and the upstream MEP pathway. These vectors were screened via transient leaf infiltrations in *N. benthamiana* to detect changes in the

metabolite profile for the targeted isoprenoid pathway branches. In order to achieve this, two sets of MEP pathway vectors were designed, targeted to the cytosol and plastid respectively. The leaf infiltrations were performed for vectors of both sets to compare the effect of location on the overexpressed genes. Experiments including a co-infiltrated vector for keto-carotenoid synthesising enzymes CRTZ and CRTW were performed to disrupt regulation by depleting the pool of β-carotene, an intermediate towards xanthophylls. The hypothesis for this study is that overexpression of the MEP pathway, internal or external from the plastid, can enlarge the pool of isoprenoid precursors (C_5 building blocks), which increase the accumulation of isoprenoids.

Whereas the multi-gene vectors for the MEP pathway were designed for targeting to both the cytosol and the plastid, the vectors for carotenoid genes *crtE* and *crtB* were generated with cytosolic targeting only. Overexpression of *crtE*, *crtB,* and *crtI* in the plastid was studied previously as demonstrated by the work of Nogueira et al. in tomato (Nogueira et al., 2013). Moreover, it would be of interest to see if carotenoids can accumulate in the cytosol, either as crystals or sequestered in the available membranes. Other organelles were considered, but with the mevalonate pathway present in the cytosol it seemed the most logical choice. Leaf infiltrations performed with the vectors for CRTE and CRTB were screened for any changes in carotenoid, chlorophyll and sterol content, to elucidate the effect of overexpressing these genes in the cytosol. The hypothesis for this study is that overexpression of the bacterial carotenoid genes *crtE* and *crtB* allows for the accumulation of the carotenoids (phytoene) in the cytosol, which can accumulate at the site of biosynthesis.

5.2. Transient leaf infiltrations in *N. benthamiana*

The infiltration of leaves in *N. benthamiana* plants with *Agrobacterium* strains containing vectors is an established system of transient plant transformation used for the screening of vector functionality. *Nicotiana* species, especially *N. benthamiana* and *N. tabaccum*, are considered useful model plants for biotechnological studies, due to their relatively rapid development and

easy transformation process. Furthermore *N. benthamiana* is used by industry for the production of therapeutic glycoproteins (Gómez et al., 2013; Gómez et al., 2009; Strasser et al., 2008).

The biosynthesis of keto-carotenoids gives a distinct orange to brown phenotype in plants as the keto-carotenoids accumulate in the leaves. Therefore the vector containing linked coding sequences for *crtZ* and *crtW* was used as a marker for the leaf infiltrations method used. The expected phenotype was observed as shown in Figure 5-1 where the CRTZ/CRTW vector caused a dark green and orange to brown colour phenotype. In further experiments the vector was used in combination with some of the vectors created with the GB method to disrupt the regulation of the plastid isoprenoid biosynthesis. The phenotype of the CRTZ/CRTW vector and the detected expression of the MEP and carotenoid genes in the GB vector infiltration demonstrate the transient expression was successful. For a complete overview, the metabolic profiling of various isoprenoids was performed (described in sub-chapter 5.3). Chromatograms of (keto-) carotenoid and chlorophyll analysis via UPLC and HPLC techniques are displayed in the appendix (Figure A-6-Figure A-10).

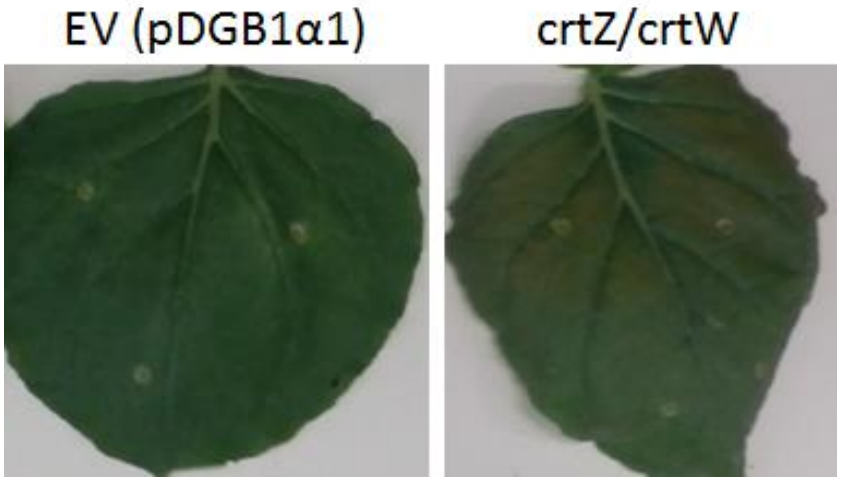

Figure 5-1. Phenotype of crtZ/crtW leaf infiltrations.
Infiltration with an expression vector (*crtZ* and *crtW* genes) leads to the production of ketocarotenoids. A darker green to orange to brown leaf colour can be observed compared to leaves infiltrated with an empty vector control.

An aspect of the infiltration results is influenced by leaf position on the infiltrated plant. Per experiment three to four leaves are infiltrated per plant for three plants per construct combination. The four leaves were selected from the middle segment of the plant at a 10-12 leaf stage, leaves were screened for shape and damages and/or health issues before selection. Plants are infiltrated at the defined developmental stage, nevertheless the leaves selected are not identical in their developmental stage, and i.e. leaves are all fully developed but not fully expanded. Therefore differences can occur between the samples derived from individual leaves as the metabolism within the leaf tissues varies based on the status of "expanding" or "maintenance". An example is demonstrated in Figure 5-2, where especially for the infiltrated crtB construct the impact between samples is noticeable. Overexpression of *crtB* caused increased carotenoid levels, especially phytoene and phytofluene, for which the highest quantities were found in the top leaves infiltrated. This effect is most relevant for compounds which are accumulating at the detection level and therefore are difficult to measure. Carotenes do not commonly accumulate in photosynthetic tissues and therefore it is likely to assume a strict regulation mechanisms is not present. Alternatively a ceiling can be detected for the photosynthetic pigments, both xanthophylls and chlorophylls, since the photosynthetic system is strictly regulated.

The climate has a strong effect on performance of the *Agrobacterium* strains, as soil-bacteria do not sustain well in temperatures above 30°C. Moreover intense sunlight can cause photo bleaching in *Nicotiana* plants (Mooney et al., 1974). Therefore some experiments described in this chapter display less impact for the constructs tested than others, which is due to trials taking place February till April and June till August. Temperatures could be maintained at ~25°C until April, from June until August temperatures regularly reached ~35°C. Leaf infiltration can be optimised by repressing potential gene silencing by using the P19 vector. Use of this vector can reduce the regulatory mechanisms that might silence any overexpressed transcripts occurring during the leaf infiltrations (Voinnet et al., 2003).

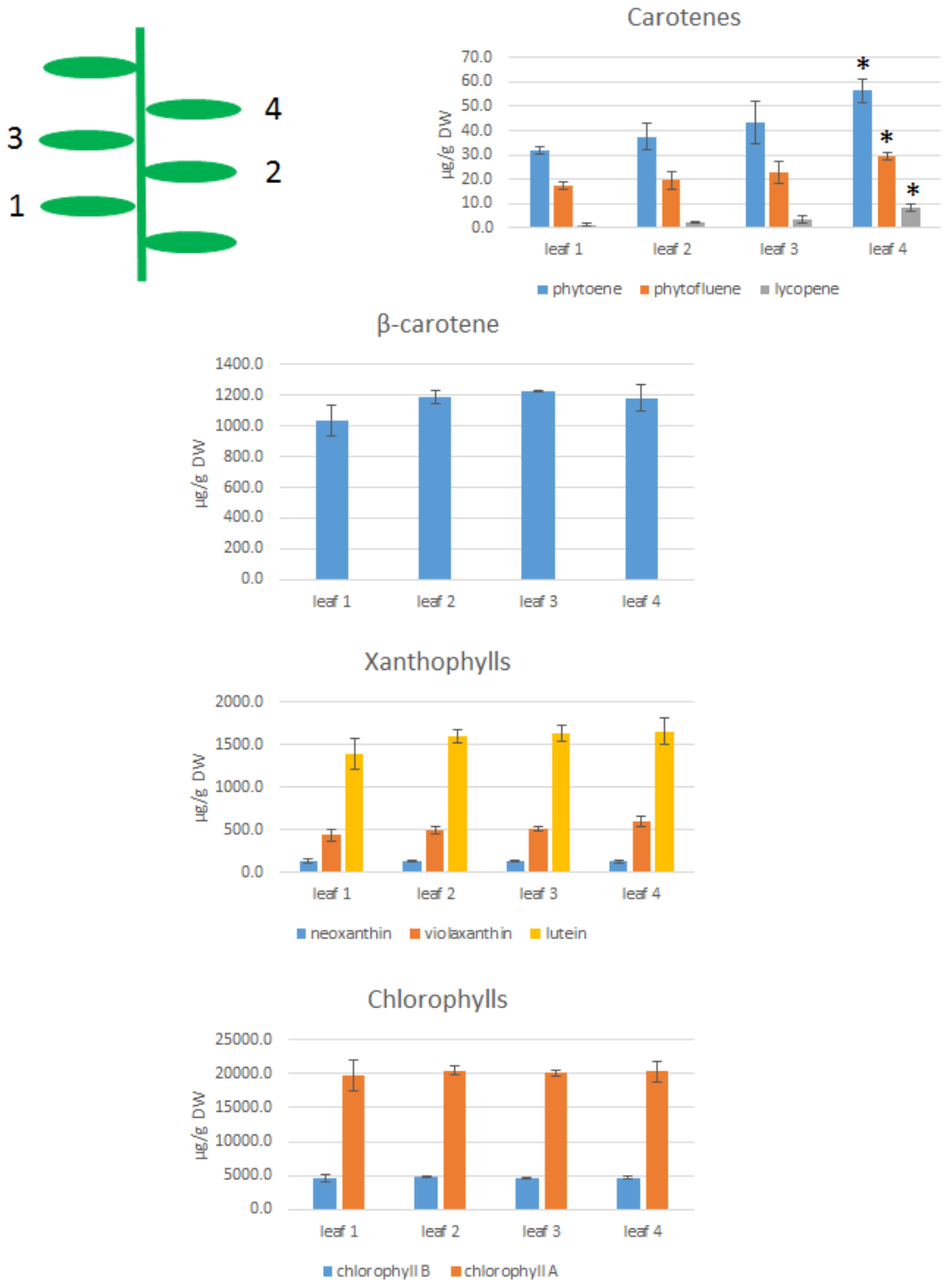

Figure 5-2. Quantitative differences of samples from different leaf positions.
Individual leaves were marked per position during infiltrations (1 base, 4 top), leaves were are fully developed but top leaves (3 & 4) would still expand during incubation period. Differences in carotenoid and chlorophyll content were compared based on leaf position. Analysis of CRTB infiltrated leaves demonstrates the effect of the constitutive expression is the strongest in the top leaves - a clear trend for carotenoids in general, and especially carotenes. * = p-value <0.05, Student's T-test compared to leaf 1.

5.3. Results

Using GB cloning a collection of vectors was generated focussed on isoprenoid biosynthesis, the bacterial carotenoid pathway and the upstream MEP pathway. Transient transformation of *N. benthamiana* demonstrated mixed outcomes related to the transcription of all genes placed in transcriptional units for overexpression. Concerns about the inaccurate assembly of the multi-gene vectors has been discussed in chapter 4, in combination with the outcome of the expression screens in *N.benthamiana*. Despite the partially unsuccessful expression results, samples of infiltrated material were screened for changes in their carotenoid and chlorophyll profiles, alternatively investigating any changes in phytosterols or keto-carotenoids.

5.3.1. Metabolic profiling of leaf infiltrations with the MEP overexpression vectors

With a large collection of GB vectors for the MEP pathway generated, an initial screen via leaf infiltrations was performed to determine the effect on carotenoid and chlorophyll levels. For this purpose the plastid targeted vectors were selected, due to their location compatibility with the endogenous MEP, carotenoid and chlorophyll pathways. The multi-gene vectors for the MEP pathway were utilised in this trial, including the single gene DXS vector and all further steps of the MEP pathway. This included the DXS-DXR, DXS-CMK, DXS-MDS, DXS-HDS, DXS-HDR, the DXS-MCT multi-gene vector was not ready for *Agrobacterium* leaf infiltration at this time; data analysis of the carotenoids and chlorophylls quantified demonstrated a significant increase of various compounds for the single gene DXS and the multi-gene vector for the MEP pathway (Figure 5-3, appendix: Table A-5). Trends suggesting increases in measured compounds were observed for other vectors screened, but no significant differences were found due to broad variation between samples. The increases caused by the DXS-vector included ~43% and 47% for violaxanthin, ~43% and 47% for chlorophyll A and B, and slightly lower increases for lutein and β-carotene at ~23% and 41% respectively. Impact of the multi-gene MEP vector was found to be higher, demonstrating significant differences for neoxanthin, violaxanthin, chlorophyll A and β-

carotene of ~67%, 65%, 68% and 62% respectively. No changes were found in the carotenoid to chlorophyll ratio (Table 5-1).

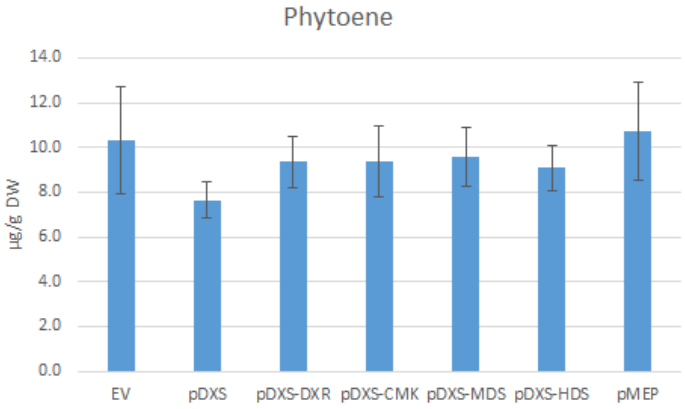

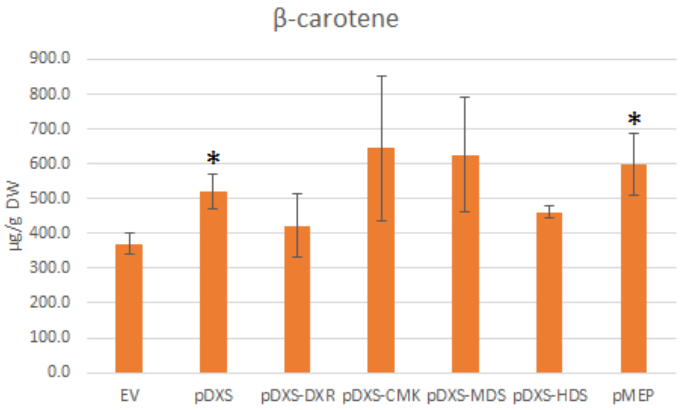

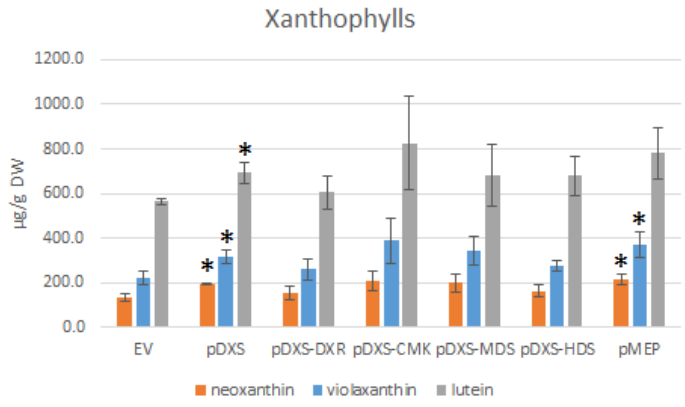

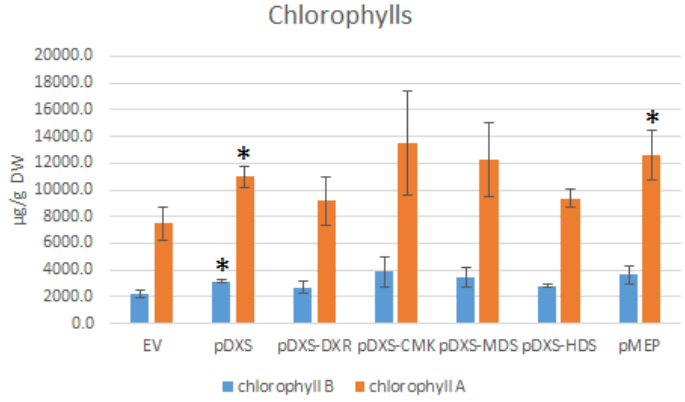

(Figure on previous page)

Figure 5-3. Carotenoid and chlorophyll content in MEP multigene infiltrated leaves.
Detection of phytoene, β-carotene, xanthophylls and chlorophylls in all samples analysed. The entire range of MEP vectors targeted to the plastid (except pDXS-MCT), from the single TU for pDXS to the multi-gene vector for the pMEP pathway were screened via transient transformation and UPLC analysis. Significant differences were observed for the DXS and MEP vectors. *= significant (p-value<0.05, Student's T-test).

In order to reduce the observed deviation between samples of the same construct, another screen was performed with less constructs, allowing more samples per construct. This screen, which only included the plastid targeted DXS and complete MEP vectors for both plastid and cytosolic targeting, still demonstrated minor differences (Figure 5-4), and the same outcome was provided in the carotenoid to chlorophyll ratio (Table 5-2). Trends in this screen of the GB-vectors shows smaller differences than observed in the initial screen with the plastid targeted vectors (Figure 5-3).

Table 5-1. Overview of carotenoid to chlorophyll ratios for GB-MEP samples.
Carotenoid/chlorophyll ratios of infiltrated leaves of GB-MEP vectors, plastid targeted series of multi-gene vectors for the MEP pathway. Sum of analysed carotenoids and chlorophyll presented besides the carotenoid/chlorophyll ratios of each vector specific sample set. No significant differences were observed between samples tested.

Screen I	EV-control	pDXS	pDXS-DXR	pDXS-CMK	pDXS-MDS	pDXS-HDS	pMEP
carotenoids	1413 ±76	1846 ±107	1559 ±208	2201 ±536	1939 ±396	1722 ±92	2068 ±287
chlorophylls	9716 ±1538	14153 ±905	11858 ±2277	17412 ±5023	15664 ±3506	12180 ±821	16220 ±2502
ratio car/chlo	0.15	0.13	0.13	0.13	0.12	0.14	0.13

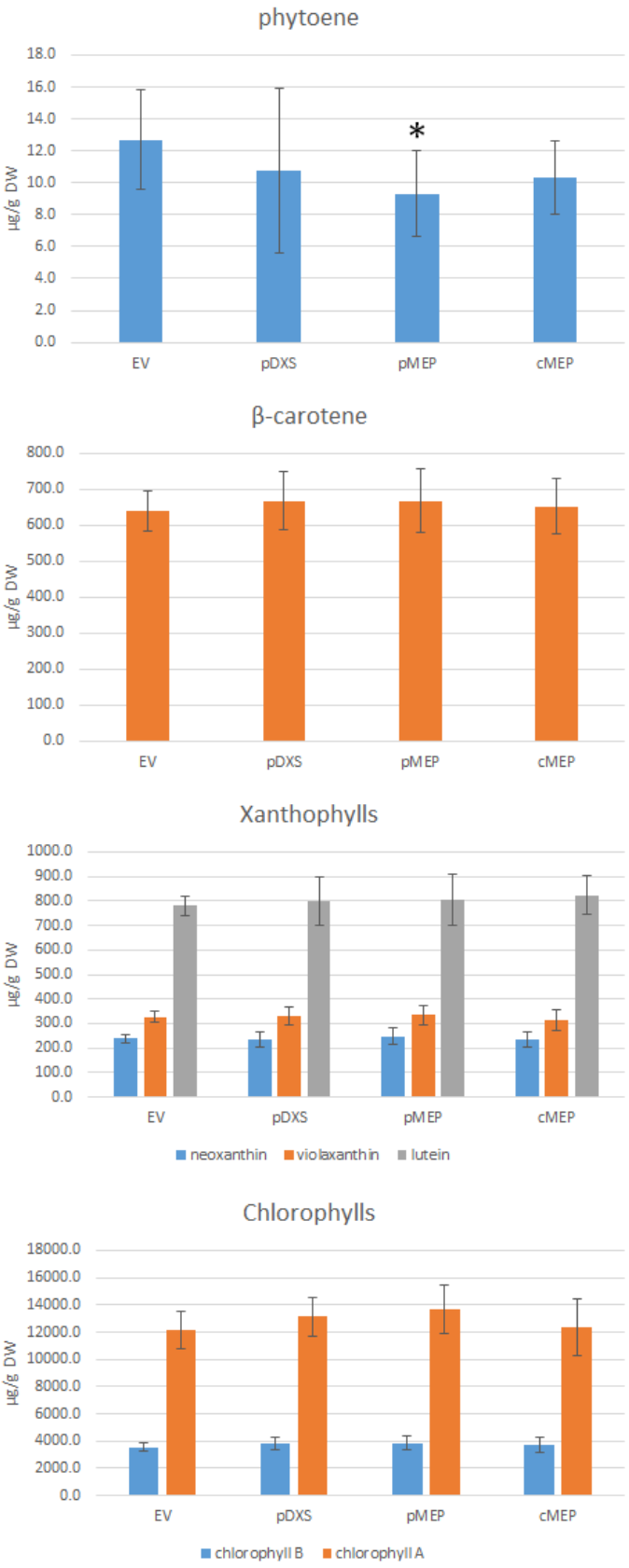

Figure 5-4. Analytical comparison of leaf infiltration for pDXS, pMEP and cMEP.
Quantification of phytoene, β-carotene, xanthophylls and chlorophylls. No significant increases were detected for any sample compared to the control (EV). * = significant (p-value<0.05, Student's T-test).

Although variation between samples infiltrated with the same vector has reduced, this effect has been matched by reduced differences between vectors. The only significant difference is a decrease in phytoene levels for the plastid targeted MEP multi-gene vector, which is reduced by ~27%. No significant differences were found for the plastid targeted DXS vector, contrary to the initial findings which demonstrated a minor increase in most compounds analysed. Any impact of the MEP multigene vector targeted to the cytosol is not detected in these infiltrations. Table A-6 in the appendix provides an overview including the negative control.

Table 5-2 Overview of carotenoid to chlorophyll ratios for samples of GB-MEP infiltrations.
Carotenoid/chlorophyll ratios of infiltrated leaves of GB-MEP vectors; plastid targeted DXS and MEP and MEP targeted to the cytosol. Sum of analysed carotenoids and chlorophyll presented next to the carotenoid/chlorophyll ratios of each vector specific sample set. Ratios do not change between samples or in comparison to the control.

Screen II	EV-control	pDXS	pMEP	cMEP
carotenoids	2055 ±107	2080 ±238	2092 ±260	2093 ±210
chlorophylls	15723 ±1718	16919 ±1870	17519 ±2278	16038 ±2644
ratio car/chlo	0.13	0.12	0.12	0.13

With the initial experiments showing little effects of the overexpression vectors, an alternative approach was used to determine functionality of the vectors. Co-infiltration of the GB MEP vectors with the earlier described overexpression vector for *crtZ* and *crtW*, responsible for the accumulation of keto-carotenoids, could potentially lead to modifications in the pathway regulation, which could cause the GB MEP vectors to demonstrate an effect. GB MEP (complete pathway) vectors targeted to both the plastid and the cytosol were screened, plastid targeted DXS and DXR vectors were included as well. A graphical overview is depicted in Figure 5-5 and Figure 5-6. Levels of carotenoids, xanthophylls, keto-carotenoids, and chlorophylls were quantified using UPLC analysis.

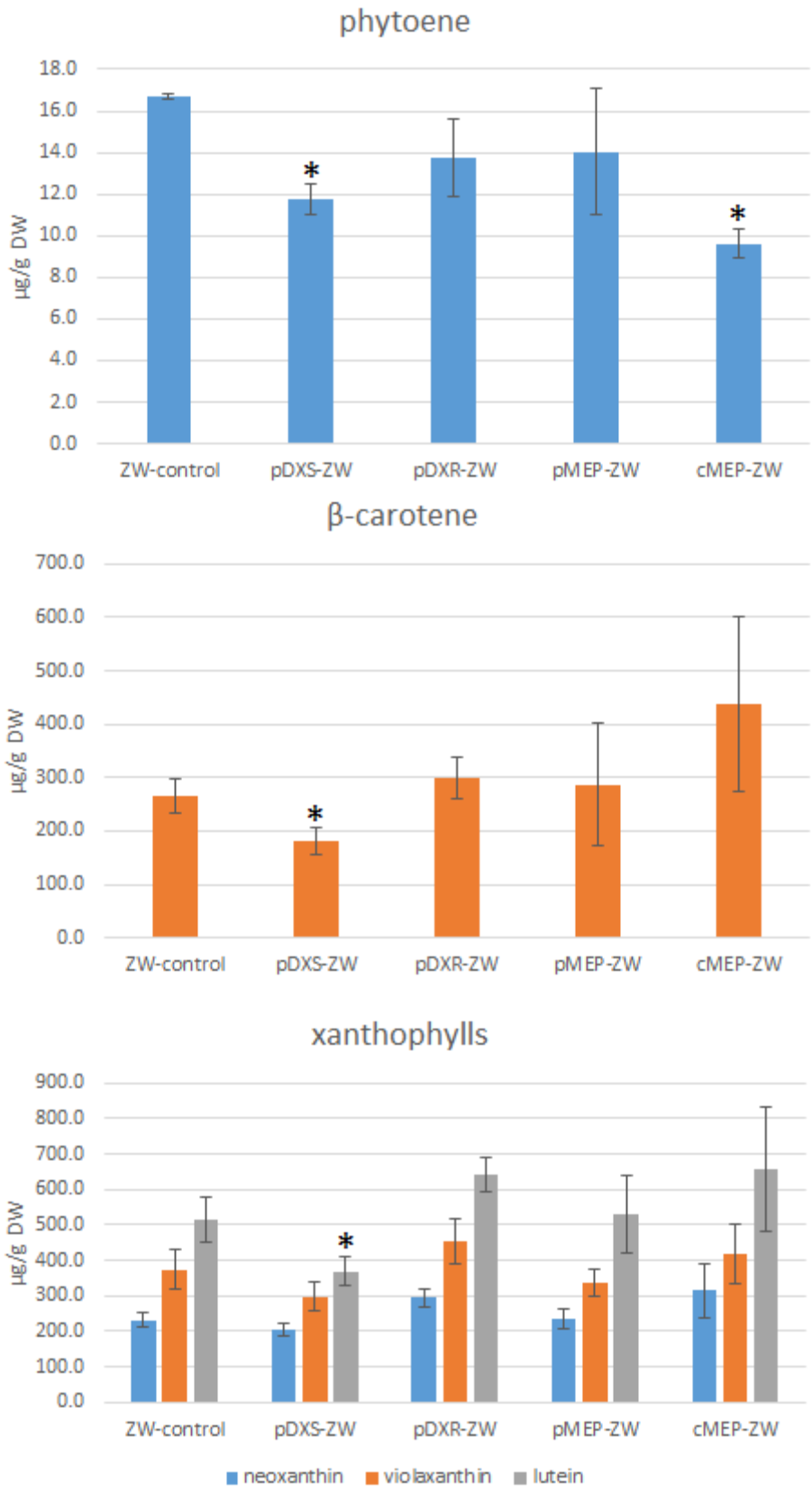

Figure 5-5. Quantification of carotenoids of GB-MEP/ZW co-infiltrated leaves.
Abundances of phytoene, β-carotene and xanthophylls for GB-MEP vectors co-infiltrated with a CRTZ/CRTW vector which accumulates ketocarotenoids (see Figure 5-6). Detected compounds were quantified via UPLC analysis and significant decreases were found for samples containing pDXS, pMEP and cMEP. * = significant (p-value<0.05, Student's T-test).

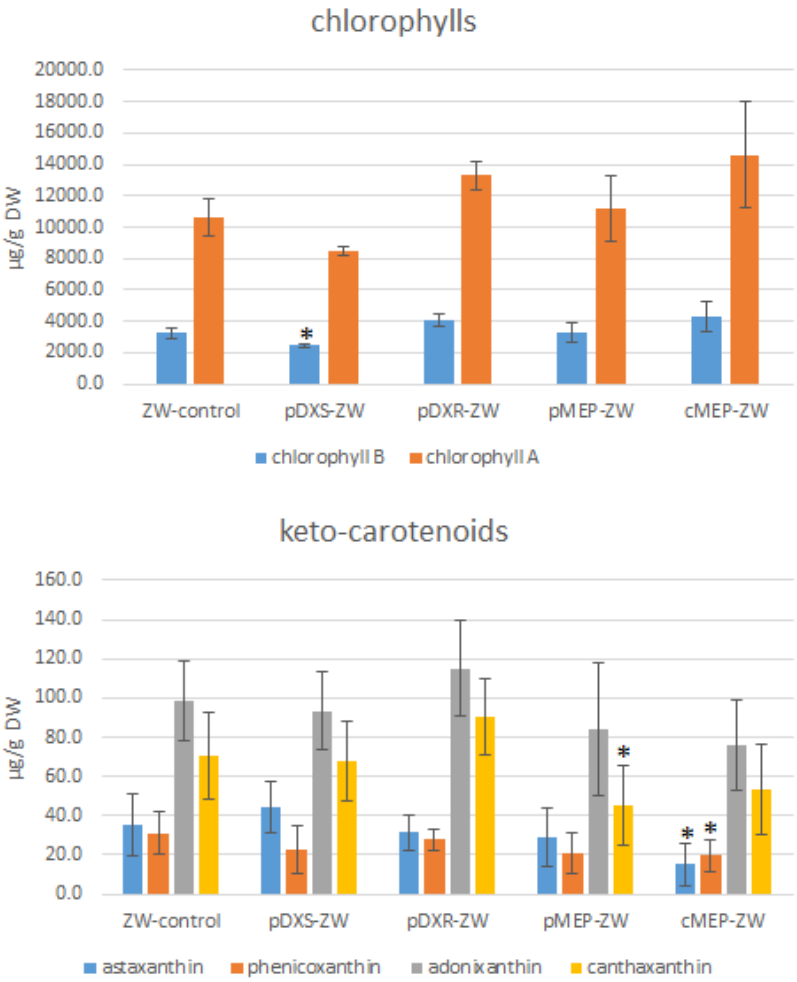

Figure 5-6. Abundances of chlorophylls and ketocarotenoids of GB-MEP/ZW infiltrated leaves. UPLC analysis of chlorophylls and ketocarotenoids, in co-infiltrated GB-MEP/CRTZW samples. Detected compounds were quantified and significant decreases were found for samples containing pDXS, pMEP and cMEP. * = significant (p-value<0.05, Student's T-test).

The impact of the ZW-vector compared to the empty vector control (not displayed in Figure 5-5 & Figure 5-6) showed no significant changes between the carotenoids and chlorophylls normally present in photosynthetic tissues except β-carotene which reduced in concentration by ~50%, and was replaced by roughly an equal amount of keto-carotenoids. Between the ZW-control and the mixtures of ZW and MEP vectors the only significant differences observed were decreased levels of phytoene, lutein, β-carotene, chlorophyll B, astaxanthin, phenicoxanthin and canthaxanthin in the ZW-pDXS, ZW-pMEP and ZW-cMEP infiltrated leaves. ZW-pDXS infiltrated leaves showed reduced levels of phytoene, lutein, β-carotene and chlorophyll B, at ~29%, 28%, 32% and 25% respectively. For the MEP multi-gene vectors, the plastid-targeted ZW-pMEP had significantly lower levels of canthaxanthin at ~36%, whilst the cytosolic ZW-cMEP showed the

highest decreases for phytoene, astaxanthin and phenicoxanthin at ~43%, 30% and 37% respectively. No changes occurred in the carotenoid to chlorophyll ratio between the sample's co-infiltration with the CRTZW-strain (Table 5-3). An additional overview including the negative controls can be found in the appendix (Table A-7).

Table 5-3. Overview of carotenoid to chlorophyll ratios for MEP/ZW samples.
Co-infiltrated GB-MEP & CRTZ/CRTW vectors. Sum of analysed carotenoids and chlorophyll presented besides the carotenoid/chlorophyll ratios of each vector specific sample set. Ratios do not change between samples or in comparison to the control.

Screen III	ZW-control	pDXS-ZW	pDXR-ZW	pMEP-ZW	cMEP-ZW
carotenoids	1727 ±178	1339 ±131	2023 ±160	1643 ±261	2038 ±441
chlorophylls	13847 ±1490	10901 ±303	17396 ±1296	14469 ±2670	18906 ±4356
ratio car/chlo	0.12	0.12	0.12	0.11	0.11

5.3.2. Metabolic profiling of leaf infiltrations with the CRTE and CRTB overexpression vectors

The CRTB single vector and CRTE-CRTB multi-gene vector were the first two constructs for the bacterial carotenoid pathway to be successfully transformed into *Agrobacterium* and screened in *N. benthamiana* leaves. The experiments conducted in the first quarter of the year demonstrated a clear impact of the infiltrated CRTB construct, which increased levels of all detected carotenoids, xantho-, and chlorophylls. The 14-fold increase of phytoene, compared to the EV-control, and the appearance of phytofluene and lycopene above detection level were most significant. Other increases were found with lutein and β-carotene at ~25% and ~30% respectively, compared to the control. A graphical overview is displayed in Figure 5-7, a numeric overview of the abundances can be found in Table A-8. As described in chapter 4, the CRTE/CRTB multigene vector did not demonstrate any gene expression when transiently screened in *N. benthamiana*, which is matched by no significant changes in carotenoid and chlorophyll content. Both the empty vector and the multi-gene CRT(EB) show a decrease in carotenoid and chlorophyll content compared to the non-infiltrated negative control, which is likely caused by the stress induced through the leaf infiltrations. For the CRTB infiltrated leaves the differences

between the negative control and the infiltrated leaves overcome or demonstrate a trend towards increased level, although these differences are not significant.

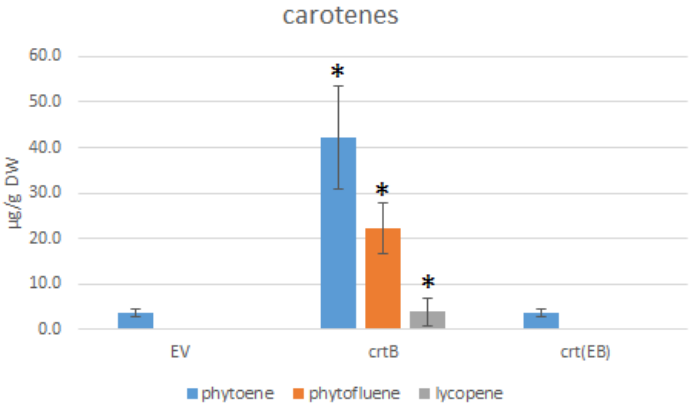

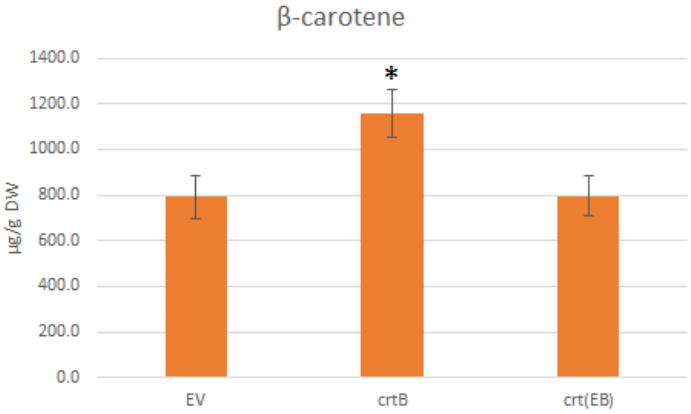

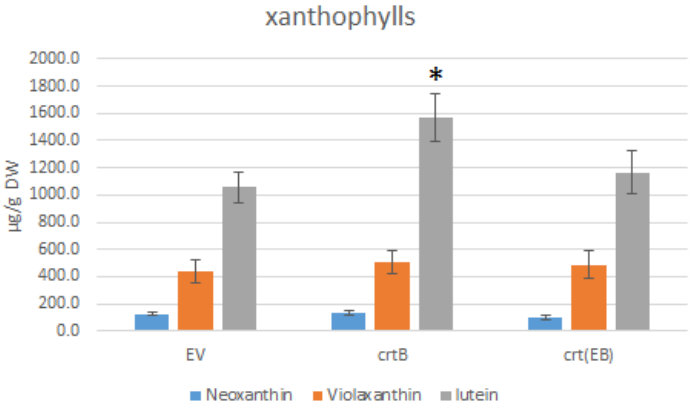

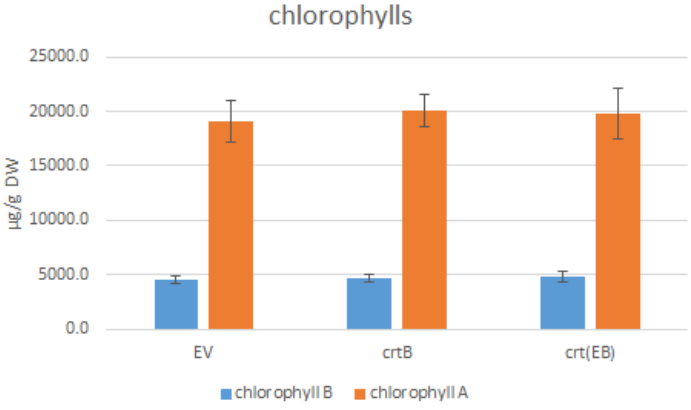

(figure on previous page)

Figure 5-7. Carotenoids and chlorophylls in leaves infiltrated with EV, CRTB and CRT(EB).
Quantifications of carotenoids and chlorophylls using UPLC techniques. The samples of the CRTB infiltrated leaves showed increased levels of phytoene, lutein and β-carotene, whilst phytofluene and lycopene were detected compared to being absent in the EV control (* is significant: p-value<0.05, Dunnett's test).

After further attempts to generate an *Agrobacterium* strain containing the overexpression vector for crtE, a strain was obtained and screening in *N. benthamiana* was performed. For this screen CRTE and CRTB overexpression vectors were tested individually and co-infiltrated, again in comparison to the CRT(EB) multi-gene vector. The impact of the vectors in this screen was less strong due to the timing of the experiment, as plants were grown over summer compared to winter for the data presented in Figure 5-7 and Table A-8. Despite a reduced impact of the overexpression vectors an increase in phytoene and phytofluene was observed. No further significant changes were detected, nor was lycopene observed in the UPLC chromatograms. Abundances as analysed from UPLC traces are displayed in Figure 5-8 (numeric overview in appendix: Table A-9).

With a less prominent change in carotenoid and chlorophyll levels a more robust method for carotenoid analysis was utilised to detect the appearance of lycopene, as the lycopene levels dropped below the threshold of detection in UPLC traces. HPLC analysis showed the presence of lycopene in samples of crtB infiltrated leaf material, whilst no lycopene was detected in the leaf control samples. An overview of the detection and confirmation of lycopene, phytoene and phytofluene using HPLC techniques is provided in Figure 5-9-Figure 5-11, chromatograms of HPLC analysis for CRTB infiltrated samples can be found in the appendix (Figure A-10).

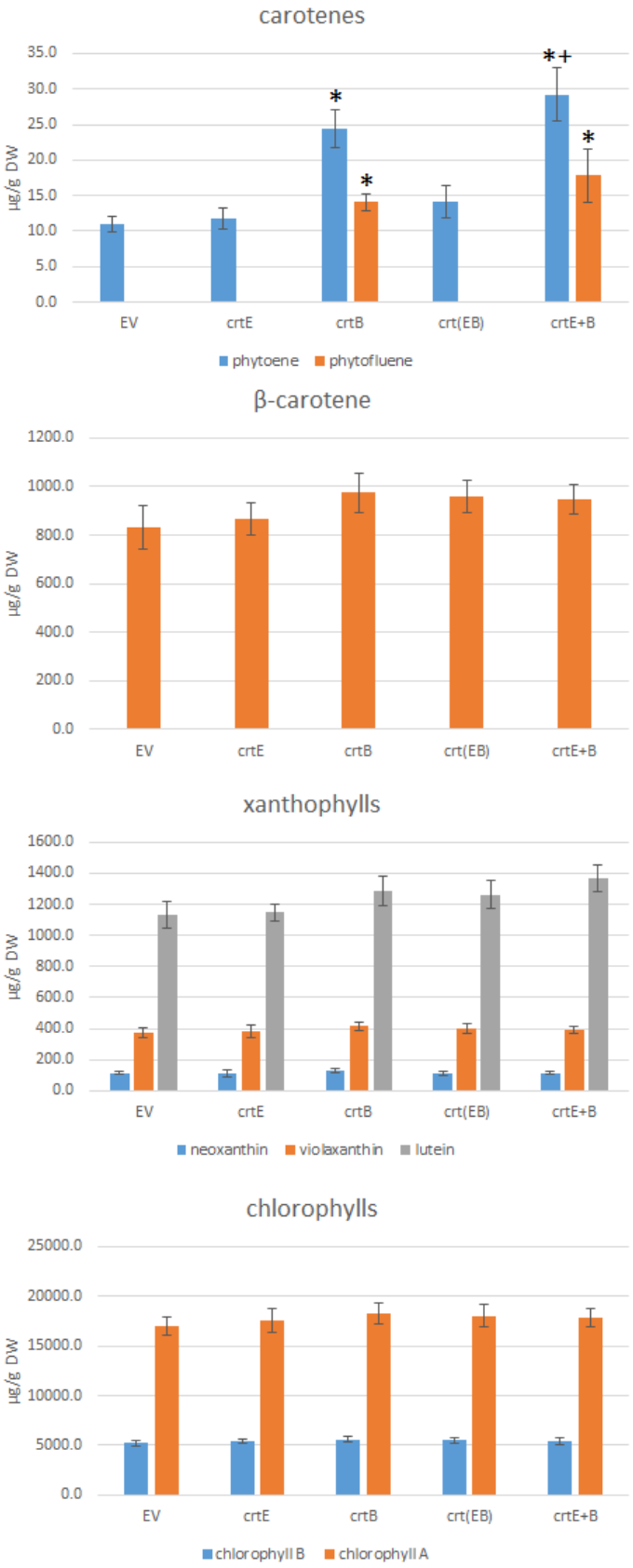

Figure 5-8. Expression of *crtE* and *crtB* in N. benthamiana leaves.
Quantification of carotenoids and chlorophylls via UPLC analysis for samples with *crtE* and *crtB* expression targeted to the cytosol. Increases in phytoene and phytofluene for CRTB and CRTE+B (co-infiltrated). (* is significant compared to the control, p-value<0.005 Student's T-test) (+ significant against crtB, p-value<0.05 Student's T-test).

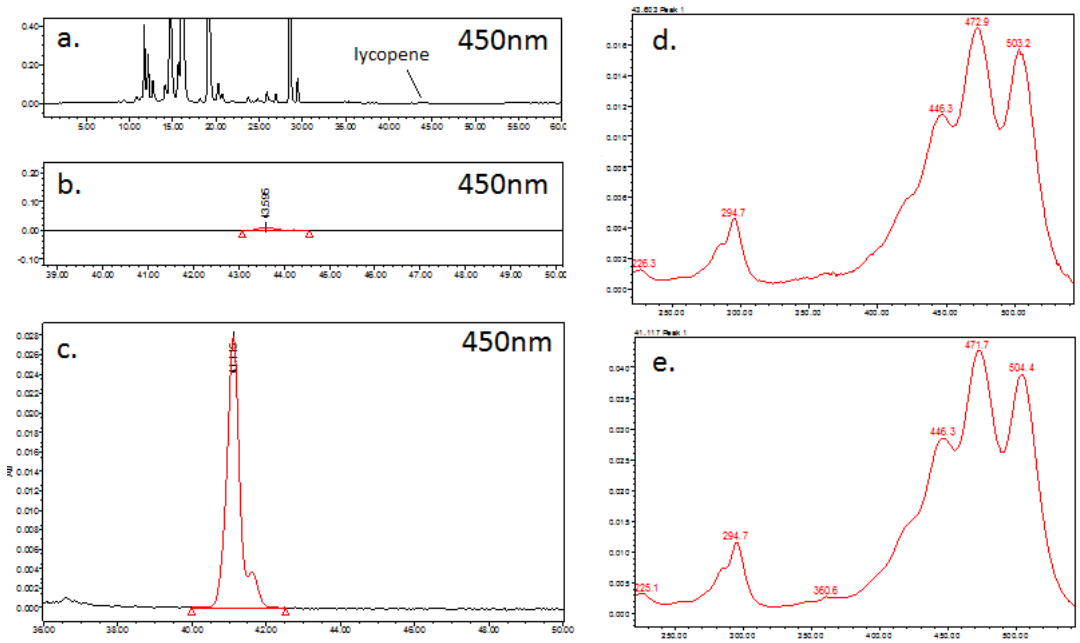

Figure 5-9 HPLC confirmation of lycopene.
Presence of lycopene in transiently transformed N.benthamiana infiltrated with CRTB. (a) Trace of CRTB sample with lycopene peak, (b) zoom in of lycopene peak, (c) lycopene standard, (d) spectrum of lycopene in sample, (e) spectrum of peak for lycopene standard.

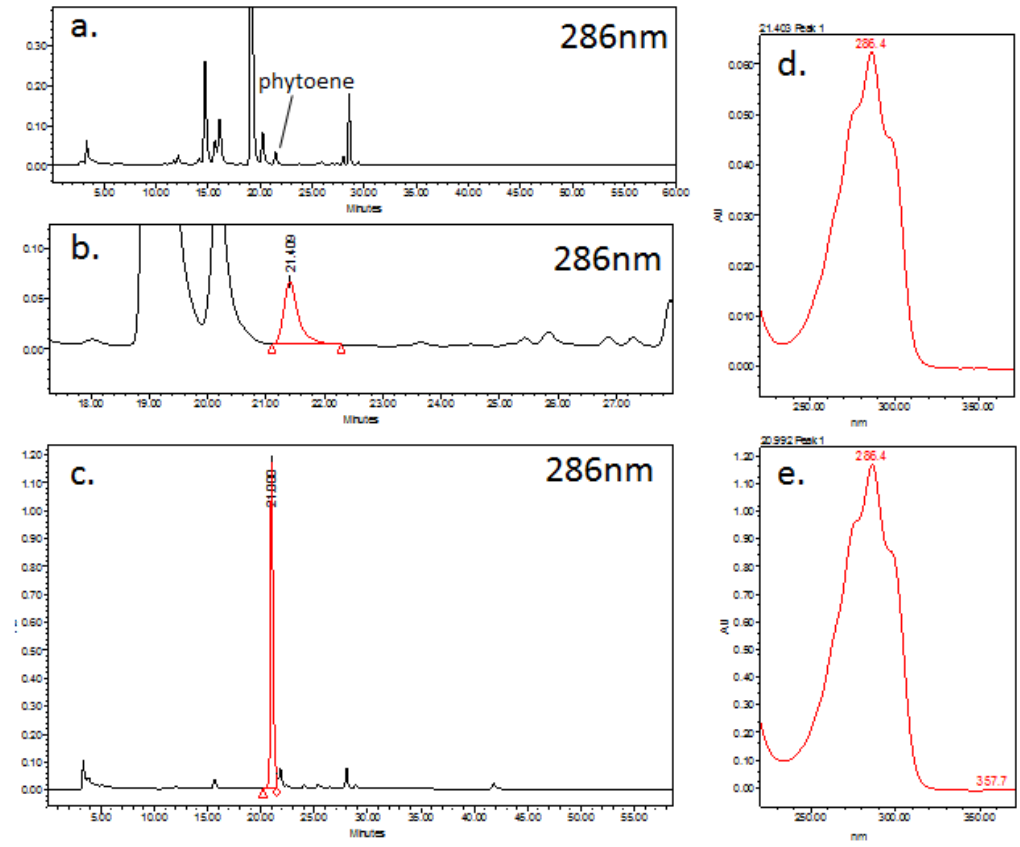

Figure 5-10. HPLC confirmation of phytoene
Presence of phytoene in transiently transformed N.benthamiana infiltrated with CRTB. (a) Trace of CRTB sample with phytoene peak, (b) zoom in of phytoene peak, (c) trace of phytoene standard, (d) spectrum of phytoene in sample, (e) spectrum of phytoene peak in standard.

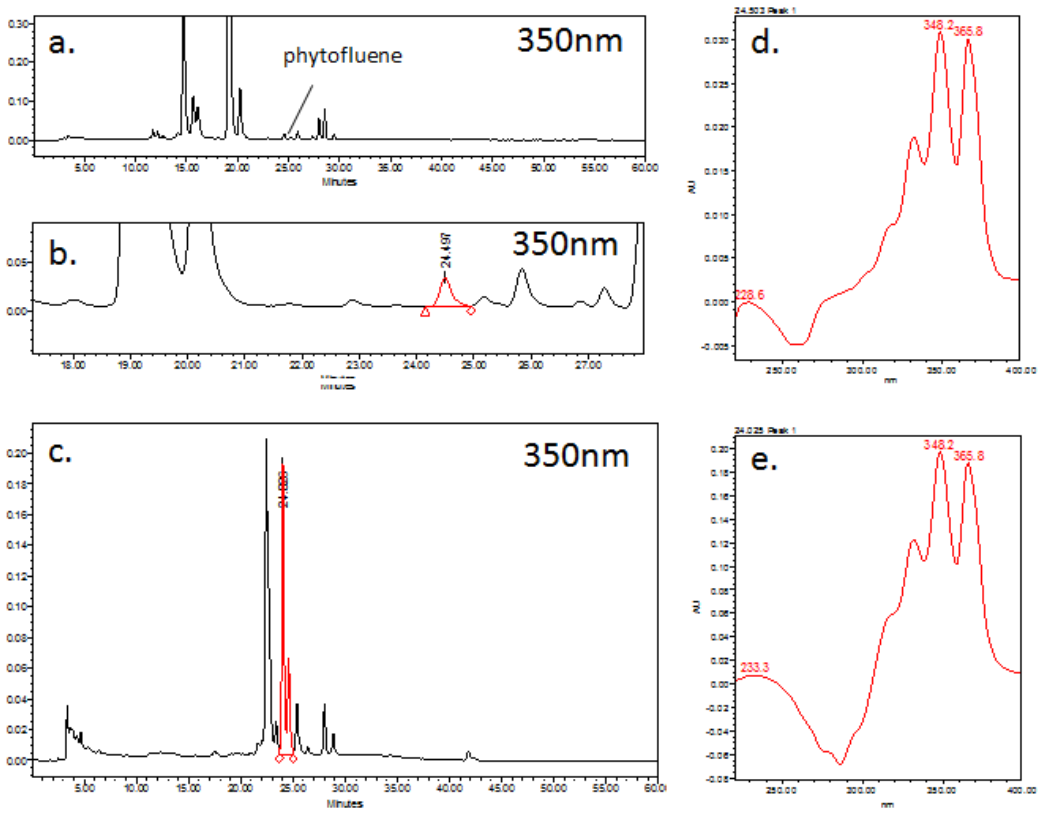

Figure 5-11 HPLC confirmation of phytofluene.
Presence of phytofluene in transiently transformed N.benthamiana infiltrated with CRTB. (a) Trace of CRTB sample with phytofluene peak, (b) zoom in of phytofluene peak, (c) phytofluene standard, (d) spectrum of phytofluene peak in sample, (e) spectrum of phytofluene peak in standard.

As infiltration mixtures were screened in combinations with co-infiltrated cultures a dose-response analysis was performed for CRTB as a single construct, in combination with a fixed percentage of the P19-vector which improves infiltration efficiency. 1/6th part of the infiltration mixture was made up of the P19-vector strain, the remaining 5/6th part of the mixture was set to 100% for the dose response trial. The CRTB strain was added in a step-wise build up from 20% (B20) up to 100% (B100), in steps of 20% (B40, B60, B80), complemented with a volume of the pDGB1α1 (empty vector control). The increase in phytoene and phytofluene levels, linked to an increased volume of CRTB *Agrobacterium* cells, demonstrates the effect of the construct. Furthermore, the gradual increase of other compounds like lutein, β-carotene, neo- and violaxanthin and chlorophyll A shows the impact of the highest added volumes, especially the B80 samples volume ratio, as the highest volume mixture does not show the highest increase in carotenoid and chlorophylls.

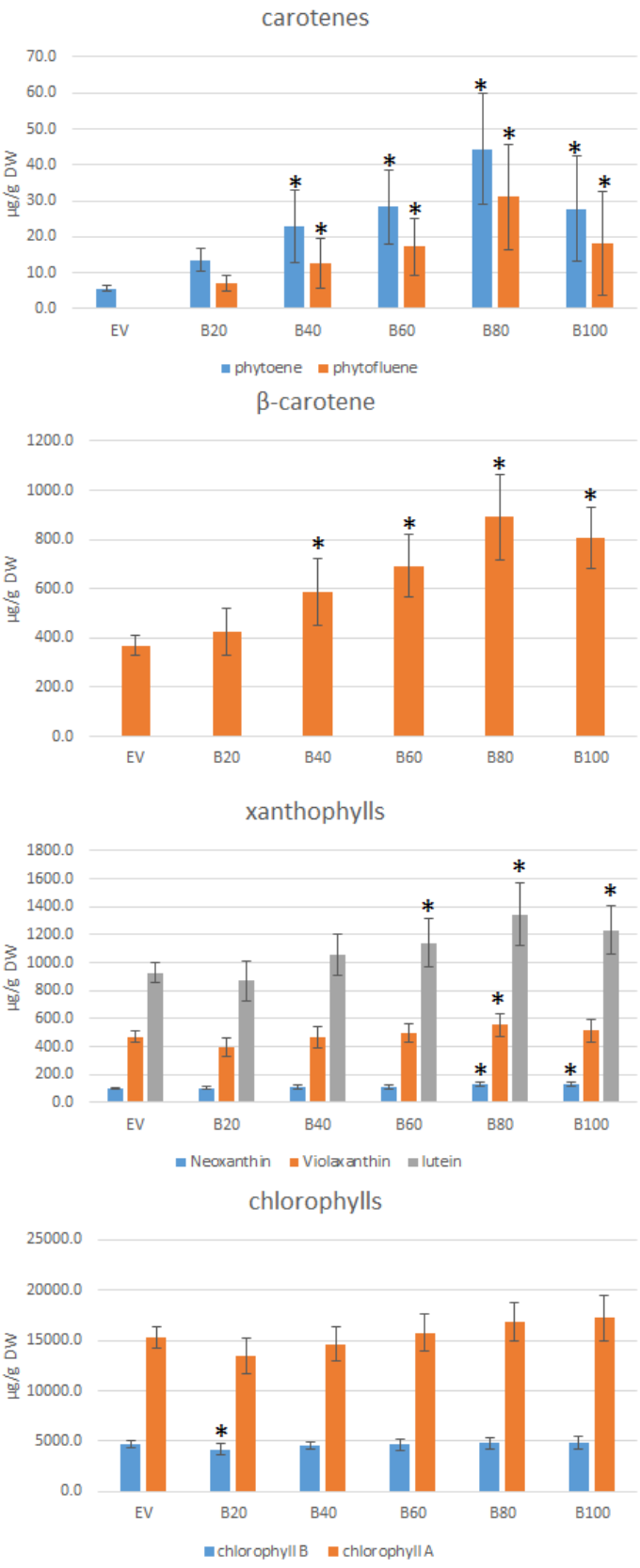

Figure 5-12. Dose response CRTB, quantification of carotenoids and chlorophylls.
An increase in Agrobacterium culture containing the CRTB vector results in a trend of increased levels for carotenoids and chlorophylls. Peak increase are found at 4/6th volume of the CRTB strain. * is significant compared to empty vector control (p-value<0.05, Dunnett's test).

Figure 5-12 displays the abundances measured for the dose response screen, indicating significant differences compared to the control. A pairwise comparison using the Duncan test for least significant difference provides the clustered means per compound analysed. Analysis demonstrated that B80 is significantly different from all other samples for carotenes phytoene and phytofluene, whilst B20 samples are not significantly different from the EV. B80 and B100 are both significantly bigger than the other samples for β-carotene, lutein and neoxanthin but cluster together, with B20 and EV not being significantly different for β-carotene, lutein. B20 is significantly lower for both chlorophylls, there is no significant changes between the other samples. B40 and B60 are mainly clustered together or with the B20 and EV samples, and for some compounds like phytofluene with B100. A complete overview can be found in the appendix (Table A-9).

5.3.3. Detection of phytosterols

With the segregation of isoprenoid pathways via compartmentalisation, the overexpression of isoprenoid genes in the cytosol potentially affects the endogenous isoprenoid synthesised. Screening of changes in the phytosterol profile in the leaf infiltrations displayed small significant increases in various sterols. Three replicate sets were analysed, outcomes of the sets were split in rep. I and rep II and III, due to a shift in detected abundances after equipment maintenance. The outcomes of the replicate sets are presented in Figure 5-13. In the first set significant changes in stigmasterol and fucosterol were observed for CRTE, CRTB and co-infiltrated CRTE/CRTB, whilst only CRTE and CRTB showed an increase in total sterol content separately. Increases for sets II and III were observed for campesterol (CRTB), stigmasterol (CRTE/CRTB) and fucosterol (CRTE, CRTB and CRTE/CRTB); CRTE/CRTB displayed a significant increase in total sterol content as well. The comparison between set I and the clustered sets II and III suggests that the increases in fucosterol (all vectors) and stigmasterol (CRTE/CRTB) are significant.

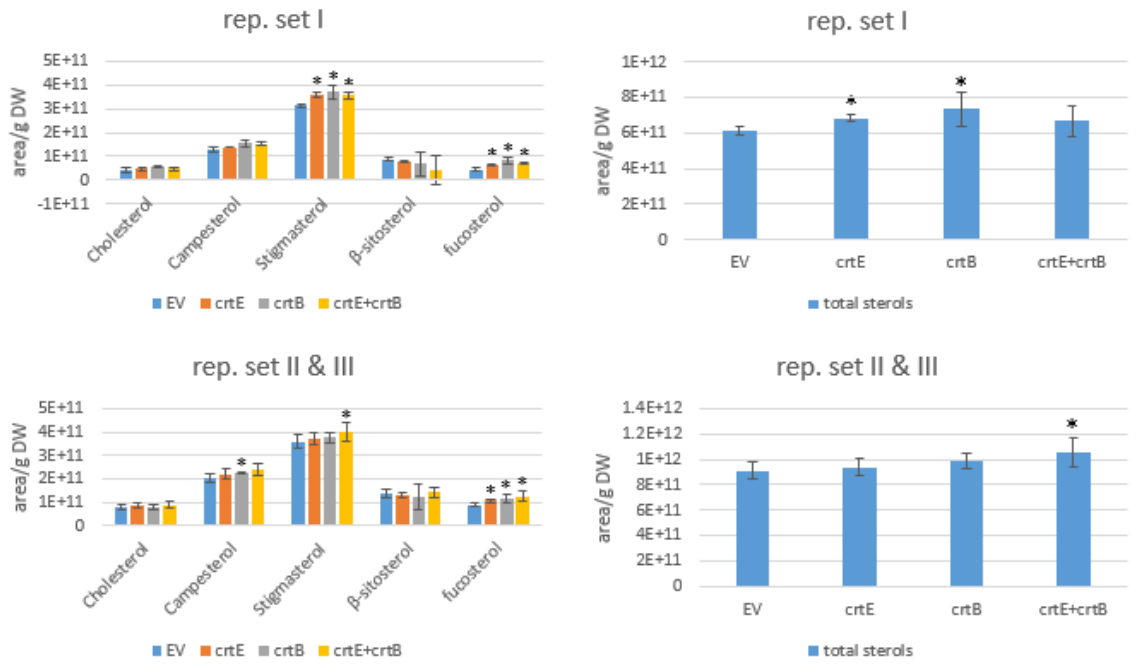

Figure 5-13. Phytosterol abundances in CRTE & CRTB samples.
GC-MS analysis of phytosterols and cholesterol on leaf samples of CRTE and CRTB infiltrated *N.benthamiana*. Cholesterol and main phytosterols presented individually (campesterol, stigmasterol β-sitosterol fucosterol) and as total sterol content. Rep I and Rep II/III presented separate due to equipment maintenance between runs. (* is significant: p-value 0.005, Student's T-test.)

5.3.4. Determination of cytosolic or plastidial targeting of isoprenoid enzymes from various organisms

Plastidial expression of the crtZ and crtW enzymes requires no further analysis as the presented phenotype can only be achieved through presence in the plastid as that is the site of accumulation for β-carotene, the precursor for these enzymes which catalyse the synthesis of keto-carotenoids. This is confirmed in the initial study on these enzymes as presented by Nogueira and coworkers (Nogueira et al., 2017). To determine the functionality of the cytosolic targeting of the CRTE and CRTB proteins a plastid isolation was performed whereby cytosolic fraction was kept for parallel analysis. Proteins were extracted from both the plastid and cytosol fraction and SDS-PAGE and Western Blots were used for analysis of the protein samples (preliminary data, not shown). Using antibodies for CRTB and TIC (Translocon on the Inner Chloroplast membrane) should clarify a potential ratio difference between the plastidial and cytosolic samples assuming some contamination between isolates would occur. Analysis with

the CRT-antibody demonstrated unspecific binding on the western blot, therefore confirmation of cytosolic targeting could not be achieved through this method. Alternative strategies to confirm the cytosolic targeting of CRTB are described in section 6.3.2. Further insights on the options to determine enzyme localisation in different organelles is described in the future perspectives section (sub-chapter 6.3).

5.4. Discussion

5.4.1. The effect on isoprenoid levels by overexpressing MEP genes

The outcomes of the GB MEP-vectors presented in this chapter suggest the vectors do not have the impact on isoprenoid profiles and content as expected. Although the concerns related to the binary assembly and expression of coding sequences in the multi-gene vectors need to be considered for these outcomes. Minor increases were found in one trial for the pDXS-vector and the pMEP vector, however none of these observations were reproducible in further trials. In later screens the effect of the vectors generated a negative impact on isoprenoid levels for some of the vectors tested. Similar to the analysis of the individual compounds, a more generic comparison between samples based on their carotenoid to chlorophyll ratio demonstrated no significant differences between the MEP-vectors and their respective empty vector controls.

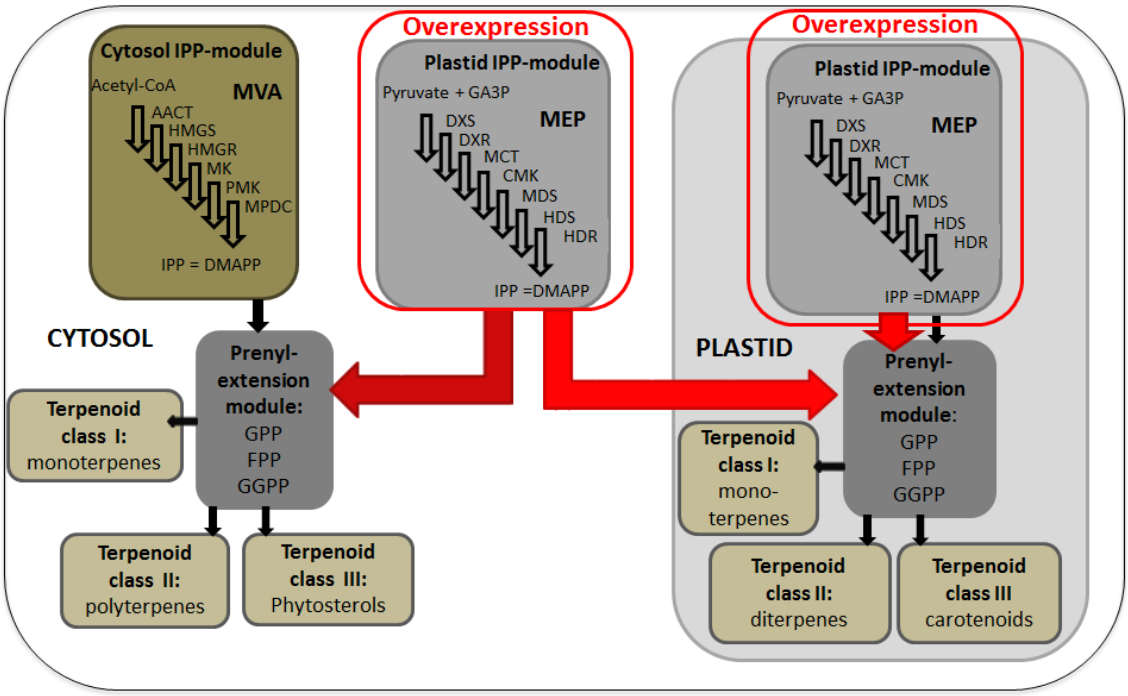

Figure 5-14. Hypothesised model for MEP-pathway overexpression between compartments. Compartment specific targeting of an overexpression module for the MEP pathway is hypothesised to enhance the pool of isoprenoid building blocks in the targeted compartment. Overexpression of the MEP pathway in the plastid should lead to an enhanced flux of isoprenoid precursors to the plastid located terpenoid branches. Constitutive "overexpression" of the MEP pathway in the cytosol would enhance the flux of isoprenoid precursors to the terpenoid biosynthesis branches in the cytosol, and potentially excess intermediates or precursors could flow back to the plastid.

The hypothesised model (Figure 5-14) as described in the introduction was based on overexpression of the MEP pathway genes, which in turn should generate an enlarged pool of isoprenoid building blocks in the targeted compartment. No novel isoprenoids were predicted, the strategy was solely focussed on enhancing the abundance of precursors for the prenyl chains, geranyl, farnesyl, and geranylgeranyl diphosphate, which provide the backbone structures for many isoprenoids. By overexpressing the MEP pathway genes targeted to the plastid or the cytosol, the additional IPP and DMAPP synthesised would supplement the endogenous MEP or MVA pathways respectively.

The lack of impact on isoprenoid biosynthesis from the screened vectors is interesting as many studies have been presented with clear correlations between overexpression of individual MEP genes and increases in isoprenoid content. An integrative overexpression study in Arabidopsis for all genes of both isoprenoid precursor pathways demonstrated the importance of DXR and MDS as key regulatory points within the MEP pathway (Lange et al., 2015), whilst a range of other studies demonstrated the impact of DXS, either overexpressed or knocked out. (Carretero-Paulet et al., 2006; Jinfen et al., 2012). Furthermore, DXR, as the first committed step of the MEP pathway, has been tested in various other studies with the same outcome (Chan et al., 2009; Yao et al., 2008). With expression of *dxs*, and *mds* confirmed in the GB multi-gene vectors for the MEP pathway (see chapter 4), one could expect increased isoprenoid levels. When investigating the reports in literature in more detail it becomes clear that it is difficult to enhance the pool of isoprenoid precursors and with that the levels of isoprenoids like carotenoids. In tomato the constitutive expression of *dxs* from *E. coli* led to an increase in carotenoids in the fruit, but not in the green tissues such as the leaves (Enfissi et al., 2005). The impact of overexpression for genes of the MEP pathway led to marginal changes for DXR and MDS enzymes in Arabidopsis; overexpression of these genes resulted in a 10% increase in total carotenoid and chlorophyll content compared to the control (Lange et al., 2015). The effect of overexpressing MEP genes might be more distinct in stable transformation than transient

expression, as outcomes of stable overexpression lines in aforementioned studies have shown (Enfissi et al., 2005; Lange et al., 2015).

Regulatory feedback processes and retrograde signalling have been observed for the MEP pathway and its downstream pathway branches, which might have some involvement in the negligible changes observed during the transient expression experiments. Feedback regulation from IPP/DMAPP to DXS, by blocking the enzymatic co-factor binding site, has been reported previously (Banerjee et al., 2013). Possibly during the leaf infiltrations, the increased accumulation of isoprenoid precursors took place, with no capacity for the downstream enzymes to utilise this enlarged pool of building blocks. As the regulation of the pathways is tightly controlled and strongly correlated to stress responses (Hemmerlin et al., 2012), this could lead to the feedback inhibition of DXS enzyme. The attempted strategy of co-infiltration with CRTZW to create a breach in the regulation taking place under normal conditions did not result in bigger fluctuations of isoprenoid levels - an outcome that was assumed to happen, as CRTZ and CRTW use β-carotene as a substrate which therefore reduced 3-fold compared to the empty vector control. The flux of β-carotene to keto-carotenoids would supposedly trigger upregulation of the MEP and carotenoid pathway, to compensate reduction in β-carotene content, which in the case of enhanced expression for MEP genes could lead to a generic increase in isoprenoids. The importance of DXS as a central regulator of isoprenoid biosynthesis is alternatively suggested on a transcriptional level, where other isoprenoid enzymes (e.g. PSY) show enhanced expression when *dxs* is highly expressed (Simpson et al., 2016). This study would suggest potentially high carotenoid levels in *N. Benthamiana* leaf samples, given the increased *dxs* transcription levels as displayed in chapter 4.

Overexpression of MEP genes in either the plastid or cytosol did not prove fruitful for the enhancement of isoprenoid levels. Given the incomplete gene expression of the genes in the MEP multi-gene vectors, it was to be expected that with missing intermediates the enzymes in

the cytosol could not generate a MEP enzyme based flux towards IPP and DMAPP. The discovery of MEcPP as a plastid to nucleus retro grade signal to trigger stress responses indicates that the MEP intermediate MEcPP, and perhaps others, can be transported to the cytosol (Xiao et al., 2012). Moreover, the finding of MEcPP transport to the cytosol, when over-accumulating in the plastid, might be reversible or function in a similar fashion for the other intermediates. Hypothetically this could mean that any excess of any MEP intermediate could be transported out of the plastid and used as a substrate in the cytosol, when the matching enzymes are present. The assumptions stated above would require the expression of i.e. *dxr*, it being a key enzyme in flux regulation, to overcome any restrictions in the flow towards IPP and DMAPP.

With the successful assembly of the MVA pathway in chloroplasts, and its functionality proven by increased levels of various isoprenoids including sterols and carotenoids (Kumar et al., 2012), the implementation of the same strategy for assembly of the MEP pathway was expected to deliver interesting results. Given the broad impact on isoprenoid levels when the MVA enzymes are active in the plastid, i.e. carotenoids in the plastid and sterols in the cytosol, one would expect that a larger pool of isoprenoid precursors in either the plastid or the cytosol via MEP overexpression leads to an increase in photosynthetic isoprenoids.

5.4.2. Cytosolic localisation of CRTE and CRTB affects the isoprenoid profile

The attempted overexpression of *crtB* targeted to the cytosol demonstrated a general increase in carotenoids and chlorophylls, especially phytoene, phytofluene, and lycopene in leaf material of *N. benthamiana*. The overexpression of *crtE* independently has not shown level changes in photosynthetic compound content. However, combined activity of CRTE and CRTB boosts the increases seen when *crtB* is expressed on its own. Furthermore both transient transformations with CRTE and CRTB demonstrated a minor trend towards increased phytosterol content, suggesting an effect in the plastid and the cytosol either directly or indirectly. Previous studies performed with bacterial carotenoid genes demonstrated the effects of the enzymes on carotenoid levels in various tissues. Fruit specific expression of *crtB* leads to a 2-4 fold increase

in carotenoid content in tomato fruit (Fraser et al., 2002). This was investigated further in a study combining CRTB, with CRTE and CRTI, where stronger increases were found for crosses of the lines (Nogueira et al., 2013). Interestingly, similarly to the results presented in this chapter, *crtE* does not show an effect on photosynthetic compounds when expressed on its own. Furthermore, higher phytoene levels, but lower β-carotene levels, were found when *crtB* is present hemizygous, but higher lycopene content was detected in homozygous lines; the combined expression of *crtE* and *crtB* led to an increase in lycopene in hemizygous lines (Nogueira et al., 2013). Expression of *crtB* in canola seeds leads to a 50-fold increase in carotenoid content (Shewmaker et al., 1999). This result has been optimised further by combining the expression of various bacterial carotenoid genes, which resulted in different carotenoid profiles (Ravanello et al., 2003). The highest impact in the studies conducted in this chapter lead to a ~14-fold increase in phytoene and a 42% increase in total carotenoid content. In potato tubers a mini pathway for carotenoid biosynthesis was assembled to enhance the carotenoid content in the tuber, with the aim to create a source of pro-vitamin A (Diretto et al., 2007). None of these examples of *crtE* and *crtB* overexpression are constitutive for the vegetative tissues and therefore no changes in carotenoid levels or profiles were found in the leaves.

The increases in chlorophyll content and lutein and β-carotene levels in the transient expression screens were unexpected, as targeting of CRTB, either independently or combined with CRTE to the cytosol, should in principle only provide accumulation of phytoene. However, the general increase in carotenoid content, especially phytofluene and lycopene, suggests an interaction is taking place between the enzymes present in the cytosol and the endogenous carotenoid pathway. Explanations could be found in the untargeted accumulation and activity of these enzymes in the plastid, or integration of the enzymes in the plastid membrane. Similar outcomes were found in a study in which the same genes were tested in a virus-based transformation system. The outcome for ectopic expression of *crtB* targeted to the cytosol was the same: a

higher general carotenoid content, this became even more apparent through the negative impact of the chloroplast function i.e. reduction in chlorophyll levels caused by the virus driven mechanism (Majer et al., 2017). The theory based on these results suggests a role of carotenoid degradation products, derived from phytoene synthesised in the cytosol, these degradation products (apocarotenoids) could cause a signalling cascade to transcriptionally increase the activity of the carotenoid pathway i.e. retrograde signalling (Majer et al., 2017). Retrograde signalling has been suggested in previous studies for a ZDS-mutant in Arabidopsis, where the excess of carotenoid precursors were cleaved into carotenoid degradation products that triggered changes in gene expression (Avendaño-Vázquez et al., 2014). The study by Majer et al. suggests carotenoid cleavage dioxygenase (CCD) could play a role in this process (Majer et al., 2017). CCD's are commonly found in plastids, since the targets of these enzymes are synthesised in the plastids, although studies in Arabidopsis and *C. sativus* demonstrated the presence of CCDs in the cytosol (Auldridge et al., 2006; Rubio et al., 2008). Non-enzymatic cleavage of carotenoids can occur through oxidation of the carotenoids by reactive oxygen species, which can take place in the cytosol under influence of the stress related hormones jasmonate and abscisic acid (Suhita et al., 2004).

The hypothesised cytosolic expression of *crtB*, and to a lesser extend *crtE*, seems to have a clear effect on carotenoids and sterols. Besides the accumulation of phytoene, the specific product of the CRTB enzyme, a general increase in endogenously synthesised carotenoids was observed. Two hypotheses can be formulated based on the data provided, retrograde signalling or untargeted transport of CRTB enzymes to the plastid. Out of these two options, the signalling cascade triggered by apocarotenoids (degradation products of phytoene) seems a very likely scenario based on reported studies on the topic (Avendaño-Vázquez et al., 2014; Majer et al., 2017). Figure 5-15 displays a hypothesised model in which the impact of the enzymes is wider than just the targeted cytosolic location, direct or indirect impact on the carotenoid pathway in the plastid is suggested for CRTB especially.

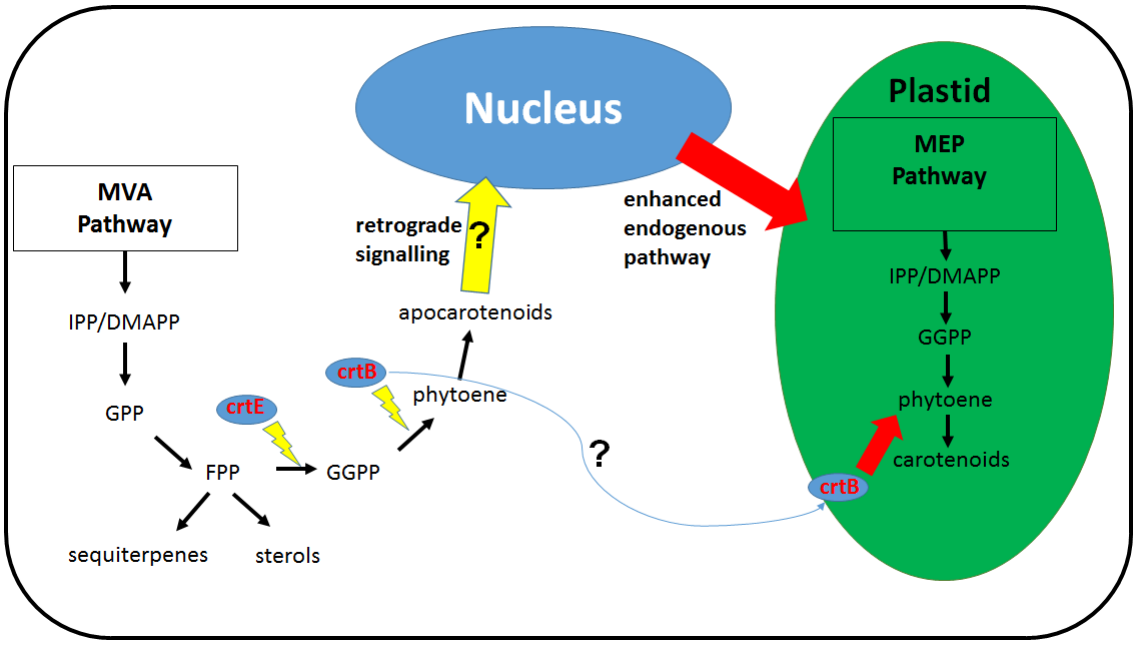

Figure 5-15. Model of transient expression of *crtE* and *crtB*.
The hypothesised model suggests that the effect of the CRTB vector is not restricted within the cytosol and impacts the endogenous carotenoid biosynthesis. Two options are suggested (i) a retrograde signalling cascade via phytoene degradation products, through CCD's or non-enzymatic oxidation or (ii) untargeted transport of CRTB enzymes to the plastid.

6. Conclusions, General discussion & Future outlook

6.1. Conclusions

The aim of this PhD project was to (i) elucidate and characterise the sequestration mechanisms for carotenoids in tomato fruits and (ii) develop and implement ectopic engineering approaches to enhance carotenoid *in planta.* Three objectives were formulated to achieve progress towards the aim and the conclusions are described below.

6.1.1. Conclusions chapter 3

The objective for this chapter was to elucidate the effect of overexpression and mutant lines, perturbed in carotenoid biosynthesis, on carotenoid sequestration mechanisms in *Tomato*. Analysis of suborganelle structures of tomato mutant lines, perturbed in carotenoid biosynthesis, demonstrated the adaptability of plastids related to the sequestration of carotenoids in tomato fruit.

- Plastids can modify their capacity for carotenoid accumulation by plastid differentiation to be more recipient to increases in carotene content in developmental stages where xanthophylls are sequestered normally.
    - Constitutive expression of the *psy1* gene led to accelerated carotene accumulation in tomato fruit which was matched by the early differentiation of chloroplasts to chromoplasts.

- Alterations in the carotenoid profile trigger differences in carotenoid uptake between storage structures e.g. plastoglobules and crystalloid membrane structures.
    - The distribution of carotenoids between plastoglobules and crystalloid membrane structures is dependent on the structural differences between *cis*-carotenes and *trans*-carotenes and xanthophylls as observed in the PSY1sense, *og*^{c}, *tan* and *tan*-crtI lines.

6.1.2. Conclusions chapter 4

For this chapter the objective was to develop a Synthetic Biology platform for ectopic engineering of the MEP and carotenoid pathway in plants. Modular cloning systems are the upcoming technological advancements in molecular biotechnology. Their ability to rapidly produce vectors for the iterative optimisation of yields and titers means the system has the ability to generate industry prototypes with more rapidity. In this study a range of vectors was created for the overexpression of genes of the MEP pathway and bacterial carotenoid genes using the GB cloning method.

- A range of parts, single gene vectors and multi-gene vectors for MEP pathway genes and bacterial carotenoid genes was assembled using the GB cloning system.
    - Screening of multi-gene vectors revealed inaccurate assembly at the binary assembly stage of the cloning system, expression analysis demonstrated the inefficiency in functionality of the multi-gene vectors.

- Expression of the selected isoprenoid genes was observed for single-gene vectors tested, whilst multi-gene vectors demonstrated only partial success in transcription of the coding sequences.
    - Transcripts for *dxs*, *mct*, *mds* and *hds* were detected in the multi-gene vectors for the MEP pathway, and single gene vectors for *crtE* and *crtB* proved functional, multi-gene expression for *dxr*, *cmk*, *hdr* and *crtE* and *crtB* was not detected.
- The success of implementation of GB cloning is considered limited compared to other modular cloning systems i.e. Golden Gate cloning.
    - The limited range of published research using the method suggests the GB method requires improvements before becoming the standard for synthetic biology in plants.

6.1.3. Conclusions chapter 5

In continuation of chapter 4 the objective for this chapter was to evaluate the impact of ectopic engineering approaches for the MEP and carotenoid pathway on carotenoid content in *Tobacco*. A selection of vectors of GB isoprenoid vector library created was screened in transient transformations in *N.benthamiana*.

- Transient transformations of MEP pathway vectors did not induce changes in the levels of isoprenoid screened for, despite confirmed expression of a number of MEP genes.
    - Modular overexpression vectors for the MEP pathway did not demonstrate significant increases when tested transiently via leaf infiltrations in *N. benthamiana*.

- The impact of a cytosolic targeted phytoene synthase (CRTB) led to increases in general carotenoid content beyond the enzyme's function suggesting an indirect role.
    - Single gene vectors for bacterial carotenoid genes *crtE* and *crtB* combined or *crtB* independently displayed clear increases in carotenoid and chlorophyll content, 42% and 5% respectively. Furthermore, a trend for increased phytosterols was observed.
    - Apocarotenoid induced retrograde signalling is a sound hypothesis for the interactions with the endogenous pathways in the plastid.

- The application of the modular pathway vectors for the MEP and carotenoid pathway, designed using the Golden Braid Cloning system, shows only limited potential. Despite expression in some of the multi-gene vectors, no impact on isoprenoid levels was observed in any screen for these vectors.

Table 6-1 Summary of chapter conclusions

OBJECTIVE	OUTCOMES
Chapter 3	
Elucidate the effect of perturbations in carotenoid biosynthesis on carotenoid sequestration mechanisms.	(i) Premature chloroplast to chromoplast differentiation can occur with increased carotenoid accumulation (ii) Modified carotenoid profiles lead to changes in carotenoid deposition between sequestration structures.
Chapter 4	
Develop a Synthetic Biology platform for ectopic engineering of the MEP and carotenoid pathway.	(i) A cloning library for isoprenoid biosynthesis was created (ii) Functionality of single-gene vectors proved successful, multi-gene vectors lacked functionality and assembly accuracy
Chapter 5	
Evaluate the impact of ectopic engineering approaches on carotenoid biosynthesis	(i) Transient transformations of the MEP-vectors did not lead to significant increases in carotenoid content. (ii) Activity of the CRTB and CRTE enzymes in the cytosol led to increased phytoene content and higher accumulation of endogenous carotenoids.

6.2. Discussion and perspectives

6.2.1. Outlook on carotenoid formation and sequestration

The sequestration of carotenoids is a complex process influenced by a range of factors depending on the tissue and plastid type. It seems that carotenoid quantity is an important factor for chromoplast biogenesis, as demonstrated in the PSY1sense line. In the sub organelle organisation of chromoplasts, the carotenoid profile plays a role in the structures the carotenoids are sequestered in, based on the ratios of *cis*-, *trans*-carotenoids and xanthophylls in the different tomato lines perturbed in carotenoid biosynthesis. Carotenoids can be synthesised and sequestered by both chloroplasts and chromoplasts, moreover both plastid types have the sub-organelle structures to sequester the carotenoids produced. Where chloroplasts require xanthophylls for their photosynthetic activity, the function of chromoplasts in flowers and fruits is carotene accumulation, to create areas with high pigment to attract pollinators or seed dispersers. An increase in carotene accumulation triggers chromoplast biogenesis in immature tomato fruit. The yellow flesh (*rr*)-mutant contains virtually no carotenoids in its ripe fruit, as the *psy1* gene is not translated (Fray and Grierson, 1993). The carotenoid profile in the ripe fruit of this PSY1 knock-out mutant represents the carotenoid profile of photosynthetic tissues more than a normal ripe fruit (Fraser et al., 1999). The accumulation of predominantly xanthophylls and the presence of chlorophylls at low concentrations suggests these compounds are perhaps remnants of the carotenoid and chlorophyll accumulation in the chloroplasts. In order to generate a broader perspective on carotenoid accumulation and chromoplast biogenesis, a sub-organelle analysis of *rr*-mutant fruits during the different developmental stages, as performed for PSY1sense, might provide further insights. The early onset of chromoplast biogenesis during fruit development when *psy1* is overexpressed could in a similar fashion delay chromoplast biogenesis when the *psy1* gene is inactivated. Where the *Or*-gene has been shown to control chromoplast differentiation from amyloplasts in various staple crops i.e. potato tubers (Lopez et al., 2008), a transcriptomics and

proteomics analysis of chloroplast to chromoplast differentiation determined the stable expression and presence respectively of an acetyl-CoA-carboxylase-D (ACCD) during the differentiation process (Barsan et al., 2012; Kahlau and Bock, 2008). The maintenance of ACCD expression and protein levels throughout chromoplast biogenesis suggests that this enzyme, which is involved in fatty acid biosynthesis, is regulating the differentiation through reorganisation of the membrane lipids. Any changes caused by perturbations in the carotenoid levels and profiles, shown for the *og*^{c}, *rr*-mutant and *tan* line, could affect membrane composition regulated by ACCD. A link between membrane and carotenoid profiles when carotenoid biosynthesis and profiles were modified has already been shown in the case of increased β-carotene levels matched by monogalactodiacylglycerol (MGDG) levels; the increased MGDG levels are suggested to change the membrane structures, which generates more space to accumulate carotenoids (Nogueira et al., 2013). The increased MGDG content in lipid membranes when β-carotene levels are increased could be extrapolated to increases of other carotenoids that demonstrate a higher accumulation in membrane structures i.e. neurosporene and poly-*cis*-lycopene. Thylakoid membrane primarily consist of MGDG and digalactosyldiacylglycerol (DGDG); MGDG is not particularly suited for the synthesis of lipid bilayers, therefore protein complexes like the light harvesting complex are required to keep the bilayers compact in plastid membranes (Janik et al., 2013). This impact of lipid properties on the stability of membrane bilayers could be an integrating factor between the levels of carotenoid accumulation and modifications in carotenoid profiles, as one could state that in both cases membrane properties change to adapt to carotenoid levels, either via the ratio between specific carotenoids or through a general increase of carotenoids content, an observation that could relate to the effect seen when membrane structures of plastids from ripe and mature green fruit material are mixed. As perturbations in the carotenoid biosynthesis are the cause for any structural modification observed in the plastid, on an organelle or sub-organelle level, results

have to be considered as responses to the changes. Therefore the outcomes can only provide an insight into the adaptability of plastids.

6.2.2. Golden Braid Cloning as syntax for plant synthetic biology

Modular cloning systems, developed within the framework of synthetic biology, provide a standardised syntax for easy exchange and scientific collaborations. Golden Gate cloning and its multi-gene extension MoClo are selected together with Golden Braid to represent the standardised cloning methods for plant biotechnology (Patron et al., 2015). The Golden Gate technique has been proven functional and has been adapted successfully in various studies. A related study on isoprenoids demonstrates the use of Golden Gate cloning for the overexpression of diterpenoid genes in *N.benthamiana* leaves (Brückner and Tissier, 2013), proving the possibilities of modular cloning systems for metabolomics engineering. By far the majority of applications for Golden Gate cloning are linked to genome editing. An example of such a study is the use of transcription activator-like effectors nucleases (TALEN) in tobacco leaves (Li et al., 2012). The Golden Braid technique has resulted in two publications since its dissemination. In a large study on phytosterols, a multi-gene overexpression vector with 10 phytosterol biosynthesis genes was successfully tested for its functionality, demonstrating a 15-fold increase in phytosterol content (Sonawane et al., 2016). In a study focussed on the biosynthesis and accumulation of solanesol in potato foliage, among environmental triggers, the impact of overexpression vectors (single gene) for the MEP pathway were tested transiently in *N. benthamiana*. 2-3 fold increases in solanesol content were detected for single gene infiltrations, increases up to 7-fold were observed for MEP genes co-infiltrated with a solanesyl diphosphate synthase (Campbell et al., 2016).

During the process of assembling GB vectors the easy construction of entry vectors was observed, followed by reasonably efficient generation of transcriptional units. The efficiency of assembly did depend on the backbone vector selected as Ω-vectors proved to be difficult to use (Sarrion-Perdigones et al., 2013). Since the issues with the Ω-vectors resulted in the failed

assembly of *crtI*$_{pa}$ into a Ω-vector, improvements would be required to improve efficiency of the technique and ease design of assembly strategies. Binary assembly of vectors seemed to result in the rapid development of a vector library containing vectors with up to seven TUs, although screening of these vectors based on restriction digestions led to concerns on the accurate assembly of the vectors. The screening of functionality for a selection of vectors confirmed the expression of some of the TUs assembled in multi-gene vectors. The absence of expression for *dxr*$_{ec}$, *cmk*$_{ec}$, *hdr*$_{ec}$, *crte*$_{pa}$ and *crtb*$_{pa}$ suggests the GB technique has some flaws in its design. The best example of this issue is the expression of both *crtE*$_{pa}$ and *crtB*$_{pa}$ when co-infiltrated in transient expression experiment, whilst the multi-gene vector for those two respective genes demonstrated no transcription for both genes.

Given the swift execution of the cloning process, samples were screened for their impact on the levels of various isoprenoids and related compounds. As increased transcription of important genes in the MEP and carotenoid pathways was detected, an increase in carotenoids and other photosynthetic compounds was expected. Despite convincing results for the multi-gene vectors described in this thesis, and limited published studies utilising this technique, GB cloning could still present itself as functional cloning technique. With the possible improvements of the GB cloning method in the updated versions, the potential of the method might increase (Vazquez-Vilar et al., 2016).

6.2.3. Isoprenoid regulation and enhanced accumulation for industrial purposes

The interest in secondary metabolites, especially plant derived, is great. Over the last decades many studies have been performed to achieve enhanced levels of those secondary metabolites in plants (Carretero-Paulet et al., 2006; Fraser et al., 2007). Strategies including breeding, mutagenesis and genetic modification have been used to produce large quantities of high value plant compounds. The attempts to genetically modify plants have been successful in many cases, although cases of restrictive feedback inhibition were revealed [reviewed by (Bramley, 2002; Hemmerlin, 2013)](Banerjee et al., 2013). Compartmentalisation within plant cells can be

utilised to reduce the impact of feedback regulation by pathway transfer i.e. expression of genes targeted to non-endogenous organelles. The attempt to target expression of the MEP pathway to the cytosol has been performed reversed by expression of the MVA pathway targeted to the plastid (Kumar et al., 2012). As that study showed a general increase in isoprenoid content, it suggests that enhancing the pool of precursors is a suitable method to increase the synthesis of high value compounds.

When looking at more a focussed approach in the case of carotenoid specific genes like *crtB* or its direct precursor *crtE*, which cover the onset of a specific isoprenoid branch, more aspects need to be taken into account. These enzymes, which are further down in the biochemical pathway, require a long track of biochemical steps to make the required substrates available. The MVA pathway in the cytosol is complemented with the prenyl extension block, constructing different isoprenoid backbone chains out of C_5-building blocks (Lange et al., 2015). Therefore the targeting of *crtE* and *crtB* to the cytosol should generate a functional biosynthetic pathway, leading to the accumulation of phytoene.

The anti-oxidant activity of carotenoids requires excess carotenoids to be sequestered in plastid membranes or globules, either as crystals or integrated with membrane lipids (Nogueira et al., 2013). This mechanism occurs to allow accumulation without a surplus of ROS-scavenging (Bouvier et al., 1998). An aspect of pathway transfer that needs to be investigated is the option of whether organelle specific compound can be accumulated to the same extent in other cellular compartments. Moreover, even if high levels of accumulation can be achieved, will it affect the general condition of the plant? Furthermore, can a conclusive explanation be found for the increase in endogenous photosynthetic compounds derived from the carotenoid and chlorophyll pathways, as the CRTE and CRTB enzymes can only synthesise geranylgeranyl diphosphate and phytoene respectively. Does the phytoene synthesised in the cytosol function as a precursor for enzymes of the carotenoid pathway in the plastid? Are the enzymes

transported untargeted to the plastid and enhance the activity there? Are there enzymes in the cytosol that can perform similar reactions as the carotenoid enzymes, which can cause isomerization of phytoene?

6.3. Future perspectives

6.3.1. Sequestration mechanisms for carotenoids

6.3.1.1. Chloroplast to chromoplast differentiation

The outcomes of the comparison of carotenoid deposition in tomato fruit of PSY1sense and its control suggests a strong link between increased carotenoid biosynthesis and chloroplast to chromoplast differentiation. It could be constructive to integrate the effect of a *psy1* knockout mutant to determine if a delayed differentiation process occurs. The results of the *rr*-mutant fruits, tested at the ripe stage, suggest primarily carotenoids from the mature green stage remain. With an inactive carotenoid pathway during the ripening process it is possible the plastid differentiation does not occur at the same time point or at the same pace. In a similar fashion the outcomes of the mixed plastid isolates, ripe and mature green fruit derived, of the control variety could be different for the overexpression and mutant varieties for the *psy1* gene. If a mechanism exists in chromoplast structures that induces degradation of thylakoid structures, the effect could be stronger in the overexpression line and less strong in the mutant line. The prominent effect of degradation of chloroplast structures in the mixed ripe and mature green samples might be partially an artefact of the technique, an element that needs to be investigated further.

Analysis of the carotenoid and chlorophyll content in the different fractions has provided useful insights into the relation between carotenoid accumulation and plastid differentiation. To complete the overview of this process it would be interesting to determine changes in plastid and sequestration related proteins such as outer and inner plastid envelope proteins and plastoglobulins. Analysis for the presence of these proteins can be executed through SDS-PAGE and Western Blots, as antibodies for these proteins are commercially available. To successfully integrate such analyses into the experimental setup the sub-plastid fractionation would need to be performed with a higher amount of starting material, to obtain sufficient proteins per fraction for further analysis. Similarly, the changes in plastid type can be linked to changes in lipid

composition, and especially MGDG, which has been connected to increased carotenoid sequestration, this could be an interesting target (Nogueira et al., 2013). Chromatography approaches (GC-MS and TLC) can be used for the analysis of lipid composition. Determination of sub-plastid structures could be performed through microscopy analysis of fractions. Previously described targeted studies on sub-chromoplast sequestration examined the presence of specific plastid structures in different fraction, whereby separation of plastoglobules, membrane structures and thylakoid remnants were observed (Nogueira et al., 2013), detection of membrane structures with and without thylakoid structures would generate useful insights on the separation of structures from different plastid types.

6.3.1.2. Sequestration mechanisms

With the changes in ratio of carotenoid deposition between plastoglobules and membrane structures for the tomato lines perturbed in carotenoid biosynthesis, a link can be made with changes in protein concentrations for proteins related to carotenoid sequestration. With increased or decreased levels of specific carotenoids being produced, the related sequestration proteins (such as plastoglobulin) involved in phytoene sequestration might be synthesised at higher levels to accommodate the formation of plastoglobules, and allow for the efficient sequestration of phytoene and other carotenoids e.g. lycopene, which have a preferred deposition in the plastoglobules. ACCD is another protein involved in carotenoid sequestration, furthermore the protein is one of the few, possibly only, protein which is maintained over the entire process of fruit ripening in tomato (Barsan et al., 2012; Kahlau and Bock, 2008), making it an important target for all elements of sequestration-related experiments in line with the work presented in this thesis. As described above in section 6.3.1.1. the analysis can be performed through SDS-PAGE, western blotting and Mass Spectrometry approaches for the detection of proteins or peptides and determine their concentrations.

The membrane composition and the potential changes triggered by changes in the carotenoid levels and profiles are relevant targets of analysis for further development for hypotheses

explaining the observed phenotypes of carotenoid deposition. The interaction between different carotenoids and lipid types was studied in in vitro models, and demonstrated clear differences between the combinations tested (Gruszecki and Strzałka, 2005; Widomska et al., 2009). The increase in MGDG as observed in the tomato lines with *crtB* and *crtI* expressed, were linked to the higher carotenoid levels and changes in carotenoid deposition towards the plastoglobules (Nogueira et al., 2013). Therefore MGDG might well be a significant factor in the differences observed between the *cis*-carotenoid and *trans*-carotenoid synthesising mutant lines, given their different sequestration profiles. Determination of changes in the lipid composition influenced by changes in carotenoid sequestration can be performed via GC-MS analysis for an untargeted approach, TLC methods can be used for the analysis of specific lipids.

6.3.2. Ectopic expression approaches

Interesting results were obtained for the carotenoid genes transiently expressed through the GB system, but the detected expression of MEP pathway genes did not lead to any significant increases in carotenoid content. More in depth analysis on the assembly of the vectors and improvements on the vector accuracy should be performed to avoid issues with functionality through inaccuracies. Analysis of expression through transient transformation for all coding sequences would still be the quickest method to screen for vector functionality. For all vectors it would be useful to determine the potential for metabolic changes via stable transformations to get a better insight into the impact during plant development and longer effect of the enzymatic activity of constitutively expressed genes on the isoprenoid and carotenoid biosynthesis in particular. An alternative strategy would be the use of a set of different promoters and terminators in case the repetitive nature of these elements is cause of some of the assembly issues.

The partial functionality of the MEP gene constructs requires further analysis to improve and complete the work done. Individual MEP gene TU's need to be tested for their functionality and also intermediate assembly steps should be screened to determine if at any point in the

assembly issues concerning the assembly or expression capacity occur. When these screens have been performed, further analysis can be done with the functional vector to determine impact on the isoprenoid precursor biosynthesis.

The impact of the CRTB enzyme has been proven significant when active in the cytosol, although accumulation of phytoene in the cytosol has not been proven. As demonstrated in a recent study on bacterial carotenoid genes targeted to the cytosol, the impact of a triple construct with *crtE*, *crtB* and *crtI* leads to the accumulation of lycopene (Majer et al., 2017). To extend upon the work done in this thesis it would be interesting to include the *crtI* gene in the GB-vector library and screen the three vectors in co-infiltration experiments and stable transformations. Again the options of using multi-gene vectors should be considered, as this element is presented as the main advantage of the GB-technique.

In the case of ectopic expression of genes and their respective functions in the cytosol, it is important to determine to which extent the targeting is specific to the cellular compartment aimed for. Experimental approaches to determine the flux towards isoprenoid biosynthesis, of isoprenoids normally found in the plastid, via the MVA pathway can be performed through inhibitor studies using mevinolin and fosmidomycin, inhibitors for HMGR and DXR respectively. Alternatively, the source of substrates for the isoprenoid precursors, through the MVA or MEP pathway respectively, could be determined via C13-labelling of MVA or MEP pathway intermediates. Localisation of proteins in the cytosol can be performed through screens with GFP-markers or cytosol and plastid isolates to be analysed via SDS-PAGE and Western blotting. A comparison of the proteins isolated from plastid isolates and the supernatant from the performed plastid isolation could give an insight in the presence of the enzymes in the different organelles. In the case of CRTB specific antibodies are available for this enzyme and western blots would be a suitable method. Screening for this enzyme through protein targeted LC-MS methods could give a targeted insight between samples.

Appendix

Appendices outline

Primers

DNA sequences for cloning

Spectra and standard curves

Chromatography traces

Sub-plastid Fractionation graphs

Sequencing data

Transient transformation data tables

Primers

Domestication primers: GB library parts

Table A-1. Primer list for domestication of GB-parts
Primers were designed using GB-cloning software and allow for SNPs on the restriction sites for required type II enzymes in the sequences used for cloning purposes. Part name, gene accession, patch number, forward (F) or reverse (R) primer and primer sequence are indicated.

Part name	**gene accession**	**patch**	**primer**	**primer sequence**
CaMV35S-5'UTR-tp	-	I	F	GCGCCGTCTCGCTCGGGAGAAGCTTGCATGCCTGCAGGT
CaMV35S-5'UTR-tp	-	I	R	GCGCCGTCTCGATACCTGCTGCGTAAGCCTC
CaMV35S-5'UTR-tp	-	II	F	GCGCCGTCTCGGTATCATCAAGACGATCTACC
CaMV35S-5'UTR-tp	-	II	R	GCGCCGTCTCGCTCGCATTGCACTTTACTCTTCCACCATT
CaMV35S-5'UTR	-	I	F	GCGCCGTCTCGCTCGGGAGAAGCTTGCATGCCTGCAGGT
CaMV35S-5'UTR	-	I	R	GCGCCGTCTCGATACCTGCTGCGTAAGCCTC
CaMV35S-5'UTR	-	II	F	GCGCCGTCTCGGTATCATCAAGACGATCTACC
CaMV35S-5'UTR	-	II	R	GCGCCGTCTCGCTCGCATTGGATCCTTATTTTTCTTGATTTCC
Thsp/Tnos	-	I	F	GCGCCGTCTCGCTCGGCTTGGATCCGAGCTCATATGAAG
Thsp/Tnos	-	I	R	GCGCCGTCTCGACCGCAAGACCGGCAACAGG
Thsp/Tnos	-	II	F	GCGCCGTCTCGCGGTGATTATCATATAATTTCTGTTG
Thsp/Tnos	-	II	R	GCGCCGTCTCGCTCGAGCGGAATTCCCGATCTAGTAACATAG
DXS_{ca}	Y15782.1	I	F	GCGCCGTCTCGCTCGAATGGCTTTATGTGCATATGCATTT
DXS_{ca}	Y15782.1	I	R	GCGCCGTCTCGGCCTCTGTGTGTAGTATTCTC
DXS_{ca}	Y15782.1	II	F	GCGCCGTCTCGAGGCCACCAACACCTATTGT
DXS_{ca}	Y15782.1	II	R	GCGCCGTCTCGGGCCTCCACTTCAACTTGCC
DXS_{ca}	Y15782.1	III	F	GCGCCGTCTCGGGCCAATAGTTCTTCCTGATC
DXS_{ca}	Y15782.1	III	R	GCGCCGTCTCGCTCGAAGCTTATGTCATGACCTCTAGAGC
DXR_{ec}	AB013300.1	I	F	GCGCCGTCTCGCTCGAATGAAGCAACTCACCATTCTG
DXR_{ec}	AB013300.1	I	R	GCGCCGTCTCGGTGTCTCACGGAAAGGGCCA
DXR_{ec}	AB013300.1	II	F	GCGCCGTCTCGACACCATTGCGCGATTTGGC
$DXR_{e}c$	AB013300.1	II	R	GCGCCGTCTCGTTGCCAGTTTCAGGCATGGA
DXR_{ec}	AB013300.1	III	F	GCGCCGTCTCGGCAATGGAGGCGTTCGAACA
DXR_{ec}	AB013300.1	III	R	GCGCCGTCTCGCTCGAAGCTCAGCTTGCAAGACGCATCA
MCT_{ec}	AB037143.1	I	F	GCGCCGTCTCGCTCGAATGGCAACCACTCATTTGGAT
MCT_{ec}	AB037143.1	I	R	GCGCCGTCTCGCTCGAAGCTTATGTATTCTCCTGATGGATGG
CMK_{ec}	AF179284.1	I	F	GCGCCGTCTCGCTCGAATGCGGACACAGTGGCCCTC

CMK_{ec}	AF179284.1	I	R	GCGCCGTCTCGCAAGACCGCCGCCCATCGGC
CMK_{ec}	AF179284.1	II	F	GCGCCGTCTCGCTTGGCGGTGGTTCATCCAA
CMK_{ec}	AF179284.1	II	R	GCGCCGTCTCGCTCGAAGCTTAAAGCATGGCTCTGTGCAA
MDS_{ec}	AF230738.1	I	F	GCGCCGTCTCGCTCGAATGCGAATTGGACACGGTTTT
MDS_{ec}	AF230738.1	I	R	GCGCCGTCTCGCTATGATAGTGACATCGACGT
MDS_{ec}	AF230738.1	II	F	GCGCCGTCTCGATAGCTCAGGCACCGAAGAT
MDS_{ec}	AF230738.1	II	R	GCGCCGTCTCGCTCGAAGCTCATTTTGTTGCCTTAATGAGTAG
HDS_{ec}	X64451.1	I	F	GCGCCGTCTCGCTCGAATGCATAACCAGGCTCCAATT
HDS_{ec}	X64451.1	I	R	GCGCCGTCTCGCGTCGCCAATCGGCACATTC
HDS_{ec}	X64451.1	II	F	GCGCCGTCTCGGACGGTGCTCCCATAGCCGTACAG
HDS_{ec}	X64451.1	II	R	GCGCCGTCTCGGCTATGAAGTTGATCCCTCG
HDS_{ec}	X64451.1	III	F	GCGCCGTCTCGTAGCCTGCCCGACCTGTTCG
HDS_{ec}	X64451.1	III	R	GCGCCGTCTCGCTCGAAGCTTATTTTTCAACCTGCTGAACGTC
HDR_{ec}	X54945.1	I	F	GCGCCGTCTCGCTCGAATGCAGATCCTGTTGGCCAA
HDR_{ec}	X54945.1	I	R	GCGCCGTCTCGCTCGAAGCTTAATCGACTTCACGAATATCGAC
$CRTE_{pa}$	D90087.2	I	F	GCGCCGTCTCGCTCGAATGACGGTCTGCGCAAAAAAACACGTT CATCTCACTCGCGACGCTGCGGAG
$CRTE_{pa}$	D90087.2	I	R	GCGCCGTCTCGTTGCGGCACCCACAACATCC
$CRTE_{pa}$	D90087.2	II	F	GCGCCGTCTCGGCAATGCGTGAAGGTGCGCT
$CRTE_{pa}$	D90087.2	II	R	GCGCCGTCTCGCTCGAAGCTTAACTGACGGCAGCGAGTT
$CRTB_{pa}$	D90087.2	I	F	GCGCCGTCTCGCTCGAATGAATAATCCGTCGTTACTCAAT
$CRTB_{pa}$	D90087.2	I	R	GCGCCGTCTCGCTCGAAGCCTAGAGCGGGCGCTGCCAGA
$CRTI_{pa}$	D90087.2	I	F	GCGCCGTCTCGCTCGAATGAAACCAACTACGGTAATTGG
$CRTI_{pa}$	D90087.2	I	R	GCGCCGTCTCGCGTCGCGGGGATTAAACTGC
$CRTI_{pa}$	D90087.2	II	F	GCGCCGTCTCGGACGTCGAAGGTTATCGTCA
$CRTI_{pa}$	D90087.2	II	R	GCGCCGTCTCGCTCGAAGCTCATATCAGATCCTCCAGCAT

Table A-2 Sequencing primers of GB parts

Primer list of primers used for sequencing purposes during confirmation of clones. GB-parts primers were designed are indicated, furthermore primer orientation forward (F) and reverse (R) and primer sequence are provided.

GB part	**primer orientation**	**sequence**
CaMV35S-5'UTR-tp	F	tggagagaacacgggggactct
CaMV35S-5'UTR-tp	R	tggacgattcaaggcttgcttcaca
CaMV35S-5'UTR	F	tggagagaacacgggggactct
CaMV35S-5'UTR	R	tggacgattcaaggcttgcttcaca
DT2, Thsp/Tnos	F	tgttttgttggatctcttctgcagca
DT2, Thsp/Tnos	R	cctgttgccggtcttgcgatga
DXS_{ca}	F1	tgtcttcaacgcaccccaagataga
DXS_{ca}	F2	gcaaaccactggaccgtgctct
DXR_{ec}	F1	tcaccattctgggctcgaccgg
DXR_{ec}	F2	gtgcgttgacatttgccgcacc

MCT_{ec}	F1	ttggatgtttgcgccgtggttc
MCT_{ec}	F2	cgtgccgaaccgggcaaaaatg
CMK_{ec}	F1	atgcggacacagtggccctctc
CMK_{ec}	F2	agagtctgaagcccgccaggtg
MDS_{ec}	F1	tgcgaattggacacggttttgacgt
MDS_{ec}	F2	tcaggcaccgaagatgttgccg
HDS_{ec}	F1	tgcataaccaggctccaattcaacgt
HDS_{ec}	F2	gctggagcaacgcctggaagat
HDR_{ec}	F1	cagatcctgttggccaacccgc
HDR_{ec}	F2	ggcgcatcggctccggatattc
$CRTE_{pa}$	F	acgttcatctcactcgcgatgc
$CRTE_{pa}$	R	tgtcaaaccaggcctgaataaaatgttga
$CRTB_{pa}$	F	tcatgcggtcgaaacgatggca
$CRTB_{pa}$	R	ccgggaagtaagggcctgacca
$CRTI_{pa}$	F	tttccactcgctgttggtgggc
$CRTI_{pa}$	R	aacctgctgtcgcttttgccga

RT-PCR primers of coding sequences

Table A-3. Primers for RT-PCR.

Usable for quantitative expression analysis using intercalating dyes. Sequences and accessions for *N. benthamiana* were obtained from https://solgenomics.net. Sequences and accessions for *E. coli* were obtained from NCBI. Gene name, accession, primer orientation forward (F) and reverse (R), fragment size and primer sequence are provided.

Gene name	*accession*	*primer*	*fragment size*	*sequence*
nb_L23	Niben101Scf01444g02009.1	F	94bp	GGTTGCCAAGGCCGTCAAGTCA
nb_L23	Niben101Scf01444g02009.1	R	94bp	TCTTCAAAGTCTTGGGTCGGTGGA
nb_EF1	Niben101Scf04639g06007.1	F	100bp	GGTGCTGCCAGCTTTACCTCCC
nb_EF1	Niben101Scf04639g06007.1	R	100bp	GCAATGTGGGAGGTGTGGCAGT
nb_Ubi	Niben101Scf00339g07001.1	F	75bp	ACAGGAAGGTGCGCGAGATTGT
nb_Ubi	Niben101Scf00339g07001.1	R	75bp	TGCTGTAACAGACGAGAGTGCGG
nb_DXS	Niben101Scf00246g04005.1	F	109bp	ACCACCATCTCGGCAGGCCTAG
nb_DXS	Niben101Scf00246g04005.1	R	109bp	GCGATGACGGCAGGTCAAGCTT
ec_DXR	NCBI: AB013300.1	F	83bp	GAATGCCGCAAACGAAATCACC
ec_DXR	NCBI:AB013300.1	R	83bp	ACGGATAAATTCAACGCAGCGA
ec_MCT	NCBI: AB037143.1	F	108bp	TGCGCGATACTATGAAACGTGC
ec_MCT	NCBI: AB037143.1	R	108bp	AGCTCACGAGGGAAAAATTGCG
ec_CMK	NCBI: AF179284.1	F	83bp	GAGGTTGATGCGGTGCTTTCC
ec_CMK	NCBI: AF179284.1	R	83bp	AATTCAGCAAAGACACAGGCCC
ec_MDS	NCBI: AF230738.1	F	99bp	ACAAATGCGCGTGTTTATTGCC
ec_MDS	NCBI: AF230738.1	R	99bp	CCACGTCCGGTAAATCCCAGTT
ec_HDS	NCBI: X64451.1	F	92bp	CGCCATTGGTTTAGGTCTGCTG
ec_HDS	NCBI: X64451.1	R	92bp	CGACTTTGATCTCTTCGACCGG
ec_HDR	NCBI: X54945.1	F	87bp	GCGATCCTGATTTTCTCCGCAC
ec_HDR	NCBI: X54945.1	R	87bp	GGTGGCATCAAACACCGTCAAA

Fasta sequences for cloning

CaMV35S-5'UTR-TP (targeting peptide: plastidial)

Aagcttgcatgcctgcaggtccccagattagccttttcaatttcagaaagaatgctaacccacagatggttagagaggcttacgcagca
ggtctcatcaagacgatctacccgagcaataatctccaggaaatcaaataccttcccaagaaggttaaagatgcagtcaaaagattca
ggactaactgcatcaagaacacagagaaagatatatttctcaagatcagaagtactattccagtatggacgattcaaggcttgcttcac
aaaccaaggcaagtaatagagattggagtctctaaaaaggtagttcccactgaatcaaaggccatggagtcaaagattcaaatagag
gacctaacagaactcgccgtaaagactggcgaacagttcatacagagtctcttacgactcaatgacaagaagaaaatcttcgtcaaca
tggtggagcacgacacacttgtctactccaaaaatatcaaagatacagtctcagaagaccaaagggcaattgagacttttcaacaaag
ggtaatatccggaaacctcctcggattccattgcccagctatctgtcactttattgtgaagatagtggaaaaggaaggtggctcctacaa
atgccatcattgcgataaaggaaaggccatcgttgaagatgcctctgccgacagtggtcccaaagatggacccccacccacgaggagc
atcgtggaaaaagaagacgttccaaccacgtcttcaaagcaagtggattgatgtgatatctccactgacgtaagggatgacgcacaatc
ccactatccttcgcaagacccttcctctatataaggaagttcatttcatttggagagaacacgggggactctagatctagagtctatttaa
ctcagtattcagaaacaacaaaagttcttctctacataaaattttcctattttagtgatcagtgaaggaaatcaagaaaaataaggatcc
atggcttctatgatatcctcttccgctgtgacaacagtcagccgtgcctctaggggcaatccgccgcagtggctccattcggcggcctca
aatccatgactggattcccagtgaagaaggtcaacactgacattacttccattacaagcaatggtggaagagtaaagtgc

DT2, succession of Thsp and Tnos terminators

Ggatccgagctcatatgaagatgaagatgaaatatttggtgtgtcaaataaaaagcttgtgtgcttaagtttgtgtttttttcttggcttgt
tgtgttatgaatttgtggctttttctaatattaaatgaatgtaagatctcattataatgaataaacaaatgtttctataatccattgtgaatg
ttttgttggatctcttctgcagcatataactactgtatgtgctatggtatggactatggaatatgattaaagataagggtaccgaatttccc
cgatcgttcaaacatttggcaataaagtttcttaagattgaatcctgttgccggtcttgcgatgattatcatataatttctgttgaattacgt
taagcatgtaataattaacatgtaatgcatgacgttatttatgagatgggtttttatgattagagtcccgcaattatacatttaatacgcga
tagaaaacaaaatatagcgcgcaaactaggataaattatcgcgcgcggtgtcatctatgttactagatcgggaattc

[DXS] deoxyxylose 5-phosphate synthase (*C.annuum*), Y15782.1

atggctttatgtgcatatgcatttcctgggattttgaacaggacagtggcagtggcttcagatgcttcaaagccaactccttattctctga
atggatcatggaacagatctgcagtttcagttccaccaaaagcttactcaggtcaagaaaaggtcacgtacggttcaggcttctttgtca
gaatccggagaatactacacacagagaccaccaacacctattgtggacactatcaactatcccattcatatgaaaaatctttctctaaag
gaacttaaacaactagcagatgagctaagatcagatacaattttcaatgtatcaaagactggtggtcaccttggttcaagtcttggcgtt
gttgagcttacagttgctcttcattatgtcttcaacgcaccccaagatagaatactctgggatgttggtcatcagtcatatcctcacaaaat
cttgactggtagaagggagaagatgtcaacattaagacaaacaaatggacttgctggatttactaaacggtcggagagtgaatatgatt
gctttgggactggccacagttccaccaccatctcagcaggcctagggatggctgttggaagagatctgaaaggaagaaacaacaatgt
tatagccgtaataggtgatggtgccatgacagcaggtcaagcttatgaagccatgaataatgctggttacctggactctgacatgattgt
tattttaaacgacaatagacaagtttctttgcctactgctactctggatgggccagttcctcctgttggagctctaagtagtgctttgagca
ggttgcagtctaataggcctctcagagaactaagagaagtcgctaaggggttactaagcagattggtggacctatgcatgagcttgct
gcaaaagttgatgaatatgctcgtggcatgatcagtggttctggatcaacattgtttgaagaacttggactttattatattggtcctgtgga
tggtcacaatattgatgatcttatttctattctcaaagaggttagaagtactaaaacaacaggtcctgtactgatccatgttgtcaccgag
aaaggcagaggttatccatatgctgagagagctgcagacaagtatcatggagttgccaaatttgatccagcaacaggaaagcaattca
aaggcagtgccaagactcagtcatatacaacatattttgcagaggctttaattgcagaagcagaagcagataaagacattgttgcaatc
catgctgccatgggggtgggaccgggatgaacctttttcctccgtcgcttcccgacacggtgttttgatgttggaatagcagaacaacat
gcagtaacctttgctgctggactggcttgtgaaggcctcaaacctttctgtgcaatttattcatctttcatgcagagggcttatgaccaggt
agtgcatgacgttgatttgcaaaagctgcctgtgaggtttgccatggacagagcaggtcttgttggagcagatggtcctacacattgtgg
tgcatttgatgttactttcatggcatgtctccctaacatggttgtaatggctccttctgatgaagcggagctatttcacattgtagcaactgc
tgctgccattgatgacagaccaagttgtttcagatacccaagaggaaatgggattggtgtagagcttccggctggaaacaaaggaattc
cccttgaggttggtaaaggcaggatattggttgaaggggagagagtggctctattgggatacggctcagcagtgcagaactgtttggct
gctgcttctgtgttagaatcccgtggcttacaagtaacagttgcagatgcacgtttctgcaaaccactggaccgtgctctcataaggagcc
ttgcaaaatcacacgaagtacttgtcactgttgaaaaaggatcaattggaggttttggatcgcatgttgttcagtttatggccttagatgg

gcttcttgatggcaagttgaagtggagaccaatagttcttcctgatcgatacattgaccatggatctcctgctgatcagttggcagaagct
ggcctaacaccatctcacattgcagcaacagtatttaacatacttggacaaaccagagaggctctagaggtcatgacataa

[DXR] deoxyxylose 5-phosphate reductase (*E. coli*), AB013300.1

atgaagcaactcaccattctgggctcgaccggctcgattggttgcagcacgctggacgtggtgcgccataatcccgaacacttccgcgta
gttgcgctggtggcaggcaaaaatgtcactcgcatggtagaacagtgcctggaattctctccccgctatgccgtaatggacgatgaagc
gagtgcgaaacttcttaaaacgatgctacagcaacagggtagccgcaccgaagtcttaagtgggcaacaagccgcttgcgatatggca
gcgcttgaggatgttgatcaggtgatggcagccattgttggcgctgctgggctgttacctacgcttgctgcgatccgcgcgggtaaaacc
attttgctggccaataaagaatcactggttacctgcggacgtctgtttatggacgccgtaaagcagagcaaagcgcaattgttaccggtc
gatagcgaacataacgccatttttcagagtttaccgcaacctatccagcataatctgggatacgctgaccttgagcaaaatggcgtggtg
tccattttacttaccgggtctggtggccctttccgtgagacgccattgcgcgatttggcaacaatgacgccggatcaagcctgccgtcatc
cgaactggtcgatggggcgtaaaatttctgtcgattcggctaccatgatgaacaaaggtctggaatacattgaagcgcgttggctgttta
acgccagcgccagccagatggaagtgctgattcacccgcagtcagtgattcactcaatggtgcgctatcaggacggcagtgttctggcg
cagctgggggaaccggatatgcgtacgccaattgcccacaccatggcatggccgaatcgcgtgaactctggcgtgaagccgctcgattt
ttgcaaactaagtgcgttgacatttgccgcaccggattatgatcgttatccatgcctgaaactggcgatggaggcgttcgaacaaggcca
ggcagcgacgacagcattgaatgccgcaaacgaaatcaccgttgctgcttttcttgcgcaacaaatccgctttacggatatcgctgcgtt
gaatttatccgtactggaaaaaatggatatgcgcgaaccacaatgtgtggacgatgtgttatctgttgatgcgaacgcgcgtgaagtcg
ccagaaaagaggtgatgcgtctcgcaagctga

[MCT] 4-diphosphocytidyl-methylerythritol synthase (*E. coli*), AB037143.1

atggcaaccactcatttggatgtttgcgccgtggttccggcggccggatttggccgtcgaatgcaaacggaatgtcctaagcaatatctct
caatcggtaatcaaaccattcttgaacactcggtgcatgcgctgctggcgcatccccgggtgaaacgtgtcgtcattgccataagtcctg
gcgatagccgttttgcacaacttcctctggcgaatcatccgcaaatcaccgttgtagatggcggtgatgagcgtgccgattccgtgctgg
caggtctgaaagccgctggcgacgcgcagtgggtattggtgcatgacgccgctcgtccttgtttgcatcaggatgacctcgcgcgattgt
tggcgttgagcgaaaccagccgcacgggggggatcctcgccgcaccagtgcgcgatactatgaaacgtgccgaaccgggcaaaaatg
ccattgctcataccgttgatcgcaacggcttatggcacgcgctgacgccgcaatttttccctcgtgagctgttacatgactgtctgacgcg
cgctctaaatgaaggcgcgactattaccgacgaagcctcggcgctggaatattgcggattccatcctcagttggtcgaaggccgtgcgg
ataacattaaagtcacgcgcccggaagatttggcactggccgagttttacctcacccgaaccatccatcaggagaatacataa

[CMK] 4-diphosphocytidyl-methylerythritol kinase (*E. coli*), AF179284.1

atgcggacacagtggccctctccggcaaaacttaatctgtttttatacattaccggtcagcgtgcggatggttaccacacgctgcaaacg
ctgtttcagtttcttgattacggcgacaccatcagcattgagcttcgtgacgatggggatattcgtctgttaacgcccgttgaaggcgtgg
aacatgaagataacctgatcgttcgcgcagcgcgattgttgatgaaaactgcggcagacagcgggcgtcttccgacgggaagcggtgc
gaatatcagcattgacaagcgtttgccgatgggcggcggtctcggcggtggttcatccaatgccgcgacggtcctggtggcattaaatca
tctctggcaatgcgggctaagcatggatgagctggcggaaatggggctgacgctgggcgcagatgttcctgtctttgttcgggggcatgc
cgcgtttgccgaaggcgttggtgaaatactaacgccggtggatccgccagagaagtggtatctggtggcgcaccctggtgtaagtattc
cgactccggtgatttttaaagatcctgaactcccgcgcaatacgccaaaaaggtcaatagaaacgttgctaaaatgtgaattcagcaat
gattgcgaggttatcgcaagaaaacgttttcgcgaggttgatgcggtgctttcctggctgttagaatacgccccgtcgcgcctgactggg
acaggggcctgtgtctttgctgaatttgatacagagtctgaagcccgccaggtgctagagcaagccccggaatggctcaatggctttgtg
gcgaaaggcgctaatctttccccattgcacagagccatgctttaa

[MDS] methylerythritol 2,4-cyclodiphosphate synthase (*E. coli*), AF230738.1

atgcgaattggacacggttttgacgtacatgcctttggcggtgaaggcccaattatcattggtggcgtacgcattccttacgaaaaagga
ttgctggcgcattctgatggcgacgtggcgctccatgcgttgaccgatgcattgcttggcgcggcggcgctgggggatatcggcaagctg
ttcccggataccgatccggcatttaaaggtgccgatagccgcgagctgctacgcgaagcctggcgtcgtattcaggcgaagggttatac
ccttggcaacgtcgatgtcactatcatcgctcaggcaccgaagatgttgccgcacattccacaaatgcgcgtgtttattgccgaagatctc
ggctgccatatggatgatgttaacgtgaaagccactactacggaaaaactgggatttaccggacgtggggaagggattgcctgtgaag
cggtggcgctactcattaaggcaacaaaatga

[HDS] Hydroxymethylbutenyl diphosphate synthase (*E. coli*), X64451.1

atgcataaccaggctccaattcaacgtagaaaatcaacacgtatttacgttgggaatgtgccgattggcgatggtgctcccatcgccgta
cagtccatgaccaatacgcgtacgacagacgtcgaagcaacggtcaatcaaatcaaggcgctggaacgcgttggcgctgatatcgtcc
gtgtatccgtaccgacgatggacgcggcagaagcgttcaaactcatcaaacagcaggttaacgtgccgctggtggctgacatccacttc
gactatcgcattgcgctgaaagtagcggaatacggcgtcgattgtctgcgtattaaccctggcaatatcggtaatgaagagcgtattcgc
atggtggttgactgtgcgcgcgataaaaacattccgatccgtattggcgttaacgccggatcgctggaaaaagatctgcaagaaaagta
tggcgaaccgacgccgcaggcgttgctggaatctgccatgcgtcatgttgatcatctcgatcgcctgaacttcgatcagttcaaagtcag
cgtgaaagcgtctgacgtcttcctcgctgttgagtcttatcgtttgctggcaaaacagatcgatcagccgttgcatctggggatcaccgaa
gccggtggtgcgcgcagcggggcagtaaaatccgccattggtttaggtctgctgctgtctgaaggcatcggcgacacgctgcgcgtatc
gctggcggccgatccggtcgaagagatcaaagtcggtttcgatattttgaaatcgctgcgtatccgttcgcgagggatcaacttcatcgc
ctgcccgacctgttcgcgtcaggaatttgatgttatcggtacggttaacgcgctggagcaacgcctggaagatatcatcactccgatgga
cgtttcgattatcggctgcgtggtgaatggcccaggtgaggcgctggtttctacactcggcgtcaccggcggcaacaagaaaagcggcc
tctatgaagatggcgtgcgcaaagaccgtctggacaacaacgatatgatcgaccagctggaagcacgcattcgtgcgaaagccagtca
gctggacgaagcgcgtcgaattgacgttcagcaggttgaaaaataa

[HDR] Hydroxymethylbutenyl diphosphate reductase (*E. coli*), X54945.1

atgcagatcctgttggccaacccgcgtggtttttgtgccggggtagaccgcgctatcagcattgttgaaaacgcgctggccatttacggc
gcaccgatatatgtccgtcacgaagtggtacataaccgctatgtggtcgatagcttgcgtgagcgtggggctatctttattgagcagatta
gcgaagtaccggacggcgcgatcctgattttctccgcacacggtgtttctcaggcggtacgtaacgaagcaaaaagtcgcgatttgacg
gtgtttgatgccacctgtccgctggtgaccaaagtgcatatggaagtcgcccgcgccagtcgccgtggcgaagaatctattctcatcggt
cacgccgggcacccggaagtggaagggacaatgggccagtacagtaacccggaagggggaatgtatctggtcgaatcgccggacgat
gtgtggaaactgacggtcaaaaacgaagagaagctctcctttatgacccagaccacgctgtcggtggatgacacgtctgatgtgatcga
cgcgctgcgtaaacgcttcccgaaaattgtcggtccgcgcaaagatgacatctgctacgccacgactaaccgtcaggaagcggtacgc
gccctggcagaacaggcggaagttgtgttggtggtcggttcgaaaaactcctccaactccaaccgtctggcggagctggcccagcgtat
gggcaaacgcgcgtttttgattgacgatgcgaaagacatccaggaagagtgggtgaaagaggttaaatgcgtcggcgtgactgcgggc
gcatcggctccggatattctggtgcagaatgtggtggcacgtttgcagcagctgggcggtggtgaagccattccgctggaaggccgtga
agaaaacattgttttcgaagtgccgaaagagctgcgtgtcgatattcgtgaagtcgattaa

[CRTE] GGPP synthase (*P. ananatis*), D90087.2

atgacggtctgcgcaaaaaaacacgttcatctcactcgcgatgctgcggagcagttactggctgatattgatcgacgccttgatcagtta
ttgcccgtggagggagaacgggatgttgtgggtgccgcgatgcgtgaaggtgcgctggcaccgggaaaacgtattcgccccatgttgct
gttgctgaccgcccgcgatctgggttgcgctgtcagccatgacggattactggatttggcctgtgcggtggaaatggtccacgcggcttc
gctgatccttgacgatatgccctgcatggacgatgcgaagctgcggcgcggacgccctaccattcattctcattacggagagcatgtggc
aatactggcggcggttgccttgctgagtaaagcctttggcgtaattgccgatgcagatggcctcacgccgctggcaaaaaatcgggcgg
tttctgaactgtcaaacgccatcggcatgcaaggattggttcagggtcagttcaaggatctgtctgaaggggataagccgcgcagcgct
gaagctattttgatgacgaatcactttaaaaccagcacgctgttttgtgcctccatgcagatggcctcgattgttgcgaatgcctccagcg
aagcgcgtgattgcctgcatcgtttttcacttgatcttggtcaggcatttcaactgctggacgatttgaccgatggcatgaccgacaccgg
taaggatagcaatcaggacgccggtaaatcgacgctggtcaatctgttaggcccgagggcggttgaagaacgtctgagacaacatctt
cagcttgccagtgagcatctctctgcggcctgccaacacgggcacgccactcaacattttattcaggcctggtttgacaaaaaactcgct
gccgtcagttaa

[CRTB] Phytoene synthase (*P. ananatis*), D90087.2

atgaataatccgtcgttactcaatcatgcggtcgaaacgatggcagttggctcgaaaagttttgcgacagcctcaaagttatttgatgca
aaaacccggcgcagcgtactgatgctctacgcctggtgccgccattgtgacgatgttattgacgatcagacgctgggctttcaggcccgg
cagcctgccttacaaacgcccgaacaacgtctgatgcaacttgagatgaaaacgcgccaggcctatgcaggatcgcagatgcacgaac
cggcgtttgcggcttttcaggaagtggctatggctcatgatatcgccccggcttacgcgtttgatcatctggaaggcttcgccatggatgt
acgcgaagcgcaatacagccaactggatgatacgctgcgctattgctatcacgttgcaggcgttgtcggcttgatgatggcgcaaatcat
gggcgtgcgggataacgccacgctggaccgcgcctgtgaccttgggctggcatttcagttgaccaatattgctcgcgatattgtggacga
tgcgcatgcgggccgctgttatctgccggcaagctggctggagcatgaaggtctgaacaaagagaattatgcggcacctgaaaaccgt
caggcgctgagccgtatcgcccgtcgtttggtgcaggaagcagaaccttactatttgtctgccacagccggcctggcagggttgcccctg

cgttccgcctgggcaatcgctacggcgaagcaggtttaccggaaaataggtgtcaaagttgaacaggccggtcagcaagcctgggatc
agcggcagtcaacgaccacgcccgaaaaattaacgctgctgctggccgcctctggtcaggcccttacttcccggatgcgggctcatcctc
cccgccctgcgcatctctggcagcgcccgctctag

[CRTI] Phytoene desaturase (*P. ananatis*), D90087.2

atgaaaccaactacggtaattggtgcaggcttcggtggcctggcactggcaattcgtctacaagctgcggggatccccgtcttactgctt
gaacaacgtgataaacccggcggtcgggcttatgtctacgaggatcaggggtttacctttgatgcaggcccgacggttatcaccgatcc
cagtgccattgaagaactgtttgcactggcaggaaaacagttaaaagagtatgtcgaactgctgccggttacgccgttttaccgcctgtg
ttgggagtcagggaaggtctttaattacgataacgatcaaacccggctcgaagcgcagattcagcagtttaatccccgcgatgtcgaag
gttatcgtcagtttctggactattcacgcgcggtgtttaaagaaggctatctaaagctcggtactgtccctttttatcgttcagagacatgc
ttcgcgccgcacctcaactggcgaaactgcaggcatggagaagcgtttacagtaaggttgccagttacatcgaagatgaacatctgcgc
caggcgttttctttccactcgctgttggtgggcggcaatcccttcgccacctcatccatttatacgttgatacacgcgctggagcgtgagtg
gggcgtctggtttccgcgtggcggcaccggcgcattagttcaggggatgataaagctgtttcaggatctgggtggcgaagtcgtgttaaa
cgccagagtcagccatatggaaacgacaggaaacaagattgaagccgtgcatttagaggacggtcgcaggttcctgacgcaagccgt
cgcgtcaaatgcagatgtggttcatacctatcgcgacctgttaagccagcaccctgccgcggttaagcagtccaacaaactgcagacta
agcgcatgagtaactctctgtttgtgctctattttggtttgaatcaccatcatgatcagctcgcgcatcacacggtttgtttcggcccgcgtt
accgcgagctgattgacgaaatttttaatcatgatggcctcgcagaggacttctcactttatctgcacgcgccctgtgtcacggattcgtc
actggcgcctgaaggttgcggcagttactatgtgttggcgccggtgccgcatttaggcaccgcgaacctcgactggacggttgaggggc
caaaactacgcgaccgtatttttgcgtaccttgagcagcattacatgcctggcttacggagtcagctggtcacgcaccggatgtttacgcc
gtttgattttcgcgaccagcttaatgcctatcatggctcagccttttctgtggagcccgttcttacccagagcgcctggtttcggccgcata
accgcgataaaaccattactaatctctacctggtcggcgcaggcacgcatcccggcgcaggcattcctggcgtcatcggctcggcaaaa
gcgacagcaggtttgatgctggaggatctgatatga

Spectra and Standard Curves

Figure A-1. Carotenoid and chlorophyll spectra for UPLC analysis.

Spectra of compounds as detected on the UPLC-PDA system. Exact spectra and retention times are provided in Table A-4.

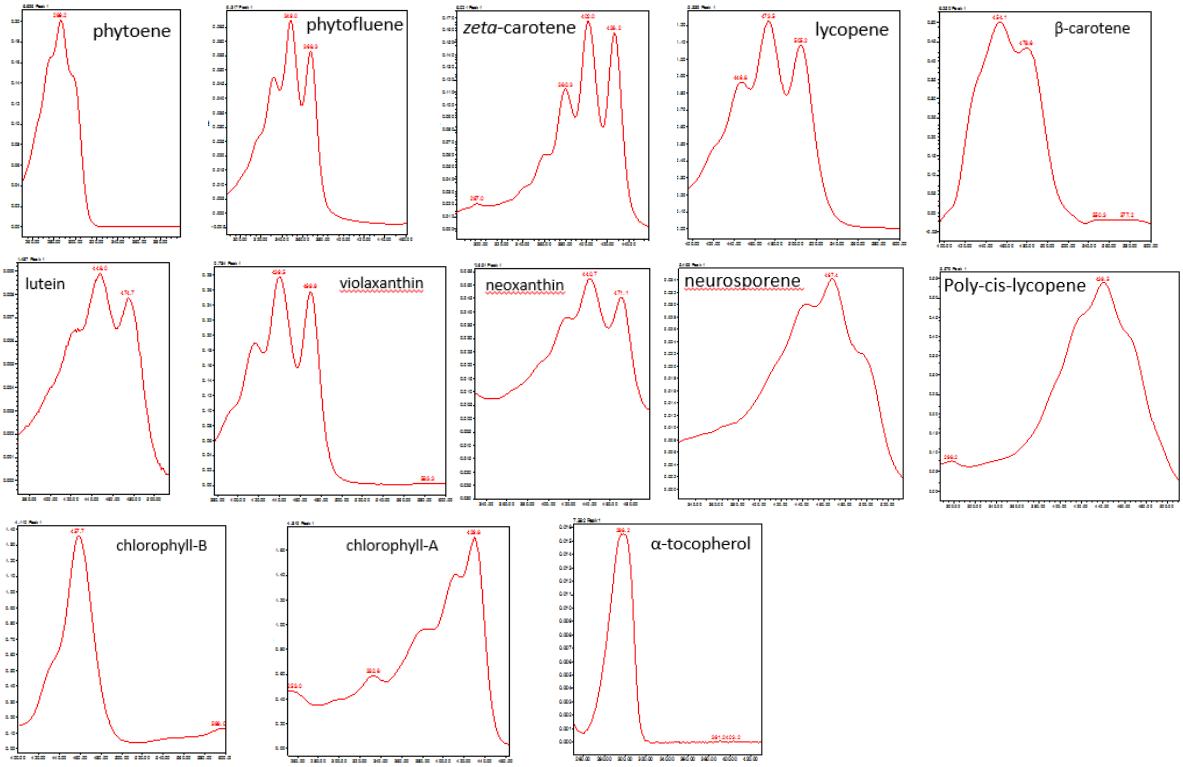

Table A-4 Carotenoids and Chlorophyll spectra and standard curves for UPLC analysis

The spectra, retention times and standard curves for compounds analysed and discussed in this thesis. * = ketocarotenoid protocol for UPLC analysis.

COMPOUND	SPECTRUM (nm)	RT (min)	STANDARD CURVE (µg)
Phytoene	286.2	6.7	y=4000000x-24989
Phytofluene	349.0, 368.3	6.4	y=3000000x-68968
ζ-carotene	400.8, 425.0	6	y=1000000x-32280
Lycopene	472.3, 502.7	5.3	y=6000000x-101170
β-carotene	454.1, 479.6	6.3	y=7000000x-408108
Lutein	448.0, 476.0	1.3	y=9000000x-462175
Violaxanthin	417.7, 442.0, 471.1	0.6	y=8000000x-205083
Neoxanthin	414.1, 438.3, 467.4	0.7	y=7000000x-182335
Neurosporene	440.5, 467.4	5.4	y=6E+06x+149819
Poly-*cis*-lycopene	439.5	5.6	y=6E+06x-156103
Chlorophyll B	456.5	4	y=3000000x-13568
Chlorophyll A	429.8	4.8	y=245786x-2630.8
α-tocopherol	293.4	4.4	y=261388x-4244.7
Astaxanthin*	479.6	3.2*	y=7000000x-58748
Adonixanthin*	466.2	3.8*	y=7000000x-202392
Phenicoxanthin*	479.6	4.6*	y=30000000x-299896
Canthaxanthin*	477.2	5.9*	y=9000000x-116270

Chromatography traces

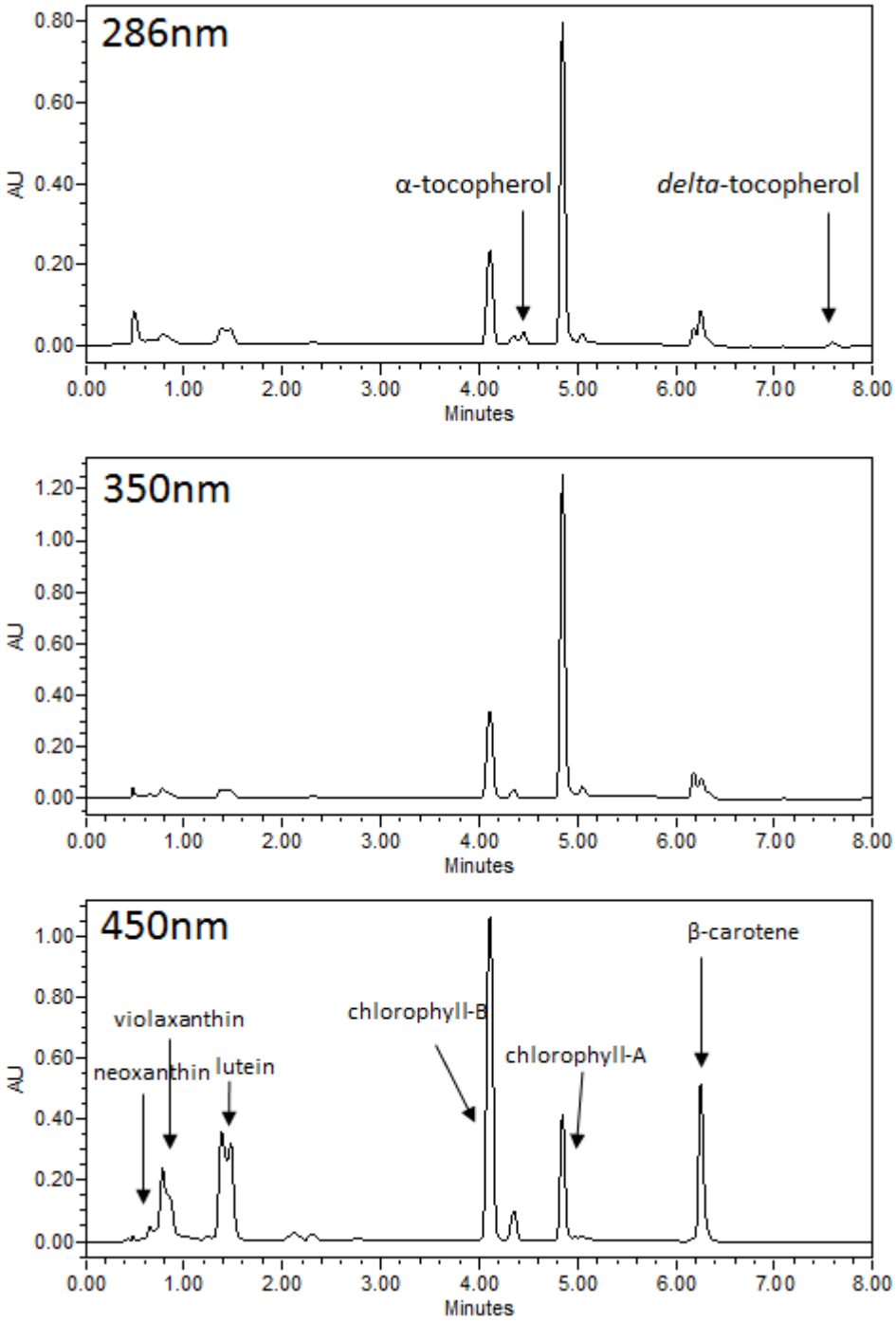

Figure A-2 UPLC traces Ailsa Craig (mature green).
UPLC traces of a mature green sample of Ailsa Craig fruit, measured at 286, 350 and 450nm. Carotenoids, tocopherols and chlorophylls detected are indicated with arrows.

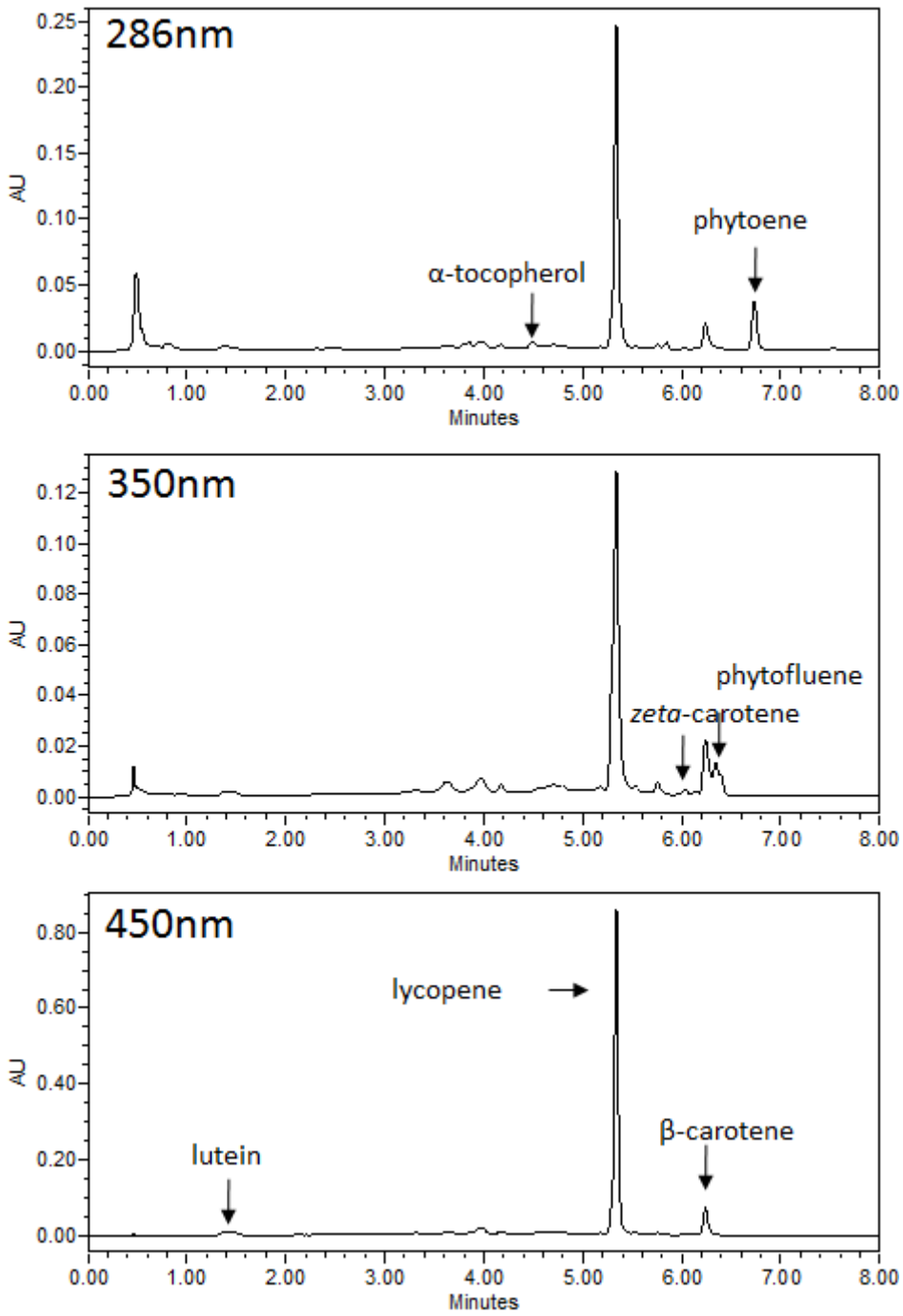

Figure A-3 UPLC traces Ailsa Craig (ripe).
UPLC traces of a ripe sample of Ailsa Craig fruit, measured at 286, 350 and 450nm. Carotenoids and tocopherols detected are indicated with arrows.

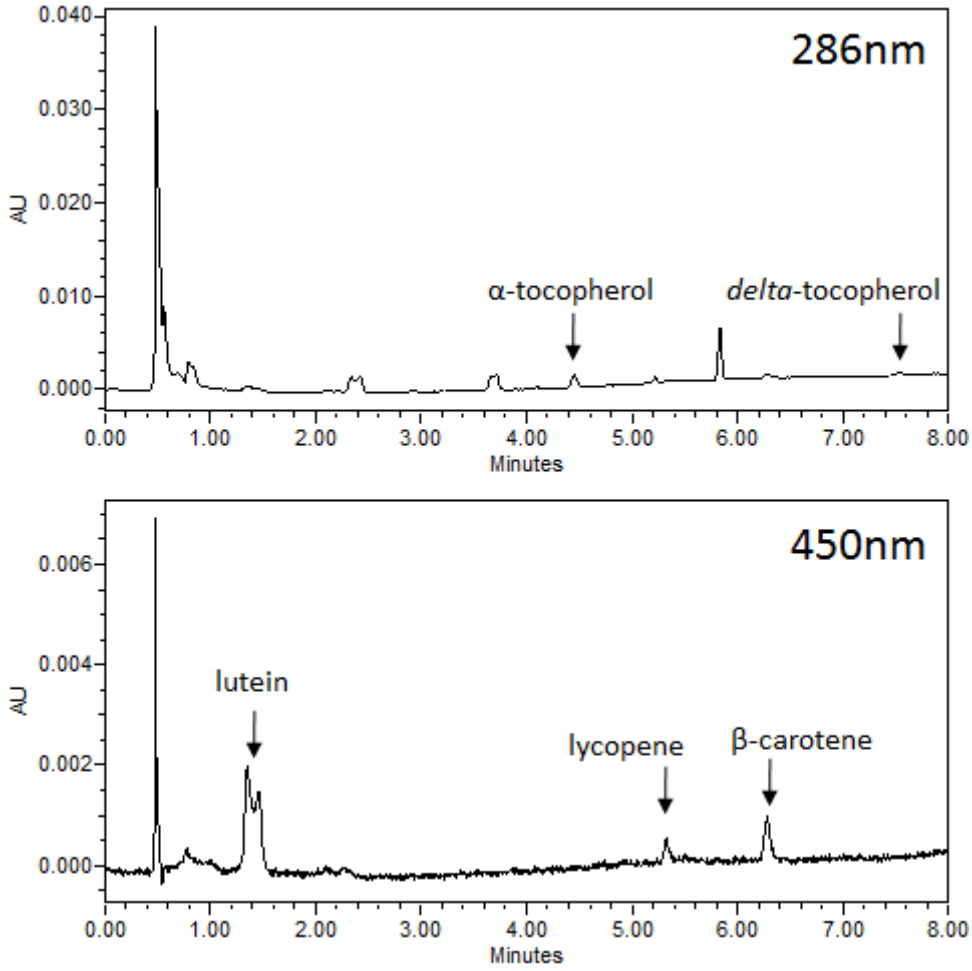

Figure A-4 UPLC traces *rr*-mutant (ripe).
UPLC traces of a ripe sample of fruit of the *rr*-mutant, measured at 286, 350 and 450nm. Carotenoids and tocopherols detected are indicated with arrows.

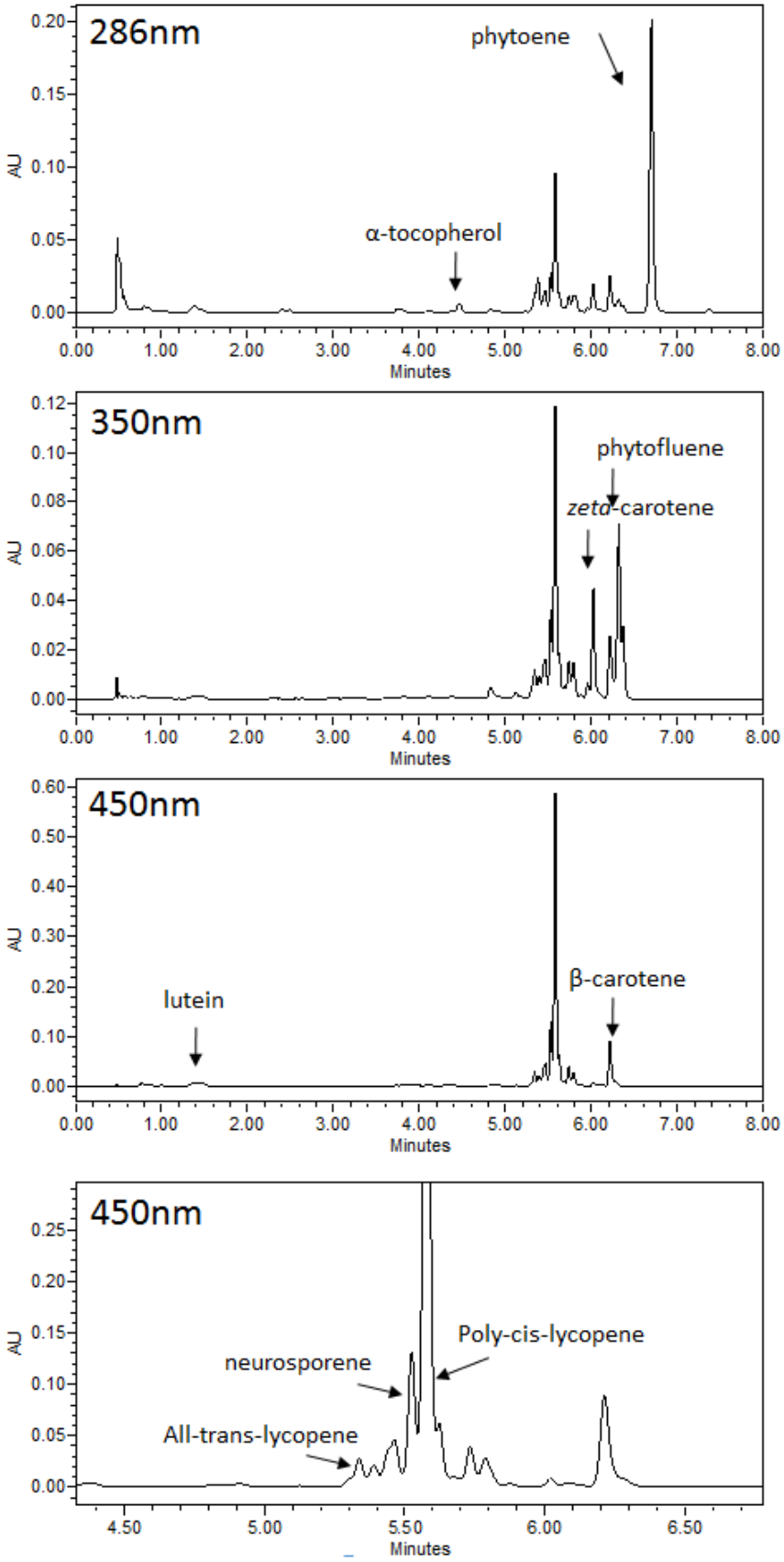

Figure A-5 UPLC traces *tangerine* mutant (ripe).
UPLC traces of a ripe fruit sample of the *tan*-mutant, measured at 286, 350 and 450nm. Carotenoids and tocopherols detected are indicated with arrows. The bottom trace zooms in on the partially co-eluted lycopene, neurosporene and poly-*cis*-lycopene

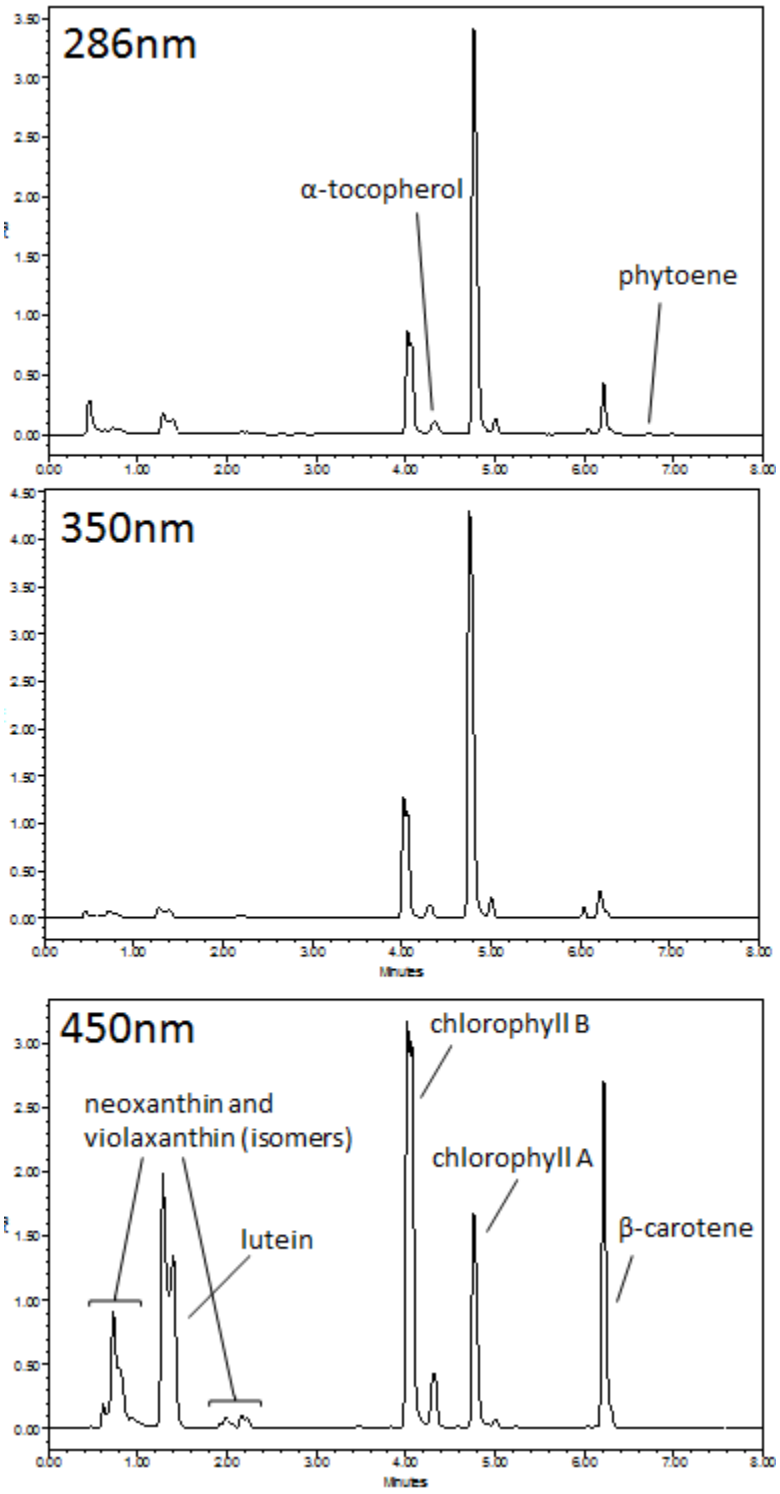

Figure A-6 UPLC traces: Transient transformation *N.benthamiana* empty vector control. Leaf sample of *N.benthamiana* infiltrated with the empty backbone vector of the GB-cloning system. Detection of compounds at 286, 350 and 450nm.

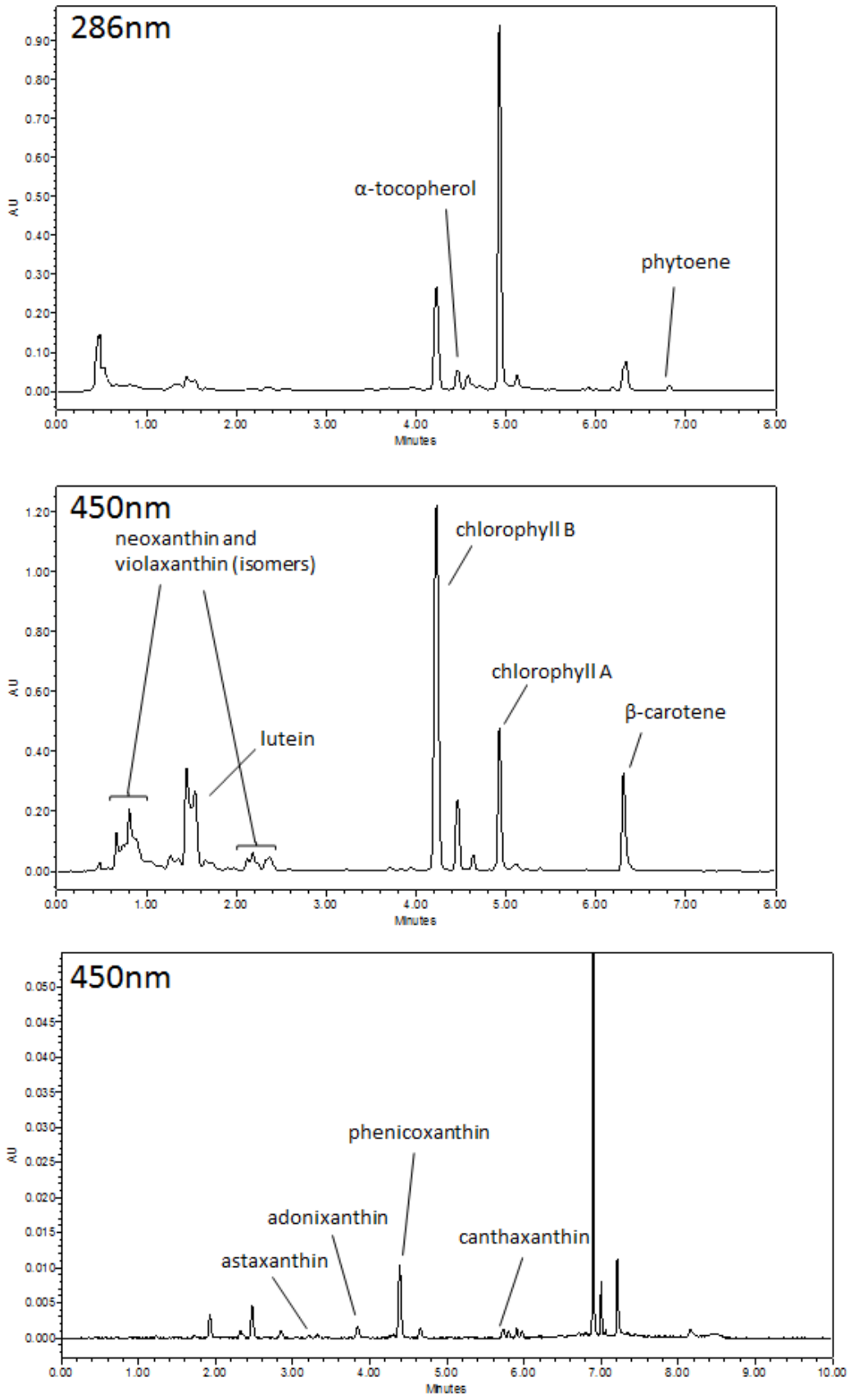

Figure A-7 UPLC traces Transient transformation *N.benthamiana* CRTZ/CRTW vector. Leaf sample of *N.benthamiana* infiltrated with the CRTZ/CRTW vector of the GB-cloning system. Detection of compounds at 286, 350 and 450nm. An additional trace with the keto-carotenoids as detected in the ketocarotenoid protocol is shown.

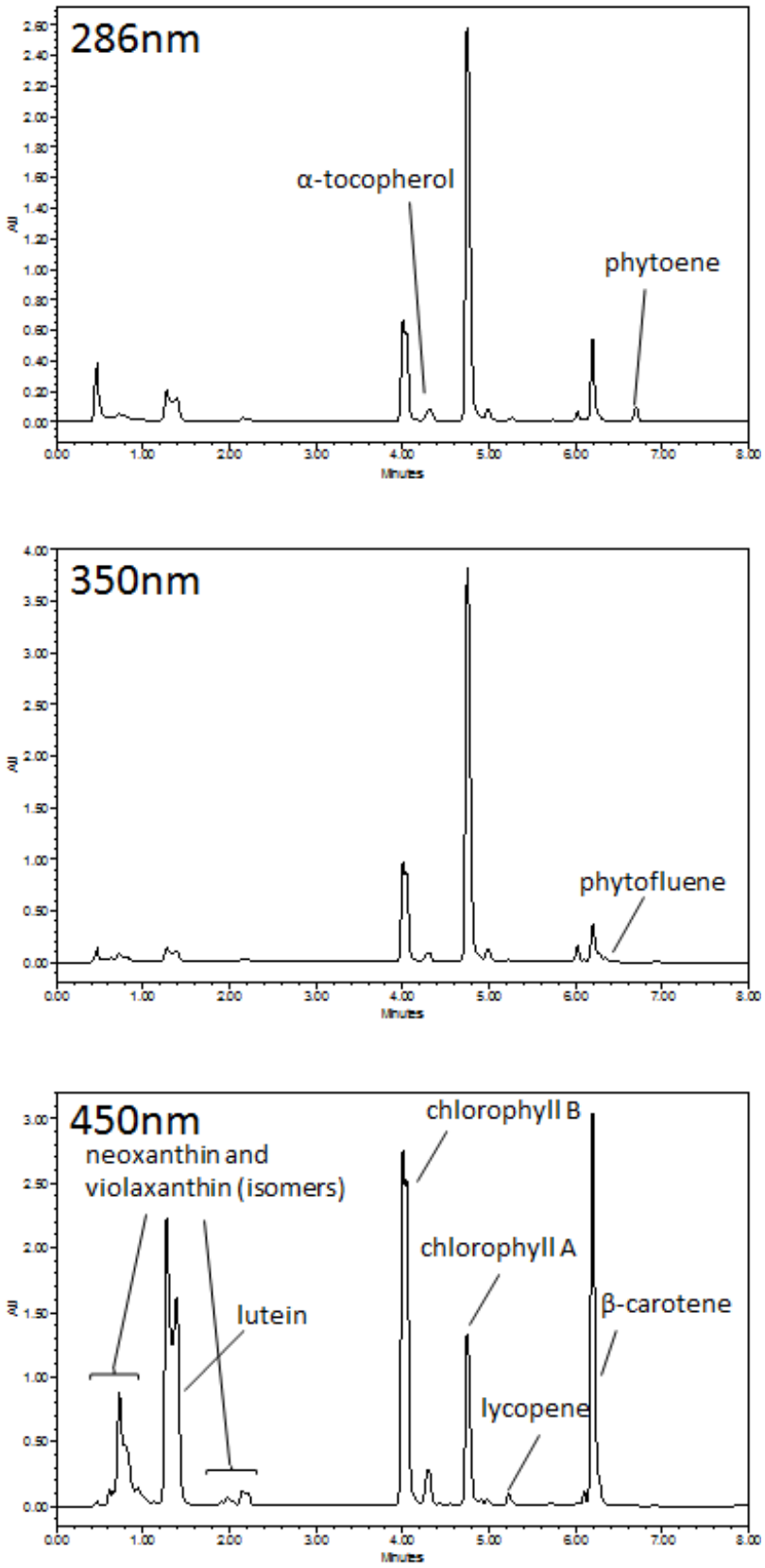

Figure A-8 UPLC traces Transient transformation *N.benthamiana* GB-crtB vector.
Leaf sample of *N.benthamiana* infiltrated with the crtB vector of the GB-cloning system. Detection of compounds at 286, 350 and 450nm. Detection of phytofluene and lycopene is novel in combination with the bigger peak for phytoene.

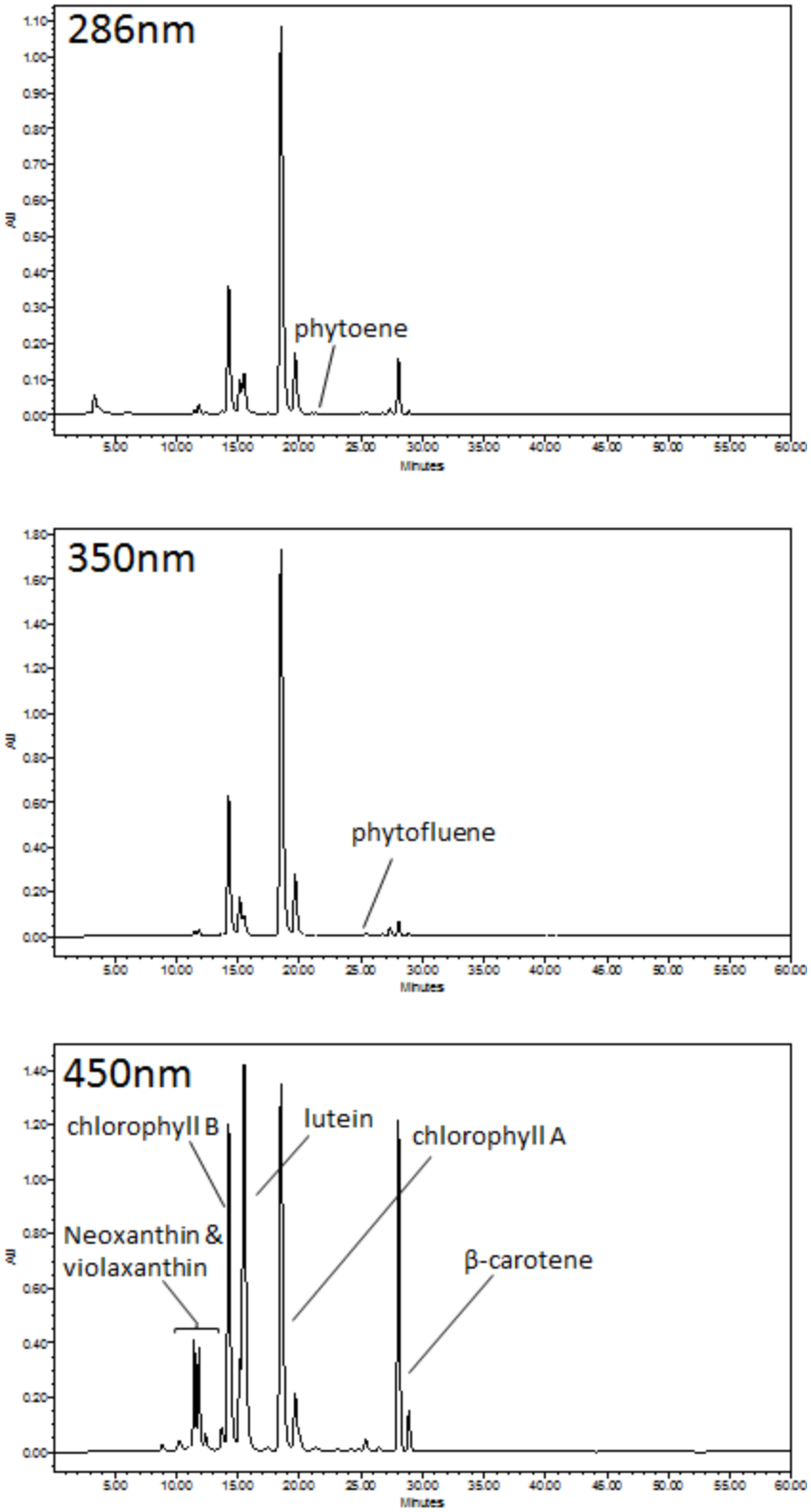

Figure A-9 HPLC traces *N. Benthamiana* leaf extract EV-control.
Leaf sample of *N.benthamiana* infiltrated with the empty vector control (backbone vector GB-cloning system). Peak detection at 286, 350 and 450nm.

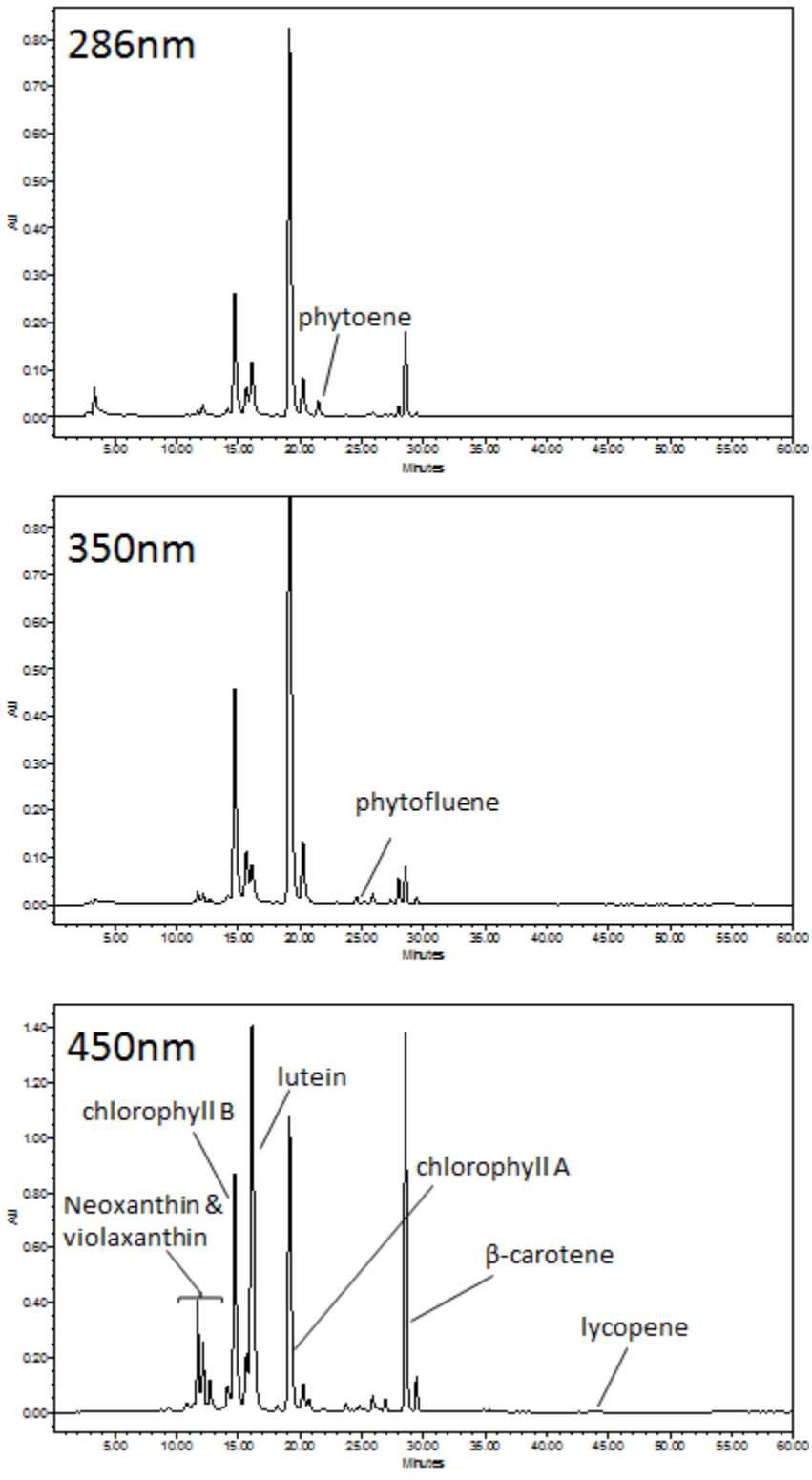

Figure A-10 HPLC trace *N. benthamiana* leaf extract crtB.
Leaf sample of *N.benthamiana* infiltrated with the crtB vector (GB-cloning system). Peak detection at 286, 350 and 450nm. Detection of phytoene and phytofluene at higher level than found in the control, appearance of lycopene is shown.

Graphs Sub-plastid Fractionation

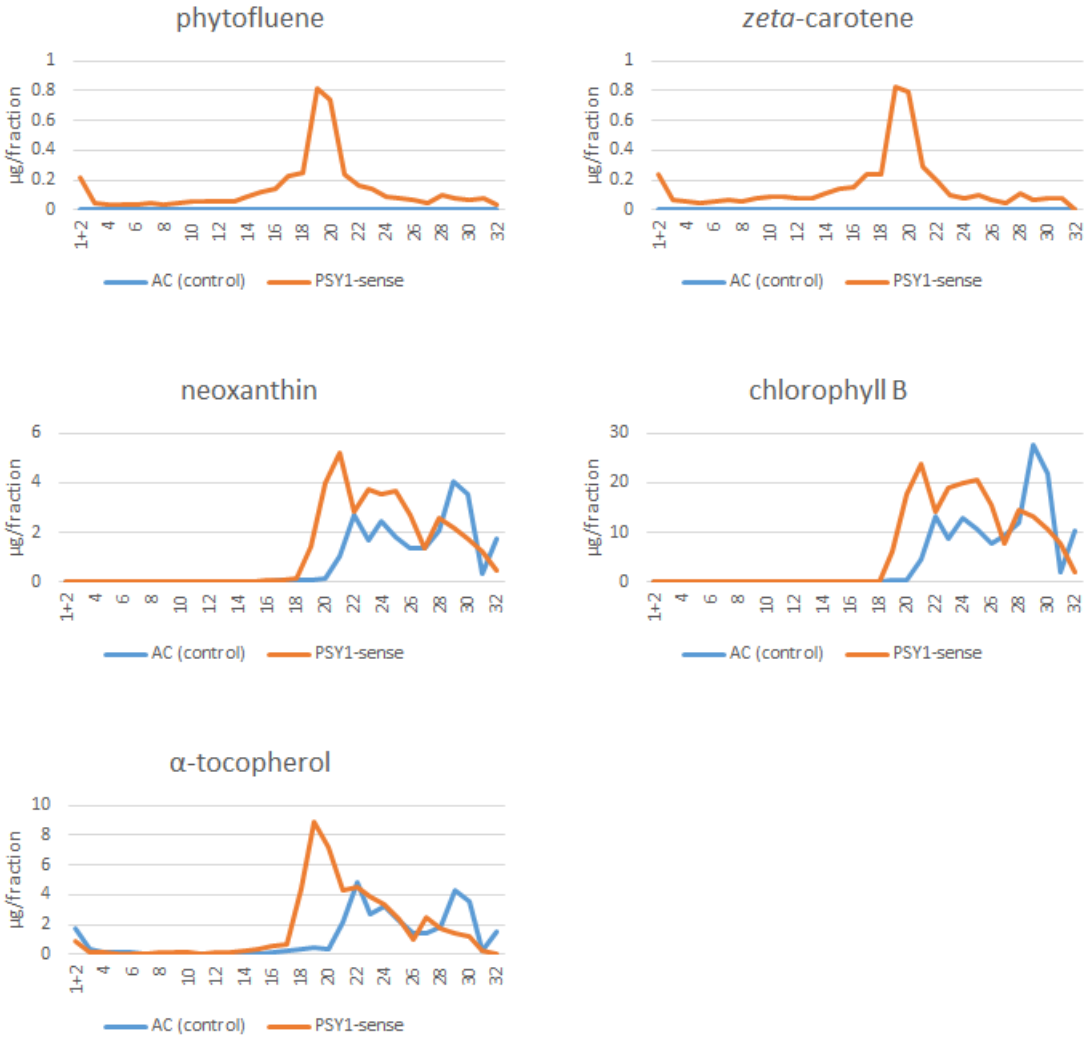

Figure A-11Graphical display of carotenoids and chlorophylls of AC and PSY1sense lines at the mature green stage.
Compounds not presented in main body of this thesis. Compounds with matching profiles are shown as an example in chapter 3.

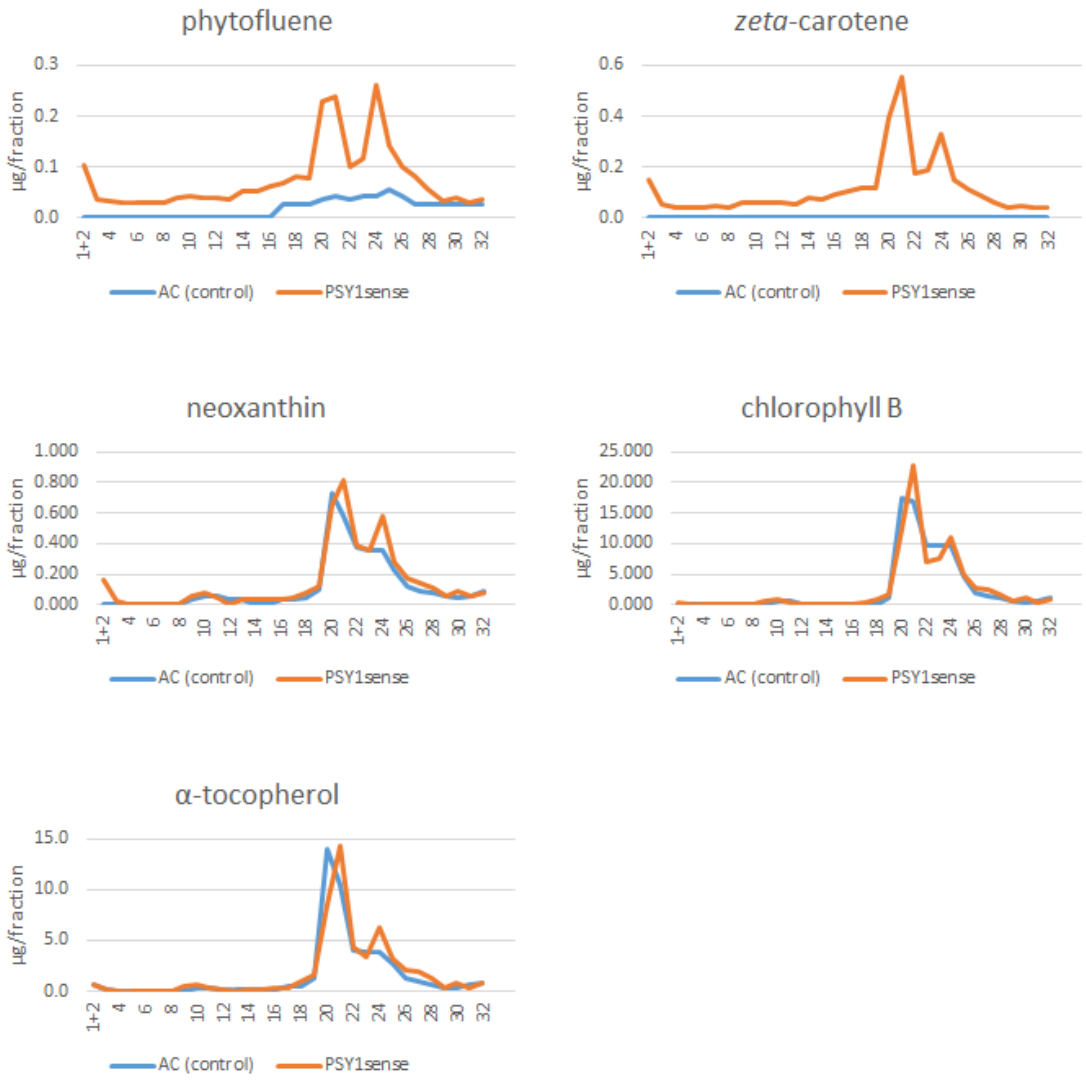

Figure A-12 Graphical display of carotenoids and chlorophylls of AC and PSY1sense lines at breaker stage.

Compounds not presented in main body of this thesis. Compounds with matching profiles are shown as an example in chapter 3.

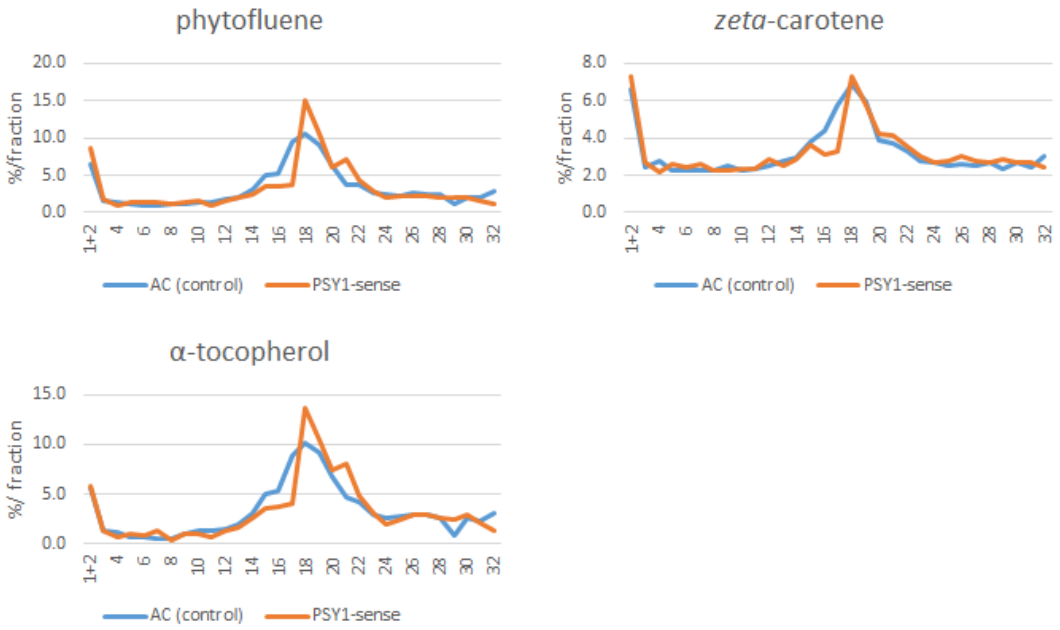

Figure A-13 Graphical display of carotenoids of AC and PSY1sense lines for ripe fruit material. Compounds not presented in main body of this thesis. Compounds with matching profiles are shown as an example in chapter 3.

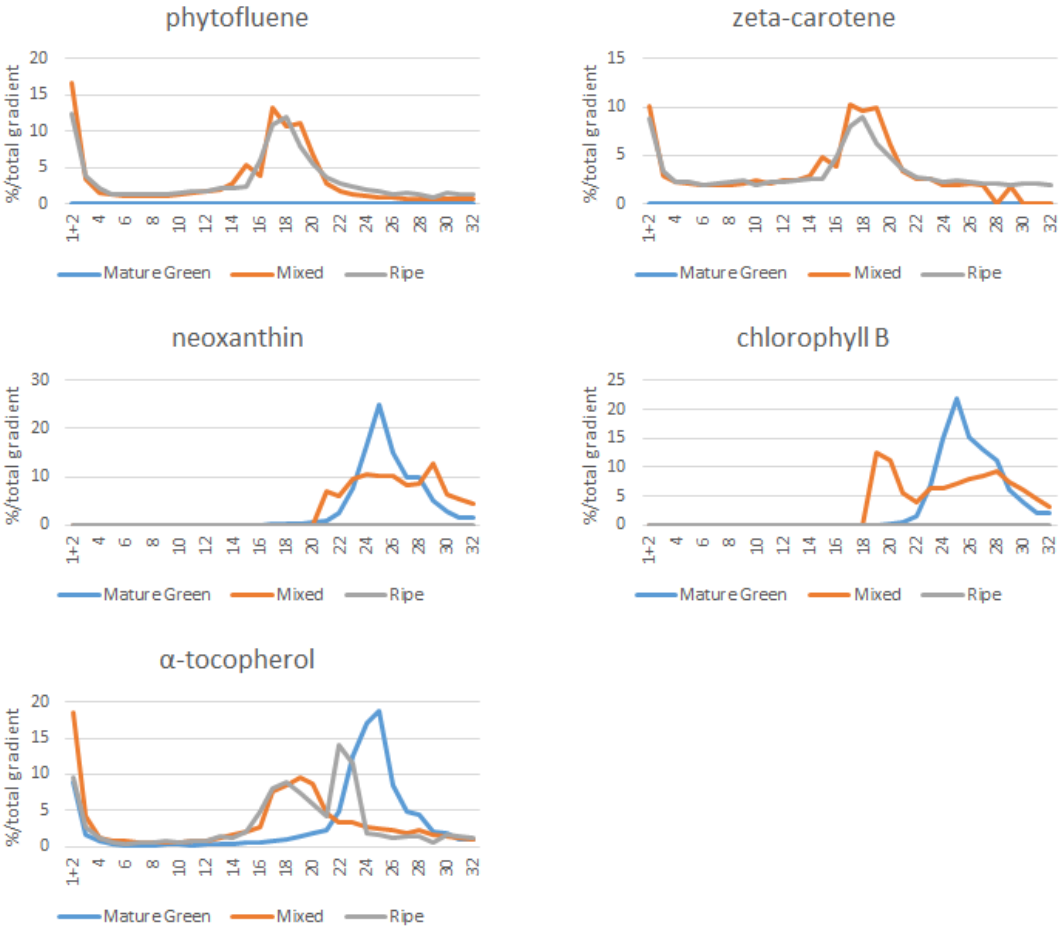

Figure A-14 Graphical display of carotenoids and chlorophylls for the AC line (ripe, mature green and mixed)
Compounds not presented in main body of this thesis. Compounds with matching profiles are shown as an example in chapter 3.

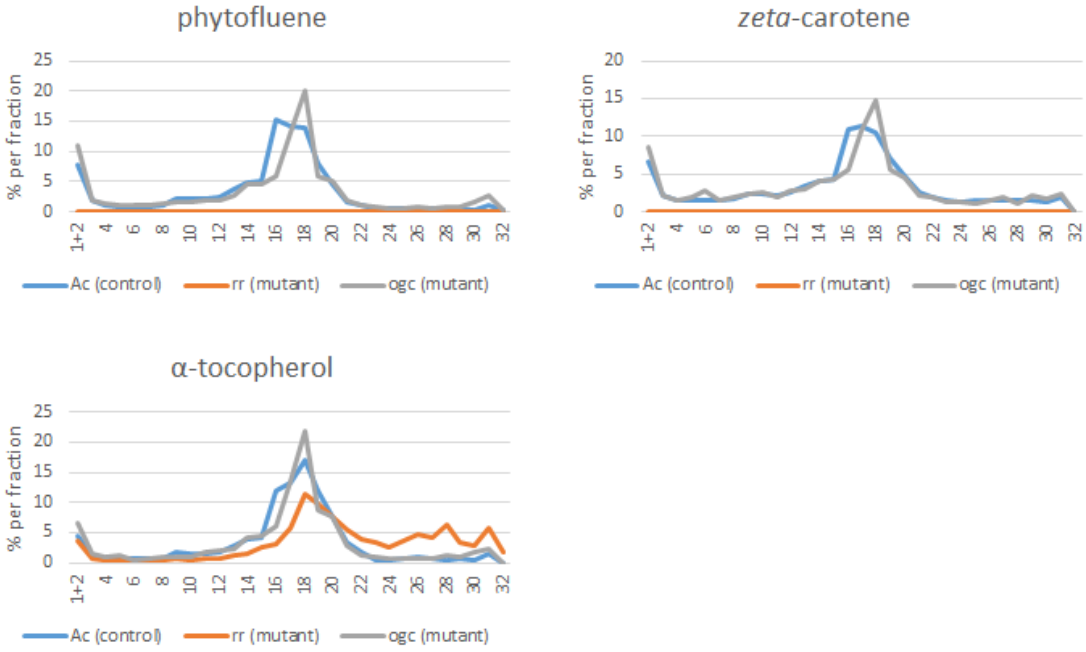

Figure A-15 Graphical display of carotenoids for the AC, *rr*, *og*^{c} lines.
Compounds not presented in main body of this thesis. Compounds with matching profiles are shown as an example in chapter 3.

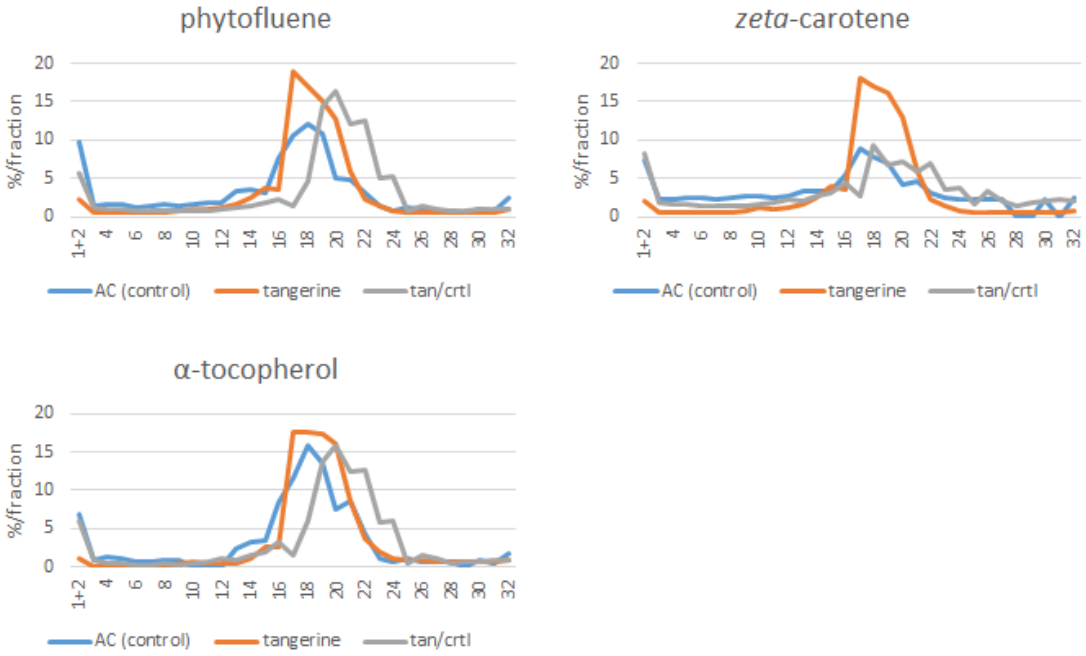

Figure A-16 Graphical display of carotenoids of the AC, *tan*, *tan*/CRTI lines
Compounds not presented in main body of this thesis. Compounds with matching profiles are shown as an example in chapter 3.

Sequencing data

Sequence analysis of GB-coding sequences

DXS (*Capsicum annuum*)

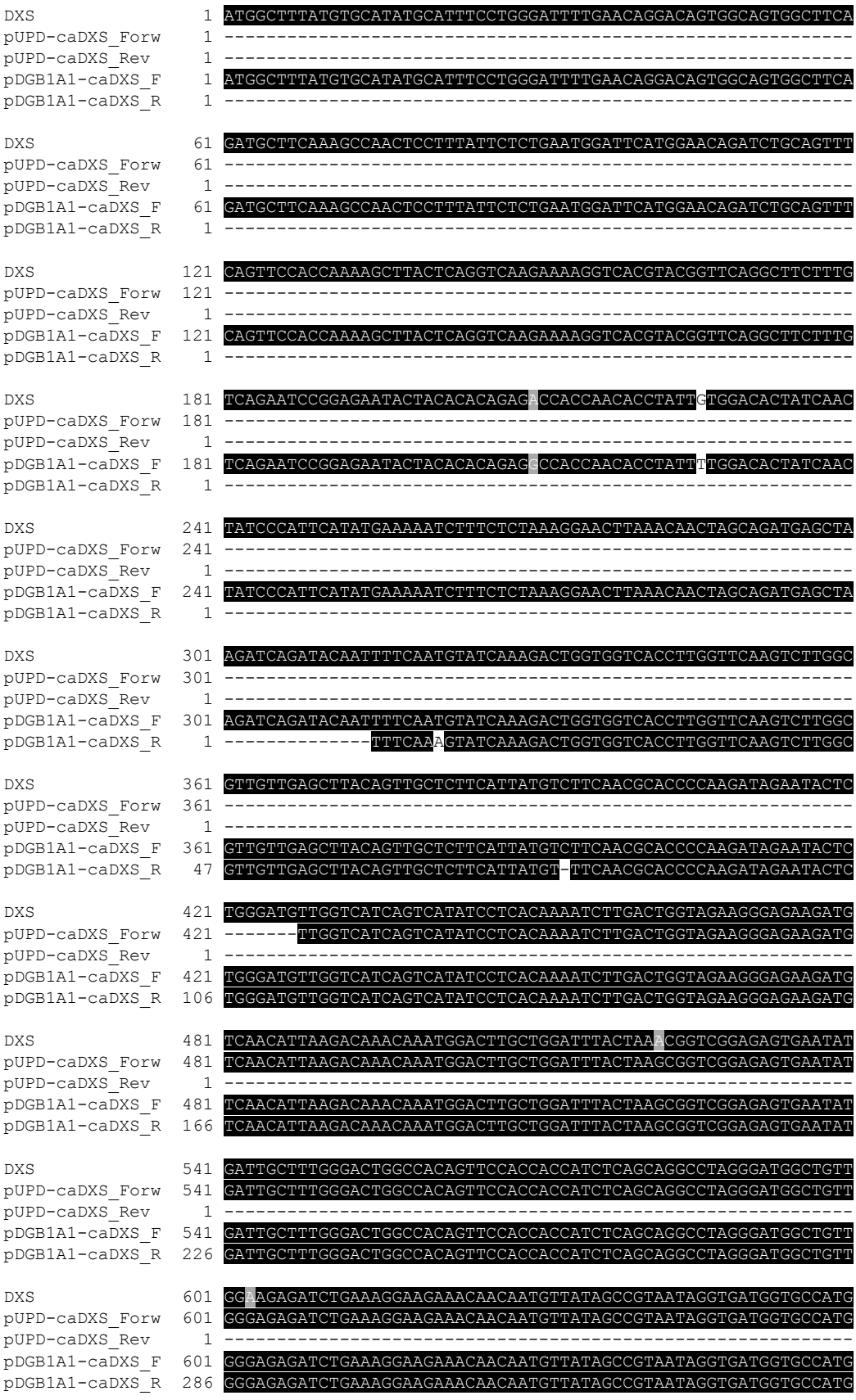

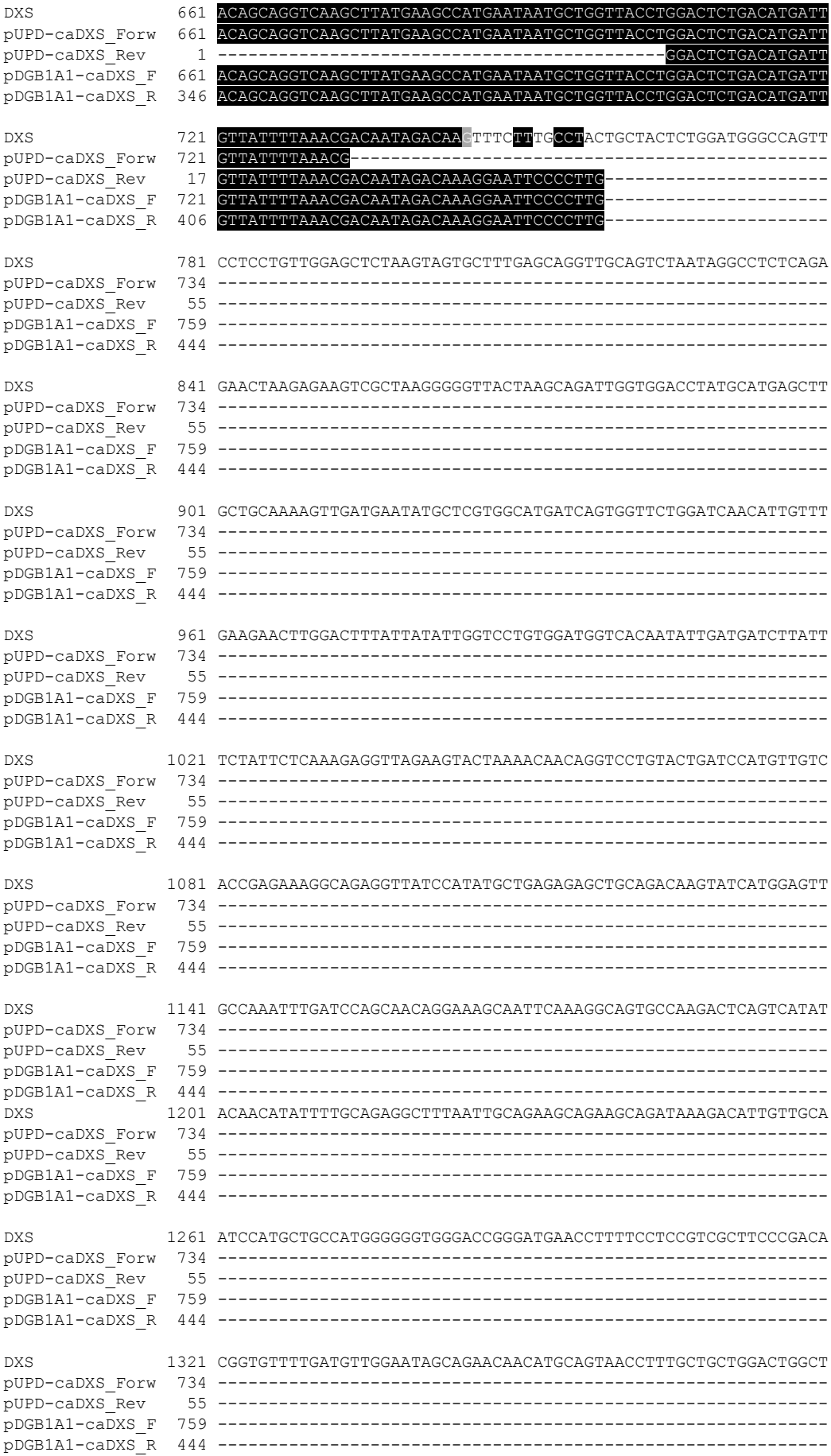
DXS 661 ACAGCAGGTCAAGCTTATGAAGCCATGAATAATGCTGGTTACCTGGACTCTGACATGATT
pUPD-caDXS_Forw 661 ACAGCAGGTCAAGCTTATGAAGCCATGAATAATGCTGGTTACCTGGACTCTGACATGATT
pUPD-caDXS_Rev 1 GGACTCTGACATGATT
pDGB1A1-caDXS_F 661 ACAGCAGGTCAAGCTTATGAAGCCATGAATAATGCTGGTTACCTGGACTCTGACATGATT
pDGB1A1-caDXS_R 346 ACAGCAGGTCAAGCTTATGAAGCCATGAATAATGCTGGTTACCTGGACTCTGACATGATT
DXS 721 GTTATTTTAAACGACAATAGACAAGTTTCTTTGCCTACTGCTACTCTGGATGGGCCAGTT
pUPD-caDXS_Forw 721 GTTATTTTAAACG
pUPD-caDXS_Rev 17 GTTATTTTAAACGACAATAGACAAAGGAATTCCCCTTG
pDGB1A1-caDXS_F 721 GTTATTTTAAACGACAATAGACAAAGGAATTCCCCTTG
pDGB1A1-caDXS_R 406 GTTATTTTAAACGACAATAGACAAAGGAATTCCCCTTG
DXS 781 CCTCCTGTTGGAGCTCTAAGTAGTGCTTTGAGCAGGTTGCAGTCTAATAGGCCTCTCAGA
pUPD-caDXS_Forw 734
pUPD-caDXS_Rev 55
pDGB1A1-caDXS_F 759
pDGB1A1-caDXS_R 444
DXS 841 GAACTAAGAGAAGTCGCTAAGGGGGTTACTAAGCAGATTGGTGGACCTATGCATGAGCTT
pUPD-caDXS_Forw 734
pUPD-caDXS_Rev 55
pDGB1A1-caDXS_F 759
pDGB1A1-caDXS_R 444
DXS 901 GCTGCAAAAGTTGATGAATATGCTCGTGGCATGATCAGTGGTTCTGGATCAACATTGTTT
pUPD-caDXS_Forw 734
pUPD-caDXS_Rev 55
pDGB1A1-caDXS_F 759
pDGB1A1-caDXS_R 444
DXS 961 GAAGAACTTGGACTTTATTATATTGGTCCTGTGGATGGTCACAATATTGATGATCTTATT
pUPD-caDXS_Forw 734
pUPD-caDXS_Rev 55
pDGB1A1-caDXS_F 759
pDGB1A1-caDXS_R 444
DXS 1021 TCTATTCTCAAAGAGGTTAGAAGTACTAAAACAACAGGTCCTGTACTGATCCATGTTGTC
pUPD-caDXS_Forw 734
pUPD-caDXS_Rev 55
pDGB1A1-caDXS_F 759
pDGB1A1-caDXS_R 444
DXS 1081 ACCGAGAAAGGCAGAGGTTATCCATATGCTGAGAGAGCTGCAGACAAGTATCATGGAGTT
pUPD-caDXS_Forw 734
pUPD-caDXS_Rev 55
pDGB1A1-caDXS_F 759
pDGB1A1-caDXS_R 444
DXS 1141 GCCAAATTTGATCCAGCAACAGGAAAGCAATTCAAAGGCAGTGCCAAGACTCAGTCATAT
pUPD-caDXS_Forw 734
pUPD-caDXS_Rev 55
pDGB1A1-caDXS_F 759
pDGB1A1-caDXS_R 444
DXS 1201 ACAACATATTTTGCAGAGGCTTTAATTGCAGAAGCAGAAGCAGATAAAGACATTGTTGCA
pUPD-caDXS_Forw 734
pUPD-caDXS_Rev 55
pDGB1A1-caDXS_F 759
pDGB1A1-caDXS_R 444
DXS 1261 ATCCATGCTGCCATGGGGGGTGGGACCGGGATGAACCTTTTCCTCCGTCGCTTCCCGACA
pUPD-caDXS_Forw 734
pUPD-caDXS_Rev 55
pDGB1A1-caDXS_F 759
pDGB1A1-caDXS_R 444
DXS 1321 CGGTGTTTTGATGTTGGAATAGCAGAACAACATGCAGTAACCTTTGCTGCTGGACTGGCT
pUPD-caDXS_Forw 734
pUPD-caDXS_Rev 55
pDGB1A1-caDXS_F 759
pDGB1A1-caDXS_R 444

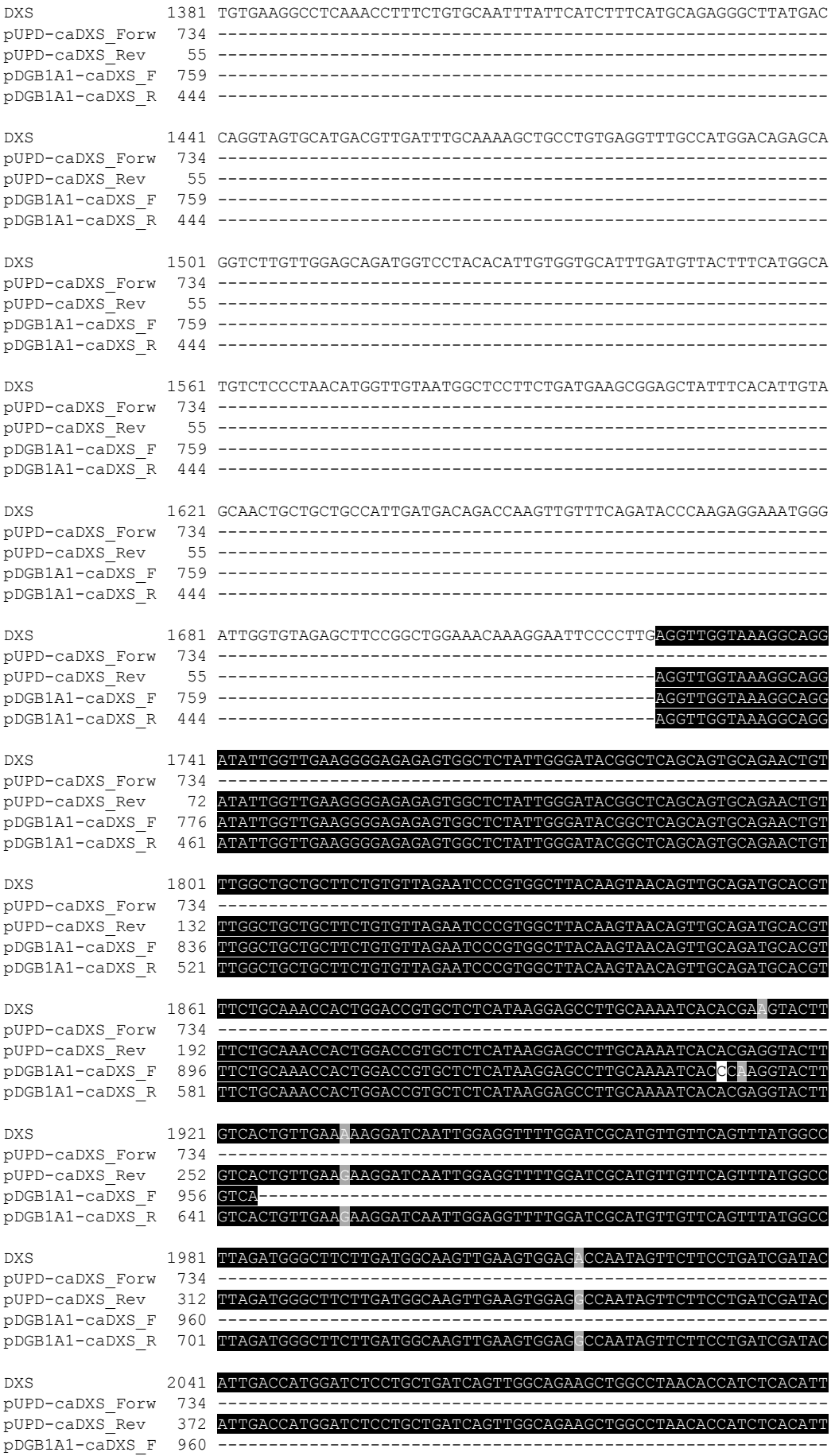
DXS 1381 TGTGAAGGCCTCAAACCTTTCTGTGCAATTTATTCATCTTTCATGCAGAGGGCTTATGAC
pUPD-caDXS_Forw 734 ----------
pUPD-caDXS_Rev 55 ----------
pDGB1A1-caDXS_F 759 ----------
pDGB1A1-caDXS_R 444 ----------
DXS 1441 CAGGTAGTGCATGACGTTGATTTGCAAAAGCTGCCTGTGAGGTTTGCCATGGACAGAGCA
pUPD-caDXS_Forw 734 ----------
pUPD-caDXS_Rev 55 ----------
pDGB1A1-caDXS_F 759 ----------
pDGB1A1-caDXS_R 444 ----------
DXS 1501 GGTCTTGTTGGAGCAGATGGTCCTACACATTGTGGTGCATTTGATGTTACTTTCATGGCA
pUPD-caDXS_Forw 734 ----------
pUPD-caDXS_Rev 55 ----------
pDGB1A1-caDXS_F 759 ----------
pDGB1A1-caDXS_R 444 ----------
DXS 1561 TGTCTCCCTAACATGGTTGTAATGGCTCCTTCTGATGAAGCGGAGCTATTTCACATTGTA
pUPD-caDXS_Forw 734 ----------
pUPD-caDXS_Rev 55 ----------
pDGB1A1-caDXS_F 759 ----------
pDGB1A1-caDXS_R 444 ----------
DXS 1621 GCAACTGCTGCTGCCATTGATGACAGACCAAGTTGTTTCAGATACCCAAGAGGAAATGGG
pUPD-caDXS_Forw 734 ----------
pUPD-caDXS_Rev 55 ----------
pDGB1A1-caDXS_F 759 ----------
pDGB1A1-caDXS_R 444 ----------
DXS 1681 ATTGGTGTAGAGCTTCCGGCTGGAAACAAAGGAATTCCCCTTGAGGTTGGTAAAGGCAGG
pUPD-caDXS_Forw 734 ----------
pUPD-caDXS_Rev 55 ----------AGGTTGGTAAAGGCAGG
pDGB1A1-caDXS_F 759 ----------AGGTTGGTAAAGGCAGG
pDGB1A1-caDXS_R 444 ----------AGGTTGGTAAAGGCAGG
DXS 1741 ATATTGGTTGAAGGGGAGAGAGTGGCTCTATTGGGATACGGCTCAGCAGTGCAGAACTGT
pUPD-caDXS_Forw 734 ----------
pUPD-caDXS_Rev 72 ATATTGGTTGAAGGGGAGAGAGTGGCTCTATTGGGATACGGCTCAGCAGTGCAGAACTGT
pDGB1A1-caDXS_F 776 ATATTGGTTGAAGGGGAGAGAGTGGCTCTATTGGGATACGGCTCAGCAGTGCAGAACTGT
pDGB1A1-caDXS_R 461 ATATTGGTTGAAGGGGAGAGAGTGGCTCTATTGGGATACGGCTCAGCAGTGCAGAACTGT
DXS 1801 TTGGCTGCTGCTTCTGTGTTAGAATCCCGTGGCTTACAAGTAACAGTTGCAGATGCACGT
pUPD-caDXS_Forw 734 ----------
pUPD-caDXS_Rev 132 TTGGCTGCTGCTTCTGTGTTAGAATCCCGTGGCTTACAAGTAACAGTTGCAGATGCACGT
pDGB1A1-caDXS_F 836 TTGGCTGCTGCTTCTGTGTTAGAATCCCGTGGCTTACAAGTAACAGTTGCAGATGCACGT
pDGB1A1-caDXS_R 521 TTGGCTGCTGCTTCTGTGTTAGAATCCCGTGGCTTACAAGTAACAGTTGCAGATGCACGT
DXS 1861 TTCTGCAAACCACTGGACCGTGCTCTCATAAGGAGCCTTGCAAAATCACACGAAGTACTT
pUPD-caDXS_Forw 734 ----------
pUPD-caDXS_Rev 192 TTCTGCAAACCACTGGACCGTGCTCTCATAAGGAGCCTTGCAAAATCACACGAGGTACTT
pDGB1A1-caDXS_F 896 TTCTGCAAACCACTGGACCGTGCTCTCATAAGGAGCCTTGCAAAATCACCCAAGGTACTT
pDGB1A1-caDXS_R 581 TTCTGCAAACCACTGGACCGTGCTCTCATAAGGAGCCTTGCAAAATCACACGAGGTACTT
DXS 1921 GTCACTGTTGAAAAAGGATCAATTGGAGGTTTTGGATCGCATGTTGTTCAGTTTATGGCC
pUPD-caDXS_Forw 734 ----------
pUPD-caDXS_Rev 252 GTCACTGTTGAAGAAGGATCAATTGGAGGTTTTGGATCGCATGTTGTTCAGTTTATGGCC
pDGB1A1-caDXS_F 956 GTCA----------
pDGB1A1-caDXS_R 641 GTCACTGTTGAAGAAGGATCAATTGGAGGTTTTGGATCGCATGTTGTTCAGTTTATGGCC
DXS 1981 TTAGATGGGCTTCTTGATGGCAAGTTGAAGTGGAGACCAATAGTTCTTCCTGATCGATAC
pUPD-caDXS_Forw 734 ----------
pUPD-caDXS_Rev 312 TTAGATGGGCTTCTTGATGGCAAGTTGAAGTGGAGGCCAATAGTTCTTCCTGATCGATAC
pDGB1A1-caDXS_F 960 ----------
pDGB1A1-caDXS_R 701 TTAGATGGGCTTCTTGATGGCAAGTTGAAGTGGAGGCCAATAGTTCTTCCTGATCGATAC
DXS 2041 ATTGACCATGGATCTCCTGCTGATCAGTTGGCAGAAGCTGGCCTAACACCATCTCACATT
pUPD-caDXS_Forw 734 ----------
pUPD-caDXS_Rev 372 ATTGACCATGGATCTCCTGCTGATCAGTTGGCAGAAGCTGGCCTAACACCATCTCACATT
pDGB1A1-caDXS_F 960 ----------

```
pDGB1A1-caDXS_R  761 ATTGACCATGGATCTCCTGCTGATCAGTTGGCAGAAGCTGGCCTAACACCATCTCACATT

DXS             2101 GCAGCAACAGTATTTAACATACTTGGACAAACCAGAGAGGCTCTAGAGGTCATGACATAA
pUPD-caDXS_Forw  734 ------------------------------------------------------------A
pUPD-caDXS_Rev   432 GCAGCAACAGTATTTAACATACTTGGACAAACCAGAGAGG--------------------
pDGB1A1-caDXS_F  960 ------------------------------------------------------------C
pDGB1A1-caDXS_R  821 GCAGCAACAGTATTTAACATACTTGGACAAACCAGAGAGGCTCTAGAGGTCATGACATAA
```

DXR (*Escherichia coli*)

```
DXR                1 ATGAAGCAACTCACCATTCTGGGCTCGACCGGCTCGATTGGTTGCAGCACGCTGGACGTG
pUPD-DXR Forw      1 ------------------------------------------------------------
pUPD-DXR_rev       1 ------------------------------------------------------------
pDGB1A2-DXR_For    1 ATGAAGCAACTCACCATTCTGGGCTCGACCGGCTCGATTGGTTGCAGCACGCTGGACGTG
pDGB1A2-DXR_rev    1 ------------------------------------------------------------

DXR               61 GTGCGCCATAATCCCGAACACTTCCGCGTAGTTGCGCTGGTGGCAGGCAAAAATGTCACT
pUPD-DXR Forw     61 ----------------------------AGTTGCGCTGGTGGCAGGCAAAAATGTCACT
pUPD-DXR_rev       1 ------------------------------------------------------------
pDGB1A2-DXR_For   61 GTGCGCCATAATCCCGAACACTTCCGCGTAGTTGCGCTGGTGGCAGGCAAAAATGTCACT
pDGB1A2-DXR_rev    1 ------------------------------------------------------------

DXR              121 CGCATGGTAGAACAGTGCCTGGAATTCTCTCCCCGCTATGCCGTAATGGACGATGAAGCG
pUPD-DXR Forw    121 CGCATGGTAGAACAGTGCCTGGAATTCTCTCCCCGCTATGCCGTAATGGACGATGAAGCG
pUPD-DXR_rev       1 ------------------------------------------------------------
pDGB1A2-DXR_For  121 CGCATGGTAGAACAGTGCCTGGAATTCTCTCCCCGCTATGCCGTAATGGACGATGAAGCG
pDGB1A2-DXR_rev    1 ------------------------------------------------------------

DXR              181 AGTGCGAAACTTCTTAAAACGATGCTACAGCAACAGGGTAGCCGCACCGAAGTCTTAAGT
pUPD-DXR_Forw    181 AGTGCGAAACTTCTTAAAACGATGCTACAGCAACAGGGTAGCCGCACCGAAGTCTTAAGT
pUPD-DXR_rev       1 ------------------------------------------------------------
pDGB1A2-DXR_For  181 AGTGCGAAACTTCTTAAAACGATGCTACAGCAACAGGGTAGCCGCACCGAAGTCTTAAGT
pDGB1A2-DXR_rev    1 ------------------------------------------------------------

DXR              241 GGGCAACAAGCCGCTTGCGATATGGCAGCGCTTGAGGATGTTGATCAGGTGATGGCAGCC
pUPD-DXR_Forw    241 GGGCAACAAGCCGCTTGCGATATGGCAGCGCTTGAGGATGTTGATCAGGTGATGGCAGCC
pUPD-DXR_rev       1 ------------------------------------------------------------
pDGB1A2-DXR_For  241 GGGCAACAAGCCGCTTGCGATATGGCAGCGCTTGAGGATGTTGATCAGGTGATGGCAGCC
pDGB1A2-DXR_rev    1 ------------------------------------------------------------

DXR              301 ATTGTTGGCGCTGCTGGGCTGTTACCTACGCTTGCTGCGATCCGCGCGGGTAAAACCATT
pUPD-DXR_Forw    301 ATTGTTGGCGCTGCTGGGCTGTTACCTACGCTTGCTGCGATCCGCGCGGGTAAAACCATT
pUPD-DXR_rev       1 ------GGCGCTGCTGGGCTGTTACCTACGCTTGCTGCGATCCGCGCGGGTAAAACCATT
pDGB1A2-DXR For  301 ATTGTTGGCGCTGCTGGGCTGTTACCTACGCTTGCTGCGATCCGCGCGGGTAAAACCATT
pDGB1A2-DXR_rev    1 -----TGGCGCTGCTGGGCTGTTACCTACGCTTGCTGCGATCCGCGCGGGTAAAACCATT

DXR              361 TTGCTGGCCAATAAAGAATCACTGGTTACCTGCGGACGTCTGTTTATGGACGCCGTAAAG
pUPD-DXR_Forw    361 TTGCTGGCCAATAAAGAATCACTGGTTACCTGCGGACGTCTGTTTATGGACGCCGTAAAG
pUPD-DXR_rev      55 TTGCTGGCCAATAAAGAATCACTGGTTACCTGCGGACGTCTGTTTATGGACGCCGTAAAG
pDGB1A2-DXR For  361 TTGCTGGCCAATAAAGAATCACTGGTTACCTGCGGACGTCTGTTTATGGACGCCGTAAAG
pDGB1A2-DXR_rev   56 TTGCTGGCCAATAAAGAATCACTGGTTACCTGCGGACGTCTGTTTATGGACGCCGTAAAG

DXR              421 CAGAGCAAAGCGCAATTGTTACCGGTCGATAGCGAACATAACGCCATTTTTCAGAGTTTA
pUPD-DXR_Forw    421 CAGAGCAAAGCGCAATTGTTACCGGTCGATAGCGAACATAACGCCATTTTTCAGAGTTTA
pUPD-DXR_rev     115 CAGAGCAAAGCGCAATTGTTACCGGTCGATAGCGAACATAACGCCATTTTTCAGAGTTTA
pDGB1A2-DXR For  421 CAGAGCAAAGCGCAATTGTTACCGGTCGATAGCGAACATAACGCCATTTTTCAGAGTTTA
pDGB1A2-DXR_rev  116 CAGAGCAAAGCGCAATTGTTACCGGTCGATAGCGAACATAACGCCATTTTTCAGAGTTTA

DXR              481 CCGCAACCTATCCAGCATAATCTGGGATACGCTGACCTTGAGCAAAATGGCGTGGTGTCC
pUPD-DXR_Forw    481 CCGCAACCTATCCAGCATAATCTGGGATACGCTGACCTTGAGCAAAATGGCGTGGTGTCC
pUPD-DXR_rev     175 CCGCAACCTATCCAGCATAATCTGGGATACGCTGACCTTGAGCAAAATGGCGTGGTGTCC
pDGB1A2-DXR For  481 CCGCAACCTATCCAGCATAATCTGGGATACGCTGACCTTGAGCAAAATGGCGTGGTGTCC
pDGB1A2-DXR_rev  176 CCGCAACCTATCCAGCATAATCTGGGATACGCTGACCTTGAGCAAAATGGCGTGGTGTCC

DXR              541 ATTTTACTTACCGGGTCTGGTGGCCCTTTCCGTGAGACGCCATTGCGCGATTTGGCAACA
pUPD-DXR_Forw    541 ATTTTACTTACCGGGTCTGGTGGCCCTTTCCGTGAGACACCATTGCGCGATTTGGCAACA
pUPD-DXR rev     235 ATTTTACTTACCGGGTCTGGTGGCCCTTTCCGTGAGACACCATTGCGCGATTTGGCAACA
pDGB1A2-DXR For  541 ATTTTACTTACCGGGTCTGGTGGCCCTTTCCGTGAGACACCATTGCGCGATTTGGCAACA
pDGB1A2-DXR_rev  236 ATTTTACTTACCGGGTCTGGTGGCCCTTTCCGTGAGACACCATTGCGCGATTTGGCAACA

DXR              601 ATGACGCCGGATCAAGCCTGCCGTCATCCGAACTGGTCGATGGGGCGTAAAATTTCTGTC
pUPD-DXR Forw    601 ATGACGCCGGATCAAGCCTGCCGTCATCCGAACTGGTCGATGGGGCGTAAAATTTCTGTC
pUPD-DXR rev     295 ATGACGCCGGATCAAGCCTGCCGTCATCCGAACTGGTCGATGGGGCGTAAAATTTCTGTC
pDGB1A2-DXR_For  601 ATGACGCCGGATCAAGCCTGCCGTCATCCGAACTGGTCGATGGGGCGTAAAATTTCTGTC
```

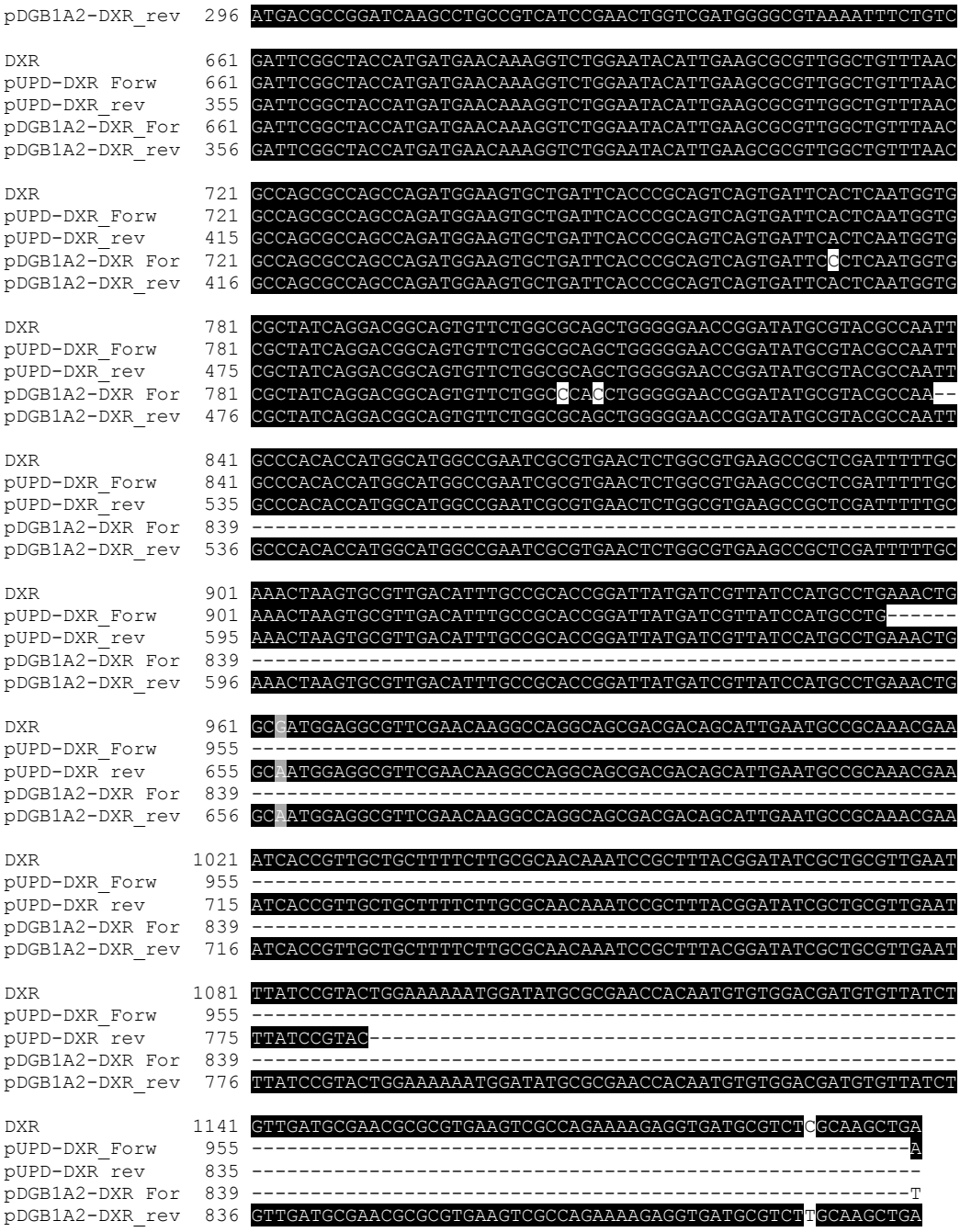

MCT (*Escherichia coli*)

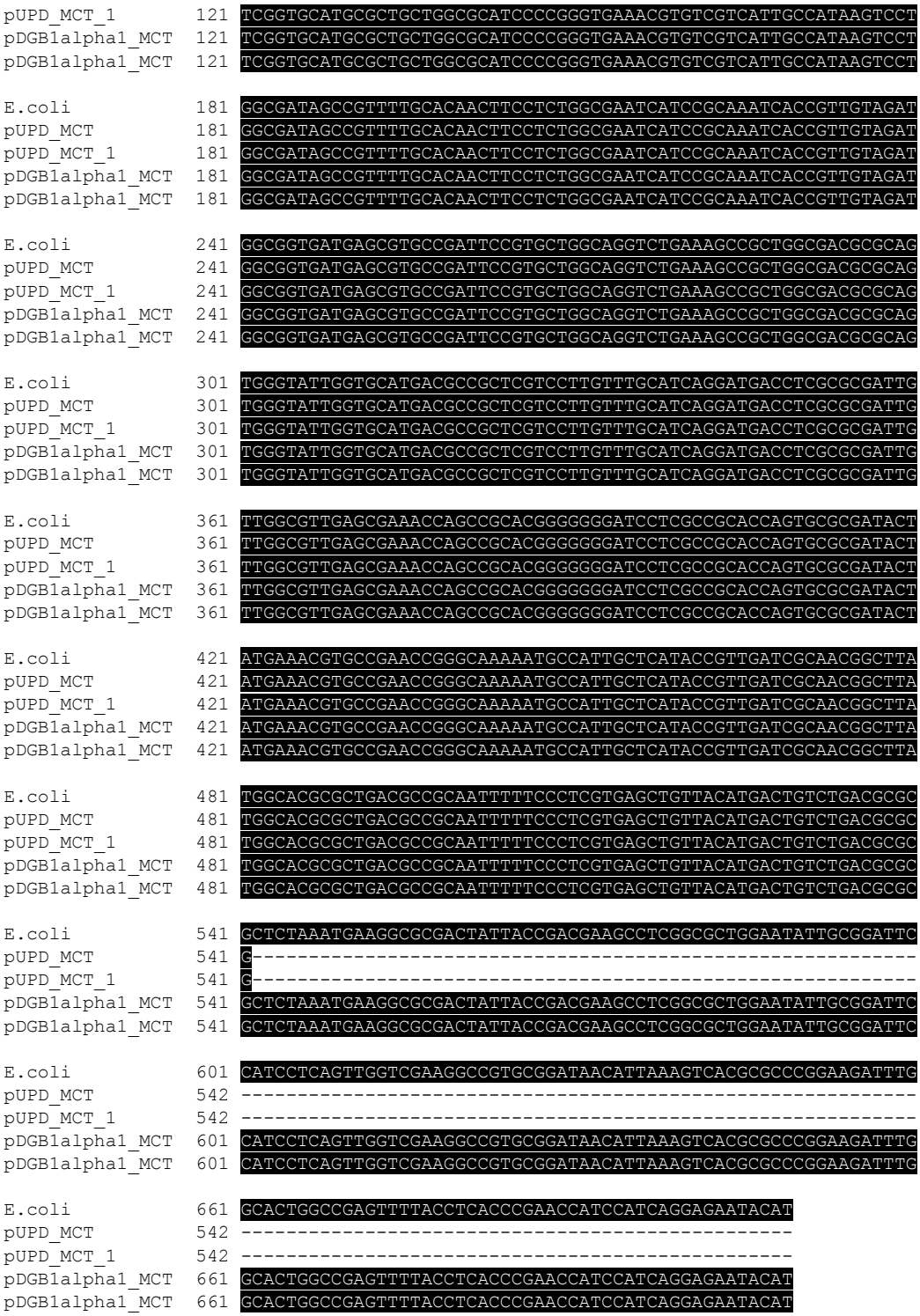

CMK (*Escherichia coli*)

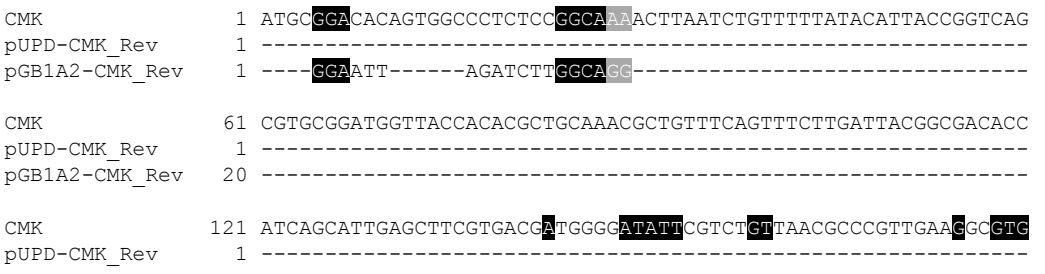

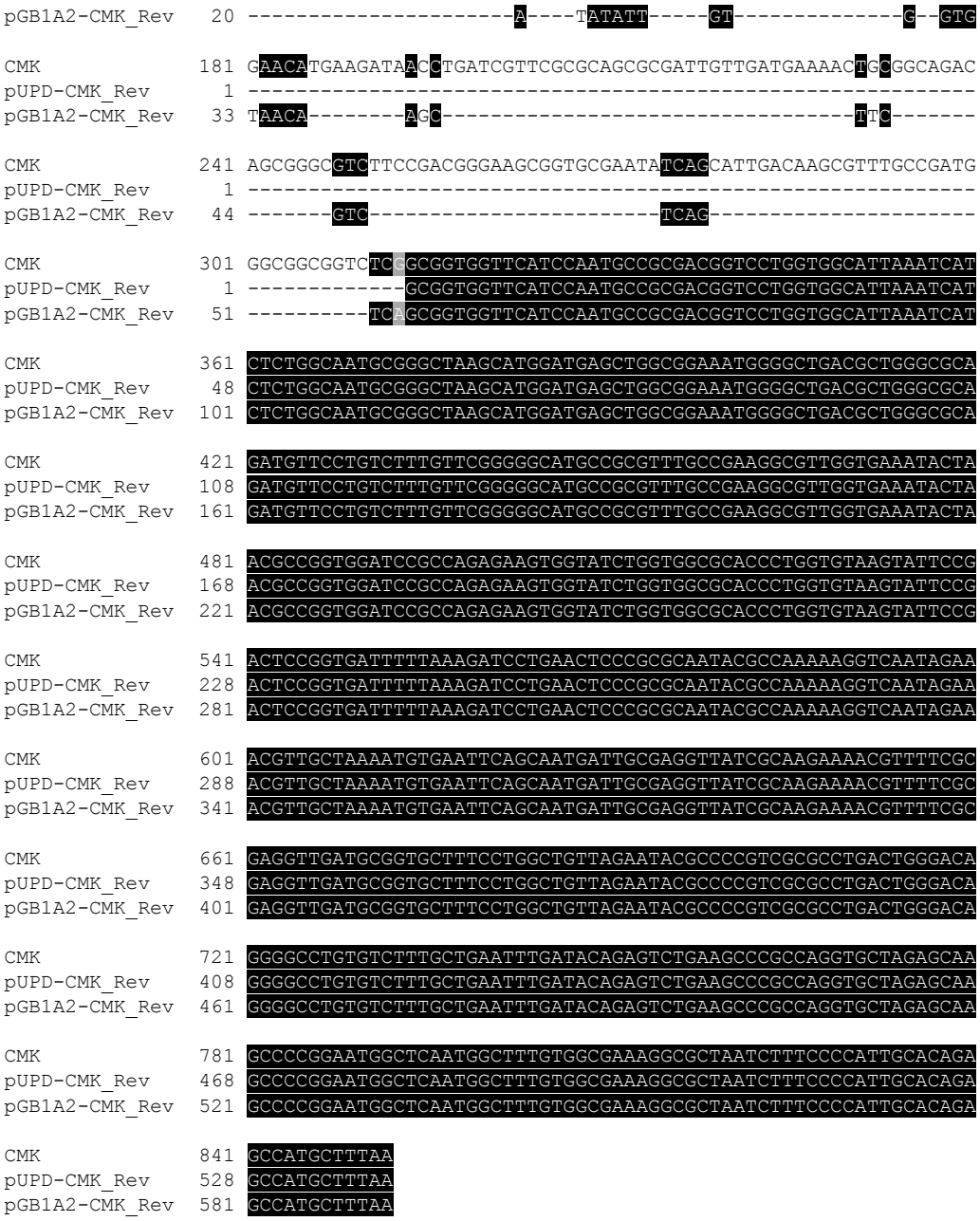

MDS (*Escherichia coli*)

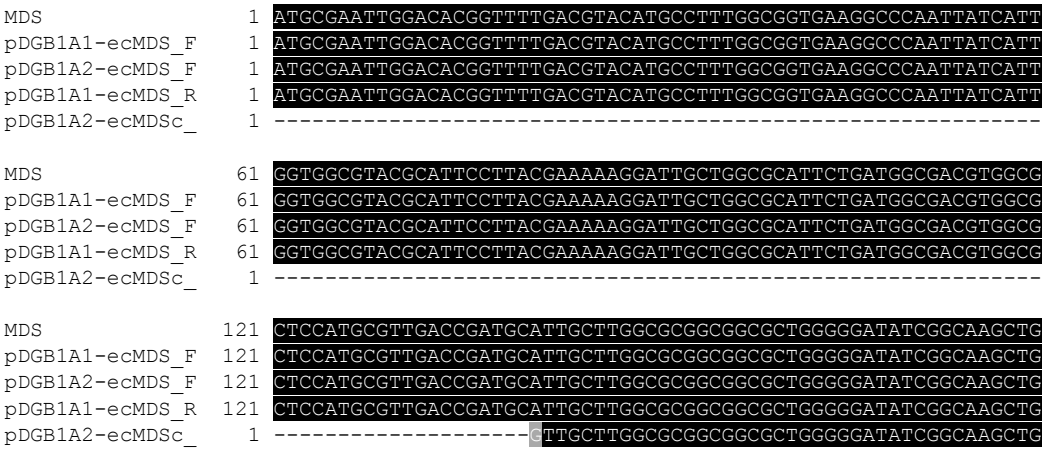

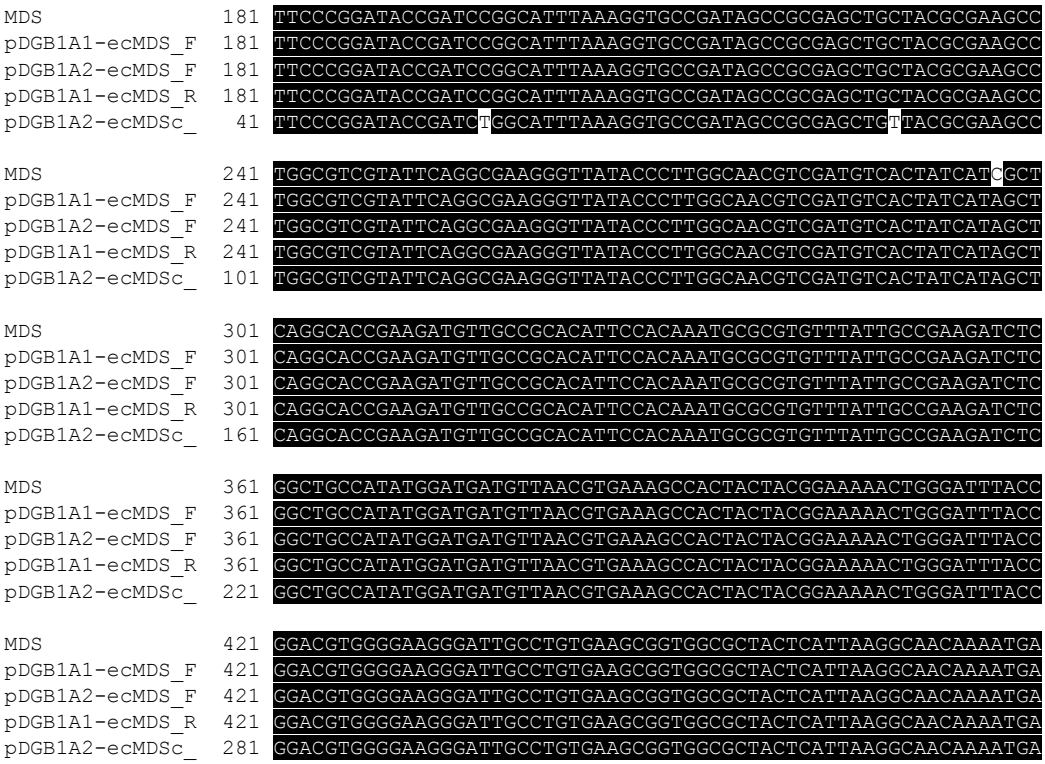

HDS (*Escherichia coli*)

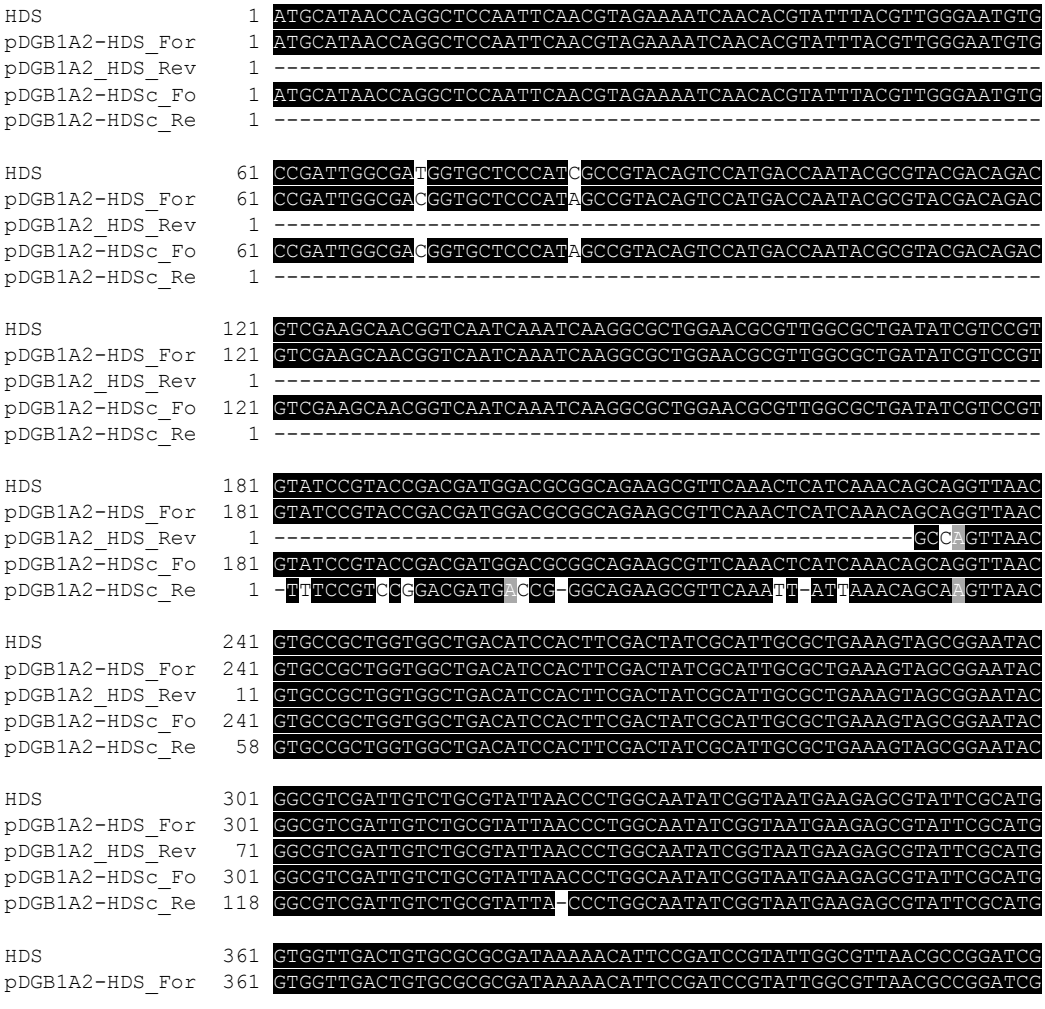

```
pDGB1A2_HDS_Rev  131 GTGGTTGACTGTGCGCGCGATAAAAACATTCCGATCCGTATTGGCGTTAACGCCGGATCG
pDGB1A2-HDSc_Fo  361 GTGGTTGACTGTGCGCGCGATAAAAACATTCCGATCCGTATTGGCGTTAACGCCGGATCG
pDGB1A2-HDSc_Re  177 GTGGTTGACTGTGCGCGCGATAAAAACATTCCGATCCGTATTGGCGTTAACGCCGGATCG

HDS              421 CTGGAAAAAGATCTGCAAGAAAAGTATGGCGAACCGACGCCGCAGGCGTTGCTGGAATCT
pDGB1A2-HDS_For  421 CTGGAAAAAGATCTGCAAGAAAAGTATGGCGAACCGACGCCGCAGGCGTTGCTGGAATCT
pDGB1A2_HDS_Rev  191 CTGGAAAAAGATCTGCAAGAAAAGTATGGCGAACCGACGCCGCAGGCGTTGCTGGAATCT
pDGB1A2-HDSc_Fo  421 CTGGAAAAAGATCTGCAAGAAAAGTATGGCGAACCGACGCCGCAGGCGTTGCTGGAATCT
pDGB1A2-HDSc_Re  237 CTGGAAAAAGATCTGCAAGAAAAGTATGGCGAACCGACGCCGCAGGCGTTGCTGGAATCT

HDS              481 GCCATGCGTCATGTTGATCATCTCGATCGCCTGAACTTCGATCAGTTCAAAGTCAGCGTG
pDGB1A2-HDS_For  481 GCCATGCGTCATGTTGATCATCTCGATCGCCTGAACTTCGATCAGTTCAAAGTCAGCGTG
pDGB1A2_HDS_Rev  251 GCCATGCGTCATGTTGATCATCTCGATCGCCTGAACTTCGATCAGTTCAAAGTCAGCGTG
pDGB1A2-HDSc_Fo  481 GCCATGCGTCATGTTGATCATCTCGATCGCCTGAACTTCGATCAGTTCAAAGTCAGCGTG
pDGB1A2-HDSc_Re  297 GCCATGCGTCATGTTGATCATCTCGATCGCCTGAACTTCGATCAGTTCAAAGTCAGCGTG

HDS              541 AAAGCGTCTGACGTCTTCCTCGCTGTTGAGTCTTATCGTTTGCTGGCAAAACAGATCGAT
pDGB1A2-HDS_For  541 AAAGCGTCTGACGTCTTCCTCGCTGTTGAGTCTTATCGTTTGCTGGCAAAACAGATCGAT
pDGB1A2_HDS_Rev  311 AAAGCGTCTGACGTCTTCCTCGCTGTTGAGTCTTATCGTTTGCTGGCAAAACAGATCGAT
pDGB1A2-HDSc_Fo  541 AAAGCGTCTGACGTCTTCCTCGCTGTTGAGTCTTATCGTTTGCTGGCAAAACAGATCGAT
pDGB1A2-HDSc_Re  357 AAAGCGTCTGACGTCTTCCTCGCTGTTGAGTCTTATCGTTTGCTGGCAAAACAGATCGAT

HDS              601 CAGCCGTTGCATCTGGGGATCACCGAAGCCGGTGGTGCGCGCAGCGGGGCAGTAAAATCC
pDGB1A2-HDS_For  601 CAGCCGTTGCATCTGGGGATCACCGAAGCCGGTGGTGCGCGCAGCGGGGCAGTAAAATCC
pDGB1A2_HDS_Rev  371 CAGCCGTTGCATCTGGGGATCACCGAAGCCGGTGGTGCGCGCAGCGGGGCAGTAAAATCC
pDGB1A2-HDSc_Fo  601 CAGCCGTTGCATCTGGGGATCACCGAAGCCGGTGGTGCGCGCAGCGGGGCAGTAAAATCC
pDGB1A2-HDSc_Re  417 CAGCCGTTGCATCTGGGGATCACCGAAGCCGGTGGTGCGCGCAGCGGGGCAGTAAAATCC

HDS              661 GCCATTGGTTTAGGTCTGCTGCTGTCTGAAGGCATCGGCGACACGCTGCGCGTATCGCTG
pDGB1A2-HDS_For  661 GCCATTGGTTTAGGTCTGCTGCTGTCTGAAGGCATCGGCGACACGCTGCGCGTATCGCTG
pDGB1A2_HDS_Rev  431 GCCATTGGTTTAGGTCTGCTGCTGTCTGAAGGCATCGGCGACACGCTGCGCGTATCGCTG
pDGB1A2-HDSc_Fo  661 GCCATTGGTTTAGGTCTGCTGCTGTCTGAAGGCATCGGCGACACGCTGCGCGTATCGCTG
pDGB1A2-HDSc_Re  477 GCCATTGGTTTAGGTCTGCTGCTGTCTGAAGGCATCGGCGACACGCTGCGCGTATCGCTG

HDS              721 GCGGCCGATCCGGTCGAAGAGATCAAAGTCGGTTTCGATATTTTGAAATCGCTGCGTATC
pDGB1A2-HDS_For  721 GCGGCCGATCCGGTCGAAGAGATCAAAGTCGGTTTCGATATTTTGAAATCGCTGCGTATC
pDGB1A2_HDS_Rev  491 GCGGCCGATCCGGTCGAAGAGATCAAAGTCGGTTTCGATATTTTGAAATCGCTGCGTATC
pDGB1A2-HDSc_Fo  721 GCGGCCGATCCGGTCGAAAAAATCAAAGTCGGTTTCGATATTTTGAAATCGCTGCGTATC
pDGB1A2-HDSc_Re  537 GCGGCCGATCCGGTCGAAGAGATCAAAGTCGGTTTCGATATTTTGAAATCGCTGCGTATC

HDS              781 CGTTCGCGAGGGATCAACTTCATCGCCTGCCCGACCTGTTCGCGTCAGGAATTTGATGTT
pDGB1A2-HDS_For  781 CGTTCGCGAGGGATCAACTTCATAGCCTGCCCGACCTGTTCGCGTCAGGAATTTGATGTT
pDGB1A2_HDS_Rev  551 CGTTCGCGAGGGATCAACTTCATAGCCTGCCCGACCTGTTCGCGTCAGGAATTTGATGTT
pDGB1A2-HDSc_Fo  781 CGTTCGCGAGGGATCAACTTCATAGCCTGCCCGACCTGTTCCGTCAGGAATTTGATGTT
pDGB1A2-HDSc_Re  597 CGTTCGCGAGGGATCAACTTCATAGCCTGCCCGACCTGTTCGCGTCAGGAATTTGATGTT

HDS              841 ATCGGTACGGTTAACGCGCTGGAGCAACGCCTGGAAGATATCATCACTCCGATGGACGTT
pDGB1A2-HDS_For  841 ATCGGTACGGTTAACGCGCTGGAGCAACGCCTGGAAGATATCATCACTCCGATGGACGTT
pDGB1A2_HDS_Rev  611 ATCGGTACGGTTAACGCGCTGGAGCAACGCCTGGAAGATATCATCACTCCGATGGACGTT
pDGB1A2-HDSc_Fo  841 ATCCGTACGGTTAACCGCCTGGAACAACGCCTGGAAAATTCCTCCTTCCAAGGAACTTT
pDGB1A2-HDSc_Re  657 ATCGGTACGGTTAACGCGCTGGAGCAACGCCTGGAAGATATCATCACTCCGATGGACGTT

HDS              901 TCGATTATCGGCTGCGTGGTGAATGGCCCAGGTGAGGCGCTGGTTTCTACACTCGGCGTC
pDGB1A2-HDS_For  901 TCGATTATCGGCTGCGTGGTGAA----------------------------------------
pDGB1A2_HDS_Rev  671 TCGATTATCGGCTGCGTGGTGAATGGCCCAGGTGAGGCGCTGGTTTCTACACTCGGCGTC
pDGB1A2-HDSc_Fo  901 C-------------------------------------------------------------
pDGB1A2-HDSc_Re  717 TCGATTATCGGCTGCGTGGTGAATGGCCCAGGTGAGGCGCTGGTTTCTACACTCGGCGTC

HDS              961 ACCGGCGGCAACAAGAAAAGCGGCCTCTATGAAGATGGCGTGCGCAAAGACCGTCTGGAC
pDGB1A2-HDS_For  924 ------------------------------------------------------------
pDGB1A2_HDS_Rev  731 ACCGGCGGCAACAAGAAAAGCGGCCTCTATGAAGATGGCGTGCGCAAAGACCGTCTGGAC
pDGB1A2-HDSc_Fo  902 ------------------------------------------------------------
pDGB1A2-HDSc_Re  777 ACCGGCGGCAACAAGAAAAGCGGCCTCTATGAAGATGGCGTGCGCAAAGACCGTCTGGAC

HDS             1021 AACAACGATATGATCGACCAGCTGGAAGCACGCATTCGTGCGAAAGCCAGTCAGCTGGAC
pDGB1A2-HDS_For  924 ------------------------------------------------------------
pDGB1A2_HDS_Rev  791 AACAACGATATGATCGACCAGCTGGAAGCACGCATTCGTGCGAAAGCCAGTCAGCTGGAC
pDGB1A2-HDSc_Fo  902 ------------------------------------------------------------
pDGB1A2-HDSc_Re  837 AACAACGATATGATCGACCAGCTGGAAGCACGCATTCGTGCGAAAGCCAGTCAGCTGGAC

HDS             1081 GAAGCGCGTCGAATTGACGTTCAGCAGGTTGAAAAATAA
```

```
pDGB1A2-HDS_For  924 ----------------------------------------G
pDGB1A2_HDS_Rev  851 GAAGCGCGTCGAATTGACGTTCAGCAGGTTGAAAAATAA
pDGB1A2-HDSc_Fo  902 ------------------------------------C
pDGB1A2-HDSc_Re  897 GAAGCGCGTCGAATTGACGTTCAGCAGGTTGAAAAATAA
```

HDR (*Escherichia coli*)

```
HDR                1 ATGCAGATCCTGTTGGCCAACCCGCGTGGTTTTTGTGCCGGGGTAGACCGCGCTATCAGC
pDGB1O1-ecHDR_F    1 ATGCAGATCCTGTTGGCCAACCCGCGTGGTTTTTGTGCCGGGGTAGACCGCGCTATCAGC
pDGB1O1-ecHDR_R    1 A-----------------------------------------------------------

HDR               61 ATTGTTGAAAACGCGCTGGCCATTTACGGCGCACCGATATATGTCCGTCACGAAGTGGTA
pDGB1O1-ecHDR_F   61 ATTGTTGAAAACGCGCTGGCCATTTACGGCGCACCGATATATGTCCGTCACGAAGTGGTA
pDGB1O1-ecHDR_R    2 --------------------------------ACCGATATATGTCCGTCACGAAGTGGTA

HDR              121 CATAACCGCTATGTGGTCGATAGCTTGCGTGAGCGTGGGGCTATCTTTATTGAGCAGATT
pDGB1O1-ecHDR_F  121 CATAACCGCTATGTGGTCGATAGCTTGCGTGAGCGTGGGGCTATCTTTATTGAGCAGATT
pDGB1O1-ecHDR_R   30 CATAACCGCTATGTGGTCGATAGCTTGCGTGAGCGTGGGGCTATCTTTATTGAGCAGATT

HDR              181 AGCGAAGTACCGGACGGCGCGATCCTGATTTTCTCCGCACACGGTGTTTCTCAGGCGGTA
pDGB1O1-ecHDR_F  181 AGCGAAGTACCGGACGGCGCGATCCTGATTTTCTCCGCACACGGTGTTTCTCAGGCGGTA
pDGB1O1-ecHDR_R   90 AGCGAAGTACCGGACGGCGCGATCCTGATTTTCTCCGCACACGGTGTTTCTCAGGCGGTA

HDR              241 CGTAACGAAGCAAAAAGTCGCGATTTGACGGTGTTTGATGCCACCTGTCCGCTGGTGACC
pDGB1O1-ecHDR_F  241 CGTAACGAAGCAAAAAGTCGCGATTTGACGGTGTTTGATGCCACCTGTCCGCTGGTGACC
pDGB1O1-ecHDR_R  150 CGTAACGAAGCAAAAAGTCGCGATTTGACGGTGTTTGATGCCACCTGTCCGCTGGTGACC

HDR              301 AAAGTGCATATGGAAGTCGCCCGCGCCAGTCGCCGTGGCGAAGAATCTATTCTCATCGGT
pDGB1O1-ecHDR_F  301 AAAGTGCATATGGAAGTCGCCCGCGCCAGTCGCCGTGGCGAAGAATCTATTCTCATCGGT
pDGB1O1-ecHDR_R  210 AAAGTGCATATGGAAGTCGCCCGCGCCAGTCGCCGTGGCGAAGAATCTATTCTCATCGGT

HDR              361 CACGCCGGGCACCCGGAAGTGGAAGGGACAATGGGCCAGTACAGTAACCCGGAAGGGGGA
pDGB1O1-ecHDR_F  361 CACGCCGGGCACCCGGAAGTGGAAGGGACAATGGGCCAGTACAGTAACCCGGAAGGGGGA
pDGB1O1-ecHDR_R  270 CACGCCGGGCACCCGGAAGTGGAAGGGACAATGGGCCAGTACAGTAACCCGGAAGGGGGA

HDR              421 ATGTATCTGGTCGAATCGCCGGACGATGTGTGGAAACTGACGGTCAAAAACGAAGAGAAG
pDGB1O1-ecHDR_F  421 ATGTATCTGGTCGAATCGCCGGACGATGTGTGGAAACTGACGGTCAAAAACGAAGAGAAG
pDGB1O1-ecHDR_R  330 ATGTATCTGGTCGAATCGCCGGACGATGTGTGGAAACTGACGGTCAAAAACGAAGAGAAG

HDR              481 CTCTCCTTTATGACCCAGACCACGCTGTCGGTGGATGACACGTCTGATGTGATCGACGCG
pDGB1O1-ecHDR_F  481 CTCTCCTTTATGACCCAGACCACGCTGTCGGTGGATGACACGTCTGATGTGATCGACGCG
pDGB1O1-ecHDR_R  390 CTCTCCTTTATGACCCAGACCACGCTGTCGGTGGATGACACGTCTGATGTGATCGACGCG

HDR              541 CTGCGTAAACGCTTCCCGAAAATTGTCGGTCCGCGCAAAGATGACATCTGCTACGCCACG
pDGB1O1-ecHDR_F  541 CTGCGTAAACGCTTCCCGAAAATTGTCGGTCCGCGCAAAGATGACATCTGCTACGCCACG
pDGB1O1-ecHDR_R  450 CTGCGTAAACGCTTCCCGAAAATTGTCGGTCCGCGCAAAGATGACATCTGCTACGCCACG

HDR              601 ACTAACCGTCAGGAAGCGGTACGCGCCCTGGCAGAACAGGCGGAAGTTGTGTTGGTGGTC
pDGB1O1-ecHDR_F  601 ACTAACCGTCAGGAAGCGGTACGCGCCCTGGCAGAACAGGCGGAAGTTGTGTTGGTGGTC
pDGB1O1-ecHDR_R  510 ACTAACCGTCAGGAAGCGGTACGCGCCCTGGCAGAACAGGCGGAAGTTGTGTTGGTGGTC

HDR              661 GGTTCGAAAAACTCCTCCAACTCCAACCGTCTGGCGGAGCTGGCCCAGCGTATGGGCAAA
pDGB1O1-ecHDR_F  661 GGTTCGAAAAACTCCTCCAACTCCAACCGTCTGGCGGAGCTGGCCCAGCGTATGGGCAAA
pDGB1O1-ecHDR_R  570 GGTTCGAAAAACTCCTCCAACTCCAACCGTCTGGCGGAGCTGGCCCAGCGTATGGGCAAA

HDR              721 CGCGCGTTTTTGATTGACGATGCGAAAGACATCCAGGAAGAGTGGGTGAAAGAGGTTAAA
pDGB1O1-ecHDR_F  721 CGCGCGTTTTTGATTGACGATGCGAAAGA-ATCCAGGAAGAGTGGGTGAAAGAGGT-AAA
pDGB1O1-ecHDR_R  630 CGCGCGTTTTTGATTGACGATGCGAAAGACATCCAGGAAGAGTGGGTGAAAGAGGTTAAA

HDR              781 TGCGTCGGCGTGACTGCGGGCGCATCGGCTCCGGATATTCTGGTGCAGAATGTGGTGGCA
pDGB1O1-ecHDR_F  779 TGCGTCGGCGTGACTGCGGGCGCATCGGCTCCGGA-ATTCTGGTGCA-AATGTGGTGGCC
pDGB1O1-ecHDR_R  690 TGCGTCGGCGTGACTGCGGGCGCATCGGCTCCGGATATTCTGGTGCAGAATGTGGTGGCA

HDR              841 CGTTTGCAGCAGCTGGGCGGTGGTGAAGCCATTCCGCTGGAAGGCCGTGAAGAAAACATT
pDGB1O1-ecHDR_F  837 C-TTTGCA-CAACTGGGCGGGGTGA--CCATTCC-CTGGAAG-----------------
pDGB1O1-ecHDR_R  750 CGTTTGCAGCAGCTGGGCGGTGGTGAAGCCATTCCGCTGGAAGGCCGTGAAGAAAACATT

HDR              901 GTTTTCGAAGTGCCGAAAGAGCTGCGTGTCGATATTCGTGAAGTCGATTAA
pDGB1O1-ecHDR_F  875 ------------------------------------------------G
pDGB1O1-ecHDR_R  810 GTTTTCGAAGTGCCGAAAGAGCTGCGTGTCGATATTCGTGAAGTCGATTAA
```

Data Transient transformation screens

Golden Braid MEP (plastid multi-gene)

Table A-5. Overview of measured quantities of carotenoids and chlorophylls.
Plastid multi-gene vectors in leaf infiltrations of *N. benthamiana*. Underlined: significantly different from the negative control, in bold: significantly different from the control (empty vector). Units in µg/g DW.

	Neg.control	EV	pDXS	pDXS-DXR	pDXS-CMK	pDXS-MDS	pDXS-HDS	pMEP
Phytoene	11.5 ±2	10.3 ±2	7.7 ±1	9.4 ±1	9.4 ±2	9.6 ±1	9.1 ±1	10.8 ±2
α-tocopherol	111.0 ±14	116.1 ±6	116.0 ±45	106.2 ±35	124.4 ±42	74.9 ±23	135.9 ±12	92.9 ±12
neoxanthin	240.5 ±41	131.2 ±19	**193.2 ±5**	156.0 ±31	209.1 ±43	200.0 ±41	162.6 ±26	**215.8 ±24**
violaxanthin	358.5 ±76	220.3 ±30	**314.9 ±28**	260.8 ±47	387.1 ±101	345.6 ±64	274.2 ±26	**367.9 ±58**
lutein	748.2 ±193	564.8 ±14	**692.4 ±45**	604.0 ±77	826.0 ±211	683.5 ±140	678.5 ±88	780.0 ±114
chlorophyll B	3363.3 ±808	2217.4 ±300	**3161.2 ±138**	2690.2 ±477	3877.7 ±1104	3409.9 ±742	**2813.9 ±129**	**3627.0 ±636**
chlorophyll A	12505.6 ±3207	7498.1 ±1239	**10992.3 ±775**	9168.1 ±1808	13534.1 ±3919	12253.6 ±2766	**9366.4 ±710**	**12592.5 ±1882**
β-carotene	591.1 ±174	370.2 ±30	**521.5 ±51**	422.5 ±92	645.2 ±208	625.1 ±165	**461.5 ±17**	**600.2 ±89**

Golden Braid MEP (plastid & cytosol multi-gene)

Table A-6. Overview of carotenoids and chlorophylls measures in infiltrated Tobacco leaves.
Samples tested with GB vectors for the MEP pathway. Underlined: significantly different from the negative control, in bold: significantly different from the control (empty vector). Units in µg/g DW.

	neg I	EV	pDXS	pMEP	cMEP
phytoene	9.1 ±2	12.7 ±3	10.7 ±5	**9.3 ±3**	10.3 ±2
α-tocopherol	58.4 ±46	56.3 ±19	37.7 ±14	**24.2 ±3**	57.2 ±25
neoxanthin	251.1 ±55	238.5 ±16	233.3 ±32	248.2 ±34	233.8 ±30
violaxanthin	342.3 ±70	326.4 ±23	329.0 ±38	334.5 ±38	314.6 ±44
lutein	911.1 ±131	780.1 ±42	800.5 ±100	807.0 ±104	824.0 ±78
chlorophyll B	4014.5 ±871	3556.8 ±339	3778.1 ±452	3858.7 ±507	3688.8 ±559

chlorophyll A	13857.9 ±3142	12166.7 ±1391	13141.1 ±1448	13660.8 ±1773	12349.4 ±2097
β-carotene	692.2 ±147	641.3 ±56	668.4 ±80	668.5 ±88	652.9 ±76

Golden Braid MEP: co-infiltration with CRTZ/CRTW

Table A-7. Overview of (keto-) carotenoids and chlorophylls.
Measures in infiltrated *N. benthamiana* leaves, tested with GB vectors for the MEP pathway. Underlined: significantly different from the negative control, in bold: significantly different from the control (ZW-control)). Units in µg/g DW.

	NC	EV	ZW control	pDXS-ZW	pDXR-ZW	pMEP-ZW	cMEP-ZW
phytoene	9.3 ±4	12.5 ±2	16.7 ±0	**11.8 ±1**	13.7 ±2	14.0 ±3	**9.6 ±1**
α-tocopherol	30.5 ±5	80.0 ±16	87.4 ±9	**50.1 ±8**	59.3 ±16	**61.2 ±4**	**38.7 ±4**
neoxanthin	234.8 ±12	213.3 ±17	232.2 ±20	202.8 ±17	293.6 ±26	234.4 ±29	314.7 ±77
violaxanthin	317.0 ±9	267.3 ±5	374.1 ±57	298.5 ±39	452.4 ±64	337.6 ±37	417.1 ±83
lutein	625.5 ±23	539.8 ±81	514.4 ±63	**367.3 ±41**	640.7 ±48	529.7 ±107	657.6 ± 174
chlorophyll B	3457.6 ±119	2989.3 ±299	3236.0 ±362	**2436.6 ±86**	4084.0 ±388	3287.5 ±587	4293.6 ±980
chlorophyll A	12962.8 ±455	10148.2 ±1241	10611.2 ±1135	8464.2 ±234	13311.8 ±911	11181.9 ±2083	14612.9 ±3378
β-carotene	573.9 ±24	436.8 ±132	266.9 ±32	**180.7 ±26**	298.6 ±39	287.2 ±114	436.8 ±164
astaxanthin	n.d.	n.d.	35.0 ±16	44.2 ±13	31.3 ±9	28.6 ±15	**15.0 ±11**
adonixanthin	n.d.	n.d.	98.8 ±20	93.1 ±20	115.2 ±24	84.1 ±34	76.0 ±23
phenicoxanthin	n.d.	n.d.	31.1 ±11	22.9 ±12	27.8 ±5	20.8 ±10	**19.6 ±8**
canthaxanthin	n.d.	n.d.	70.3 ±22	67.9 ±20	90.6 ±19	**45.2 ±20**	53.0 ±23

Golden Braid carotenoid pathway: infiltration with crtB and crt(EB)

Table A-8. Display of abundances of agro-infiltrated *N. benthamiana* with crtB and crt(EB).
Transiently expressing crtB (single vector) and crt(EB) (multi-gene vector). Significant differences between the empty vector are underlined (p-value<0.05, Dunnett's test).

	neg. control	empty vector	crtB	crt(EB)
phytoene	5.7 ±0.9	3.7 ±0.9	42.2 ±11.3	3.6 ±1.0
a-tocopherol	12.0 ±5.2	9.8 ±2.1	9.7 ±4.1	11.7 ±3.1
phytofluene	n.d.	n.d.	22.3 ±5.7	n.d.
neoxanthin	146.5 ±18.2	127.3 ±11.9	132.0 ±15.6	98.9 ±13.3

violaxanthin	527.0 ±75.6	435.4 ±85.3	509.1 ±82.7	486.8 ±101.4
lutein	1419.8 ±168.9	1057.8 ±114.4	1569.5 ±175.8	1166.5 ±155.3
chlorophyll B	5341.3 ±412.1	4552.6 ±403.5	4700.4 ±332.5	4800.0 ±517.2
chlorophyll A	23718.6 ±2420.7	19098.0 ±1894.1	20082.1 ±1516.9	19777.7 ±2293.4
β-carotene	1004.7 ±95.5	790.8 ±95.0	1157.9 ±107.1	797.1 ±90.3
lycopene	n.d.	n.d.	3.8 ±3.0	n.d.

Golden Braid carotenoid pathway: crtB dose response

Dose response screen for Golden Braid crtB (phytoene synthase)

Table A-9. Overview of quantities detected for the dose response samples.

Significance of samples compared to the control (EV) is indicated by underlining, in bold the significance between sample 1/6 and 2/6, 2/6 and 3/6 etc. units represent µg/g DW.

	NC	**EV**	**crtB (1/6)**	**crtB (2/6)**	**crtB (3/6)**	**crtB (4/6)**	**crtB (5/6)**
phytoene	5.2 ±1	5.7 ±1	13.6 ±3	**22.9 ±10**	28.3 ±10	**44.5 ±15**	**27.8 ±15**
α-tocopherol	15.8 ±13	0.0 ±0	3.1 ±2	**8.6 ±6**	6.3 ±3	6.0 ±3	7.4 ±4
phytofluene	0.0 ±0	0.0 ±0	7.0 ±2	**12.7 ±7**	17.2 ±8	**31.1 ±15**	**18.2 ±15**
Neoxanthin	126.8 ±11	103.3 ±8	105.7 ±13	113.8 ±13	110.7 ±14	**131.4 ±12**	133.6 ±13
Violaxanthin	541.1 ±82	468.5 ±41	398.5 ± 69	**466.4 ±78**	501.1 ±68	556.7 ±81	516.6 ±82
lutein	1141.5 ±133	927.1 ±73	870.3 ±146	**1056.5 ±149**	1143.1±169	**1344.6 ±225**	1230.8 ±172
chlorophyll B	5250.0 ±535	4720.9 ±301	4162.4 ±569	**4591.0 ±365**	4654.2 ±550	4788.3 ±516	4890.6 ±625
chlorophyll A	18296.5 ±2201	15285.7 ±1026	13460.0 ±1704	14663.4 ±1677	15785.4 ±1873	16893.8 ±1882	17231.4 ±2230
β-carotene	677.4 ±107	368.1 ±41	424.8 ±94	**585.6 ±135**	692.8 ±127	**890.1 ±171**	805.2 ±125

References

Accuray Research LLP (2017). Global Carotenoids Market Analysis & Trends- Industry Forecast to 2025. 164.

Allorent, G., Courtois, F., Chevalier, F., and Lerbs-Mache, S. (2013). Plastid gene expression during chloroplast differentiation and dedifferentiation into non-photosynthetic plastids during seed formation. Plant Mol Biol *82*, 59-70.

Arie, T., Takahashi, H., Kodama, M., and Teraoka, T. (2007). Tomato as a model plant for plant-pathogen interactions. Plant Biotechnology *24*, 135-147.

Auldridge, M.E., Block, A., Vogel, J.T., Dabney-Smith, C., Mila, I., Bouzayen, M., Magallanes-Lundback, M., DellaPenna, D., McCarty, D.R., and Klee, H.J. (2006). Characterization of three members of the Arabidopsis carotenoid cleavage dioxygenase family demonstrates the divergent roles of this multifunctional enzyme family. The Plant Journal *45*, 982-993.

Avendaño-Vázquez, A.-O., Cordoba, E., Llamas, E., San Román, C., Nisar, N., De la Torre, S., Ramos-Vega, M., Gutiérrez-Nava, M.d.l.L., Cazzonelli, C.I., Pogson, B.J*., et al.* (2014). An Uncharacterized Apocarotenoid-Derived Signal Generated in ζ-Carotene Desaturase Mutants Regulates Leaf Development and the Expression of Chloroplast and Nuclear Genes in Arabidopsis. The Plant Cell Online *26*, 2524-2537.

Banerjee, A., Wu, Y., Banerjee, R., Li, Y., Yan, H., and Sharkey, T.D. (2013). Feedback Inhibition of Deoxy-d-xylulose-5-phosphate Synthase Regulates the Methylerythritol 4-Phosphate Pathway. Journal of Biological Chemistry *288*, 16926-16936.

Barros, M., Poppe, S., and Bondan, E. (2014). Neuroprotective Properties of the Marine Carotenoid Astaxanthin and Omega-3 Fatty Acids, and Perspectives for the Natural Combination of Both in Krill Oil. Nutrients *6*, 1293-1317.

Barsan, C., Zouine, M., Maza, E., Bian, W., Egea, I., Rossignol, M., Bouyssie, D., Pichereaux, C., Purgatto, E., Bouzayen, M*., et al.* (2012). Proteomic Analysis of Chloroplast-to-Chromoplast Transition in Tomato Reveals Metabolic Shifts Coupled with Disrupted Thylakoid Biogenesis Machinery and Elevated Energy-Production Components. Plant Physiology *160*, 708-725.

Battilana, J., Emanuelli, F., Gambino, G., Gribaudo, I., Gasperi, F., Boss, P.K., and Grando, M.S. (2011). Functional effect of grapevine 1-deoxy-D-xylulose 5-phosphate synthase substitution K284N on Muscat flavour formation. Journal of Experimental Botany.

Benn, G., Bjornson, M., Ke, H., De Souza, A., Balmond, E.I., Shaw, J.T., and Dehesh, K. (2016). Plastidial metabolite MEcPP induces a transcriptionally centered stress-response hub via the transcription factor CAMTA3. Proceedings of the National Academy of Sciences *113*, 8855-8860.

Beyer, P., Al-Babili, S., Ye, X., Lucca, P., Schaub, P., Welsch, R., and Potrykus, I. (2002). Golden Rice: Introducing the β-Carotene Biosynthesis Pathway into Rice Endosperm by Genetic Engineering to Defeat Vitamin A Deficiency. The Journal of Nutrition *132*, 506S-510S.

Beyer, P., Mayer, M., and Kleinig, H. (1989). Molecular oxygen and the state of geometric isomerism of intermediates are essential in the carotene desaturation and cyclization reactions in daffodil chromoplasts. European Journal of Biochemistry *184*, 141-150.

Bian, W., Barsan, C., Egea, I., Purgatto, E., Chervin, C., Zouine, M., Latché, A., Bouzayen, M., and Pech, J.-C. (2011). Metabolic and Molecular Events Occurring during Chromoplast Biogenesis. Journal of Botany *2011*.

Bick, J.A., and Lange, B.M. (2003). Metabolic cross talk between cytosolic and plastidial pathways of isoprenoid biosynthesis: unidirectional transport of intermediates across the chloroplast envelope membrane. Archives of Biochemistry and Biophysics *415*, 146-154.

Bino, R.J., De Vos, C.H.R., Lieberman, M., Hall, R.D., Bovy, A., Jonker, H.H., Tikunov, Y., Lommen, A., Moco, S., and Levin, I. (2005). The light-hyperresponsive high pigment-2dg mutation of tomato: alterations in the fruit metabolome. New Phytologist *166*, 427-438.
Bombarely, A., Rosli, H.G., Vrebalov, J., Moffett, P., Mueller, L.A., and Martin, G.B. (2012). A Draft Genome Sequence of *Nicotiana benthamiana* to Enhance Molecular Plant-Microbe Biology Research. Molecular Plant-Microbe Interactions *25*, 1523-1530.
Botella-Pavía, P., Besumbes, Ó., Phillips, M.A., Carretero-Paulet, L., Boronat, A., and Rodríguez-Concepción, M. (2004). Regulation of carotenoid biosynthesis in plants: evidence for a key role of hydroxymethylbutenyl diphosphate reductase in controlling the supply of plastidial isoprenoid precursors. The Plant Journal *40*, 188-199.
Botté, C.Y., and Maréchal, E. (2013). Plastids with or without galactoglycerolipids. Trends in Plant Science *19*, 71-78.
Bouvier, F., Backhaus, R.A., and Camara, B. (1998). Induction and Control of Chromoplast-specific Carotenoid Genes by Oxidative Stress. Journal of Biological Chemistry *273*, 30651-30659.
Bouvier, F., D'Harlingue, A., Backhaus, R.A., Kumagai, M.H., and Camara, B. (2000). Identification of neoxanthin synthase as a carotenoid cyclase paralog. European Journal of Biochemistry *267*, 6346-6352.
Bovy, A., de Vos, R., Kemper, M., Schijlen, E., Pertejo, M.A., Muir, S., Collins, G., Robinson, S., Verhoeyen, M., and Hughes, S. (2002). High-flavonol tomatoes resulting from the heterologous expression of the maize transcription factor genes LC and C1. The Plant Cell *14*, 2509-2526.
Bramley, P.M. (2002). Regulation of carotenoid formation during tomato fruit ripening and development. Journal of Experimental Botany *53*, 2107-2113.
Breitenbach, J., Nogueira, M., Farré, G., Zhu, C., Capell, T., Christou, P., Fleck, G., Focken, U., Fraser, P.D., and Sandmann, G. (2016). Engineered maize as a source of astaxanthin: processing and application as fish feed. Transgenic research *25*, 785-793.
Brückner, K., and Tissier, A. (2013). High-level diterpene production by transient expression in Nicotiana benthamiana. Plant Methods *9*, 46.
Butelli, E., Titta, L., Giorgio, M., Mock, H.-P., Matros, A., Peterek, S., Schijlen, E.G.W.M., Hall, R.D., Bovy, A.G., Luo, J.*, et al.* (2008). Enrichment of tomato fruit with health-promoting anthocyanins by expression of select transcription factors. Nat Biotech *26*, 1301-1308.
Campbell, R., Freitag, S., Bryan, G.J., Stewart, D., and Taylor, M.A. (2016). Environmental and Genetic Factors Associated with Solanesol Accumulation in Potato Leaves. Frontiers in Plant Science *7*.
Campbell, R., Morris, W.L., Mortimer, C.L., Misawa, N., Ducreux, L.J.M., Morris, J.A., Hedley, P.E., Fraser, P.D., and Taylor, M.A. (2015). Optimising ketocarotenoid production in potato tubers: Effect of genetic background, transgene combinations and environment. Plant Science *234*, 27-37.
Canene-Adams, K., Campbell, J.K., Zaripheh, S., Jeffery, E.H., and Erdman, J.W. (2005). The Tomato As a Functional Food. The Journal of Nutrition *135*, 1226-1230.
Carretero-Paulet, L., Cairó, A., Botella-Pavía, P., Besumbes, O., Campos, N., Boronat, A., and Rodríguez-Concepción, M. (2006). Enhanced flux through the methylerythritol 4-phosphate pathway in Arabidopsis plants overexpressing deoxyxylulose 5-phosphate reductoisomerase. Plant Mol Biol *62*, 683-695.
Cazzonelli, C.I., and Pogson, B.J. (2010). Source to sink: regulation of carotenoid biosynthesis in plants. Trends in Plant Science *15*, 266-274.
Chalker-Scott, L. (1999). Environmental significance of anthocyanins in plant stress responses. Photochemistry and photobiology *70*, 1-9.
Chan, K.X., Crisp, P.A., Estavillo, G.M., and Pogson, B.J. (2010a). Chloroplast-to-nucleus communication: Current knowledge, experimental strategies and relationship to drought stress signaling. Plant Signaling & Behavior *5*, 1575-1582.

Chan, L.K., Koay, S.S., Boey, P.L., and Bhatt, A. (2010b). Effects of abiotic stress on biomass and anthocyanin production in cell cultures of Melastoma malabathricum. Biological Research *43*, 127-135.
Chan, W.-S., Abdullah, J.O., Namasivayam, P., and Mahmood, M. (2009). Molecular characterization of a new 1-deoxy-d-xylulose 5-phosphate reductoisomerase (DXR) transcript from Vanda Mimi Palmer. Scientia Horticulturae *121*, 378-382.
Chang, K., Chen, M., Zeng, L., Lan, X., Wang, Q., and Liao, Z. (2014). Abscisic acid enhanced ajmalicine biosynthesis in hairy roots of Rauvolfia verticillata by upregulating expression of the MEP pathway genes. Russ J Plant Physiol *61*, 136-140.
Chappell, J. (2002). The genetics and molecular genetics of terpene and sterol origami. Current Opinion in Plant Biology *5*, 151-157.
Cheng, H.-R., and Jiang, N. (2006). Extremely Rapid Extraction of DNA from Bacteria and Yeasts. Biotechnology Letters *28*, 55-59.
Christiansen, R., Lie, O., and Torrissen, O.J. (1995). Growth and survival of Atlantic salmon, *Salmo salar L*., fed different dietary levels of astaxanthin. First-feeding fry. Aquaculture Nutrition *1*, 189-198.
Christie, P.J., Alfenito, M.R., and Walbot, V. (1994). Impact of low-temperature stress on general phenylpropanoid and anthocyanin pathways: Enhancement of transcript abundance and anthocyanin pigmentation in maize seedlings. Planta *194*, 541-549.
Cordoba, E., Salmi, M., and León, P. (2009). Unravelling the regulatory mechanisms that modulate the MEP pathway in higher plants. Journal of Experimental Botany *60*, 2933-2943.
Cunningham, F.X., and Gantt, E. (2011). Elucidation of the Pathway to Astaxanthin in the Flowers of *Adonis aestivalis*. The Plant Cell *23*, 3055-3069.
Dall'Osto, L., Lico, C., Alric, J., Giuliano, G., Havaux, M., and Bassi, R. (2006). Lutein is needed for efficient chlorophyll triplet quenching in the major LHCII antenna complex of higher plants and effective photoprotection in vivo under strong light. BMC Plant Biology *6*, 32.
Del Campo, J.A., García-González, M., and Guerrero, M.G. (2007). Outdoor cultivation of microalgae for carotenoid production: current state and perspectives. Applied microbiology and biotechnology *74*, 1163-1174.
DellaPenna, D., and Pogson, B.J. (2006). VITAMIN SYNTHESIS IN PLANTS: Tocopherols and Carotenoids. Annual Review of Plant Biology *57*, 711-738.
Demmig-Adams, B., and Adams, W. (1996a). Chlorophyll and Carotenoid Composition in Leaves of *Euonymus kiautschovicus* Acclimated to Different Degrees of Light Stress in the Field. Functional Plant Biology *23*, 649-659.
Demmig-Adams, B., and Adams, W.W. (1996b). The role of xanthophyll cycle carotenoids in the protection of photosynthesis. Trends in Plant Science *1*, 21-26.
Demmig-Adams, B., and Adams, W.W. (2002). Antioxidants in Photosynthesis and Human Nutrition. Science *298*, 2149-2153.
Deruère, J., Römer, S., d'Harlingue, A., Backhaus, R.A., Kuntz, M., and Camara, B. (1994). Fibril assembly and carotenoid overaccumulation in chromoplasts: a model for supramolecular lipoprotein structures. The Plant Cell *6*, 119-133.
Diretto, G., Al-Babili, S., Tavazza, R., Papacchioli, V., Beyer, P., and Giuliano, G. (2007). Metabolic Engineering of Potato Carotenoid Content through Tuber-Specific Overexpression of a Bacterial Mini-Pathway. PLOS ONE *2*, e350.
Dudareva, N., Andersson, S., Orlova, I., Gatto, N., Reichelt, M., Rhodes, D., Boland, W., and Gershenzon, J. (2005). The nonmevalonate pathway supports both monoterpene and sesquiterpene formation in snapdragon flowers. Proceedings of the National Academy of Sciences of the United States of America *102*, 933-938.
Egea, I., Barsan, C., Bian, W., Purgatto, E., Latché, A., Chervin, C., Bouzayen, M., and Pech, J.-C. (2010). Chromoplast Differentiation: Current Status and Perspectives. Plant and Cell Physiology *51*, 1601-1611.

Egea, I., Bian, W., Barsan, C., Jauneau, A., Pech, J.-C., Latché, A., Li, Z., and Chervin, C. (2011). Chloroplast to chromoplast transition in tomato fruit: spectral confocal microscopy analyses of carotenoids and chlorophylls in isolated plastids and time-lapse recording on intact live tissue. Annals of Botany *108*, 291-297.
Enfissi, E.M.A., Barneche, F., Ahmed, I., Lichtlé, C., Gerrish, C., McQuinn, R.P., Giovannoni, J.J., Lopez-Juez, E., Bowler, C., Bramley, P.M.*, et al.* (2010). Integrative Transcript and Metabolite Analysis of Nutritionally Enhanced DE-ETIOLATED1 Downregulated Tomato Fruit. The Plant Cell Online *22*, 1190-1215.
Enfissi, E.M.A., Fraser, P.D., Lois, L.-M., Boronat, A., Schuch, W., and Bramley, P.M. (2005). Metabolic engineering of the mevalonate and non-mevalonate isopentenyl diphosphate-forming pathways for the production of health-promoting isoprenoids in tomato. Plant Biotechnology Journal *3*, 17-27.
Enfissi, E.M.A., Nogueira, M., Bramley, P.M., and Fraser, P.D. (2017). The regulation of carotenoid formation in tomato fruit. The Plant Journal *89*, 774-788.
Engel, P., and Wyss, A. (2010). Beta-Carotene Intake Recommendations (nutri-facts).
Engler, C., Gruetzner, R., Kandzia, R., and Marillonnet, S. (2009). Golden Gate Shuffling: A One-Pot DNA Shuffling Method Based on Type IIs Restriction Enzymes. PLoS ONE *4*, e5553.
Engler, C., Kandzia, R., and Marillonnet, S. (2008). A One Pot, One Step, Precision Cloning Method with High Throughput Capability. PLoS ONE *3*, e3647.
FAOSTAT2014.
Farré, G., Bai, C., Twyman, R.M., Capell, T., Christou, P., and Zhu, C. (2011). Nutritious crops producing multiple carotenoids – a metabolic balancing act. Trends in Plant Science *16*, 532-540.
Fraser, P.D., and Bramley, P.M. (2004). The biosynthesis and nutritional uses of carotenoids. Progress in Lipid Research *43*, 228-265.
Fraser, P.D., Enfissi, E.M.A., and Bramley, P.M. (2009). Genetic engineering of carotenoid formation in tomato fruit and the potential application of systems and synthetic biology approaches. Archives of Biochemistry and Biophysics *483*, 196-204.
Fraser, P.D., Enfissi, E.M.A., Halket, J.M., Truesdale, M.R., Yu, D., Gerrish, C., and Bramley, P.M. (2007). Manipulation of Phytoene Levels in Tomato Fruit: Effects on Isoprenoids, Plastids, and Intermediary Metabolism. The Plant Cell *19*, 3194-3211.
Fraser, P.D., Kiano, J.W., Truesdale, M.R., Schuch, W., and Bramley, P.M. (1999). Phytoene synthase-2 enzyme activity in tomato does not contribute to carotenoid synthesis in ripening fruit. Plant Mol Biol *40*, 687-698.
Fraser, P.D., Misawa, N., Linden, H., Yamano, S., Kobayashi, K., and Sandmann, G. (1992). Expression in *Escherichia coli,* purification, and reactivation of the recombinant Erwinia uredovora phytoene desaturase. Journal of Biological Chemistry *267*, 19891-19895.
Fraser, P.D., Pinto, M.E.S., Holloway, D.E., and Bramley, P.M. (2000). Application of high-performance liquid chromatography with photodiode array detection to the metabolic profiling of plant isoprenoids. The Plant Journal *24*, 551-558.
Fraser, P.D., Romer, S., Shipton, C.A., Mills, P.B., Kiano, J.W., Misawa, N., Drake, R.G., Schuch, W., and Bramley, P.M. (2002). Evaluation of transgenic tomato plants expressing an additional phytoene synthase in a fruit-specific manner. Proceedings of the National Academy of Sciences *99*, 1092-1097.
Fray, R., and Grierson, D. (1993). Identification and genetic analysis of normal and mutant phytoene synthase genes of tomato by sequencing, complementation and co-suppression. Plant Mol Biol *22*, 589-602.
Frusciante, L., Carli, P., Ercolano, M.R., Pernice, R., Di Matteo, A., Fogliano, V., and Pellegrini, N. (2007). Antioxidant nutritional quality of tomato. Molecular nutrition & food research *51*, 609-617.
George, B., Kaur, C., Khurdiya, D., and Kapoor, H. (2004). Antioxidants in tomato (*Lycopersium esculentum*) as a function of genotype. Food chemistry *84*, 45-51.

Gerszberg, A., Hnatuszko-Konka, K., Kowalczyk, T., and Kononowicz, A.K. (2015). Tomato (*Solanum lycopersicum L*.) in the service of biotechnology. Plant Cell, Tissue and Organ Culture (PCTOC) *120*, 881-902.
Gibson, D.G., Benders, G.A., Axelrod, K.C., Zaveri, J., Algire, M.A., Moodie, M., Montague, M.G., Venter, J.C., Smith, H.O., and Hutchison, C.A. (2008). One-step assembly in yeast of 25 overlapping DNA fragments to form a complete synthetic Mycoplasma genitalium genome. Proceedings of the National Academy of Sciences *105*, 20404-20409.
Gibson, D.G., Young, L., Chuang, R.-Y., Venter, J.C., Hutchison, C.A., and Smith, H.O. (2009). Enzymatic assembly of DNA molecules up to several hundred kilobases. Nat Meth *6*, 343-345.
Giovannoni, J.J. (2007). Fruit ripening mutants yield insights into ripening control. Current Opinion in Plant Biology *10*, 283-289.
Giovannucci, E., Rimm, E.B., Liu, Y., Stampfer, M.J., and Willett, W.C. (2002). A Prospective Study of Tomato Products, Lycopene, and Prostate Cancer Risk. Journal of the National Cancer Institute *94*, 391-398.
Giuliano, G., Bartley, G.E., and Scolnik, P.A. (1993). Regulation of carotenoid biosynthesis during tomato development. The Plant Cell Online *5*, 379-387.
Gómez, E., Lucero, M.S., Zoth, S.C., Carballeda, J.M., Gravisaco, M.J., and Berinstein, A. (2013). Transient expression of VP2 in *Nicotiana benthamiana* and its use as a plant-based vaccine against infectious bursal disease virus. Vaccine *31*, 2623-2627.
Gómez, E., Zoth, S.C., Asurmendi, S., Rovere, C.V., and Berinstein, A. (2009). Expression of Hemagglutinin-Neuraminidase glycoprotein of Newcastle Disease Virus in agroinfiltrated *Nicotiana benthamiana* plants. Journal of biotechnology *144*, 337-340.
Gonzali, S., Mazzucato, A., and Perata, P. (2009). Purple as a tomato: towards high anthocyanin tomatoes. Trends in plant science *14*, 237-241.
Goodin, M.M., Zaitlin, D., Naidu, R.A., and Lommel, S.A. (2008). *Nicotiana benthamiana*: Its History and Future as a Model for Plant–Pathogen Interactions. Molecular Plant-Microbe Interactions *21*, 1015-1026.
Gould, S., Waller, R., and McFadden, G. (2008). Plastid Evolution. Annual Review of Plant Biology *59*, 491-517.
Gruszecki, W.I., and Strzałka, K. (2005). Carotenoids as modulators of lipid membrane physical properties. Biochimica et Biophysica Acta (BBA) - Molecular Basis of Disease *1740*, 108-115.
Gupta, P., and Phulara, S.C. (2015). Metabolic engineering for isoprenoid-based biofuel production. Journal of Applied Microbiology *119*, 605-619.
Guzman, I., Hamby, S., Romero, J., Bosland, P.W., and O'Connell, M.A. (2010). Variability of carotenoid biosynthesis in orange colored Capsicum spp. Plant Science *179*, 49-59.
Hahlbrock, K., Bednarek, P., Ciolkowski, I., Hamberger, B., Heise, A., Liedgens, H., Logemann, E., Nürnberger, T., Schmelzer, E., and Somssich, I.E. (2003). Non-self recognition, transcriptional reprogramming, and secondary metabolite accumulation during plant/pathogen interactions. Proceedings of the National Academy of Sciences *100*, 14569-14576.
Haili, D., Yan, D., Jinye, M., Qingtao, L., Yiqin, W., Yunyuan, X., Chengcai, C., Kang, C., Congming, L., and Jianru, Z. (2007). The Arabidopsis Spontaneous Cell Death1 gene, encoding a ζ-carotene desaturase essential for carotenoid biosynthesis, is involved in chloroplast development, photoprotection and retrograde signalling. Cell Research *17*, 458-470.
Halling, K.K., and Slotte, J.P. (2004). Membrane properties of plant sterols in phospholipid bilayers as determined by differential scanning calorimetry, resonance energy transfer and detergent-induced solubilization. Biochimica et Biophysica Acta (BBA) - Biomembranes *1664*, 161-171.
Handelman, G.J., Nightingale, Z.D., Lichtenstein, A.H., Schaefer, E.J., and Blumberg, J.B. (1999). Lutein and zeaxanthin concentrations in plasma after dietary supplementation with egg yolk. The American Journal of Clinical Nutrition *70*, 247-251.
Harada, H., Maoka, T., Osawa, A., Hattan, J.-i., Kanamoto, H., Shindo, K., Otomatsu, T., and Misawa, N. (2014). Construction of transplastomic lettuce (*Lactuca sativa*) dominantly

producing astaxanthin fatty acid esters and detailed chemical analysis of generated carotenoids. Transgenic Research *23*, 303-315.
Harris, W.M., and Spurr, A.R. (1969). Chromoplasts of Tomato Fruits. II. The Red Tomato. American Journal of Botany *56*, 380-389.
Hemmerlin, A. (2013). Post-translational events and modifications regulating plant enzymes involved in isoprenoid precursor biosynthesis. Plant Science *203–204*, 41-54.
Hemmerlin, A., Harwood, J.L., and Bach, T.J. (2012). A raison d'être for two distinct pathways in the early steps of plant isoprenoid biosynthesis? Progress in Lipid Research *51*, 95-148.
Hornero-Méndez, D., Gómez-Ladrón de Guevara, R., and Mínguez-Mosquera, M.I. (2000). Carotenoid Biosynthesis Changes in Five Red Pepper (Capsicum annuum L.) Cultivars during Ripening. Cultivar Selection for Breeding. Journal of Agricultural and Food Chemistry *48*, 3857-3864.
Horton, P., and Ruban, A. (2005). Molecular design of the photosystem II light-harvesting antenna: photosynthesis and photoprotection. Journal of Experimental Botany *56*, 365-373.
Howitt, C.A., and Pogson, B.J. (2006). Carotenoid accumulation and function in seeds and non-green tissues. Plant, cell & environment *29*, 435-445.
Hsieh, M.-H., and Goodman, H.M. (2005). The Arabidopsis IspH Homolog Is Involved in the Plastid Nonmevalonate Pathway of Isoprenoid Biosynthesis. Plant Physiology *138*, 641-653.
Huang, J.-C., Zhong, Y.-J., Liu, J., Sandmann, G., and Chen, F. (2013). Metabolic engineering of tomato for high-yield production of astaxanthin. Metabolic Engineering *17*, 59-67.
Huang, J.-Z., Cheng, T.-C., Wen, P.-J., Hsieh, M.-H., and Chen, F.-C. (2009). Molecular characterization of the Oncidium orchid HDR gene encoding 1-hydroxy-2-methyl-2-(E)-butenyl 4-diphosphate reductase, the last step of the methylerythritol phosphate pathway. Plant Cell Rep *28*, 1475-1486.
Isaacson, T., Ronen, G., Zamir, D., and Hirschberg, J. (2002). Cloning of tangerine from Tomato Reveals a Carotenoid Isomerase Essential for the Production of β-Carotene and Xanthophylls in Plants. The Plant Cell Online *14*, 333-342.
Jackson, H., Braun, C.L., and Ernst, H. (2008). The Chemistry of Novel Xanthophyll Carotenoids. The American Journal of Cardiology *101*, S50-S57.
Jahns, P., and Holzwarth, A.R. (2012). The role of the xanthophyll cycle and of lutein in photoprotection of photosystem II. Biochimica et Biophysica Acta (BBA) - Bioenergetics *1817*, 182-193.
Janik, E., Bednarska, J., Zubik, M., Puzio, M., Luchowski, R., Grudzinski, W., Mazur, R., Garstka, M., Maksymiec, W., Kulik, A*., et al.* (2013). Molecular Architecture of Plant Thylakoids under Physiological and Light Stress Conditions: A Study of Lipid–Light-Harvesting Complex II Model Membranes. The Plant Cell *25*, 2155-2170.
Janská, A., Maršík, P., Zelenková, S., and Ovesná, J. (2010). Cold stress and acclimation – what is important for metabolic adjustment? Plant Biology *12*, 395-405.
Jinfen, Y., Adhikari, M.N., Hui, L., Guozhen, H., Hui, X., Ruoting, Z., and Weiwen, C. (2012). Molecular Cloning, Characterization and Functional Analysis of the Genes Encoding DXR and DXS, the Two Enzymes in the MEP Pathway, from *Amomum villosum Lour*. Paper presented at: Biomedical Engineering and Biotechnology (iCBEB), 2012 International Conference on.
Kachanovsky, D.E., Filler, S., Isaacson, T., and Hirschberg, J. (2012). Epistasis in tomato color mutations involves regulation of phytoene synthase 1 expression by cis-carotenoids. Proceedings of the National Academy of Sciences *109*, 19021-19026.
Kahlau, S., and Bock, R. (2008). Plastid Transcriptomics and Translatomics of Tomato Fruit Development and Chloroplast-to-Chromoplast Differentiation: Chromoplast Gene Expression Largely Serves the Production of a Single Protein. The Plant Cell *20*, 856-874.
Kang, B., Gu, Q., Tian, P., Xiao, L., Cao, H., and Yang, W. (2014). A chimeric transcript containing Psy1 and a potential mRNA is associated with yellow flesh color in tomato accession PI 114490. Planta, 1-11.

Karadas, F., Grammenidis, E., Surai, P., Acamovic, T., and Sparks, N. (2006). Effects of carotenoids from lucerne, marigold and tomato on egg yolk pigmentation and carotenoid composition. British poultry science *47*, 561-566.
Kessler, D., and Baldwin, I.T. (2007). Making sense of nectar scents: the effects of nectar secondary metabolites on floral visitors of *Nicotiana attenuata*. The Plant Journal *49*, 840-854.
Kilambi, H.V., Kumar, R., Sharma, R., and Sreelakshmi, Y. (2013). Chromoplast-Specific Carotenoid-Associated Protein Appears to Be Important for Enhanced Accumulation of Carotenoids in hp1 Tomato Fruits. Plant Physiology *161*, 2085-2101.
Kilambi, H.V., Manda, K., Mitra, S., Charakana, C., Bagri, J., Sharma, R., and Sreelakshmi, Y. (2014). Diverse Networks Regulate carotenogenesis in the Tomato Clade.
Kim, O.T., Kim, S.H., Ohyama, K., Muranaka, T., Choi, Y.E., Lee, H.Y., Kim, M.Y., and Hwang, B. (2010). Upregulation of phytosterol and triterpene biosynthesis in *Centella asiatica* hairy roots overexpressed ginseng farnesyl diphosphate synthase. Plant Cell Rep *29*, 403-411.
Kimura, S., and Sinha, N. (2008). Tomato (*Solanum lycopersicum*): A Model Fruit-Bearing Crop. Cold Spring Harbor Protocols *2008*, pdb.emo105.
Knight, T. (2003). Idempotent vector design for standard assembly of biobricks (DTIC Document).
Kudoh, K., Kawano, Y., Hotta, S., Sekine, M., Watanabe, T., and Ihara, M. (2014). Prerequisite for highly efficient isoprenoid production by cyanobacteria discovered through the over-expression of 1-deoxy-d-xylulose 5-phosphate synthase and carbon allocation analysis. Journal of Bioscience and Bioengineering.
Kumar, S., Hahn, F.M., Baidoo, E., Kahlon, T.S., Wood, D.F., McMahan, C.M., Cornish, K., Keasling, J.D., Daniell, H., and Whalen, M.C. (2012). Remodeling the isoprenoid pathway in tobacco by expressing the cytoplasmic mevalonate pathway in chloroplasts. Metabolic Engineering *14*, 19-28.
Lange, B.M., Rujan, T., Martin, W., and Croteau, R. (2000). Isoprenoid biosynthesis: The evolution of two ancient and distinct pathways across genomes. Proceedings of the National Academy of Sciences *97*, 13172-13177.
Lange, I., Poirier, B.C., Herron, B.K., and Lange, B.M. (2015). Comprehensive Assessment of Transcriptional Regulation Facilitates Metabolic Engineering of Isoprenoid Accumulation in Arabidopsis. Plant Physiology.
LE Frucht, and S Kanon (2005). https://www.israel21c.org/israel-grows-red-algae-in-the-desert-to-fight-disease/ (Israel21c).
Leister, D. (2012). Retrograde signaling in plants: from simple to complex scenarios. Frontiers in Plant Science *3*.
Leivar, P., Monte, E., Al-Sady, B., Carle, C., Storer, A., Alonso, J.M., Ecker, J.R., and Quail, P.H. (2008). The Arabidopsis phytochrome-interacting factor PIF7, together with PIF3 and PIF4, regulates responses to prolonged red light by modulating phyB levels. Plant Cell *20*, 337-352.
Li, J.F., Norville, J.E., Aach, J., McCormack, M., Zhang, D., and Bush, J. (2013). Multiplex and homologous recombination-mediated genome editing in Arabidopsis and *Nicotiana benthamiana* using guide RNA and Cas9. Nat Biotechnol *31*.
Li, L., Paolillo, D.J., Parthasarathy, M.V., DiMuzio, E.M., and Garvin, D.F. (2001). A novel gene mutation that confers abnormal patterns of β-carotene accumulation in cauliflower (Brassica oleracea var. botrytis). The Plant Journal *26*, 59-67.
Li, L., Piatek, M.J., Atef, A., Piatek, A., Wibowo, A., Fang, X., Sabir, J.S.M., Zhu, J.-K., and Mahfouz, M.M. (2012). Rapid and highly efficient construction of TALE-based transcriptional regulators and nucleases for genome modification. Plant Molecular Biology *78*, 407-416.
Li, Z., and Sharkey, T.D. (2013). Metabolic profiling of the methylerythritol phosphate pathway reveals the source of post-illumination isoprene burst from leaves. Plant, Cell & Environment *36*, 429-437.
Li, Z., Wakao, S., Fischer, B.B., and Niyogi, K.K. (2009). Sensing and Responding to Excess Light. Annual Review of Plant Biology *60*, 239-260.

Lichtenthaler, H.K., Rohmer, M., and Schwender, J. (1997). Two independent biochemical pathways for isopentenyl diphosphate and isoprenoid biosynthesis in higher plants. Physiologia Plantarum *101*, 643-652.
Liu, Y., Nakayama, N., Schiff, M., Litt, A., Irish, V.F., and Dinesh-Kumar, S.P. (2004). Virus Induced Gene Silencing of a DEFICIENS Ortholog in *Nicotiana Benthamiana*. Plant Mol Biol *54*, 701-711.
Llorente, B., D'Andrea, L., Ruiz-Sola, M.A., Botterweg, E., Pulido, P., Andilla, J., Loza-Alvarez, P., and Rodriguez-Concepcion, M. (2016). Tomato fruit carotenoid biosynthesis is adjusted to actual ripening progression by a light-dependent mechanism. The Plant Journal *85*, 107-119.
Lois, L.M., Rodríguez-Concepción, M., Gallego, F., Campos, N., and Boronat, A. (2000). Carotenoid biosynthesis during tomato fruit development: regulatory role of 1-deoxy-D-xylulose 5-phosphate synthase. The Plant Journal *22*, 503-513.
López-Juez, E. (2007). Plastid biogenesis, between light and shadows. Journal of Experimental Botany *58*, 11-26.
Lopez, A.B., Van Eck, J., Conlin, B.J., Paolillo, D.J., O'Neill, J., and Li, L. (2008). Effect of the cauliflower Or transgene on carotenoid accumulation and chromoplast formation in transgenic potato tubers. Journal of Experimental Botany *59*, 213-223.
Lorenz, R.T., and Cysewski, G.R. (2000). Commercial potential for *Haematococcus* microalgae as a natural source of astaxanthin. Trends in Biotechnology *18*, 160-167.
Lowder, L.G., Zhang, D., Baltes, N.J., Paul, J.W., Tang, X., and Zheng, X. (2015). A CRISPR/Cas9 toolbox for multiplexed plant genome editing and transcriptional regulation. Plant Physiol *169*.
Luengwilai, K., and Beckles, D.M. (2009). Starch Granules in Tomato Fruit Show a Complex Pattern of Degradation. Journal of Agricultural and Food Chemistry *57*, 8480-8487.
M.L.Cipollini, and D.J.Levey (1997). Secondary Metabolites of Fleshy Vertebrate-Dispersed Fruits: Adaptive Hypotheses and Implications for Seed Dispersal. The American Naturalist *150*, 346-372.
Ma, X., Zhang, Q., Zhu, Q., Liu, W., Chen, Y., and Qiu, R. (2015). A robust CRISPR/Cas9 system for convenient, high-efficiency multiplex genome editing in monocot and dicot plants. Mol Plant.
Maass, D., Arango, J., Wüst, F., Beyer, P., and Welsch, R. (2009). Carotenoid Crystal Formation in Arabidopsis and Carrot Roots Caused by Increased Phytoene Synthase Protein Levels. PLoS ONE *4*, e6373.
Mahajan, S., and Tuteja, N. (2005). Cold, salinity and drought stresses: An overview. Archives of Biochemistry and Biophysics *444*, 139-158.
Majer, E., Llorente, B., Rodríguez-Concepción, M., and Daròs, J.-A. (2017). Rewiring carotenoid biosynthesis in plants using a viral vector. Scientific Reports *7*, 41645.
Manabe, Y., Hirata, T., and Sugawara, T. (2014). Suppressive Effects of Carotenoids on the Antigen-induced Degranulation in RBL-2H3 Rat Basophilic Leukemia Cells. Journal of Oleo Science *63*, 291-294.
Mann, V., Harker, M., Pecker, I., and Hirschberg, J. (2000). Metabolic engineering of astaxanthin production in tobacco flowers. Nature biotechnology *18*, 888-892.
Mannen, K., Matsumoto, T., Takahashi, S., Yamaguchi, Y., Tsukagoshi, M., Sano, R., Suzuki, H., Sakurai, N., Shibata, D., Koyama, T*., et al.* (2014). Coordinated transcriptional regulation of isopentenyl diphosphate biosynthetic pathway enzymes in plastids by phytochrome-interacting factor 5. Biochemical and Biophysical Research Communications *443*, 768-774.
Mayne, S.T. (2003). Antioxidant Nutrients and Chronic Disease: Use of Biomarkers of Exposure and Oxidative Stress Status in Epidemiologic Research. The Journal of Nutrition *133*, 933S-940S.
McNulty, H.P., Byun, J., Lockwood, S.F., Jacob, R.F., and Mason, R.P. (2007). Differential effects of carotenoids on lipid peroxidation due to membrane interactions: X-ray diffraction analysis. Biochimica et Biophysica Acta (BBA) - Biomembranes *1768*, 167-174.

Meissner, R., Jacobson, Y., Melamed, S., Levyatuv, S., Shalev, G., Ashri, A., Elkind, Y., and Levy, A. (1997). A new model system for tomato genetics. The Plant Journal *12*, 1465-1472.
Misawa, N., and Shimada, H. (1998). Metabolic engineering for the production of carotenoids in non-carotenogenic bacteria and yeasts. Journal of Biotechnology *59*, 169-181.
Mooney, H.A., Harrison, A.T., and Gulmon, S.L. (1974). Photobleaching in High and Low Elevation Plants at Different Intensities. The American Midland Naturalist *91*, 254-256.
Morandini, P. (2013). Control limits for accumulation of plant metabolites: brute force is no substitute for understanding. Plant biotechnology journal *11*, 253-267.
Moreno, J.A., Díaz-Gómez, J., Nogareda, C., Angulo, E., Sandmann, G., Portero-Otin, M., Serrano, J.C.E., Twyman, R.M., Capell, T., Zhu, C*., et al.* (2016). The distribution of carotenoids in hens fed on biofortified maize is influenced by feed composition, absorption, resource allocation and storage. Scientific Reports *6*, 35346.
Morison, J.I.L., and Lawlor, D.W. (1999). Interactions between increasing CO2 concentration and temperature on plant growth. Plant, Cell & Environment *22*, 659-682.
Müller, P., Li, X.-P., and Niyogi, K.K. (2001). Non-Photochemical Quenching. A Response to Excess Light Energy. Plant Physiology *125*, 1558-1566.
Nambara, E., and Marion-Poll, A. (2005). ABSCISIC ACID BIOSYNTHESIS AND CATABOLISM. Annual Review of Plant Biology *56*, 165-185.
Narusaka, M., Seki, M., Umezawa, T., Ishida, J., Nakajima, M., Enju, A., and Shinozaki, K. (2004). Crosstalk in the responses to abiotic and biotic stresses in Arabidopsis: analysis of gene expression in cytochrome P450 gene superfamily by cDNA microarray. Plant Mol Biol *55*, 327-342.
Natesan, S.K.A., Sullivan, J.A., and Gray, J.C. (2005). Stromules: a characteristic cell-specific feature of plastid morphology*. Journal of Experimental Botany *56*, 787-797.
Nekrasov, V., Staskawicz, B., Weigel, D., Jones, J.D.G., and Kamoun, S. (2013). Targeted mutagenesis in the model plant *Nicotiana benthamiana* using Cas9 RNA-guided endonuclease. Nat Biotech *31*, 691-693.
Neuhaus, H.E., and Emes, M.J. (2000). NONPHOTOSYNTHETIC METABOLISM IN PLASTIDS. Annual Review of Plant Physiology and Plant Molecular Biology *51*, 111-140.
Niinemets, Ü., Kännaste, A., and Copolovici, L. (2013). Quantitative patterns between plant volatile emissions induced by biotic stresses and the degree of damage. Frontiers in Plant Science *4*, 262.
Niyogi, K.K., Grossman, A.R., and Björkman, O. (1998). Arabidopsis mutants define a central role for the xanthophyll cycle in the regulation of photosynthetic energy conversion. The Plant Cell *10*, 1121-1134.
Nogueira, M., Berry, H., Nohl, R., Klompmaker, M., Holden, A., and Fraser, P.D. (2016). Subchromoplast Fractionation Protocol for Different *Solanaceae* Fruit Species. Bio-protocol 6(13): e1861
Nogueira, M., Enfissi, E.M.A., Martínez Valenzuela, M.E., Menard, G.N., Driller, R.L., Eastmond, P.J., Schuch, W., Sandmann, G., and Fraser, P.D. (2017). Engineering of tomato for the sustainable production of ketocarotenoids and its evaluation in aquaculture feed. Proceedings of the National Academy of Sciences *114*, 10876-10881.
Nogueira, M., Mora, L., Enfissi, E.M.A., Bramley, P.M., and Fraser, P.D. (2013). Subchromoplast Sequestration of Carotenoids Affects Regulatory Mechanisms in Tomato Lines Expressing Different Carotenoid Gene Combinations. The Plant Cell Online *25*, 4560-4579.
Noviendri, D., Hasrini, R.F., and Octavianti, F. (2011). Carotenoids: Sources, medicinal properties and their application in food and nutraceutical industry. Journal of Medicinal Plants Research *5*, 7119-7131.
Oldenburg, D.J., and Bendich, A.J. (2004). Most Chloroplast DNA of Maize Seedlings in Linear Molecules with Defined Ends and Branched Forms. Journal of Molecular Biology *335*, 953-970.

Osganian, S.K., Stampfer, M.J., Rimm, E., Spiegelman, D., Manson, J.E., and Willett, W.C. (2003). Dietary carotenoids and risk of coronary artery disease in women. The American Journal of Clinical Nutrition *77*, 1390-1399.
Paetzold, H., Garms, S., Bartram, S., Wieczorek, J., Urós-Gracia, E.-M., Rodríguez-Concepción, M., Boland, W., Strack, D., Hause, B., and Walter, M.H. (2010). The Isogene 1-Deoxy-D-Xylulose 5-Phosphate Synthase 2 Controls Isoprenoid Profiles, Precursor Pathway Allocation, and Density of Tomato Trichomes. Molecular Plant *3*, 904-916.
Paine, J.A., Shipton, C.A., Chaggar, S., Howells, R.M., Kennedy, M.J., Vernon, G., Wright, S.Y., Hinchliffe, E., Adams, J.L., Silverstone, A.L.*, et al.* (2005). Improving the nutritional value of Golden Rice through increased pro-vitamin A content. Nature Biotechnology *23*, 482.
Park, H., Kreunen, S.S., Cuttriss, A.J., DellaPenna, D., and Pogson, B.J. (2002). Identification of the Carotenoid Isomerase Provides Insight into Carotenoid Biosynthesis, Prolamellar Body Formation, and Photomorphogenesis. The Plant Cell Online *14*, 321-332.
Patron, N.J., Orzaez, D., Marillonnet, S., Warzecha, H., Matthewman, C., and Youles, M. (2015). Standards for plant synthetic biology: a common syntax for exchange of DNA parts. New Phytol.
Pedranzani, H., Racagni, G., Alemano, S., Miersch, O., Ramírez, I., Peña-Cortés, H., Taleisnik, E., Machado-Domenech, E., and Abdala, G. (2003). Salt tolerant tomato plants show increased levels of jasmonic acid. Plant Growth Regulation *41*, 149-158.
Pedranzani, H., Sierra-de-Grado, R., Vigliocco, A., Miersch, O., and Abdala, G. (2007). Cold and water stresses produce changes in endogenous jasmonates in two populations of *Pinus pinaster Ait*. Plant Growth Regulation *52*, 111-116.
Petrusa, L.M., and Winicov, I. (1997). and plants in response to NaCl. Plant Physiol Biochem *35*, 303-310.
Pogson, B.J., Niyogi, K.K., Björkman, O., and DellaPenna, D. (1998). Altered xanthophyll compositions adversely affect chlorophyll accumulation and nonphotochemical quenching in Arabidopsis mutants. Proceedings of the National Academy of Sciences *95*, 13324-13329.
Qin, C., Yu, C., Shen, Y., Fang, X., Chen, L., Min, J., Cheng, J., Zhao, S., Xu, M., Luo, Y.*, et al.* (2014). Whole-genome sequencing of cultivated and wild peppers provides insights into *Capsicum* domestication and specialization. Proceedings of the National Academy of Sciences *111*, 5135-5140.
Raiola, A., Rigano, M.M., Calafiore, R., Frusciante, L., and Barone, A. (2014). Enhancing the Health-Promoting Effects of Tomato Fruit for Biofortified Food. Mediators of Inflammation *2014*, 16.
Ravanello, M.P., Ke, D., Alvarez, J., Huang, B., and Shewmaker, C.K. (2003). Coordinate expression of multiple bacterial carotenoid genes in canola leading to altered carotenoid production. Metabolic Engineering *5*, 255-263.
Rodríguez-Concepción, M., and Boronat, A. (2002). Elucidation of the Methylerythritol Phosphate Pathway for Isoprenoid Biosynthesis in Bacteria and Plastids. A Metabolic Milestone Achieved through Genomics. Plant Physiology *130*, 1079-1089.
Rodriguez-Concepcion, M., and Stange, C. (2013). Biosynthesis of carotenoids in carrot: An underground story comes to light. Archives of Biochemistry and Biophysics *539*, 110-116.
Rodríguez-Villalón, A., Gas, E., and Rodríguez-Concepción, M. (2009). Phytoene synthase activity controls the biosynthesis of carotenoids and the supply of their metabolic precursors in dark-grown Arabidopsis seedlings. The Plant Journal *60*, 424-435.
Rohmer, M., Seemann, M., Horbach, S., Bringer-Meyer, S., and Sahm, H. (1996). Glyceraldehyde 3-Phosphate and Pyruvate as Precursors of Isoprenic Units in an Alternative Non-mevalonate Pathway for Terpenoid Biosynthesis. Journal of the American Chemical Society *118*, 2564-2566.
Ronen, G., Carmel-Goren, L., Zamir, D., and Hirschberg, J. (2000). An alternative pathway to β-carotene formation in plant chromoplasts discovered by map-based cloning of Beta and old-

gold color mutations in tomato. Proceedings of the National Academy of Sciences *97*, 11102-11107.
Rubio, A., Rambla, J.L., Santaella, M., Gómez, M.D., Orzaez, D., Granell, A., and Gómez-Gómez, L. (2008). Cytosolic and Plastoglobule-targeted Carotenoid Dioxygenases from *Crocus sativus* Are Both Involved in β-Ionone Release. Journal of Biological Chemistry *283*, 24816-24825.
Ruiz-Sola, M.Á., and Rodríguez-Concepción, M. (2012). Carotenoid Biosynthesis in Arabidopsis: A Colorful Pathway. The Arabidopsis Book / American Society of Plant Biologists *10*, e0158.
Sakuma, T., Nishikawa, A., Kume, S., Chayama, K., and Yamamoto, T. (2014). Multiplex genome engineering in human cells using all-in-one CRISPR/Cas9 vector system. Sci Rep *4*.
Sarrion-Perdigones, A., Falconi, E.E., Zandalinas, S.I., Juarez, P., Fernandez-del-Carmen, A., and Granell, A. (2011). GoldenBraid: an iterative cloning system for standardized assembly of reusable genetic modules. PLoS ONE *6*.
Sarrion-Perdigones, A., Vazquez-Vilar, M., Palaci, J., Castelijns, B., Forment, J., and Ziarsolo, P. (2013). GoldenBraid 2.0: a comprehensive DNA assembly framework for plant synthetic biology. Plant Physiol *162*.
Schauer, N., Semel, Y., Roessner, U., Gur, A., Balbo, I., Carrari, F., Pleban, T., Perez-Melis, A., Bruedigam, C., Kopka, J.*, et al.* (2006). Comprehensive metabolic profiling and phenotyping of interspecific introgression lines for tomato improvement. Nat Biotech *24*, 447-454.
Schmidt, G.W., and Delaney, S.K. (2010). Stable internal reference genes for normalization of real-time RT-PCR in tobacco (*Nicotiana tabacum*) during development and abiotic stress. Molecular Genetics and Genomics *283*, 233-241.
Schmidt, I., Schewe, H., Gassel, S., Jin, C., Buckingham, J., Hümbelin, M., Sandmann, G., and Schrader, J. (2011). Biotechnological production of astaxanthin with *Phaffia rhodozyma*/*Xanthophyllomyces dendrorhous*. Applied Microbiology and Biotechnology *89*, 555-571.
Shewmaker, C.K., Sheehy, J.A., Daley, M., Colburn, S., and Ke, D.Y. (1999). Seed-specific overexpression of phytoene synthase: increase in carotenoids and other metabolic effects. The Plant Journal *20*, 401-412.
Simpson, K., Quiroz, L.F., Rodriguez-Concepción, M., and Stange, C.R. (2016). Differential Contribution of the First Two Enzymes of the MEP Pathway to the Supply of Metabolic Precursors for Carotenoid and Chlorophyll Biosynthesis in Carrot (Daucus carota). Frontiers in Plant Science *7*, 1344.
Singh, K.B., Foley, R.C., and Oñate-Sánchez, L. (2002). Transcription factors in plant defense and stress responses. Current opinion in plant biology *5*, 430-436.
Smita, S., Rajwanshi, R., Lenka, S., Katiyar, A., Chinnusamy, V., and Bansal, K. (2013). Expression profile of genes coding for carotenoid biosynthetic pathway during ripening and their association with accumulation of lycopene in tomato fruits. J Genet *92*, 363-368.
Sonawane, P.D., Pollier, J., Panda, S., Szymanski, J., Massalha, H., Yona, M., Unger, T., Malitsky, S., Arendt, P., Pauwels, L.*, et al.* (2016). Plant cholesterol biosynthetic pathway overlaps with phytosterol metabolism. Nature Plants *3*, 16205.
Sparkes, I.A., Runions, J., Kearns, A., and Hawes, C. (2006). Rapid, transient expression of fluorescent fusion proteins in tobacco plants and generation of stably transformed plants. Nat Protocols *1*, 2019-2025.
Strasser, R., Stadlmann, J., Schähs, M., Stiegler, G., Quendler, H., Mach, L., Glössl, J., Weterings, K., Pabst, M., and Steinkellner, H. (2008). Generation of glyco-engineered *Nicotiana benthamiana* for the production of monoclonal antibodies with a homogeneous human-like N-glycan structure. Plant biotechnology journal *6*, 392-402.
Suhita, D., Raghavendra, A.S., Kwak, J.M., and Vavasseur, A. (2004). Cytoplasmic Alkalization Precedes Reactive Oxygen Species Production during Methyl Jasmonate- and Abscisic Acid-Induced Stomatal Closure. Plant Physiology *134*, 1536-1545.

Takabayashi, J., Dicke, M., and Posthumus, M.A. (1994). Volatile herbivore-induced terpenoids in plant-mite interactions: variation caused by biotic and abiotic factors. Journal of Chemical Ecology *20*, 1329-1354.
Taylor, A., Jacques, P.F., Chylack, L.T., Hankinson, S.E., Khu, P.M., Rogers, G., Friend, J., Tung, W., Wolfe, J.K., Padhye, N.*, et al.* (2002). Long-term intake of vitamins and carotenoids and odds of early age-related cortical and posterior subcapsular lens opacities. The American Journal of Clinical Nutrition *75*, 540-549.
Télef, N., Stammitti-Bert, L., Mortain-Bertrand, A., Maucourt, M., Carde, J.P., Rolin, D., and Gallusci, P. (2006). Sucrose deficiency delays lycopene accumulation in tomato fruit pericarp discs. Plant Mol Biol *62*, 453-469.
Terfrüchte, M., Joehnk, B., Fajardo-Somera, R., Braus, G.H., Riquelme, M., Schipper, K., and Feldbrügge, M. (2014). Establishing a versatile Golden Gate cloning system for genetic engineering in fungi. Fungal Genetics and Biology *62*, 1-10.
The Tomato Genome Consortium (2012). The tomato genome sequence provides insights into fleshy fruit evolution. Nature *485*, 635-641.
Toledo-Ortiz, G., Johansson, H., Lee, K.P., Bou-Torrent, J., Stewart, K., Steel, G., Rodríguez-Concepción, M., and Halliday, K.J. (2014). The HY5-PIF Regulatory Module Coordinates Light and Temperature Control of Photosynthetic Gene Transcription. PLOS Genetics *10*, e1004416.
Tong, C., Huang, G., Ashton, C., Wu, H., Yan, H., and Ying, Q.-L. (2012). Rapid and Cost-Effective Gene Targeting in Rat Embryonic Stem Cells by TALENs. Journal of Genetics and Genomics *39*, 275-280.
Tsuda, T. (2012). Dietary anthocyanin-rich plants: biochemical basis and recent progress in health benefits studies. Molecular nutrition & food research *56*, 159-170.
Vallabhaneni, R., and Wurtzel, E.T. (2009). Timing and biosynthetic potential for carotenoid accumulation in genetically diverse germplasm of maize. Plant Physiology *150*, 562-572.
Van Cutsem, E., Simonart, G., Degand, H., Faber, A.M., Morsomme, P., and Boutry, M. (2011). Gel-based and gel-free proteomic analysis of *Nicotiana tabacum* trichomes identifies proteins involved in secondary metabolism and in the (a) biotic stress response. Proteomics *11*, 440-454.
Van Norman, J.M., and Sieburth, L.E. (2007). Dissecting the biosynthetic pathway for the bypass1 root-derived signal. The Plant Journal *49*, 619-628.
Vazquez-Vilar, M., Bernabé-Orts, J.M., Fernandez-del-Carmen, A., Ziarsolo, P., Blanca, J., Granell, A., and Orzaez, D. (2016). A modular toolbox for gRNA–Cas9 genome engineering in plants based on the GoldenBraid standard. Plant Methods *12*, 10.
Vazquez-Vilar, M., Sarrion-Perdigones, A., Ziarsolo, P., Blanca, J., Granell, A., and Orzaez, D. (2015). Software-assisted stacking of gene modules using GoldenBraid 2.0 DNA-assembly framework. Methods Mol Biol *1284*.
Vincent, H., Wiersema, J., Kell, S., Fielder, H., Dobbie, S., Castañeda-Álvarez, N.P., Guarino, L., Eastwood, R., León, B., and Maxted, N. (2013). A prioritized crop wild relative inventory to help underpin global food security. Biological Conservation *167*, 265-275.
Vishnevetsky, M., Ovadis, M., and Vainstein, A. (1999). Carotenoid sequestration in plants: the role of carotenoid-associated proteins. Trends in Plant Science *4*, 232-235.
Visser, H., Ooyen, A.J., and Verdoes, J.C. (2003). Metabolic engineering of the astaxanthin-biosynthetic pathway of *Xanthophyllomyces dendrorhous*. FEMS yeast research *4*, 221-231.
Voinnet, O., Rivas, S., Mestre, P., and Baulcombe, D. (2003). An enhanced transient expression system in plants based on suppression of gene silencing by the p19 protein of tomato bushy stunt virus. Plant J *33*.
von Oppen-Bezalel, L. (2007). UVA, A Main Concern in Sun Damage: Protection from the Inside and Outside with Phytoene, Phytofluene, the Colorless Carotenoids and more. SÖFW-Journal *133*.

von Oppen-Bezalel, L., Fishbein, D., Havas, F., Ben-Chitrit, O., and Khaiat, A. (2015). The photoprotective effects of a food supplement tomato powder rich in phytoene and phytofluene, the colorless carotenoids, a preliminary study.
von Oppen-Bezalel, L., Lerner, E., Kern, D.G., Fuller, B., Soudant, E., and Shaish, A. (2006). Colorless carotenoids from IBR: phytoene and phytofluene from unicellular algae-applications in cosmetics, wellness and nutrition. Fragrance Journal *34*, 48.
Vranova, E., Coman, D., and Gruissem, W. (2013). Network Analysis of the MVA and MEP Pathways for Isoprenoid Synthesis. Annual Review of Plant Biology *64*, 665-700.
Walley, J., Xiao, Y., Wang, J.-Z., Baidoo, E.E., Keasling, J.D., Shen, Z., Briggs, S.P., and Dehesh, K. (2015). Plastid-produced interorgannellar stress signal MEcPP potentiates induction of the unfolded protein response in endoplasmic reticulum. Proceedings of the National Academy of Sciences *112*, 6212-6217.
Wang, H., Nagegowda, D.A., Rawat, R., Bouvier-Navé, P., Guo, D., Bach, T.J., and Chye, M.-L. (2012). Overexpression of *Brassica juncea* wild-type and mutant HMG-CoA synthase 1 in Arabidopsis up-regulates genes in sterol biosynthesis and enhances sterol production and stress tolerance. Plant Biotechnology Journal *10*, 31-42.
Weber, E., Engler, C., Gruetzner, R., Werner, S., and Marillonnet, S. (2011). A Modular Cloning System for Standardized Assembly of Multigene Constructs. PLoS ONE *6*, e16765.
Widomska, J., Kostecka-Gugała, A., Latowski, D., Gruszecki, W.I., and Strzałka, K. (2009). Calorimetric studies of the effect of cis-carotenoids on the thermotropic phase behavior of phosphatidylcholine bilayers. Biophysical Chemistry *140*, 108-114.
Wydro, M., Kozubek, E., and Lehmann, P. (2006). Optimization of transient Agrobacterium-mediated gene expression system in leaves of *Nicotiana benthamiana*. ACTA BIOCHIMICA POLONICA-ENGLISH EDITION- *53*, 289.
Xiao, Y., Savchenko, T., Baidoo, E.E., Chehab, W.E., Hayden, D.M., Tolstikov, V., Corwin, J.A., Kliebenstein, D.J., Keasling, J.D., and Dehesh, K. (2012). Retrograde signaling by the plastidial metabolite MEcPP regulates expression of nuclear stress-response genes. Cell *149*.
Xie, Z., Kapteyn, J., and Gang, D.R. (2008). A systems biology investigation of the MEP/terpenoid and shikimate/phenylpropanoid pathways points to multiple levels of metabolic control in sweet basil glandular trichomes. The Plant Journal *54*, 349-361.
Yang, J., Adhikari, M., Liu, H., Xu, H., He, G., Zhan, R., Wei, J., and Chen, W. (2012). Characterization and functional analysis of the genes encoding 1-deoxy-d-xylulose-5-phosphate reductoisomerase and 1-deoxy-d-xylulose-5-phosphate synthase, the two enzymes in the MEP pathway, from *Amomum villosum Lour*. Mol Biol Rep *39*, 8287-8296.
Yao, H., Gong, Y., Zuo, K., Ling, H., Qiu, C., Zhang, F., Wang, Y., Pi, Y., Liu, X., Sun, X*., et al.* (2008). Molecular cloning, expression profiling and functional analysis of a DXR gene encoding 1-deoxy-d-xylulose 5-phosphate reductoisomerase from *Camptotheca acuminata*. Journal of Plant Physiology *165*, 203-213.
Ye, X., Al-Babili, S., Klöti, A., Zhang, J., Lucca, P., Beyer, P., and Potrykus, I. (2000). Engineering the provitamin A (β-carotene) biosynthetic pathway into (carotenoid-free) rice endosperm. Science *287*, 303-305.
Yuan, J.-P., and Chen, F. (2000). Purification of trans-astaxanthin from a high-yielding astaxanthin ester-producing strain of the microalga *Haematococcus pluvialis*. Food Chemistry *68*, 443-448.
Zhou, C., Li, Z., Wiberley-Bradford, A.E., Weise, S.E., and Sharkey, T.D. (2013). Isopentenyl diphosphate and dimethylallyl diphosphate/isopentenyl diphosphate ratio measured with recombinant isopentenyl diphosphate isomerase and isoprene synthase. Analytical Biochemistry *440*, 130-136.
Zhou, K., Zou, R., Stephanopoulos, G., and Too, H.-P. (2012). Metabolite Profiling Identified Methylerythritol Cyclodiphosphate Efflux as a Limiting Step in Microbial Isoprenoid Production. PLoS ONE *7*, e47513.

Zhou, X., Welsch, R., Yang, Y., Riediger, M., Alvarez, D., Yuan, H., Fish, T., Liu, J., Thannhauser, T.W., and Li, L. (2015). Arabidopsis OR proteins are the Major Post-Transcriptional Regulators of Phytoene Synthase in Mediating Carotenoid Biosynthesis.